Aus dem Adolf-Butenandt-Institut der

Ludwig-Maximilians-Universität München

Lehrstuhl: Stoffwechselbiochemie

Vorstand: Prof. Dr. rer. nat. Dr. h.c. Christian Haass

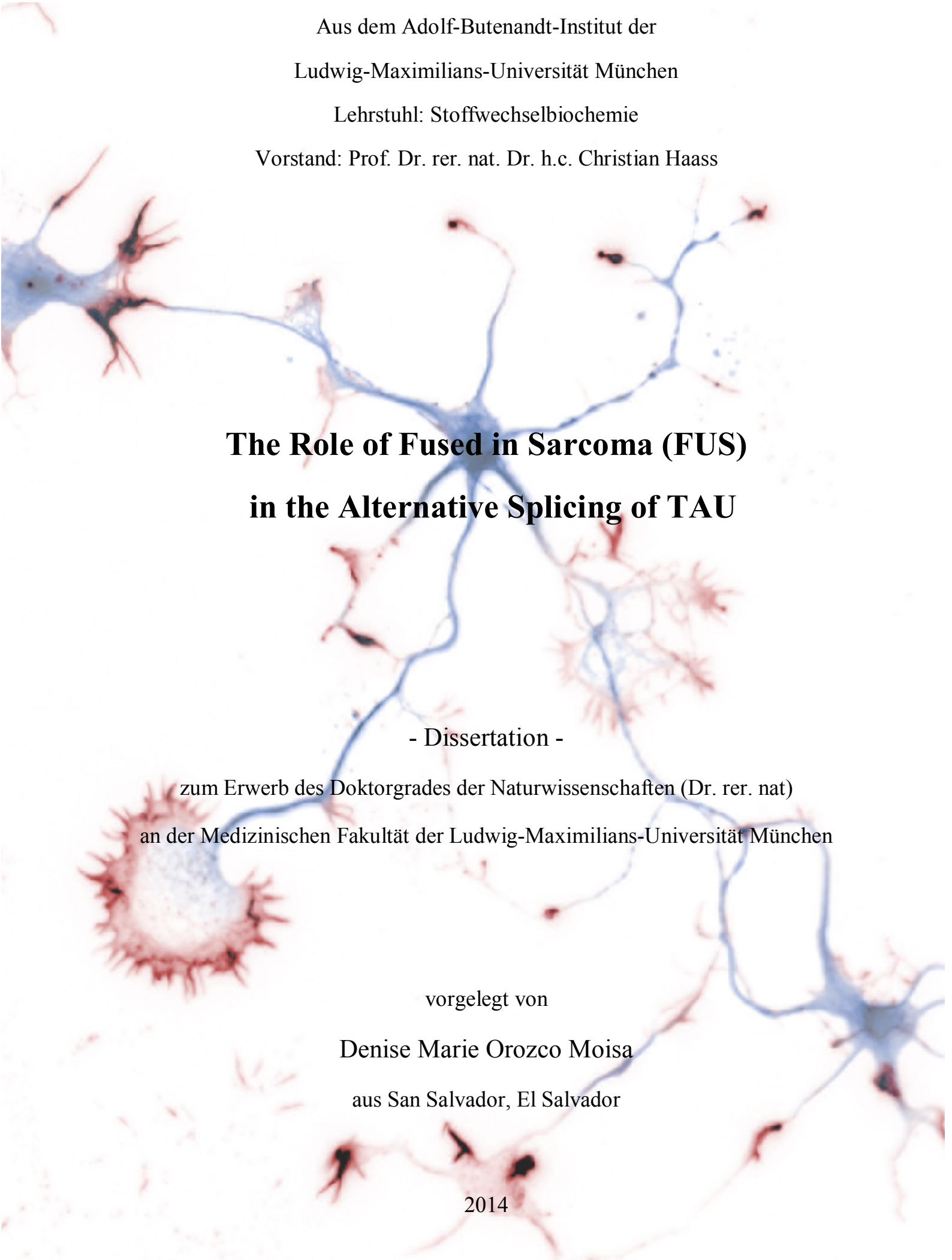

The Role of Fused in Sarcoma (FUS) in the Alternative Splicing of TAU

- Dissertation -

zum Erwerb des Doktorgrades der Naturwissenschaften (Dr. rer. nat)

an der Medizinischen Fakultät der Ludwig-Maximilians-Universität München

vorgelegt von

Denise Marie Orozco Moisa

aus San Salvador, El Salvador

2014

Gedruckt mit Genehmigung der Medizinischen Fakultät der Ludwig-Maximilians-Universität München

Betreuer: Prof. Dr. rer. nat. Dr. h.c. Christian Haass

Zweitgutachter: Prof. Dr. rer. nat. Michael Kiebler

Dekan: Herr Prof. Dr.med. Dr.h.c. Maximilian Reiser, FACR, FRCR

Dissertation eingereicht am 08.April. 2014.

Tag der mündlichen Prüfung:16.September.2014.

Eidesstattliche Versicherung

Ich erkläre hiermit an Eides statt, dass ich die vorliegende Dissertation mit dem Thema *The Role of Fused in Sarcoma (FUS) in the Alternative Splicing of Tau* selbständig verfasst, mich außer der angegebenen keiner weiteren Hilfsmittel bedient und alle Erkenntnisse, die aus dem Schrifttum ganz oder annähernd übernommen sind, als solche kenntlich gemacht und nach ihrer Herkunft unter Bezeichnung der Fundstelle einzeln nachgewiesen habe.

Ich erkläre des Weiteren, dass die hier vorgelegte Dissertation nicht in gleicher oder in ähnlicher Form bei einer anderen Stelle zur Erlangung eines akademischen Grades eingereicht wurde.

München, 08.April. 2014

_____

Denise Marie Orozco Moisa

Andrea: Die Wissenschaft kennt nur ein Gebot: den wissenschaftlichen Beitrag
- Leben des Galilei, Bertolt Brecht

Let us keep looking in spite of everything. Let us keep searching
It is indeed the best method of finding, and perhaps thanks to our efforts,
the verdict we will give such a patient tomorrow
will not be the same we must give this patient today.
- Jean-Martin Charcot

Gracias a la vida que me ha dado tanto
Me dio el corazón que agita su marco
Cuando miro el fruto del cerebro humano
- Violeta Parra

A mi familia, por su apoyo incondicional

Summary

Neurodegenerative disease patients suffer from cognitive decline and/or motor dysfunctions, depending on the different regions affected by the neuron loss. With aging being the major risk factor and a society with increased life expectancy, there is an urgent need to develop new effective treatments to alleviate the situation faced by patients, their families and society. Although neurodegenerative diseases including Alzheimer's disease (AD), amyotrophic lateral sclerosis (ALS) or frontotemporal dementia (FTD) lead to different clinical symptoms, they share common pathomechanisms, such as protein aggregation and altered RNA metabolism. A subset of ALS and FTD cases, for instance, is pathologically characterized by neuronal cytoplasmic inclusions containing aggregated Fused in Sarcoma (FUS) protein. There is also a genetic link, since *FUS* mutations cause ALS with FUS pathology. FUS is a DNA/RNA-binding protein known to regulate different steps of RNA metabolism, however, its exact function and target genes in neurons were unknown.

In this study, I evaluated the neuronal role of FUS in alternative splicing using a candidate approach focusing on the microtubule-associated protein TAU. TAU is one of the most widely studied proteins in neurodegeneration research due to its aggregation in different tauopathies, most notably AD. Mutations in the TAU gene *MAPT*, that affect alternative splicing of exon 10, are known to cause another subtype of FTD. Here, I demonstrate that FUS depleted rat neurons, although having normal viability, show aberrant alternative splicing of TAU, with increased inclusion of exon 3 and exon 10, resulting in higher expression of the 2N and 4R TAU isoforms. Importantly, reintroduction of human FUS rescues aberrant splicing of TAU in FUS depleted neurons. Accordingly, overexpression of FUS decreases expression of 2N and 4R TAU isoforms. In mouse brain lysates, I detected direct FUS binding to TAU pre-mRNA, with strong binding around the regulated exon 10, often at AUU-rich RNA stretches. Since TAU splicing is regulated differently in humans and rodents, I also confirmed the role of human FUS in TAU exon 10 splicing using a TAU minigene and a human neuronal cell line. In addition, I analyzed the morphology and development of axons to evaluate the functional consequences of FUS depletion in neurons. Although FUS depleted neurons develop neurites normally, their axons are significantly shorter than in the control cells. Similar to observations in TAU/MAP1B knockout neurons, axons of FUS depleted

neurons develop significantly larger growth cones with abnormal cytoskeletal organization. The development of growth cones *in vivo* is an essential step in axonal maintenance and repair.

Altogether, this study identified TAU as the first physiological splice target of FUS in neurons. The newly discovered role of FUS in regulating the axonal cytoskeleton indicates that aberrant axonal function could contribute to the neuron loss seen in ALS/FTD cases with FUS aggregates.

Zusammenfassung

Patienten mit neurodegenerativen Erkrankungen können an kognitivem Abbau und/oder motorische Störungen leiden, je nachdem welche Gehirnregion von dem Verlust von Neuronen betroffen ist. Da sich das Risiko einer neurodegenerativen Erkrankung mit zunehmendem Alter drastisch erhöht und wir eine Gesellschaft mit steigender Lebenserwartung haben, ist es dringend notwending, neue wirksame Behandlungsmethoden zu entwickeln, um die Situation, mit der sich Patienten, ihre Familien und die Gesellschaft konfrontiert sehen, zu erleichtern. Obwohl sich verschiedene neurodegenerative Erkrankungen wie die Alzheimer-Erkrankung (AD), Amyotrophe Lateralsklerose (ALS) oder Frontotemporale Demenz (FTD) klinisch unterscheiden, gibt es gemeinsame Pathomechanismen, wie Proteinaggregation und Störungen im RNA-Metabolismus. Bei einem Teil der ALS und FTD Patienten beobachtet man Ablagerungen aus aggregiertem Fused in Sarcoma (FUS) Protein. Des Weiteren verursachen *FUS* Mutationen ALS mit FUS neuronalen Aggregaten. FUS ist ein DNA/RNA-bindendes Protein, das verschiedene Schritte des RNA-Metabolismus reguliert. Die genaue Funktion von FUS und seine Zielgene in Neuronen waren jedoch bisher unbekannt.

In dieser Studie habe ich die Funktion von FUS auf neuronales alternatives Spleißen mit einem Kandidaten-Ansatz untersucht, und mich insbesondere auf das Mikrotubuli-bindende Protein TAU fokussiert. Tau ist eines der bekanntesten Proteine in der Demenzforschung, da TAU Aggregate in verschiedenen sogenannten Tauopathien, insbesondere AD, gefunden wurden. Mutationen im TAU Gen *MAPT*, die das alternative Spleißen von TAU Exon 10 beeinflussen, können einen anderen Subtyp der FTD verursachen. Diese Studie zeigt, dass die Herunterregulierung (*Gen-Knockdown*) von FUS in murinen Neuronen das Überleben der Neuronen nicht beeinträchtigt, aber zu verändertem alternativen Spleißen von TAU mit einem erhöhten Einschluss von Exon 3 und Exon 10 führt und somit eine höhere Expression von den 2N und 4R TAU Isoformen verursacht. Eine wichtige Beobachtung dieser Studie war auch, dass die Expression von humanem FUS in FUS *knockdown* Neuronen aberrantes TAU Spleißen korrigieren kann. Dementsprechend führte auch die alleinige Überexpression von FUS zu einer verminderten Expression von 2N und 4R TAU. In Lysaten von Mausgehirnen konnte ich eine direkte Interaktion zwischen FUS und TAU RNA nachweisen, und zwar mit

bevorzugter FUS Bindung nahe am regulierten TAU Exon 10 und oft an AUU-reichen RNA-Abschnitten. Da das Spleißen von TAU in Menschen und Nagetieren unterschiedlich reguliert wird, bestätigte ich mit sowohl einer menschlichen neuronalen Zelllinie als auch einem TAU-Minigen Konstrukt die Rolle von humanem FUS in TAU Exon 10 Spleißen. Um die funktionalen Konsequenzen von FUS *knockdown* in Neuronen zu bewerten, analysierte ich die Morphologie und Entwicklung der Axone. Obwohl Neuronen mit FUS *knockdown* normalen Neuriten bilden, sind ihre Axone deutlich kürzer als die der Kontroll-Neuronen. Wie auch schon in TAU/MAP1B *knockout* Neuronen beobachtet wurde, entwickeln FUS *knockdown* Neuronen Axone mit einem deutlich größeren Wachstumskegel und abnormer Zytoskelett-Organisation. Die dynamische Bildung axonaler Wachstumskegel ist ein wesentlicher Schritt in der axonalen Aufrechterhaltung und Reparatur *in vivo*.

Insgesamt konnte diese Studie TAU als erstes physiologisches *splice* Zielgen von FUS in Neuronen identifizieren. Die neu entdeckte Funktion von FUS bei der Regulation des axonalen Zytoskelettes spricht für eine mögliche Rolle der veränderten axonalen Funktion beim Verlust von Neuronen in ALS/FTD Fällen mit FUS Aggregaten.

.

Table of Contents

List of Figures

List of Abbreviations

µm	micrometer
A	adenine
AD	Alzheimer's disease
ADNP	activity-dependent neuroprotective protein
aFTLD-U	atypical frototemporal lobar degeneration with ubiquitin pathology
AGD	argyrophilic grain disease
ALS	amyotrophic lateral sclerosis
ANOVA	analysis of variance
APS	ammonium persulfate
BAC	bacterial artificial chromosome
bFGF	basic fibroblast growth factor
BIBD	basophilic inclusions body disease
bvFTD	behavioral variant frontotemporal dementia
C	cytosine
C. elegans	Caenorhabditis elegans
CBD	corticobasal degeneration
CHMP2B	charged multivesicular body protein 2b
CLIP	UV crosslinking and immunoprecipitation
CLK1	cdc2-like kinases
CNS	central nervous system
CSF	cerebral spinal fluid
CT	computed tomography
D. melanogaster	Drosophila melanogaster
dcAMP	dibutyril cyclic adenosine monophosphate
DIV	days in vitro
DNA	deoxyribonucleic acid
DSCAM	down syndrome cell adhesion molecule
E. coli	Escherichia coli
e.g.	exempli gratia
E18	embryonic day 18
ET	essential tremor
EWS	Ewing sarcoma protein
FDA	food and drug administration
FTD	frontotemporal dementia
FTLD	frototemporal lobar degeneration
FUS	Fused in sarcoma
G	guanine
GAPDH	glyceraldehyde-3-phosphate dehydrogenase
GDB	gelatin dilution buffer
GDNF	glial cell-derived neurotrophic factor
GFP	green fluorescent protein
GST	glutathione s-transferase
GWAS	genome wide association study
HA	hemagglutinin
HD	Huntington's disease
HDAC1	histone deacetylase 1 protein
HEK cells	human embryonic kidney cells

IP	immunoprecipitation
IT	*in vitro* transcription
kDa	kilodalton
KO	knock-out
LB	lysogeny broth medium
LTR	long terminal repeat
MAPT	microtubule-associated protein TAU gene
Meg3	maternally expressed gene 3
min.	minute
MRI	magnetic resonance imaging
mRNA	messenger ribonucleic acid
N6	random hexanucleotides
NCI	neuronal cytoplasmic inclusions
NEAT1	Nuclear paraspeckle assembly transcript 1
NFT	neurofibrillary tangles
NIFID	neuronal intermediate filament inclusion disease
NII	neuronal intranuclear inclusions
NLS	nuclear localization signal
NMDAR	N-methyl-D-aspartate receptor
NMJ	neuromuscular junction
NRC	N-methyl-D-aspartate receptor NMDAR multiprotein complex
NTNG1	Netrin-G1
PCR	polymerase chain reaction
PD	Parkinson's disease
PDL	poly-D-lysine
PET	positron emission tomography
PFA	paraformaldehyde
PGRN	Progranulin
PHF	paired helical filaments
PiD	Pick's disease
PLL	poly-L-lysine
PNFA	progressive non-fluent aphasia
PPA	primary progressive aphasia
PSP	progressive supranuclear palsy
PY-NLS	proline-tyrosine nuclear localization signal
RGG	arginine-glycine-glycine
RNA	ribonucleic acid
RRM	RNA recognition motif
RT-qPCR	reverse transcription and quantitative polymerase chain reaction
SD	semantic dementia
SDS-PAGE	sodium dodecyl sulfate polyacrylamide gel electrophoresis
shRNA	short hairpin RNA
SMA	spinal muscular atrophy
SMN 1	Survival of motor neuron 1
SOD1	Superoxide dismutase 1
SR protein	serine-arginine protein
SSRIs	selective serotonin reuptake inhibitors
SYGQ	serine-tyrosine-glycine-glutamine
T	thymine
TAF-15	TATA box binding protein (TBP)-associated factor 68 kDa

TDP-43	transactive response DNA binding protein 43 kDa
TEMED	tetramethylethylendiamin
TLS	translocated in liposarcoma
U	uracil
Ub	Ubiquitin
UBQLN2	Ubiquilin2
UPS	ubiquitin-proteasome system
UV	ultraviolet light
VCP	Valosin-containing protein
WT	wildtype
XTT	(2,3-Bis(2-methoxy-4-nitro-5-sulfophenyl)-5-((phenylamino)carbonyl)-2H-tetrazoliumhydroxid)

1. Introduction

1.1. Neurodegenerative diseases

Neurodegenerative diseases are caused by the chronic and progressive loss of neurons (neurodegeneration) in the central and peripheral nervous system, which leads to impaired cognitive function (dementia), movement dysfunction or both. Currently 35.6 million people are estimated to suffer from dementia worldwide (WHO, 2012), with aging being the most important risk factor (Bertram & Tanzi, 2005). Without a preventive or curative treatment, predictions estimate this number could double every 20 years, reaching 81 million by 2040 (Ferri et al, 2005). The worldwide increase in life expectancy and the progressive nature of neurodegenerative diseases underscore the alarming situation (CDC, 2003; Trojanowski, 2008).

Scientific research has responded to the pressing public health problem with huge progress achieved by applying the tools of modern molecular biology and genetics. The identification of disease-associated gene mutations has revealed the cellular processes affected and has directed the efforts towards causal therapies for Alzheimer's disease (AD), amyotrophic lateral sclerosis (ALS) and other dementias. Some of the common cellular processes affected are proteosomal degradation, RNA metabolism, and aggregation of misfolded proteins (Bai et al, 2013; Ross & Poirier, 2004; Thomas et al, 2013). It is still unclear if the protein aggregation, observed in virtually all neurodegenerative diseases, acts as a disease causing agent, a protective agent, or an innocent bystander (Ross & Poirier, 2004; Taylor et al, 2002).

The existence of underlying common mechanisms in neurodegenerative diseases opens up the possibility of expanding our understanding from one disease to the others (Ross & Poirier, 2004). In order to establish such links, an adequate classification based on symptoms, pathology, and genetics is required. The focus of my thesis is the molecular parallels between two related neurodegenerative diseases: ALS and frontotemporal lobar degeneration (FTLD). I will provide an overview of ALS and FTLD, including their classification and a current understanding of the pathomechanisms. This overview also introduces the questions that are experimentally addressed in this study.

1.2. Amyotrophic lateral sclerosis - ALS

Amyotrophic lateral sclerosis (ALS), also known as Charcot disease or Lou Gehrig's disease, is a fatal neurodegenerative disease that affects both upper and lower motor neurons (Cleveland & Rothstein, 2001; Kiernan et al, 2011). Upper motor neurons are located in the motor cortex (Brodmann area 4) and extend their long axons along the spinal cord. They communicate with the lower motor neurons in the spinal cord via the neurotrasmitter glutamate. In turn, they transmit information to muscles primarily with the neurotransmitter acetylcholine (ACh) at the neuromuscular junction (NMJ) (Nishimaru et al, 2005).

ALS is one of the most common neuromuscular diseases worldwide with an incidence rate of 2.08 in 100,000 and a prevalence of 5.40 in 100,000 (Chiò et al, 2013). It affects all races and ethnic backgrounds equally, except for the Guam Island in the South Pacific, which shows a higher incidence of disease (ALS-Guam variant). Although the cause for this is still unknown, genetic and environmental factors unique to the indigenous Chamorro population have been proposed (Steele & McGeer, 2008).

Early symptoms may vary among patients and can include muscle weakness, spasticity (stiffness) or fasciculations (muscle twitches). Other patients present initial symptoms of dysarthria or dysphagia (difficulties in forming words or swallowing, respectively). A characteristic feature of ALS patients is hyperreflexia without sensory disturbance (Kinsley et al, 2001; NINDS, 2013). Regardless of the type of initial symptom, muscle atrophy and weakness spread progressively in the body, eventually preventing voluntary control of arms and legs (Figure 1A). At late stages of ALS respiratory muscles also succumb to this disease, increasing the risk of pneumonia. Respiratory failure is the primary cause of death in ALS and typically occurs within 2 to 10 years after disease onset.

ALS is diagnosed based on a combination of physical examination and neurologic tests including electromyography (EMG) and nerve conduction velocity (NCV) test. Differential diagnosis excludes other conditions with ALS-resembling symptoms such as spinal muscular atrophy (SMA), multiple sclerosis (MS), and spinal cord tumors.

The vast majority (about 90%) of ALS patients shows no clear history of neurodegenerative disease in the family and is thus classified as sporadic cases. In contrast, about 10% of patients are affected by familial ALS (Ling et al, 2013). The

occurrence of recessive inherited mutations, missing familial medical history, and paternity issues hinder, however, correct classification between sporadic and familial cases. Although familial cases tend to have earlier disease onset (46 years) than sporadic cases (56 years), they are virtually indistinguishable in terms of symptoms and disease course. The juvenile form of familial ALS has a remarkably early age of onset before 25 years (Aggarwal & Shashiraj, 2006).

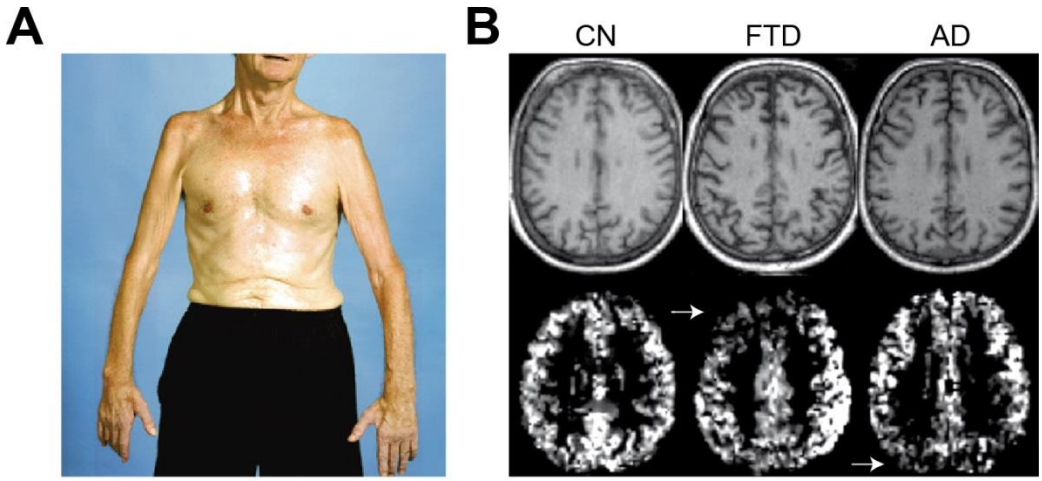

Figure 1 Clinical presentation of amyotrophic lateral sclerosis and frontotemporal dementia

(A) Amyotrophic lateral sclerosis (ALS) patients present symmetrical upper limb wasting. Note also the ALS typical feature of a "split-hand", which is caused by disproportionate wasting of the hand muscles. Adapted from: (Kiernan et al, 2011). **(B)** Frontotemporal dementia (FTD) patients show reduced perfusion in frontal brain regions (arrow, middle panel) compared to a cognitive normal (CN) individual and an Alzheimer disease patient (AD). In contrast, AD patients show diminished perfusion in the posterior region of the brain (arrow, right panel) in comparison to CN individual and FTD patient. This is visualized here by structural and arterial spin labeling magnetic resonance perfusion images after partial volume corrections. Adapted from:(Du et al, 2006).

Treatment opportunities for ALS patients are very limited and the lack of specific reliable biomarkers hinders the development of treatments. The only FDA approved drug available for ALS is Riluzole (Rilutek, Sanofi-Aventis), which appears to protect neurons from glutamate excitotoxicity either by blocking receptors or by stimulating glutamate uptake. Riluzole prolongs survival of patients by several months and delays the need for mechanical ventilation. Symptomatic treatment aims to reduce pain, cramps, fatigue, and excess saliva. As normal cognitive functions are often sustained in ALS patients, the progressive deterioration of health can cause depression. Overall, a multidisciplinary team of physicians, physiotherapists, and nutritionists is recommended to support the patients and caregivers.

1.3. Frontotemporal lobar degeneration - FTLD

Frontotemporal lobar degeneration (FTLD) is the pathological entity underlying a group of diseases classified by the umbrella term of frontotemporal dementia (FTD). In the following sections the term FTLD is used to designate both disease and pathology. FTLD, as indicated in the name, is characterized by specific degeneration of the frontal and temporal cortex, brain areas that usually control emotional and social behavior. As a consequence, FTLD patients typically suffer from difficulties in controlling emotions, speech/language dysfunction and changes in social behavior, while memory, perception and spatial skills are generally preserved.

FTLD is the second most common dementia after AD in the presenile group (<65 years) with an incidence of 3.5 - 4.1 per 100,000/year and a prevalence of 10-20 per 100,000 (van Langenhove et al, 2012). The typical age of onset is around 60 years and the life expectancy after diagnosis ranges from 2-10 years (Bird et al, 2003; Hsiung & Feldman, 2013). FTLD is a rapidly progressing disease and patients eventually require full-time care. The combination of disease onset at presenile age and a rapid progression of disease results in a devastating emotional and financial situation for the patients and families. Interestingly, in comparison to other neurodegenerative diseases, FTLD has a strong genetic component with about 50% familial and 50% sporadic cases (Rademakers et al, 2012; Rohrer et al, 2009).

Depending on the main symptom FTLD is subdivided in three different variants: behavioral variant (bvFTD), primary progressive aphasia (PPA), and variant with combined dementia and movement disorders. The most common variant is bvFTD, which results in patients suffering from progressive deterioration of behavior and diminished executive functions. Some examples include impulsive actions, apathy, repetitive movements, and dietary changes (overeating) (Rascovsky et al, 2011). Primary progressive aphasia (PPA) is the second most common clinical variant. PPA patients have difficulties in word naming or word comprehension, and are eventually unable to communicate and become mute. PPA cases are further subclassified as progressive non-fluent aphasia (PNFA) or semantic dementia (SD) based on clinical features and neuroimaging techniques (Gorno-Tempini et al, 2011). PNFA is characterized by patients showing apraxia of speech and impaired comprehension of complex sentences. Object knowledge or single-word comprehension is, however, unaffected. In contrast, SD is characterized by impaired single-word comprehension and recognition of objects or

familiar faces, while speech production is spared. In FTLD with movement disorders, patients present dementia and bradykinesia (slow movement), akinesia (no movement), or limb dystonia often causing postural disequilibrium (Hsiung & Feldman, 2013). Eventually patients lose the ability to walk. The accompanying movement disorder can manifest early on or it may develop with the disease. Importantly, the current classification is not definite as there is also significant overlap between variants (Seeley et al, 2005). It has been reported, for example, that the vast majority of bvFTD patients with *GRN* mutations eventually develop language problems (Josephs, 2007).

The clinical variants are diagnosed based on clinical features and neuroimaging findings from magnetic resonance imaging (MRI), computed tomography (CT), or positron emission tomography (PET). CT and MRI typically show asymmetric atrophy in frontal and/or temporal regions of FTLD patients (Figure 1B). Differential diagnosis excludes AD or psychiatric conditions such as depression or psychosis, which result in similar unusual behavior. A definite diagnosis is only possible with postmortem neuropathological evidence or if a disease causing mutation is detected.

There is currently no cure for FTLD, but symptomatic treatment is available for behavioral symptoms. Selective serotonin reuptake inhibitors (SSRIs), for example, are used to control compulsive behaviors. Although there is no FTLD specific biomarker available, TAU and Progranulin protein levels in the cerebral spinal fluid (CSF) are useful monitoring tools. Caregivers also need training and psychological support due to the difficulties in managing the behavioral changes of some patients.

1.4. ALS-FTLD disease spectrum

1.4.1. Clinical overlap

In ALS cases cognition and memory are usually not affected, however, about 5-20% of cases present symptoms related to FTD (Kinsley et al, 2001; Ringholz et al, 2005). Similarly, 14% of FTD patients also meet the criteria for ALS (Lomen-Hoerth et al, 2002) (Figure 2). Cases with overlapping clinical presentation of ALS symptoms and FTLD symptoms are classified as ALS-FTD.

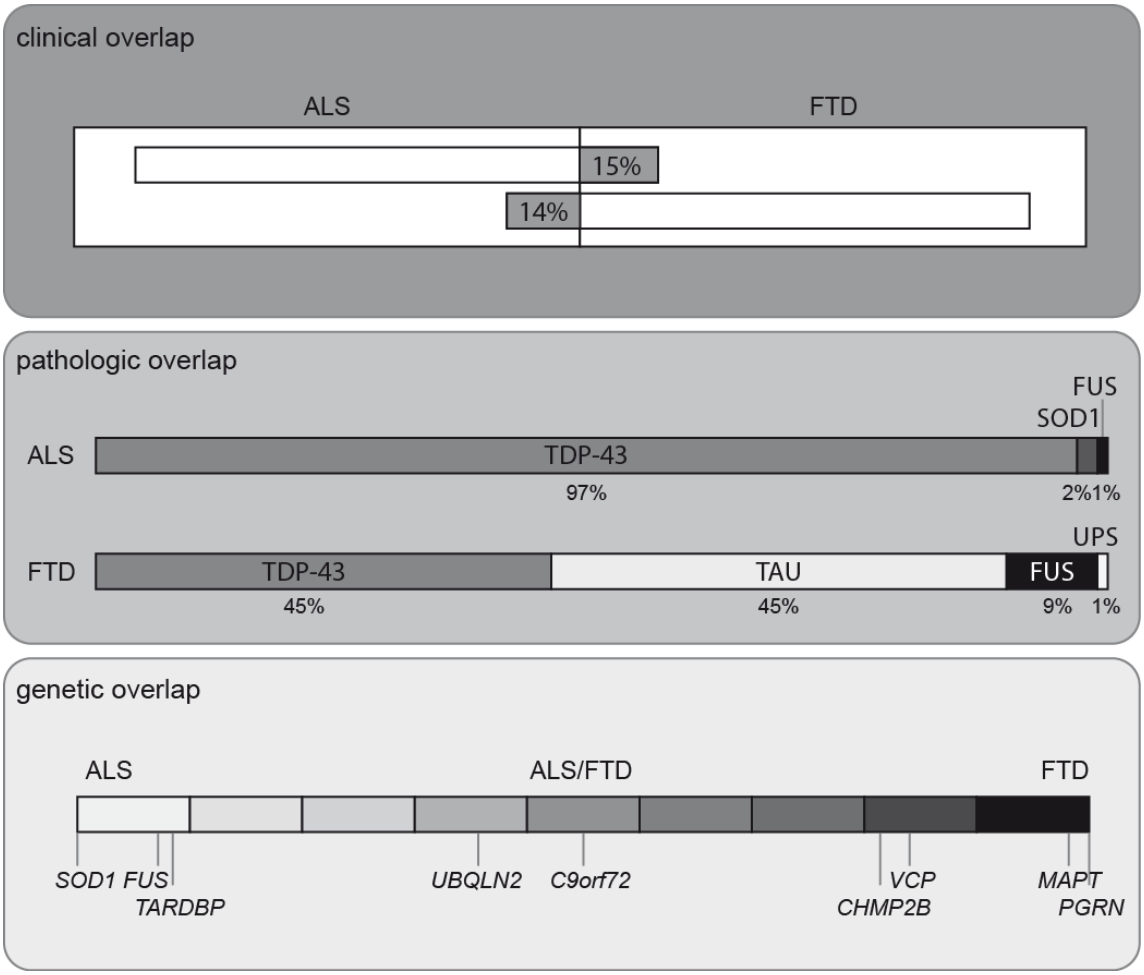

Figure 2 Overview on clinical, pathological and genetic overlap between ALS and FTLD

Clinical overlap: The scheme presents the clinical overlap between ALS and FTD, and denotes the percentage of ALS cases with significant FTD symptoms and vice versa. **Pathologic overlap:** The frequencies of the different pathological subtypes are depicted according to protein deposited. Note that the pathology is usually mutually exclusive so that the main aggregating protein defines the classification. Note also that TDP-43 and FUS pathology is observed in ALS and FTD subtypes. **Genetic overlap:** The spectrum is presented as a gradient between pure ALS and pure FTD. The major genes are plotted along the gradient according to the disease caused by mutations. Mutations in *SOD1* or *GRN* cause pure ALS or FTD respectively, while mutation in *C9orf72* can cause ALS or FTD. Adapted partially from: (Al-Chalabi et al, 2012; Ling et al, 2013).

1.4.2. Molecular pathology of ALS and FTLD

In the last decade, tremendous progress has been made in ALS and FTLD research, with new disease causing mutations, new histological markers for classification, and new risk factor genes being discovered every year. This poses a challenge in updating the classification scheme of the diseases. The table presented here corresponds to a summary of the latest classifications available (Figure 3) (Bahia et al, 2013; Dormann & Haass, 2013; Ling et al, 2013; Rademakers et al, 2012; Sieben et al, 2012; Thomas et al, 2013). In stark contrast to AD, where amyloid-beta pathology co-occurs with TAU pathology,

the aggregating marker proteins of ALS or FTLD subtypes are usually mutually exclusive and are used to classify the different subtypes. In ALS, the main aggregating proteins are either transactive response DNA binding protein 43 kDa (TDP-43) (97%), SOD1 (2%) or FUS (1%) (Ling et al, 2013) (Figure 2). The major ALS subtypes are termed accordingly: ALS-TDP, ALS-SOD1 and ALS-FUS (Figure 3). In FTLD, the most common neuropathologic findings are either aggregated TAU (45%) or aggregated TDP-43 (45%) (Ling et al, 2013). Additionally, about 9% of the cases show aggregated FUS as the pathologic hallmark (Ling et al, 2013) (Figure 2). FUS pathology is observed in the vast majority of TDP-43 and TAU negative cases, thus constituting an important subtype of FTLD (Urwin et al, 2010b). The remaining 1% of cases (TDP-43, TAU and FUS negative) are positive for markers of the ubiquitin-proteasome system (UPS). Analogous to ALS, the major FTLD subtypes are classified accordingly as: FTLD-TAU, FTLD-TDP, FTLD-FUS or FTLD-UPS (Figure 3). Importantly, there is no perfect correlation between the histopathological and the clinical variants. Thus each pathology subtype can be associated with any clinical variant, however, with somewhat different frequencies (Sieben et al, 2012; Van Langenhove et al, 2013). There is, therefore, a growing notion that the anatomical distribution of degeneration rather than the type of pathology define the symptoms (Morrison & Hof, 1997; Skovronsky et al, 2006). Similar to the selective vulnerability found in ALS for motor neurons, in FTD (bvFTD), a selective vulnerability has been proposed for spindle neurons or von Economo neurons (VENs) located in the anterior cingulate cortex (ACC) (Santillo et al, 2013; Seeley, 2008). Early bvFTD seems to affect focally the ACC, in contrast to AD, where it is spared (Seeley, 2008). The exact mechanism behind this selective vulnerability remains, however, unknown.

1.4.3. Pathomechanism behind major ALS and FTLD subtypes

This thesis focuses on the molecular link between FUS and TAU and the consequences for ALS and FTLD. In order to provide an appropriate context to this link, the major ALS and FTLD subtypes are discussed first, including their genetic components and potential molecular pathomechanisms.

1.4.3.1. ALS-TDP and FTLD-TDP

TDP-43 pathology is observed in all major neurodegenerative diseases including AD (Amador-Ortiz et al, 2007), Huntington's disease (HD) (Schwab et al, 2008) and Parkinson's disease (PD) (Lattante et al, 2013; Nakashima-Yasuda et al, 2007). In ALS-TDP, TDP-43 pathology is mainly found in spinal cord and cortex (Arai et al, 2006;

Lattante et al, 2013; Neumann et al, 2006). In FTLD-TDP, TDP-43 pathology is observed in various cortical layers and TDP-43 positive inclusions can be detected in the nucleus or cytoplasm of affected neurons (Mackenzie et al, 2011b). Biochemical characteristics of TDP-43 aggregates in both ALS and FTLD include hyperphosphorylation, truncation, and cytoplasmic localization accompanied with a nuclear clearance of TDP-43 (Lee et al, 2012; Ling et al, 2013).

TDP-43 is a multifunctional DNA/RNA-binding protein involved in different steps of RNA metabolism (Buratti & Baralle, 2008; Buratti & Baralle, 2010; Lagier-Tourenne et al, 2010); including transcription, alternative splicing and transport of RNA (Polymenidou et al, 2011; Tollervey et al, 2011). Additionally, TPD-43 may be involved in microRNA biogenesis (Kawahara & Mieda-Sato, 2012).

Heterozygous mutations in *GRN* cause autosomal dominant FTLD-TDP, while mutations in *C9orf72*, *VCP*, *UBQLN2* or the TDP-43 coding gene *TARDBP* can cause familial ALS-TDP or FTLD-TDP (Figure 3). *GRN* mutations were first described in 2006, solving the mystery of TAU negative familial cases with a strong genetic linkage to chromosome 17q21. Currently 69 *GRN* mutations have been identified in 231 families and all mutations are considered loss of function because they result in haploinsufficency ((Cruts et al, 2012), http://www.molgen.vib-ua.be/FTDMutations). *GRN* codes for the Progranulin protein, which is ubiquitously expressed and proteolytically processed to 7.5 Granulin peptides. In the CNS, Progranulin functions as a neurotrophic factor with an important role in neurite survival and outgrowth. Progranulin also functions in inflammation and wound repair, where it antagonizes the Granulins function (Eriksen & Mackenzie, 2008).

The recently discovered mutations in the uncharacterized *C9orf72* gene are now considered the major genetic cause for both FTLD-TDP and ALS-TDP (DeJesus-Hernandez et al, 2011; Gijselinck et al, 2012; Renton et al, 2011). The *C9orf72* gene of healthy individuals contains only 3 to 25 GGGGCC repeats in the first intron. In ALS-FTLD patients with *C9orf72* mutations, the gene contains a massive expansion of 700-1,600 GGGGCC repeats (DeJesus-Hernandez et al, 2011). The C9orf72 protein is ubiquitously expressed but its function is still unknown.

The massive repeat expansion leads to a reduction of expression, which indicates a possible loss of function component in the disease (Belzil et al, 2013; Ciura et al, 2013;

DeJesus-Hernandez et al, 2011; Mori et al, 2013b). However, alternative mechanisms are also being investigated, such as non-ATG translation of the repeat and RNA toxic gain-of-function (Ling et al, 2013; Mori et al, 2013a; Mori et al, 2013b).

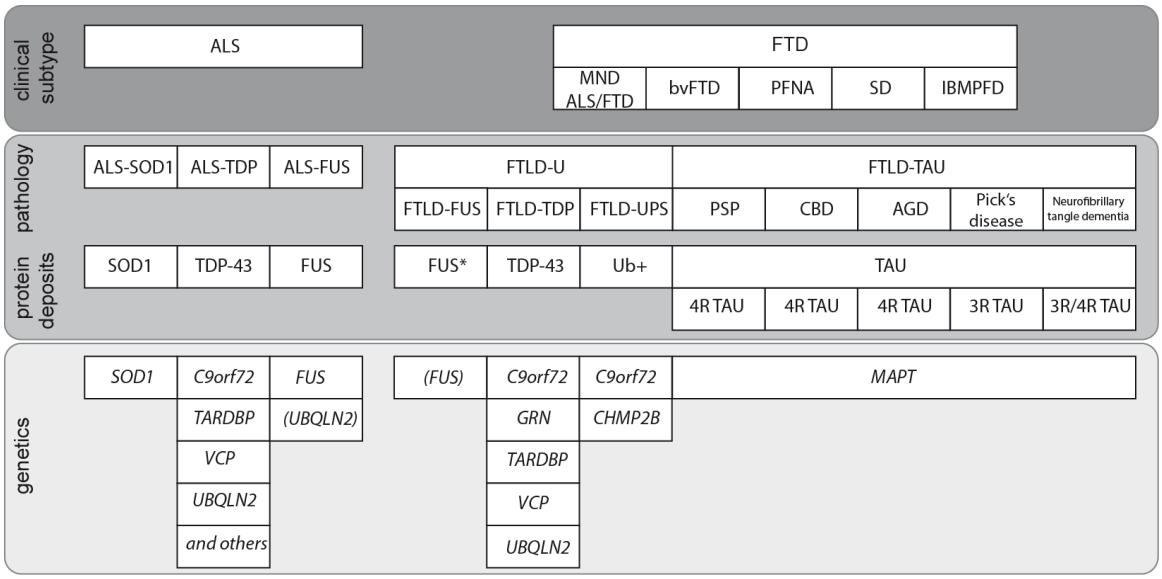

Figure 3 Clinical, pathological and genetic classification of ALS and FTD

Clinics: Based on the symptoms, FTD can be diagnosed as: FTD with motor neuron disease (MND, ALS/FTD); behavioral variant FTD (bvFTD); semantic dementia (SD) or progressive nonfluent aphasia (PFNA). The proximal muscle weakness disease inclusion body myopathy with Paget's disease of bone (IBMPPD) is caused by mutations in the *VCP* gene. The classification presented here is not absolute, since significant overlap is seen between clinical variants. **Pathology:** According to the aggregated protein, ALS is classified as ALS-SOD1, ALS-TDP or ALS-FUS with SOD1, TDP-43 or FUS protein deposits, respectively. In FTLD, cases are divided as FTLD-TAU with TAU protein deposits or as FTLD-U with ubiquitin (Ub) positive aggregates. The subdivision of FTLD-TAU cases (also called tauopathies) as progressive supranuclear palsy (PSP), argyrophilic grain disease (AGD), Pick's disease or neurofibrillary tangle dementia is based on the nature and location of TAU aggregates. In the case of PSP, CBD and AGD, the aggregates consist mainly of the 4R TAU isoform. In contrast, Pick's disease is characterized by aggregates consisting of 3R TAU. In neurofibrillary tangle dementia, both isoforms 3R and 4R are present in aggregates. FTLD-U cases are subdivided as FTLD-FUS, FTLD-TDP or FTLD-UPS when the aggregates are positive for FUS, TDP-43 or markers of the ubiquitin-proteasome system (UPS), respectively. *Note that in FTLD-FUS the related proteins TAF-15 and EWS also co-aggregate, which contrasts the sole aggregation of FUS in ALS-FUS. **Genetics:** ALS causing mutations have been found in the *SOD1*, *TARDBP* (coding for TDP-43) and *FUS* genes. Mutations associated with TDP-43 pathology have also been found in *C9orf72*, *UBQLN2*, *VCP*, and other genes. Rare mutations in *UBQLN2* are associated to ALS with TDP-43 and FUS pathology. FTLD-TAU cases are usually linked to mutations in the *MAPT* gene, coding for TAU. FTLD-TDP pathology is associated with mutations in *GRN*, *C9orf72*, *VCP*, *UBQLN2*, or in rare cases *TARDBP*. FTLD-U cases are associated with mutations in *C9orf72* or *CHMP2B*. Only rare cases of mutations in *FUS* have been reported to cause FTLD-FUS, thus most cases are currently classified as sporadic cases. Despite the significant genetic component, in FTD and less in ALS, many sporadic cases remain to be resolved. Note that the size of the boxes is not proportional to the relative incidence. Adapted from: (Bahia et al, 2013; Dormann & Haass, 2013; Ling et al, 2013; Rademakers et al, 2012; Sieben et al, 2012; Thomas et al, 2013; Van Langenhove et al, 2010)

Mutations in the *TARDBP* gene are usually associated with pure ALS (Figure 2). However, mutation carrier families can have members affected by FTD, ALS or a combination of both (Al-Chalabi et al, 2012). Up to now, more than 40 mutations have been identified and the majority cluster around the C-terminal glycine-rich region, which functions in alternative splicing and mediates protein-protein interactions (Al-Chalabi et al, 2012; Lagier-Tourenne et al, 2010; Renton et al, 2014).

Additionally, rare mutations in *VCP* have also been implicated in ALS-TDP and FTLD-TDP (Johnson et al, 2010; Neumann et al, 2007). Previously, *VCP* mutations were known to cause inclusion body myositis and Paget's disease of bone (IBMPFD) (Watts et al, 2004). *VCP* codes for the valosin containing protein (VCP), which is an ATPase that interacts with ubiquitinated proteins and functions in protein clearance pathway, autophagy, and protein sorting (Ling et al, 2013). Therefore, mutations are thought to disturb the ubiquitin dependent proteasomal degradation. Also *Ubqln-2* mutations that impair protein degradation and autophagy regulated by the Ubiquilin-2 protein are associated with ALS and FTLD. Curiously, Ubiquilin 2 pathology may be accompanied by TDP-43 and FUS pathology (Deng et al, 2011; Ling et al, 2013; Williams et al, 2012). In summary, mutations in genes involved in diverse pathways as RNA metabolism and protein degradation can cause ALS or FTLD with TDP pathology.

1.4.3.2. ALS-FUS and FTLD-FUS

In ALS-FUS cases, severe motor neuron loss is observed in the spinal cord and to a lesser extend in the brain stem (Al-Chalabi et al, 2012). Histopathologically, FUS is found mislocalized to the cytoplasmic compartment and aggregates are found in both neurons and glia cells (Kwiatkowski et al, 2009; Tateishi et al, 2010; Vance et al, 2009) (Figure 4A). Two different types of pathology are observed depending on the severity of the disease. Neuronal basophilic inclusions and round aggregates in the cytoplasm are typical for early-onset ALS. In late-onset ALS, tangle-like FUS inclusions are found in both neurons and glia (Ling et al, 2013). Also in FTLD-FUS, FUS pathology is observed in both neurons and glia cells (Mackenzie et al, 2011a; Neumann et al, 2009a) (Figure 4A). The location and morphology of the inclusions define the three pathology subtypes: atypical FTLD-U (aFTLD-U), basophilic inclusions body disease (BIBD), and neuronal intermediate filament inclusion disease (NIFID) (Lashley et al, 2011; Mackenzie et al, 2011a; Munoz et al, 2009; Neumann et al, 2009b; Sieben et al, 2012). aFTLD-U is the most common FTLD-FUS subtype and is associated with early onset disease (40-50 years

of age) with a mean duration of disease of about 7 years (Lashley et al, 2011). aFLTD-U cases show neuropathologically severe atrophy in the caudate nucleus and the frontotemporal cortex. FUS inclusions can be either compact oval shaped neuronal cytoplasmic inclusions (NCI) or vermiform neuronal intranuclear inclusions (NII) located in the neocortex, granule layer of the dentate gyrus and striatum, while the cerebral cortex is spared (Mackenzie et al, 2011a; Munoz et al, 2009). In BIBD, in contrast, basophilic NCI are found in the pontine nuclei, brain stem, cerebral and frontal cortex. BIBD is also typically found in early-onset disease (Sieben et al, 2012). The third subtype, NIFID, is characterized by FUS inclusions that are also positive for interfilaments, alpha-internexin, and neurofilaments (Neumann et al, 2009b). Asymmetric atrophy is additionally seen in the frontotemporal cortex and neostriatum (Sieben et al, 2012). In contrast to aFTLD-U, NIFID FUS inclusions are abundant in the CA1 layer, leaving the granular layer of the dentate gyrus largely spared. NIFID is often associated with bvFTD and has an age of onset between 40-60 years of age, with a rapid progression (3 years disease duration) (Sieben et al, 2012).

Interestingly, one key distinction between ALS-FUS and FTLD-FUS is the co-aggregation of the FET family members, Ewing sarcoma protein (EWS) and TATA-binding protein (TBP)-associated factor (TAF15 or TAFII68), present only in FTLD-FUS and not in ALS-FUS. Nuclear FUS aggregates have also been observed in HD (Doi et al, 2008) and spinocerebellar ataxias (Doi et al, 2010) cases without *FUS* mutations.

Mutations in the *FUS* gene are the main genetic cause for ALS-FUS, but in rare cases also *UBQLN2* mutations can cause ALS with Ubiquilin-2, TDP-43 and FUS pathology (Deng et al, 2011; Williams et al, 2012). ALS *FUS* mutations, considered loss of function mutations, usually cluster around the C-terminus or around the G-rich domain (Figure 4B). So far *FUS* mutations have been reported only in a few FTLD-FUS cases and their pathogenicity is still unclear. Thus, almost all FTLD-FUS cases are considered sporadic cases (Snowden et al, 2011; Van Langenhove et al, 2010). Although it is still under debate how exactly FUS mutations or aggregation cause neurodegeneration, multiple functions might be impaired, including regulation of transcription, genomic stability, microRNA biogenesis, mRNA transport, and alternative splicing.

1.4.3.3. ALS-SOD1

As discussed in a recent review, ALS and FTLD are related but different disorders (Dormann & Haass, 2013). Contrary to the neuropathological and genetic overlap seen with TDP-43 and FUS, *SOD1* or *TAU* mutations cause pure ALS or FTD, respectively (Figure 2). In ALS-SOD1, the main aggregating protein is the copper/zinc superoxide dismutase 1 (SOD1). Mutations in *SOD1* were first discovered in 1993 (Rosen et al, 1993) and, in contrast to TDP-43 or FUS mutations, *SOD1* mutations do not cluster in any specific gene region. The current understanding is that *SOD1* mutations cause a toxic gain of function, possibly by increasing the propensity to aggregate (Al-Chalabi et al, 2012).

1.4.3.4. FTLD-TAU

FTLD cases with TAU pathology are the major form of FTLD, apart from FTLD-U cases, and are further subclassified, among others, as Pick's disease (PiD), corticobasal degeneration (CBD), progressive supranuclear palsy (PSP) or argyrophilic grain disease (AGD) (Bahia et al, 2013; Lee et al, 2001), depending on the characteristics of the pathology and the aggregated TAU isoforms (Figure 3). These diseases belong to a wider class termed tauopathies, which are neurodegenerative diseases that show characteristic aggregation of hyperphosphorylated TAU in the somatodentritic compartment. TAU forms paired helical filaments (PHF) that can aggregate into insoluble neurofibrillary tangles (NFT) (Ballatore et al, 2007). NFTs are, together with amyloid-beta plaques, the pathological hallmark of AD, thus AD is the most common tauopathy (Ballatore et al, 2007).

Pick's disease is a tauopathy with characteristic TAU aggregates called Pick bodies and Pick cells, named after the Czech neurologist Arnold Pick, who made the initial observations of this characteristic pathology in 1892 (Pick, 1892). Pick bodies consist of predominantly 3R TAU isoform. This is in contrast to CBD, PSP and AGD, where the predominantly aggregated TAU isoform is the 4R isoform (Bahia et al, 2013). In AD, all TAU isoforms aggregate in apparently similar proportions. CBD is characterized by typical glial TAU pathology termed astrocytic plaques (Feany & Dickson, 1995; Lee et al, 2001). 4R TAU aggregates in CBD are found, among other regions, in the neocortex and subcortical white matter. In PSP, neuronal loss is found predominantly in the substantia nigra and the anterior thalamus. Lesions can also be found in the primary motor and premotor cortices. PSP is neuropathologically characterized by tufted

astrocytes and globose neurofibrillary tangles. Finally, AGD typically presents as the neuropathological hallmark hyperphosphorylated 4R TAU and often truncated TAU in so called pre-tangle neurons and in oligodendroglial cells (Ferrer et al, 2008).

Mutations in the TAU coding gene *MAPT* in chromosome 17q21 were the first mutations identified to cause a form of familial FTLD (Frontotemporal dementia and parkinsonism linked to chromosome 17 (FTDP-17)). Currently, 44 different mutations have been identified in 134 families. The most common mutations are P301L and the intronic mutation IVS10+16C>T (Rademakers et al, 2004). *MAPT* mutations typically cluster around exons 9-13, which code the microtubule binding domains (Figure 5). Mutations can cause altered binding to microtubules either by disturbing the balance between isoforms or by changing the binding properties of the protein. This has functional consequences in terms of neuronal plasticity, axonal transport and cytoskeleton dynamic stability (Ballatore et al, 2007).

1.4.3.5. FTLD-UPS

Finally, some FTLD cases remain unclassifiable because protein aggregates are negative for TAU, TDP-43 or FUS but positive for ubiquitin and p62, which label most aggregating proteins. These cases are termed ubiquitin-proteasome system positive cases or FTLD-UPS (Figure 3). Note that for the purpose of clarity the distinction is made here between FTLD-U and FTLD-UPS, with FTLD-U cases being all Ubiquitin positive and TAU negative cases that can be further divided into FTLD-TDP, FTLD-FUS and FTLD-UPS. Mutations in the charged multivesicular body protein 2B gene *CHMP2B* are linked to some cases of FTLD-UPS (Momeni et al, 2006; van der Zee et al, 2008) and ALS (Cox et al, 2010; Parkinson et al, 2006). CHMP2B is a core component of the endosomal sorting complexes required for transport-III (ESCRT-III), which regulates protein trafficking in the lysosomal degradation pathway. *CHMP2B* mutations are known to disrupt the endosome-lysosomal pathway, but the detailed pathomechanism is still unknown (Han et al, 2012; Urwin et al, 2010a).

1.4.4. Other genes, epigenetic and environmental risk factors related to ALS/FTLD

Curiously, other genes associated with rare cases of ALS and FTLD also have functions in either transport, cytoskeleton stability or in RNA metabolism. They include: *DCTN1*, a gene encoding a subunit of the dynactin transporter protein (Puls et al, 2003); *NEFH*, a gene encoding the heavy neurofilament unit (Al-Chalabi et al, 1999); *PRPH*, a gene encoding the type III intermediate filament peripherin (Leung et al, 2004); and *SMN1*,

encoding the survival motor neuron protein 1, which functions in RNA metabolism (Blauw et al, 2012).

Although some risk factors and susceptibility genes have recently been discovered, little is still known about their function in pathological and physiological context. In the case of FTLD, the *APOE* E2 allele is reported to be a risk factor (Verpillat et al, 2002), but not the E4 allele, which is usually associated with AD (Geschwind et al, 1998). ApoE transports lipoproteins and regulates the lipid metabolism in the brain. Also, a polymorphism in *TMEM106B* was identified in a genome wide association study (GWAS) as the strongest risk factor for FTLD-TDP (Van Deerlin et al, 2010; van der Zee et al, 2011). TMEM106B is a transmembrane protein that is primarily found in late endosomes and lysosomes (Brady et al, 2013; Chen-Plotkin et al, 2012; Lang et al, 2012). TMEM106B has been shown to control dendritic trafficking of lysosomes via its interaction with the microtubule associated protein MAP6 (Schwenk et al, 2013). The *MAPT* H1 haplotype is also considered a genetic risk for FTLD, because it is overrepresented in the group of 4R TAU disorders (Baker et al, 1999; Houlden et al, 2001; Sobrido et al, 2003).

The abundance of sporadic cases and the different age of onset among ALS and FTLD subtypes already point towards the influence of non-genetic factors on the disease progression. There are variations regarding type and severity of disease even between individuals carrying the same mutation. As in the case of *TARDBP* mutations, families carrying *C9orf72* mutations can have members suffering from ALS, FTLD, or a combination of ALS-FTLD (Gijselinck et al, 2012; Renton et al, 2011). Epigenetic and environmental factors could account for such differences and are being extensively studied (Jakovcevski & Akbarian, 2012; Morahan et al, 2009). Additionally, for ALS, elevated levels of glutamate in the nervous system have been proposed to be a risk factor (Rothstein et al, 1992; Shaw & Ince, 1997). One possible mechanism behind this is the selective vulnerability of motor neurons to glutamate mediated excitotoxicity due to their high expression of glutamate receptors (Kawahara & Kwak, 2005).

1.5. The role of FUS and TAU in disease

The pathological and genetic link between FUS or TAU and different subtypes of ALS or FTLD is now well-established. TAU is one of the most widely studied proteins in the field of neurodegeneration because of its pathological link to AD, FTLD and the

ALS/Parkinsonism-dementia (ALS-Guam variant). However, the exact role of FUS and TAU in disease onset or progression remains still unclear. In order to gain further insight into possible pathomechanisms, a more in depth study of protein structure, location, and physiological function is required.

1.5.1. FUS

1.5.1.1. FUS protein domain structure

The N-terminal part of FUS contains a region rich in glutamine, glycine, serine, and tyrosine (QGSY), and a glycine-rich region (G-rich). The N-terminal part of FUS acts as a transcriptional activation domain, which is responsible for the oncogenic potential of the FUS fusion proteins found in some sarcoma patients (Crozat et al, 1993; Prasad et al, 1994; Rabbitts et al, 1993; Zinszner et al, 1994). The QGSY domain confers aggregation propensity *in vitro* (Kato et al, 2012) and has been predicted to have prion-like properties (King et al, 2012). The C-terminal part of the protein mediates DNA/RNA-binding through a RNA recognition motif (RRM), two arginine-/glycine-rich regions (RGG), and a zinc finger domain (ZnF) (Iko et al, 2004; Lagier-Tourenne et al, 2010) (Figure 4B). Finally, FUS contains a proline-tyrosine nuclear localization signal (PY-NLS) at the C-terminus. This protein structure is common to the FET family of proteins including EWS and TAF15 (Tan & Manley, 2009).

1.5.1.2. FUS protein function

FUS binds single and double stranded DNA, regulates transcription and different stages of RNA metabolism (Lagier-Tourenne et al, 2010; Tan & Manley, 2009). FUS regulation of transcription involves, on the one hand, the direct binding to RNA polymerase II and regulation of its phosphorylation, which can affect general transcription and elongation (Schwartz et al, 2012; Yang et al, 2000). On the other hand, FUS can also regulate transcription of specific targets by binding to specific DNA sequences in the promoter region of target genes (Tan et al, 2012) or by binding to nuclear hormone receptors (Powers et al, 1998). The DNA binding function of FUS is generally associated with the role in transcription; however, it could also be important for the role of FUS in genomic stability (Hicks et al, 2000). FUS interaction with the histone deacetylase 1 protein (HDAC1) has been reported as crucial for FUS function in DNA damage response (Wang et al, 2013).

FUS regulation of transcription and RNA splicing could function simultaneously, since both processes are tightly interdependent (Das et al, 2007; Lagier-Tourenne et al, 2010; Reed, 2003).

FUS is also part of the spliceosome (Hartmuth et al, 2002; Rappsilber et al, 2002; Zhou et al, 2002), and upon loss of FUS almost 1,000 transcripts are affected in their abundance or splicing in the adult mouse brain (Lagier-Tourenne et al, 2012). FUS shuttles between nucleus and cytosol (Zinszner et al, 1997) and has been proposed to localize to dendrites in response to neuronal activation (Fujii et al, 2005). The Transportin 1 dependent FUS nuclear import is mediated through the PY-NLS and by its arginine-methylation (Dormann et al, 2012; Dormann et al, 2010; Tradewell et al, 2012). Additionally, FUS is phosphorylated, but the function of this post-translational modification remains largely unknown (Klint et al, 2004; Rappsilber et al, 2003). FUS can also regulate synaptic function probably through its role in RNA transport and local translation at the synapse where it is also part of the N-methyl-D-aspartate receptor NMDAR multiprotein complex (NRC) (Husi et al, 2000). One FUS target RNA transported along dendrites is the *Nd1-L* mRNA, which codes an actin-stabilizing protein (Fujii & Takumi, 2005).

In addition to the conserved protein domain structure, the FET family members also share various protein functions in DNA/RNA processing (Tan & Manley, 2009). They all have important functions both in the nucleus and in the cytoplasm, for example pre-mRNA splicing and mRNA transport, respectively (Law et al, 2006; Tan & Manley, 2009). Also their nuclear import is regulated by PY-NLS (Lee et al, 2006; Marko et al, 2012; Zakaryan & Gehring, 2006).

1.5.1.3. FUS animal models

Animal models have been generated to better understand FUS physiological function and to evaluate potential pathomechanisms behind ALS/FTD-FUS. Two FUS knockout mouse (KO) lines show quite different phenotypes (Hicks et al, 2000; Kuroda et al, 2000). Inbred KO mice die within a few hours postnatal, due to inability to suckle (Hicks et al, 2000) and outbred KO mice, although they do reach adulthood, show sterility in male mice (Kuroda et al, 2000). Both KO mouse lines show one common phenotype: genomic instability. Cells from inbred FUS KO mouse line showed an increased number of karyotypic aberrations (e.g. chromosome breakage) (Hicks et al, 2000) and the outbred FUS KO mice showed increased sensitivity to ionizing irradiation (Kuroda et al, 2000).

When cultured, FUS KO neurons show less mature spines and more filopodia-like dendritic protrusions than the control neurons (Fujii et al, 2005).

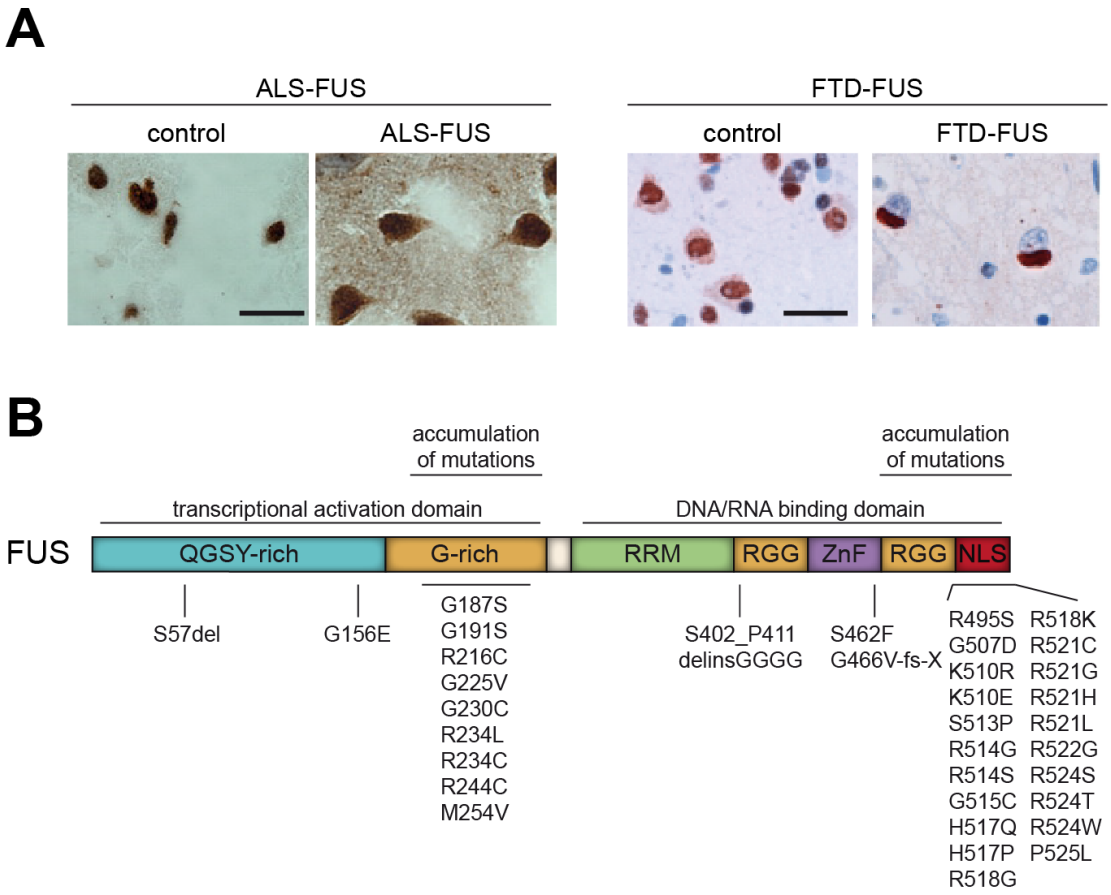

Figure 4 FUS pathology in ALS/FTD-FUS, FUS protein structure and mutations

FUS pathology in ALS-FUS and FTD-FUS cases. **(A, left panel)** FUS immunohistochemical staining of frontal cortex sections from a control individual or a *FUS* mutation carrier (ALS-FUS). FUS staining in the control section shows normal nuclear localization (left). In contrast, the ALS-FUS section shows FUS cytoplasmic inclusions (right). Scale bar: 20µm. Adapted from (Kwiatkowski et al, 2009). **(A, right panel)** FUS immunohistochemical staining of neocortex sections from controls or aFTLD-U/FTD-FUS cases. The control staining shows normal FUS nuclear staining and weak cytoplasmic staining. FTD-FUS sections show FUS positive neuronal cytoplasmic inclusions (NCI) with oval shape and some of the affected cells show partial FUS nuclear clearence. Scale bar: control 20 µm, FTD-FUS 15 µm. Adapted from (Neumann et al, 2009a). **(B)** FUS protein structure including domains responsible for its transcriptional activity (QGSY-rich domain, and G-rich domain) and DNA/RNA binding domains (RRM, RGG, ZnF and the C-terminal NLS). Below, is a schematic representation of the mutations known to cause ALS-FUS. Note the prominent accumulation of mutations at the G-rich domain and the C-terminal NLS. Adapted from (Dormann & Haass, 2011).

Also rat and mouse FUS overexpression models have been generated. Rats with inducible expression of mutant FUS (R521C) show strong motor deficits and neurodegeneration already at an early age (Huang et al, 2011). Interestingly, rat expressing wildtype human FUS, although asymptomatic at an early age, develop spatial learning and memory

deficiency at an advanced age (Huang et al, 2011). Overexpression of wildtype human FUS in mice is highly deleterious and the mice show severe paralysis and die after 12 weeks. The pathology observed is reminiscent of the human FUS pathology (Mitchell et al, 2012). Recently, a mouse model expressing mutated FUS (R521C) was reported showing severe motor behavioral deficits and higher postnatal lethality (Qiu et al, 2014). Despite the deleterious effects of increased FUS expression, there is generally no FUS aggregation observed in the different models (Shelkovnikova, 2013). This raises the question of a missing additional stress factor needed to induce the aggregation and propagation cascade in the different animal models. Also FUS overexpression in non-mammalian models as *D. melanogaster* (fruitfly) and *C. elegans* (worm) have demonstrated, although with some variation, that increased levels of wildtype or mutant FUS can cause decreased lifespan, cell loss and locomotor deficiencies, even in the absence of FUS aggregates (Chen et al, 2011; Lanson et al, 2011; Miguel et al, 2012; Shelkovnikova, 2013; Vaccaro et al, 2012; Xia et al, 2012). FUS knockout and overexpression models consequently demonstrate that a balanced FUS expression is required to maintain normal cellular function.

1.5.1.4. The role of FUS in neurodegeneration

RNA and protein homeostasis are the recurring themes constantly identified when evaluating the function of genes and proteins involved in neurodegeneration (Dormann & Haass, 2013; Renton et al, 2014; Thomas et al, 2013). In the case of FUS, the prominent clustering of mutations around the C-terminal part of the protein, which mislocalizes the protein to the cytoplasm, also offers clues on the pathomechanism behind ALS-FUS (Dormann et al, 2010; Kwiatkowski et al, 2009; Vance et al, 2009). However, FUS pathology is also observed in the absence of *FUS* mutations, for example in FTLD-FUS and HD cases, which indicates that other mechanisms can also cause disease. Disease could therefore result from a loss of FUS nuclear function or from a gain-of-toxic function of mislocalized FUS. Furthermore, based on the animal models presented above, the enigma about the origin and function of FUS aggregates in disease also gains relevance. Two mechanisms have been proposed for the origin of FUS aggregates. The first one includes a sequential development of inclusions starting from stress granules that at some point cannot longer be dissolved (Bentmann et al, 2013). The second mechanism proposes a sudden generation of aggregates due to an increase in local protein concentration. FUS protein that loses normal interaction with other proteins or RNA

could start a cascade of aberrant interactions resulting in aggregates (Ross & Poirier, 2004; Shelkovnikova, 2013). The characteristic prion-like domain of FUS has been proposed to mediate its aggregation propensity in yeast models (Sun et al, 2011) and the *in vitro* formation of hydrogels (Kato et al, 2012). Importantly, the prion-like properties of FUS could also have a major role in cell-to-cell propagation of the disease (Gitler & Shorter, 2011; King et al, 2012; Ling et al, 2013).

1.5.2. TAU

1.5.2.1. TAU protein domain structure

The TAU protein can be divided into a N-terminal projection domain and a microtubule binding domain close to the C-terminus (Mandelkow et al, 1996) (Figure 5A, Annex I). TAU binds to the outside of microtubules primarily with the microtubule binding domains and adjacent regions, which leaves the N- and C-terminal regions pointing outwards (Gustke et al, 1994; Kar et al, 2003; Santarella et al, 2004). The interaction with the microtubules is mediated by the positive net charge of the microtubule binding domains and the negative charge from the tubulin units.

1.5.2.2. TAU protein function

TAU can directly regulate transport along the highly polarized neurons (Dixit et al, 2008) by binding and stabilizing microtubules (Gustke et al, 1994; Weingarten et al, 1975). TAU is highly phosphorylated at sites that affect the microtubule binding affinity. The degree of phosphorylation together with the isoform abundance offers a delicate regulation of affinity to the microtubules. The projection domain of TAU has been shown to be responsible for the microtubule spacing (Al-Bassam et al, 2002; Chen et al, 1992; Frappier et al, 1994) and may affect cellular signaling by mediating interaction with the kinase Fyn (Morris et al, 2011). Additional functions attributed to TAU include the role as scaffolding protein in cell signaling mediated by multiple lipids and protein binding partners (Morris et al, 2011). TAU has also been proposed to mediate toxicity in cellular and mouse models of AD (Ballatore et al, 2007; Haass & Mandelkow, 2010; Ittner et al, 2010), which provides an interesting pathomechanism that combines the roles of amyloid-beta and TAU in AD. Research focusing on TAU's multifaceted functions may contribute to a better understanding of its role in major neurodegenerative diseases, and as a result treatment opportunities could expand.

1.5.2.3. TAU/*MAPT* alternative splicing

The TAU coding gene *MAPT* consists of 16 exons and is expressed in the central and peripheral nervous system, mainly in neurons. However, some TAU isoforms are also expressed in the skeletal muscle (Wei & Andreadis, 1998). In the brain, TAU protein is translated from six main transcripts generated by alternative splicing of exons 2 and 3, and exon 10 (Figure 5A). In the projection domain, inclusion of exon 2 only or exon 2 and exon 3 introduces one or two short acidic regions (1N, 2N) (Figure 5A). Exon 10 inclusion inserts a fourth microtubule binding domain (4R) at the C-terminal part of the protein. The combination of these splicing events leads to the six isoforms termed: 0N3R, 1N3R, 2N3R, 0N4R, 1N4R, 2N4R (Figure 5A).

MAPT alternative splicing is regulated tightly during development and expression shifts toward longer isoforms at mature age. The regulation of alternative splicing involves the interplay of *cis*- and *trans*-elements (Andreadis, 2012). The RNA-binding protein SRp75, for example, inhibits the splicing of exon 10 via its interaction with an intronic splicing silencer sequence downstream of exon 10 (Wang et al, 2011). Other factors do not bind RNA directly, but rather regulate splicing by binding other splicing factors. HnRNPG acts synergistically with SRp75 to regulate TAU exon 10 and, in contrast, this effect is antagonized by hnRNPE2 (Wang et al, 2011). Additionally, TAU splicing can also be regulated at the level of kinases that phosphorylate splicing factors and regulate their activity. One such example is the group of CDC2-like kinases CLK1, 2, 3, and 4 and CDK5 that regulate TAU exon 10 splicing (Hartmann et al, 2001). Although the exact target remains to be identified, a general change in phosphorylation status across different splice factors could mediate the effect (Hartmann et al, 2001).

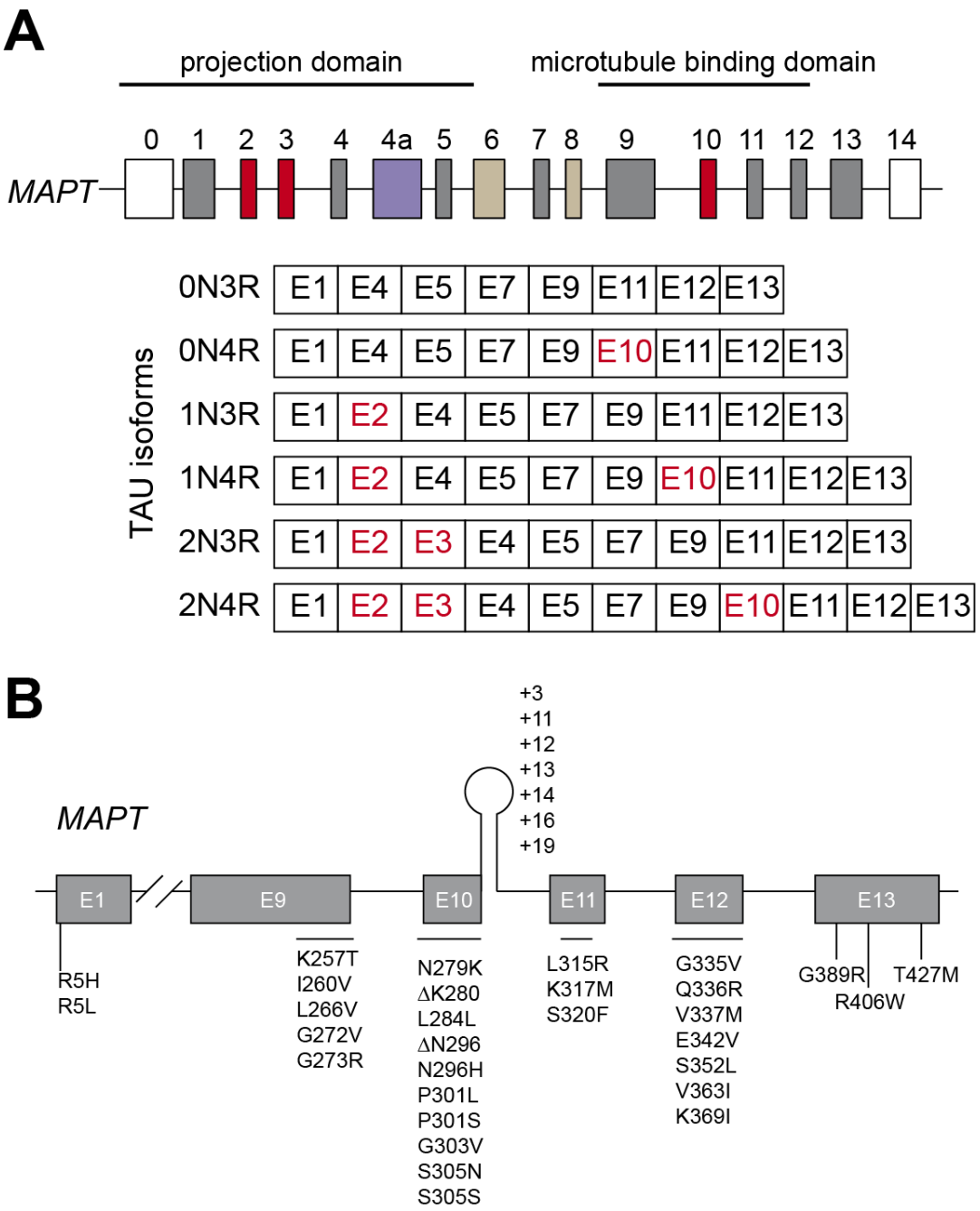

Figure 5 *MAPT*/TAU genetic structure and disease causing mutations

(A) Genetic structure of the human *MAPT* gene coding for the TAU protein. Exons 6 and 8 (brown) are not expressed in the human brain, and exon 4a (violet) is only expressed in the peripheral nervous system. Exons 0 and 14 (white) are noncoding. Exons 2, 3 and 10 (red) are alternatively spliced and give rise to six different isoforms (0N3R, 0N4R, 1N3R, 1N4R, 2N3R, 2N4R). Inclusion of E2 or E2/E3 adds one or two acidic regions (1N, 2N) in the projection domain (N-terminal part). Alternative splicing of E10 is regulated independently. Exons 9–12 code for microtubule binding domains. Inclusion of E10 adds a fourth microtubule binding domain (4R). Taken from (Orozco & Edbauer, 2013). **(B)** Mutations in *MAPT* known to cause frontotemporal dementia and parkisonism linked to chromosome 17 (FTDP-17) are shown for the coding region in exons 1, 9-13 (lower part) and in the intronic regions flanking exon 10 (upper part). Note that the intronic region next to exon 10 is predicted to form a stem loop structure. Adapted from (Goedert & Spillantini, 2006).

1.6. The role of alternative splicing in neurodegeneration

1.6.1. Mechanism and regulation alternative splicing

Alternative splicing is the mechanism that, on the one hand, extends the diversity of the transcriptome and proteome and, on the other hand, offers a third level of regulation of protein homeostasis next to transcription and translation. Different protein isoforms, often with distinct functions, are transcribed from one single gene (Dredge et al, 2001; Li et al, 2007; Licatalosi & Darnell, 2010). With this, it is possible to have tailored protein functions specific to each tissue and developmental stage. The high degree of diversity is best exemplified by the *D. melanogaster* Down syndrome cell adhesion molecule (*DSCAM*) gene, which is expressed in up to 38.016 different isoforms through alternative splicing of variable exon clusters. Different isoforms of *DSCAM* regulate the binding affinity in the crucial process of dendritic self-avoidance (homophilic repulsion) during neuronal development (Hattori et al, 2008). In the case of TAU, alternative splicing of exon 2, exon 3, and exon 10 result in 6 different isoforms. The expression of these isoforms is tightly regulated during development.

Alternative splicing is regulated through a complex interplay of *cis*- and *trans*-acting elements. *Cis*-acting elements are, for example, splicing enhancer and inhibitory sequences within the pre-mRNA that recruit *trans*-acting RNA-binding proteins. Posttranscriptional modification of these *trans*-acting factors allows the integration of cellular signaling and the regulation of alternative splicing. Furthermore, the relative abundance of targeted transcript and regulatory factors also determines alternative splicing (Licatalosi & Darnell, 2010). A combination of biochemical methods, next-generation sequencing and bioinformatics is currently being applied to unravel the regulatory code of alternative splicing (Licatalosi & Darnell, 2010).

The human brain relies, more than other tissues, on alternative splicing to regulate expression, with more than 40% of the genes presenting one or more alternative splicing events, followed by the testis and the liver with <40% of genes spliced (Yeo et al, 2004).

1.6.2. Alternative splicing in neurodegeneration

The role of alternative spicing in neurodegeneration has repeatedly been demonstrated. In AD brains, for example, a recent study identified 3,014 mRNAs with altered splicing through an unbiased RNA sequencing approach (Bai et al, 2013). Additionally, pathogenic mutations affecting alternative splicing have been identified at the level of *cis*-

acting elements or *trans*-acting factors (Keene, 2007). For example, mutations in the TAU gene *MAPT* located around the alternatively spliced exon 10 affect correct splicing and cause TAU aggregation (Hong et al, 1998). Mutations in the RNA-binding protein *(trans*-acting factor) survival motor neuron protein 1 (SMN1) cause spinal muscular atrophy (Cooper et al, 2009; Lorson & Androphy, 1998). SMN1 has an important role in the assembly of ribonucleoprotein complexes. Defects in alternative splicing or RNA transport are still discussed as pathomechanism behind SMA (Burghes & Beattie, 2009). Similar to SMN1, FUS could also affect different stages of alternative splicing in the disease. Understanding which targets are affected by FUS under normal and disease conditions would contribute to our understanding of the pathogenesis of ALS/FTD-FUS.

2. Aims of the Study

The DNA/RNA-binding protein FUS is pathologically and genetically linked to ALS and FTD, however, the pathomechanism is still unclear (Kwiatkowski et al, 2009; Mackenzie et al, 2011a; Neumann et al, 2009a; Vance et al, 2009). The redistribution of nuclear FUS into the cytoplasm in ALS/FTD-FUS immediately suggests two potential pathomechanisms that are not mutually exclusive. On the one hand, loss of nuclear FUS function may have detrimental consequences for normal cell physiology. On the other hand, mislocalized cytoplasmic FUS may cause a toxic gain-of-function (Ling et al, 2013).

The aim of my thesis project was to evaluate the FUS loss-of-function component in ALS/FTD-FUS by focusing on mRNA splicing, because ample evidence supports a key role of FUS in alternative splicing, although no physiological splice target was known. First, FUS binds pre-mRNA directly (Ishigaki et al, 2012; Lagier-Tourenne et al, 2012; Nakaya, 2013; Rogelj et al, 2012). Second, FUS is a known component of the spliceosome (Hartmuth et al, 2002; Rappsilber et al, 2002; Zhou et al, 2002) and third, it interacts with multiple splice factors (Gerbino et al, 2013; Meissner et al, 2003; Yang et al, 1998). Therefore, I aimed to identify physiological FUS splice targets. I focused on genes that are crucial to maintain normal neuronal function, such as the axonal protein TAU. Already slight alterations in the splicing of TAU affect the binding affinity for microtubules and mutations near the exon 10 splice site can cause FTD with TAU inclusions (Dredge et al, 2001; Liu & Gong, 2008). Finally, I asked how FUS loss-of-function in neurons affects axonal morphology and development.

In summary, my aims for this thesis were:

- to identify a physiological FUS splicing target in neurons and elucidate its regulation
- to assess the impact of FUS pathogenic mutations on its function in alternative splicing
- to validate the identified splice target in a human neuronal cell line
- to evaluate functional consequences of FUS depletion in neurons and link them to ALS/FTD pathophysiology

Together, these findings could help to understand the pathomechanisms of FUS related neurodegenerative disorders and elucidate therapeutic opportunities.

3. Materials and Methods

3.1. Materials

3.1.1. Equipment and tools

3.1.1.1. General equipment

Name	**Company**
Amaxa 4D-Nucleofector	Lonza
analytical balance (0.0001 – 200 g)	Mettler-Toledo
autoclave	Systec
automated Potter Multifix Record	Johann Gg Bachhofer
balance (0.01 – 2000 g)	Mettler-Toledo
Bunsen burner	Heraeus
CFX384 Real-Time System quantitative PCR	Biorad
CO_2-incubator	Thermo Scientific
cooling centrifuge 5417R	Eppendorf
digital sonifier 250	Branson
DNA electrophoresis gel system	Thermo Scientific
Dynabeads magnet	Life technologies
film cassette	G. Kisker
film developer	CaWo
freezer (-20°C)	Liebherr
freezer (-80°C)	Heraeus
fridge	Santo electronic
glassware	VWR
heating block MR Hei-Tec	Heidolph instrument
hemocytometer	Optik Labor
hood for cell culture	Heraeus
incubator	B. Braun Biotech International
microsurgical instruments (Dumont forceps and scissors)	FST
microwave	Sharp
Milli Q plus filtration system	Merck Millipore
N_2-tank	Messer Griesheim
Nano Drop	Implen
oven	Memmert
PCR thermal cycler	Eppendorf
pH meter	Thermo Scientific
pipette boy	Integra
power suppliers	Biorad, Major Science
Powerwave XS plate reader	BioTek
protein electrophoresis gel system	Bio-Rad
rotors (TLA-55, SW28)	Beckmann Coulter
scanner	Epson
shaker	Edmund Bühler GMBH
thermomixer	Eppendorf
ultracentrifuge	Beckmann Coulter
UV crosslinker StrataLinker 1800	Stratagene
UV lamp	Intas
vortex	Scientific Industries
water bath	GFL

3.1.1.2. Microscope equipment

Name	**Company**
confocal laser scanning microscope (LSM510, LSM 710)	Zeiss
epifluorescence microscope (Axiovert.A2)	Zeiss
Immersol 518 F	Zeiss
light microscope (Wilovert S)	Hund Wetzlar
microscope cover glasses (18 mm, 20 mm)	VWR
microscope slides Superfrost plus	Thermo Scientific
objective (Plan Apochromat, 40x/1.4 oil DIC)	Zeiss
objective (Plan Apochromat, 63x/1.4 oil DIC)	Zeiss
phase contrast microscope (CKX41)	Olympus
Vectashield H-1000 mounting medium	Vectorlabs

3.1.1.3. Consumables

Name	**Company**
cell culture dish (3.5 cm, 6 cm, 10 cm)	Nunc
cell culture plate (12 well, 96 well)	Nunc
centrifuge tubes (1.5 ml for TLA-55)	Beckmann Coulter
centrifuge tubes for rotor SW28	Beckmann Coulter
filter paper	Schleicher & Schüll
gloves (Latex)	Semperit
gloves (Nitrile)	Meditrade
hard shell PCR plates 384-well	BioRad
Immobilon-P membrane, PVDF, 0.45 µM	Merck Millipore
nitrocellulose membran	GE Healthcare
parafilm “M“	Pechiney Plastic Packaging
PCR tubes, strips, 96 well plates	Sarstedt
PES membrane filter (0.45 µm)	VWR International
pH indicator strips	Merck Millipore
pipette tips (10 µl, 200 µl, 1000 µl)	Sarstedt, VWR
pipettes	Gilson, Raynon
serological pipettes (2 ml, 5 ml, 10 ml, 25 ml)	Sarstedt
tubes (1.5 ml, 2 ml)	Sarstedt
tubes (15 ml, 50 ml)	Sarstedt
X-ray films	Fuji

3.1.1.4. List of software and online tools

Name	**Company/Link**
Adobe Illustrator	Adobe Systems
APE	Wayne Davis
AxioVision	Zeiss
BioRad CFX manager	BioRad
BLAST	NCBI, http://blast.ncbi.nlm.nih.gov/Blast.cgi?CMD=Web&PAGE_TYPE=BlastHome
CLC bio	CLC bio
Ensembl	EMBL-EBI, Sanger Centre http://www.ensembl.org/index.html
GraphPad Prism	GraphPad Software, Inc
ImageJ	NIH

iScore designer	KAKENHI, http://www.med.nagoya-u.ac.jp/neurogenetics/i_Score/i_score.html
LSM	Zeiss
NCBI	http://www.ncbi.nlm.nih.gov/
Primer3	Whitehead Institute for Biomedical Research, http://bioinfo.ut.ee/primer3/
Spidey	NCBI, http://www.ncbi.nlm.nih.gov/spidey/

3.1.1.5. List of services

Name	**Company**
antibody production	Eurogentec
DNA sequencing	GATC Biotech
oligonucleotide synthesis	Sigma-Aldrich

3.1.2. Chemicals

3.1.2.1. General chemicals

Name	**Company**
4-(2-hydroxyethyl)-1-piperazineethanesulfonic acid (HEPES)	Biomol
acrylamide (19:1 / 40 % (w/v))	Bio-Rad
agarose ultrapure	Life Technologies
ammonium persulfate (APS)	Roche
ampicillin	Boehringer Mannheum
boric acid	Merck Millipore
bovine serum albumin	Sigma-Aldrich
bromophenol blue	Merck Millipore
$CaCl_2$	AppliChem
DMSO	Roth
DTT	Biomol
ECL	Thermo Scientific
ECL plus	Thermo Scientific
EDTA	USB
EGTA	Sigma-Aldrich
ethanol	Sigma-Aldrich
ethidiumbromide	ROTH
fish gelatin	Sigma-Aldrich
gelatin	Sigma-Aldrich
glutaraldehyde	Sigma-Aldrich
glycerol	USB
glycine	Biomol
I-Block	Tropix
IPTG	ROTH
isopropanol	Merck Millipore
kanamycine	ROTH
KCl	USB
KH_2PO_4	Merck Millipore
methanol	Merck Millipore
$MgSO_4$	Sigma-Aldrich
$Na_2[B_4O_5(OH)_4]$	Sigma-Aldrich

Na_2HPO_4	Merck Millipore
NaCl	Merck Millipore
NaH_2PO_4	Sigma-Aldrich
$NaHCO_3$	Merck Millipore
NaN_3	Merck Millipore
NaOH	Merck Millipore
NH_4HCO_3	Merck Millipore
N-N'-Methylene-bisacrylamide (bisacrylamide)	SERVA
paraformaldehyde	Sigma-Aldrich
PIPES	Sigma-Aldrich
sodium borate decahydrate (Borax)	Sigma-Aldrich
sodium deoxycholate	Sigma-Aldrich
sodium dodecyl sulfate (SDS)	Roth
staurosporine	Sigma-Aldrich
suberic acid bis(3-sulfo-N-hydroxysuccinimide ester) sodium salt (BS3)	Sigma-Aldrich
sucrose	Sigma-Aldrich
tetramethylethylenediamine (TEMED)	USB
TO-PRO-3	Life Technologies
tris base	AppliChem
Triton X100	Merck Millipore
tryptone	BD Biosciences
yeast extract	BD Biosciences
β-mercaptoethanol	ROTH

3.1.2.2. List of kits

Name	**Company**
DNase digest kit	Qiagen
Electrophoretic Mobility-Shift Assay (EMSA) Kit with SYBR® Green & SYPRO® Ruby	Molecular Probes
endofree plasmid Maxi kit	Qiagen
Gel and PCR clean-up kit	Macherey-Nagel
MAXIscript T7 in vitro transcription kit	Ambion
neurons nucleoporation kit primary culture kit P3 amaxa	Lonza
NucleoBond Xtra Midi EF	Macherey-Nagel
Nucleospin Plasmid kit	Macherey-Nagel
Red/ET system	Gene Bridges
RNeasy Mini Kit	Qiagen
RT-PCR kit TaqMan MicroRNA Reverse Transcription Kit	Applied Biosystems
SsoFast™ EvaGreen® Supermix	BioRad
XTT assay	Roche

3.1.3. Molecular Biology and Biochemistry

3.1.3.1. General reagents

Name	**Company**
biotin-16-UTP	Roche

calf-intestinal alkaline phosphatase (CIP)	NEB
DNA ladder	Life Technologies
DNA polymerase (Pfu Ultra II Fusion)	Agilent
DNA polymerase (Pfu)	Agilent
DNA polymerase (Pwo)	PEQLAB Biotechnologie
DNA polymerase (Taq)	Roche Applied Science
deoxyribonucleotides (dNTPs)	Roche Applied Sciences
glutathion sepharose 4B	GE Healthcare
lysozyme	Merck Millipore
phosphatase inhibitor	Sigma-Aldrich
Protein A sepharose beads	GE Healthcare
Protein G Dynabeads	Life Technologies
proteinase inhibitor	Sigma-Aldrich
restriction enzymes	NEB
RNA Later	Ambion
RNAse A	Sigma-Aldrich
SeaBlue Prestained Protein Ladder Plus2	Life Technologies
Streptavidin-Peroxidase	Sigma-Aldrich
SUPERase RNase inhibitor	Ambion
T4-Ligase	NEB

3.1.3.2. List of antibodies

Name	**Company**
3R TAU, clone 8E6/C11	Millipore
4R TAU, clone 1E1/A6	Millipore
acetylated tubulin, clone 6-11B-1	Sigma-Aldrich
actin, clone AC-15	Sigma-Aldrich
Alexa secondary antibodies	Life Technologies
anti-mouse HRP	Promega
anti-rabbit HRP	Promega
anti-rat HRP	Santa Cruz Biotechnology
EWS	Santa Cruz Biotechnology
FUS, clone A300-292A	Bethyl
GFP	Neuromab, Fitzgerald Industries International
GluR2, clone L21/32	Neuromab
HA, clone 3F10	Roche
MAP2, AP-20	Sigma-Aldrich
NR1, clone 54.1	BD
NR2A, clone PRB-513P	Covance
Phalloidin	Life Technologies
PSD-95, clone K28/43	Neuromab
streptavidin HRP	Sigma-Aldrich
synaptophysin, clone SY38	Millipore
TAU, clone A 0024	Dako
Tau1, clone PC1C6	Millipore
TDP-43	Sigma-Aldrich
tubulin beta 3, SDL.3D10	Sigma-Aldrich
tubulin beta 3, Tuj1	Covance
tyrosinated tubulin, clone YL1/2	Abcam

3.1.3.3. Cloning vectors and oligonucleotides

Cloning vectors

Name	**Company**
FUW lentivirus vector	Lois et al (Lois et al, 2002)
mouse MAPT genomic BAC	Imagenes
pBUD-CE4	Invitrogen
pCR-blunt2 TOPO	Invitrogen
pGEM3	Promega
pSUPER	Oligoengine

List of oligonucleotide sequences for shRNA cloning
The target sequence is marked in bold. Oligonucleotides were cloned in pSuper using BglII/HindIII.

Name	**Species**	**Sequence sense**
shC9orf72	mr	gatcccc**GGATGGAAGATCAGGGTCA**ttcaagagaTGACCCTGATCTTCCATCCttttggaaa
shEWS	hmr	gatcccc**CAGCAGAGTTCATTCCGAC**ttcaagagaGTCGGAATGAACTCTGCTGttttggaaa
shFUS #1	mr	gatcccc**GTGCAAGGCCTAGGCGAtA**ttcaagagaTCTCGCCTAGGCCTTGCACttttggaaa
shFUS #2	mr	gatcccc**GGCCTAGGCGAGAATGTTA**ttcaagagaTAACATTCTCGCCTAGGCCttttggaaa
sh-hFUS	h	gatcccc**GGACAGCAGCAAAGCTATG**ttcaagagaCATAGCTTTGCTGCTGTCCttttggaaa
shLuc	-	gatcccc**CGTACGCGGAATACTTCGA**ttcaagagaTCGAAGTATTCCGCGTACGttttggaaa
shTAF15	mr	gatcccc**TATGATGAGCAGTCCAATTAT**ttcaagagaATAATTGGACTGCTCATCATAttttttggaaa
shTDP	mr	gatcccc**GTAGATGTCTTCATTCCCAAA**ttcaagagaTTTGGGAATGAAGACATCTACttttttggaaa

h= human, m= mouse, r= rat

List of primers for cloning

Name	**Species**	**sense**	**antisense**
GAPDH e3	m	atgGAATTCtcagctcccctgtttcttgtctttca	gatTCTAGAaccttcagctttccggccacttac
GAPDH e5	m	atgGAATTCcctcactcattgcccccgtgtttt	gatGCTAGCactgtcacaccagagacaagccca
HA-FUS* mutagenesis 3’	h	GGCCTGGGTGAaAAcGTgAcaattgagtctgtggctg	gaGATATCTTAATACGGCCTCTCCCTtCGgTCtTGcCTGTGCTCACCCCTGGAA
HA-FUS* mutagenesis 5’	h	gaggatccGCGGACATGTACCCATACGACGTC	caattgTcACgTTtTCACCCAGGCCttgcacaaagatgg
MAPT exon 1-4	m	gtgtaatctccagcatggtcttccattgtgtcaaactcctggcgagggtcagcCAGGTCCTCCTCCGAGATAAGCTTCTGCTC	catcggagacaccccgaaccaggaggaccaagccgctgggcatgtgactcaaACGCGTTACCCATACGACGTCCCAGACTAC
MAPT exon 9-11	m	caatcttcgacctgacattcttttaggtctggcatgggcacaggggcagtctgcagCAGGTCCTCCTCCGAGATAAGCTTCTGCTC	gagcaaagtgacctccaagtgtggctcgttagggaacatccatcacaagccaACGCGTTACCCATACGACGTCCCAGACTAC

TAU e10	m	atgGAATTCgccatcccaggcagc ttctgagc	gatTCTAGAggaacagggagggga gtctgggg
TAU e11	m	atgGAATTCgcagcagctgatggg agccactg	gatTCTAGAagacccaggtccaag gccacaca
TAU e3	m	atgGAATTCcactccttgcactgc ccctgcat	gatTCTAGAtgcacccgactatga gggtgacct
TAU e9	m	atgGAATTCctcagggactttgca gacgccgc	gatTCTAGAtactggctaggtggg agtctggct
TAU i10-1	m	atgGAATTCgctgcagtgcctagg gtatcaggga	gatTCTAGAtagatcccacagagc agcccgagag
TAU i10-2	m	atgGAATTCtccactgGGtgtcAT Tggcctttca	gatTCTAGACCACCggcttgtaga ctatttgcaCCt
TAU i10-3	m	atgGAATTCtgcaggggtgggctc tctttcct	gatTCTAGAgtagccaacagcccc gcctttcc
TAU i2-1	m	atgGAATTCctgaacatggcttgg gcattctgtt	gatTCTAGAcctgccccagctttg gctcc
TAU i9-1	m	atgGAATTCaggaatgacagcctg tttctacacct	gatTCTAGAacacctttgaaggag aaagatgaagtctttga
TAU i9-2	m	atgGAATTCaccgtgtgcgattgc ttaatgtcct	gatTCTAGATgctattttgaggcg gggtctctct
TAU i9-3	m	atgGAATTCaaggtcgatctccac cacaggcaaa	gatTCTAGAccatctcaccagacc caagcccttt
TAU i9-4	m	atgGAATTCTaggttggggcttgt cactagaggg	ataGTCGACggcacacactattcc tggagccaca
TAU i9-5	m	atgGAATTCagtcaggcATTgaaG GTGGtgcaga	ataGTCGACgtgcttggtgagagg acgcaggAAT
TAU i9-6	m	atgGAATTCtcttggcccactcac agttgttgct	ataGTCGACtcccggaagccAATg aggaaaaagga
TAU isoforms	r	atggctAGCAGCATGGCTGAACCC CGCCAGGAG	catgaattcTCACAAACCCTGCTT GGCCAAAGAGGCGG

h= human, m= mouse, r= rat

3.1.3.4. List of qPCR primers

Name	**Species**	**sense**	**antisense**
0N TAU	r	ccatggcttaaaaGCtgaaga	cctgtcctgtctttgcttacg
0N TAU	h	cgaagtgatggaagatcacg	ctgcttcttcagctttcagg
1N TAU	r	tgctgaaGCtgaagaagcag	cctgtcctgtctttgcttacg
1N TAU	h	aagaccaagagggtgacacg	cttcttcagcttccgctgtt
2N TAU	r	gaagagagagctcccgacaa	cagcttggtcctccatgttc
2N TAU	h	tgtgacagcacccttagtgg	tctccaatgcctgcttcttc
3R TAU	r	gcggcaaGGtgcaaatagt	acgatttctgctccatggtc
3R TAU	h	gtccgtactccacccaagtc	ggtttgtagactatttgcaccttc
4R endpoint PCR	mr	gcactccccctaagtcacc	ctggcttgtgatggatgttc
4R TAU	m/r	aagaagctggatcttagcaacg	ctggcttgtgatggatgttc
4R TAU	h	aagatcggctccactgagaa	cacacttggactggacgttg
C9orf72	mr	ccagaaaattgtcttggaagg	cagctgtcaccaatgtcatca
EWS	hmr	cccagcctaggatatggaca	ctgcccatagctgctttgtt
FUS	m/r	ctggcaagttgaagggtgaggc	gctcgttgctgtcctccacctc
FUS	h	acggacacttcaggctatgg	tagccagggtaggaggactg
GAPDH	m/r	ccgcatcttcttgtgcagtgcc	agactccacgacatactcagcacc
pre-mRNA GAPDH exon 4	m	tctgaaatcaacttctttccctta	tgtctccccactgcctacat
pre-mRNA TAU exon 10	m	ctccggtgtggttgtctctc	agcacacctcatggagactg
SON	m/r	tcttctcagcttgctctgga	caggcaaaggtccctctatg
TAF15	hmr	acttggggagggtgtgtcta	tcaatggctgccttagctg

TDP-43	m/r	agtgttgggtctcccctggaaa	acagtcacaccatcgcccatct
total TAU	m/r	tccagtcgaagattggctccttgg	aggtgccgtggagatgtgtccc
total TAU	h	tccagtcgaagattgggtccctgg	agatgccgtggagacgtgtccc
YWHAZ	m/r	tgagcagaagacggaaggtgctg	tctgatggggtgtgtcggctgc
YWHAZ	h	ttcttgatccccaatgcttc	aggctttctctggggagttc

h= human, m= mouse, r= rat

3.1.4. Cell culture

3.1.4.1. Cell culture reagents

Name	**Company**
B27 supplement	Life Technologies
basic fibroblast growth factor (bFGF)	R&D
bovine serum albumin	Sigma-Aldrich
dibutyril cAMP (dcAMP)	Sigma-Aldrich
DMEM glutamax-I	Life Technologies
DMEM/F12	Lonza
DNAse	Sigma-Aldrich
fetal bovine serum	Life Technologies
fibronectin	Sigma-Aldrich
glial cell-derived neurotrophic factor (GDNF)	R&D
laminin	Roche Applied Science
L-glutamate	Sigma-Aldrich
L-glutamine	Sigma-Aldrich
Lipofectamine 2000	Life Technologies
N2 supplement	Invitrogen
Neurobasal	Life Technologies
non-essential amino acids (NEAA)	Life Technologies
OptiMEM	Life Technologies
penicillin/streptomycin	Life Technologies
poly-D-lysine (PDL)	Sigma-Aldrich
poly-L-lysine (PLL)	Sigma-Aldrich
tetracycline	Sigma-Aldrich
trypsin (2.5 %)	Life Technologies
trypsin-EDTA	Life Technologies

3.1.4.2. List of cell lines and bacteria strains

Name	**Company**
DH5α – *E. coli* competent cells	Life Technologies
HEK 293-FT	Life Technologies
LUHMES	(Lotharius et al, 2002; Lotharius et al, 2005; Scholz et al, 2011)

3.1.5. Buffers and Media

All buffers are prepared with dH_2O unless otherwise specified.

3.1.5.1. Protein biochemistry

Name	**Composition**
4x Laemmli buffer	4% SDS 20% glycerol 5% β-mercaptoethanol 200 mM Na_2HPO_4 bromophenol blue adjust to pH 7.4
4x SDS PAGE running gel	1.5 M Tris base 0.4 % (w/v) SDS adjust to pH 8.8
4x SDS PAGE stacking gel	0.5 M Tris base 0.4 % (w/v) SDS adjust to pH 6.8
acrylamide-Schägger buffer	49.5% acrylamide 3% bisacrylamide
anode buffer	0.2 M Tris-HCl adjust to pH 8.9
blotting buffer	25 mM Tris 0.2 M Glycine
cathode buffer	0.1 M Tris-HCl 0.1 M Tricine 0.1% SDS
I-block buffer	0.2% I-block in TBSTx
IP lysis buffer (TNE 450)	20 mM Tris–HCl, pH 7.4 450 mM NaCl 0.1 mM EDTA 1.5 mM $MgCl_2$ 1 mM $CaCl_2$ 0.6% Triton X-100
IP lysis buffer no salt (TNE 0)	20 mM Tris–HCl, pH 7.4 0.1 mM EDTA 1.5 mM $MgCl_2$ 1 mM $CaCl_2$ 0.6% Triton X-100
RIPA buffer	137 mM NaCl 20 mM Tris, pH 7.5 0.1% SDS 10% glycerol 1% Triton X-100 0.5% sodium deoxycholate 2 mM EDTA
SDS PAGE running buffer 1x with SDS	25 mM Tris 0.2 M Glycine 0.1% SDS
separating gel buffer	1.5 M Tris 0.4% (w/v) SDS adjust to pH 8.8

stacking gel buffer	0.5 M Tris 0.4 % (w/v) SDS adjust to pH 6.8
TBSTx	20 mM Tris 0.14 M NaCl 0.2% Triton X-100 adjust to pH 7.6
tricine-Schägger gel buffer	3 M Tris-HCl 0.3% SDS adjust to pH 8.45

3.1.5.2. Antibody purification

Name	**Composition**
100x lysozyme stock	20 mg/mL lysozyme stock in STE buffer
100x NaN_3 for antibody dilutions	10% NaN_3
acid elution buffer	0.1 M Glycine-HCl 150 mM NaCl adjust to pH 2.5
BS3 stock solution (25mM)	25 mg suberic acid bis(3-sulfo-N-hydroxysuccinimide ester) sodium salt (BS3) in 1.75 mL 20mM sodium phosphate buffer adjust to pH 7.4
column wash buffer	0.2 M Tris-HCl 0.5 M NaCl adjust to pH 8
conjugation buffer	20 mM sodium phosphate Na_2HPO_4 0.15 M NaCl adjust to pH 8
neutralization buffer	1 M Tris, adjust to pH 9.5
quenching buffer for antibody purification	1 M Tris adjust to pH 7.5
STE	10 mM Tris-HCl 150 mM NaCl 1 mM EDTA adjust pH 8

3.1.5.3. Immunofluorescence

Name	**Composition**
2x GDB	0.2% gelatin powder 0.33 M Na_2HPO_4 0.9 M NaCl 0.6% Triton X-100 adjust to pH 7.4
immunofluorescence blocking buffer	2% fetal bovine serum 2% bovine serum albumin 0.2% fish gelatin dissolved in PBS
permeabilization/quenching buffer for nuclear proteins	0.2% Triton X-100 50 mM NH_4Cl dissolved in PBS

PFA-fix	4 % PFA 0.15 mM NaOH 0.13 mM NaH_2PO_4 sodium phosphate monobasic 0.12 mM sucrose adjust to pH 7.5
PHEM buffer	60 mM PIPES 25 mM HEPES 10 mM EGTA 2 mM $MgCl_2$ adjust to pH 6.9
PHEM fixative	3.7% (w/v) PFA/sucrose 0.25% (w/v) glutaraldehyde 0.1% (v/v) Triton X-100 dissolved in PHEM buffer

3.1.5.4. DNA Biochemistry

Name	**Composition**
20x SB agarose gel buffer (100mM)	38.17 g sodium borate decahydrate (Borax) 33 g boric acid 1L dH_2O adjust to pH 8.0
5x DNA loading buffer	50 % glycerol 50 mM Na_2EDTA 0.05 % bromophenol blue adjust to pH 8.0

3.1.5.5. Cell and bacterial culture

Name	**Composition**
borate buffer	40 mM boric acid 10 mM sodium tetra borate $Na_2B_4O_7 \cdot 10H_2O$ adjust to pH 8.5
coating solution for cover glasses	1.5% PDL 0.5% Laminin dissolve in borat buffer
coating solution for plastic culture plates	1.5 % PDL dissolve in borat buffer
cortical primary neurons medium	0.25% L-Glutamine (200 mM stock) 2% B27 1% penicillin/streptomycin in Neurobasal medium
HBSS	0.14 M NaCl 5.4 mM KCl 0.25 mM Na_2HPO_4 5.6 mM glucose 0.44 mM KH_2PO_4 1.3 mM $CaCl_2$ 1.0 mM $MgSO_4$ 4.2 mM $NaHCO_3$

HEK 293-FT cells medium	1% penicillin/streptomycin 1% NEAA 10% FCS in DMEM Glutamax
high BSA HEK medium	6.4% high BSA stock in HEK medium prepare fresh
high BSA stock	20% BSA in DMEM medium sterile filter
hippocampal primary neurons medium	2% B27 0.25% L-Glutamine (200 mM stock) 0.125% L-Glutamate (10 mM stock) 1% penicillin/streptomycin in Neurobasal medium
LB agar	1.5% agar dissolve in LB medium
LB medium	1% tryptone 0.5% yeast extract 86 mM NaCl
LUHMES differentiation medium	1 µg/mL tetracycline 2 ng/mL GDNF 0.49 mg/mL dcAMP 1% N2 supplement 1% penicillin/streptomycin in DMEM/F12 medium
LUHMES growth medium	1% N2 supplement 0.04 µg/mL bFGF 1% penicillin/streptomycin in DMEM/F12 medium
phosphate-buffered saline (PBS)	0.14 M NaCl 10 mM Na_2HPO_4 2.8 mM KH_2PO_4 2.7 mM KCl ajust to pH 7.4
poly-D-lysine stock	10 mg/mL in borate buffer

3.2. Methods

3.2.1. Biochemistry

3.2.1.1. Protein biochemistry

Neuron lysates

Protein lysates from primary neuronal culture were prepared by adding 2x Laemmli buffer directly to the culture dish after washing once with PBS. Samples were then boiled at 95°C for 10 min and used immediately or frozen for storage.

HEK 293-FT lysates and LUHMES lysates

Protein lysates from HEK 293-FT cells or LUHMES cells were prepared with cold RIPA buffer supplemented with proteinase and phosphatase inhibitors. After washing the culture dish once with PBS, RIPA buffer was added directly to the cells and the plate was incubated 15 min on ice. The lysate was centrifuged for 15 min at 17 000 *g*. The supernatant was mixed with 1/3 volume of 4x Laemmli buffer. Samples were boiled at 95 °C for 10 min and used immediately or frozen for storage.

SDS PAGE

10% acrylamide gels with a 4% stacking gel were prepared by mixing the following components (for 4 gels):

4% stacking gel	6.5 mL H_2O 2.5 mL stacking buffer 1 mL acrylamide
10% separating gel	10 mL H_2O 5 mL running buffer 5 mL acrylamide

The gels were polymerized by adding 100µL APS and 10µL TEMED for 10mL mixture. After complete polymerization, the samples were loaded and the gel was run first at 90V, and afterwards at 120V after the samples formed a single front. The gel was then blotted onto a PVDF or nitrocellulose membrane with a wet blotting chamber at 400 mA for 1 hour. After blotting, the membranes were blocked with blocking buffer (0.2% I-block in TBST) while shaking at room temperature (RT) for 1 hour.

The membranes were incubated overnight with the first antibody in blocking buffer while shaking at 4°C. On the next day, the membranes were washed for at least one hour

extensively with TBSTx before and after incubation with the secondary antibody. ECL or ECL plus was used following the manufacturer's instructions to develop the membranes.

Tricine-SDS-Schägger Gels

The tricine-SDS gels, developed by Schägger et al (Schägger & Von Jagow, 1987), were used here to detect proteins below 20 kDa. The following solutions are used:

4% stacking gel	2.1 mL H_2O 0.775 mL tricine-Schägger gel buffer 0.25 mL acrylamide Schägger buffer
16.5% running gel	1.75 mL 32% glycerol 1.75 mL tricine-Schägger gel buffer 1.75 mL acrylamide Schägger buffer
10% running gel	1.75 mL H_2O 1.25 mL tricine-Schägger gel buffer 0.75 mL acrylamide Schägger buffer

The gradient in the running gel was prepared by adding APS and TEMED and overlaying 16.5% acrylamide solution with the 10% acrylamide solution. The acrylamide solutions were let to polymerize together. A 4% acrylamide solution was used for the stacking gel. To run the gels, the cathode buffer (inner chamber) and anode buffer (bottom chamber) were filled accordingly in the gel chamber without mixing. In order to increase the detection of small proteins, a nitrocellulose membrane was used for the transfer. After completion of the transfer, the nitrocellulose membrane was heated to 95°C in PBS for 5 min. The membrane was then blocked and used as described above.

3.2.1.2. RNA binding assay

In vitro transcription (IT)

To generate RNA probes for the crosslinking experiments, the DNA plasmids were first linearized with a single cutter restriction enzyme for several hours. A small amount of DNA was visualized with an agarose gel to confirm the completion of the reaction. The linearized plasmid was *in vitro* transcribed using the MAXIscript T7 kit with biotin-16-UTP to label the RNA according to the manufacturer's instructions. The RNA probes were visualized in acrylamide gels with SYBR® Green (Molecular Probes) to assess the reaction and semi-quantify the product.

FUS immunoprecipitation and RNA extraction (RIP)

For the immunoprecipiation of endogenous FUS from mouse brain (P15), the brains were homogenized with a potter homogenizer in 2 mL IP lysis buffer (TNE 450) containing RNase inhibitor SUPERase-In (1 U/mL) and protease and phosphatase inhibitor cocktail. The lysate was centrifuged for 20 min at 70 000 *g* at 4°C in a TLA55 rotor to clear the sample. The supernatant was immunoprecipitated for 1 hour at 4°C with Dynabeads Protein G that had been previously coupled to FUS or GST antibody (3 µg antibody/25 µL beads). After immunoprecipitation, the beads were washed four times with lysis buffer. The bound RNA was then extracted with the RNeasy mini kit including the optional DNase treatment step. RNA and protein samples were collected accordingly during the process to compare input and IP samples. RNA samples were further analyzed with quantitative PCR and the Ct values of the IP samples were compared to the Ct values of the input to determine the percentage of recovery.

Crosslinking binding assay of FUS to TAU pre-mRNA probes

As in the FUS immunoprecipitation, the RNA binding assay is used to test the binding of endogenous mouse FUS to RNA. However, in this case, the lysate is incubated with labeled RNA probes prior to the immunoprecipitation. First, the mouse brains were homogenized as described above, however in the absence of RNase inhibitor. The lysate was centrifuged for 20 min at 70,000 *g* as described above, except that the supernatant was diluted with 2 volumes of lysis buffer lacking salt (TNE 0) to allow binding of protein to the RNA probes. In order to clear the lysate from endogenous biotinylated proteins, the lysate was incubated with streptavidin agarose before adding the RNA probes. After clearing, protein extracts (500 µg) were incubated with biotinylated RNA probes (4 µl of a 20 µL IT reaction) at RT for 30 min. The samples were crosslinked on ice with ultraviolet light irradiation at 254 nm, 400 mJ/cm^2 with a StrataLinker 1800 and then treated with RNase A (10 mg/ml) for 15 min to digest unprotected RNA. After RNAse digestion, the samples were subjected to immunoprecipitation with FUS or GST antibodies as detailed above. The eluted protein samples were loaded on a SDS-PAGE gel and biotinylated RNA crosslinked to FUS was detected using streptavidin-peroxidase.

3.2.1.3. 2N TAU antibody purification

A 2N TAU specific polyclonal rabbit antibody was generated by immunizing rabbits with a GST-TAU exon 3 antigen (sequence DVTAPLVEERAPDKQATAQSHTEIPEGTTA).

The antibody was then purified from the rabbit final bleed in two steps, first negative selection against GST followed by positive selection against GST-TAU exon 3 and elution from the purification column. The GST and GST-TAU exon 3 antigens were produced in bacteria induced with IPTG and extracted by disrupting the bacteria with lysozyme (100 µg/mL), 5 mM DTT and 1% Triton X-100 followed by short sonication. The extracts were incubated with glutathion-beads for 30 min and washed with conjugation buffer before crosslinking with BS3 for 45 min at RT. After quenching with 50 mM Tris buffer, the unbound GST fraction was eluted with acid elution buffer. The GST-Glutathion beads were loaded on a column for removal of anti-GST antibodies by negative selection. The diluted rabbit serum was passed three times through the column, the flow through being collected and reused each time. The negative selected serum, depleted from anti-GST antibodies, was then transferred to a column for the positive selection with GST-TAU exon 3 Glutathion beads. After several washes, the antibody was eluted in 1 mL fractions with elution buffer. The fractions were immediately neutralized with Tris buffer pH 9.5. The antibody concentration was determined and the fractions with the highest concentration were pooled. The antibody was tested by immunoblotting for specificity.

3.2.2. Molecular Biology

3.2.2.1. Molecular cloning

Standard bacterial transformation

Competent *E. coli* bacteria (eg. DH5α) were thawed on ice. The ligation reaction (see below) or 1µL of the plasmid to be re-transformed were incubated with 100 µL bacteria on ice for 20 min. A heat shock was then performed for 45 sec at 42°C to promote take-up of the DNA. After adding 400µL LB medium without antibiotics, the mixture was incubated for 1h at 37°C with slow shaking. The small bacteria culture was finally plated on agarose LB plate containing the adequate antibiotics.

Subcloning

For subcloning, 3 µg of a plasmid containing the insert of interest was digested with enzymes that digest both ends usually for 1h at 37°C in the corresponding NEB buffer. Whenever possible, the reaction was stopped with a heat kill at 65°C for 20 min. The insert was isolated with agarose gel electrophoresis, the corresponding band cut out of the gel and extracted with a Gel Extraction kit (Macherey-Nagel). The backbone was

prepared in the same way, except for an extra dephosphorylation step after the enzyme digestion. For this, the same reaction was further mixed with new NEB buffer and the phosphatase CIP and incubated for 1h at 37°C. A second heat kill was performed to stop the reaction. The backbone was then isolated with agarose gel electrophoresis as described above. Insert and backbone were ligated with T4 DNA ligase for >30 min at RT. The reaction was then transformed in competent bacteria, as detailed above.

Cloning with oligonucleotides

In order to clone oligonucleotides, for example for shRNAs, oligonucleotides were first dissolved in H_2O to a concentration of 100 µM. They were then annealed by mixing 1µL of each forward and reverse oligonucleotide, with NEB buffer 4 and H_2O. The reaction was heated to 95°C for 4 min and then let to cool down at RT. The backbone was prepared by digesting the plasmid with the corresponding enzymes, but without dephosphorylation of the ends. The annealed oligonucleotides were then ligated with the digested backbone using T4 DNA ligase for 1h at RT. In case the restriction sites were destroyed by correct oligo insertion, an extra digest was performed before bacteria transformation to exclude empty re-ligated backbones. The reaction was then transformed as usual in competent bacteria.

shRNAs were cloned into a pSUPER backbone and then subcloned into a FUW lentivirus packaging vector (FU2) co-expressing mCherry or TagRFP from the human ubiquitin C promoter. 25 nucleotide long oligonucleotides were designed by assigning a specific seed region generally unique to the target using the iScore designer (http://www.med.nagoya-u.ac.jp/neurogenetics/i_Score/i_score.html) and the BLAST web tool (http://blast.ncbi.nlm.nih.gov/Blast.cgi?CMD=Web&PAGE_TYPE=BlastHome). Whenever possible, shRNAs were first tested in HEK 293-FT cells for their knockdown efficiency by co-transfecting with a tagged overexpression construct. All constructs were verified by DNA sequencing.

PCR product cloning

The primers used for cloning PCR products were designed with restriction sites at both ends. The PCR product was first digested with the corresponding restriction enzymes usually overnight at 37°C followed by heat kill to stop the digestion. The digested PCR product was used as insert in the ligation reaction with the corresponding vector. In some cases, a TOPO cloning kit was used according to the manufacturer’s instructions.

The TAU pre-mRNA probes for the crosslinking experiments were generated by cloning 250-400 bp PCR products, using genomic mouse DNA or MAPT BAC as template, into the pGEM3 vector or pCR-blunt2 TOPO. Overexpression constructs were cloned using the same strategy, except that cDNA was used as template for the PCR. For rescue experiments with human FUS, a silent mutation was added to make the HA-tagged human FUS construct resistant to the shRNAs. The HA-tagged human FUS construct was expressed under the human synapsin promoter in a lentiviral vector.

The different TAU isoform expression constructs were cloned by first generating cDNA from rat neurons at different developmental stages (DIV1, DIV7, DIV14, DIV21). The PCR products were then cloned, followed by a selection based on the correct sequence corresponding to the different TAU isoforms.

TAU minigene cloning

The TAU minigene constructs containing mouse *MAPT* exon 9-11 or exon 1-4 were cloned by homologous recombination using the Red/ET system (Gene Bridges) starting with a mouse genomic BAC and a modified expression vector pBUD-CE, where the NheI/PciI fragment containing the EF1 expression cassette was excised. For better detection, the expression vector contained a myc-tag (N-term.) and a HA-tag (C-term.).

3.2.2.2. Reverse transcription and quantitative PCR (RT-qPCR)

RNA isolation

RNA was isolated with the Qiagen RNAeasy kit following the manufacturer's instructions. In case the RNA was not immediately isolated, cells were kept in RNAlater at 4 °C. Whenever necessary, an additional DNase digest was performed during RNA extraction, according to manufacturer's instructions.

Reverse transcription RT-PCR

The isolated RNA was first diluted with RNAse-free H_2O and reversely transcribed with random hexamer primers (N6) using TaqMan MicroRNA Reverse Transcription Kit following the manufacturer’s instructions to generate complementary DNA (cDNA). For the cDNA standard series, a mixture was prepared by pooling equal amounts of all RNA samples and this mixture was then serially diluted in 1/10 steps. The following table gives the details for the reaction. For each reaction the RNA sample was diluted nuclease-free H_2O in 15µL and combined with 30µL reaction mix.

components	µL
100 mM dNTPs (with dTTP)	0.45
MultiScribe™ Reverse Transcriptase (50 U/µL)	3
10X RT buffer	4.5
RNase inhibitor	0.55
nuclease-free H_2O	17
N6 primer (50 ng/µl)	4.5
reaction mix	30
RNA sample diluted	15

The mix was incubated on ice for 5 minutes before starting the reverse transcription reaction. The program for the RT-PCR reaction was:

time	temperature
30 min	16 °C
30 min	42 °C
5 min	85 °C
hold	4 °C

Quantitative PCR (qPCR)

The qPCR reaction with the SsoFast™ EvaGreen® (BioRad) reaction mix was prepared according to the manufacturer's instructions by adding the cDNA diluted in H_2O (usually 1:1) and gene specific primers. YWHAZ was usually used as housekeeping gene. The relative mRNA expression was calculated with the BioRad CFX manager software using the delta-delta-Ct method. The following table gives the details for the reaction.

components	µL
SsoFast™ EvaGreen®	2.5
primer forward (400 nM)	0.05
primer reverse (400 nM)	0.05
H_2O	0.4
cDNA template	2
total mix	5

The qPCR ran for 50 cycles in the CFX384 Real-Time System quantitative PCR (BioRad) with the following program:

step	time	temperature
start	30 sec	95°C
cycle (50x)	5 sec	95°C
	5 sec	60°C
	10 sec	95°C
melt curve	5 sec (increment 0.5 °C)	65°C - 95°C

The PCR products were usually sequenced to confirm the correct amplification.

Quantitative PCR primer design

qPCR primers were design based on the NCBI database genomic and mRNA sequences of the gene and species of interest. The Spidey web tool (NCBI, http://www.ncbi.nlm.nih.gov/spidey/) was used to generate a multiple alignment between sequences. Regions (>22 bp) with perfect alignment were selected if a large intron (>1000 bp) was being spanned, to avoid detection of genomic DNA. The selected regions were then processed with the Primer3 web tool (http://bioinfo.ut.ee/primer3/) to generate primers with a product size 200-300 bp at an optimal temperature of 60°C.

Endpoint PCR

Endpoint PCRs were used to estimate the relative abundance of different PCR products, for example between inclusion and exclusion of a specific exon. A standard PCR reaction was prepared and run for 30 cycles. The PCR products were visualized with an agarose gel and the band intensities were quantified. A ratio was then calculated based on the intensities.

3.2.3. Cell culture and lentivirus production

Rat primary neurons

For the neuronal culture, the brains of rat embryos (E18-E19) were collected from a pregnant mother that was sacrificed with CO_2. The cortex or hippocampal region was cut out with microsurgical instruments. After washing cortices and hippocampi separately in 5 mL cold HBSS, 500µL 2.5% trypsin was added to dissociate the tissue. For cortical neurons, DNase was also added (final concentration 0.7 mg/mL). After digestion, the tissue was washed with warm HBSS and gently dissociated into a cell suspension. For the feeder-free culture system, cells were plated in cell culture dishes previously coated with poly-D-Lysin (PDL) or PDL and Laminin, for culture on plastic or cover glasses, respectively (see buffer list). For immunofluorescence experiments, cover glasses were treated with nitric acid, washed, sterilized, before coating. Cortical neurons were kept in culture in Neurobasal medium supplemented with B27, penicillin/streptomycin and L-glutamine. For hippocampal neurons, culture media was further supplemented with L-glutamate (see buffer list).

Cell culture of LUHMES cells

LUHMES were cultured as dividing cells in DMEM/F12 medium supplemented with N2, bFGF and penicillin/streptomycin (see buffer list) in a cell culture flask previously coated

with poly-L-Lysin (PLL). LUHMES were passaged at 60-70% confluency and full confluency was avoided. For differentiating LUHMES into post-mitotic neuronal-like cells, cells were plated in normal medium on cell culture dishes previously coated in two steps, first with PLL and then with fibronectin. One day after plating, normal medium was changed to differentiating medium, consisting of DMEM/F12, penicillin/streptomycin, tetracycline, GDNF and dcAMP (see buffer list). Half of the culture media was exchanged every 2-3 days.

Cell culture of human Embryonic Kidney cells (HEK 293-FT)

HEK 293-FT cells were cultured in DMEM/Glutamax medium supplemented with 10% FCS, 1% penicillin/streptomycin and 1% non-essential amino acids (NEAA). HEK 293-FT cells were used only at a low passage and full confluency was avoided for virus production. For passaging, cells were detached from culture flask with Trypsin/EDTA and replated with new medium.

Virus production

Virus was produced in packaging HEK 293-FT cells. For this, HEK 293-FT cells were expanded from a freshly thawed aliquot. One day after seeding, HEK 293-FT cells were transfected with Lipofectamine with three constructs: two that allow the formation of the lentivirus particles (pVSVg and pSPAX) and the construct of interest (lentivirus packaging construct). Usually, three 10 cm culture dishes were transfect for each construct. First, Lipofectamine was diluted in Optimem and incubated for 5 min at RT.

for 3x10 cm dishes	volume (µl)
Lipofectamine	108
in Optimem	4500

The DNA was also diluted in Optimem, as follows:

for 3x10 cm dishes	DNA (µg)
LTR-vector	18.6
pSPAX2	11
pVSVg	6.4
total	36
in Optimem (µl)	4500

The DNA and Lipofectamine mixture was incubated for 20 min at RT prior to adding the 3mL of the mixture to each dish. One day after transfection, medium was changed to high BSA HEK 293-FT medium (see buffer list). Two days after transfection, the supernatants

were recovered, filtered through a 0.45 µm PES membrane filter to remove cell debris and ultracentrifuged for 2 h at 64,000 *g* in a SW28 rotor. The virus pellet was re-suspended slowly in Neurobasal medium for 5 h at 4°C. Aliquots were stored at -80°C.

Cytotoxicity test

XTT metabolic assay kit from Roche Applied Science was used for cytotoxicity measurements according to the manufacturer's instructions. Cells were treated with staurosporine (final concentration 1 µM for 4h) as a positive control.

Splicing assay in HEK 293-FT cells

For the splicing assays with TAU minigenes, HEK 293-FT cells were transfected sequentially. First with shRNA construct to allow sufficient knockdown and two days later with the TAU minigene construct using Lipofectamine. Before the second transfection HEK 293-FT cells were replated to avoid differences in cell number due to possible growth delay caused by the shRNA constructs. The transfections were performed as follows:

first transfection in 10 cm dish	
10 µg DNA in 1,5 mL Optimem	add 3mL per dish
108 µL L2K in 1,5 mL Optimem	

second transfection in 12 well	
1 µg DNA in 100 µL Optimem	add 200µL per well
3 µL Lipofectamine in 100 µL Optimem	

Transfection of neurons with Lipofectamine

Primary neurons were transfected in a 12 well culture plate, after changing medium to transfection medium (primary neurons medium without B27). For one well of the 12 well culture plate, 1.8 µg DNA and 3.2 µL Lipofectamine were diluted individually in 100 µL Neurobasal. The DNA and Lipofectamine transfection mixture was incubated for 20 min at RT prior to adding it to each well. After 45 min, transfection medium was discarded and the cells were washed once and placed back to the conditioned medium.

Amaxa transfection of neurons

For the analysis of neuronal morphology, neurons were transfected before plating using the Amaxa 4D-nucleofector with the primary culture kit P3 (Lonza) and using the program EM110. Neurons were then cultured on astrocyte feeder cells in N2 media.

3.2.4. Immunofluorescence

Microscopy

All images were taken either with a confocal laser scanning microscope (LSM510 or LSM 710, Zeiss) or with an epifluorescence microscope (Axiovert.A2, Zeiss). Confocal images were usually taken as Z-stacks and processed with LSM software or ImageJ.

Immunostaining

Neurons cultured on cover glasses were fixed with 4% PFA (PFA-fix) for 20 min at RT and then washed with PBS. The cover glasses were incubated with the primary antibody diluted in 1x GDB buffer at 4°C overnight. After several washes with PBS, the cover glasses were incubated with the secondary antibody diluted in 1x GDB at RT for 1 h. Nuclear staining with TO-PRO-3 diluted in H_2O was performed after the incubation with the secondary antibody. After several washes with PBS, the cover glasses were briefly dipped in dH_2O and mounted on object slides with Vectashield and fixed on the sides with clear nail polish.

In order to better visualize nuclear proteins such as FUS, an additional permeabilization step was performed with Triton X-100. In summary, after fixing with 4% PFA for 20 min at RT, hippocampal neurons were quenched and permeabilized with 0.1% Triton X-100 in 50 mM ammonium chloride. The fixed cells were then blocked with 2% fetal bovine serum, 2% bovine serum albumin and 0.2% fish gelatin dissolved in PBS. After blocking, neurons were handled as described above, except that 10% blocking solution was used instead of 1x GDB buffer.

Fixation to visualize cytoskeleton in neurons

A special fixation method modified from (Smith, 1994), was needed for the visualization of microtubules in neurons. The PHEM fixative, containing glutaraldehyde, was freshly prepared and pre-warmed at 37°C (see buffer list). The neurons were fixed with PHEM fixative for 15 min at RT and then washed three times with PBS. The neurons were then quenched for 10 min with 50 mM ammonium chloride and washed again three times with PBS. The fixed neurons were treated as usual for the immunostaining.

Quantification of neuronal morphology

The software Axio Vision (Zeiss) was used for length and area measurements. Image acquisition and quantification were done blind to the experimental conditions. Axonal

growth cone area, neurite number and axonal branching were quantified from a minimum of 45 cells per condition in three independent experiments. Axonal length, defined by the length of the longest process at the time point of analysis (DIV0+4), were quantified from a minimum of 99 cells per condition in three independent experiments.

3.2.5. Statistical analysis

All statistical analysis was performed with the GraphPad Prism software using t-test, one-way or two-way ANOVA. Morphological analysis and quantification was performed blind to the experimental conditions. Statistical significance was considered as follows: * $p<0.05$, ** $p<0.01$, *** $p<0.001$, **** $p<0.0001$

4. Results

4.1. FUS function in neurons

4.1.1. FUS localizes predominantly in the nucleus of hippocampal rat neurons

FUS is a predominantly nuclear protein, although prevalent dendritic/synaptic localization of transfected and endogenous FUS has been reported in some studies with cultured neurons (Belly et al, 2005; Fujii et al, 2005; Husi et al, 2000). I assessed the localization of endogenous FUS in cultured rat hippocampal neurons with immunofluorescence (IF) and detected exclusive nuclear FUS staining (Figure 6). There was no co-localization with the dendritic marker MAP2 (Figure 6A) nor with the synaptic marker synaptophysin (Figure 6B). This result strongly contrasts the studies mentioned above; however it does not exclude the possibility that a small FUS population, below the detection limit, could be localized in dendrites.

Thus, FUS localizes predominantly in the nucleus of cultured rat neurons. Based on this, I focused on FUS nuclear function and its relevance in the pathomechanism behind ALS and FTLD.

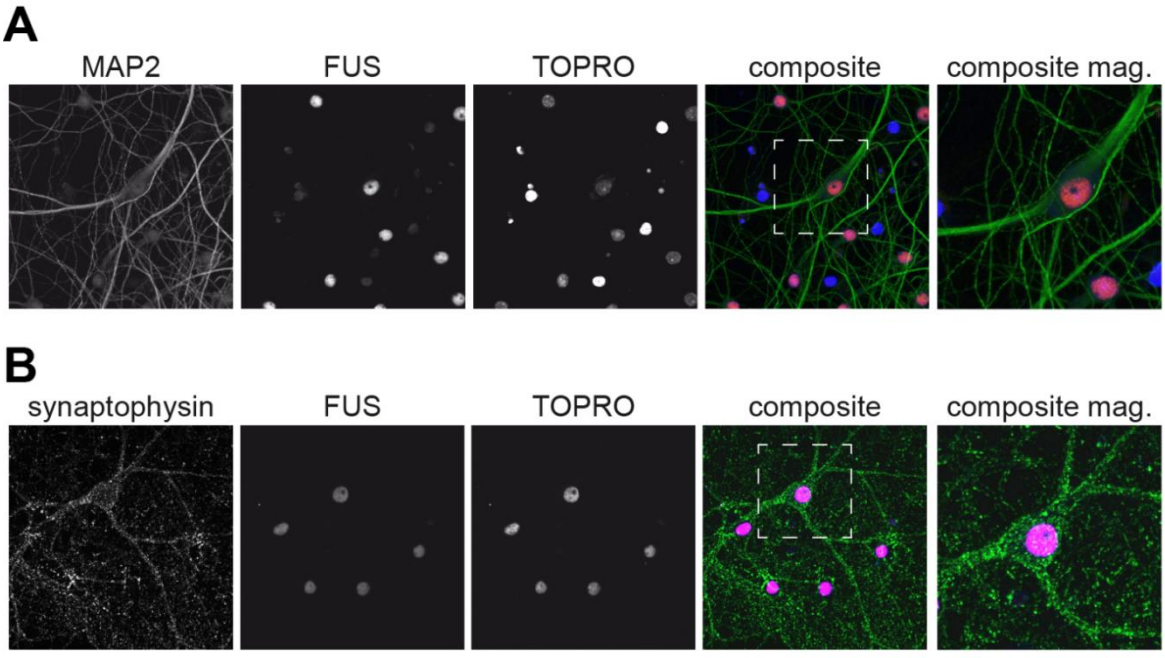

Figure 6 FUS is localized to the nucleus in rat hippocampal neurons

Immunofluorescence images of untransfected mature neurons (DIV 20) with the indicated antibodies and TO-PRO-3 to label nuclear DNA. **(A)** MAP2 defines dendrites and **(B)** synaptophysin defines synapses. Note that FUS localizes exclusively to the nucleus and does not colocalize with MAP2 or synaptophysin. The rightmost panel (composite mag.) shows a magnification of the field marked with white box in the composite.

4.1.2. FUS knockdown in neurons is not toxic but enhances expression of 4R TAU

In order to evaluate the physiological function of FUS, I cloned two shRNAs against rat FUS in a viral transfer vector and produced lentivirus to knockdown FUS in neurons. Hippocampal neurons were transduced with purified virus after two days in culture and harvested seven days later (DIV 2+7). Both shRNAs against FUS showed a knockdown efficiency of about 90% compared to a control shRNA (shLuc) targeting the non-expressed gene firefly luciferase (Figure 7A). The abundance of synaptic proteins (GluR2, NR1, NR2A, synaptophysin) and cytoskeletal proteins β-actin and β-tubulin remained unaltered, as shown in the immunoblots (Figure 7A,C). TDP-43, another disease related DNA/RNA-binding protein, also remained unaltered (Figure 7C). Cell viability, assessed by a metabolic XTT assay, was also not affected (Figure 7B). In contrast, the immunoblots using a TAU antibody showed increased levels of heavier variants of TAU in FUS knockdown treated neurons (Figure 7C,D). TAU is alternatively spliced (Figure 8) and the two prominent bands observed in the shortly exposed immunoblots (Figure 7D) correspond to the most abundant 3R and 4R TAU isoforms, as shown by the immunoblots with isoform specific antibodies (Figure 7D). At this stage, more 3R TAU is expressed than 4R TAU, with a ratio of 80% 3R TAU to 20% 4R TAU (Figure 7D, note also the difference in abundance on mRNA level in Figure 9A). Immunoblots using the isoform specific antibodies showed a significant increase in 4R TAU upon FUS knockdown, but no effect on the 3R TAU. The lack of a reciprocal decrease in 3R TAU can be explained by differences in relative amounts.

Together, this data indicates that FUS knockdown alters relative abundance of TAU isoforms, resulting in an enhanced expression of 4R TAU.

4.1.3. FUS knockdown in neurons results in increased expression of 2N and 4R TAU isoforms

In order to evaluate the abundance of individual TAU isoforms, I focused on quantitative PCR (qPCR) and endpoint PCR studies. Figure 8A shows the genomic structure of the *MAPT* gene, coding for TAU, with the alternatively spliced exons marked in red. Primers for qPCR were designed to amplify PCR products unique to each spliced exon (Figure 8B). Primers for endpoint PCR are placed around exon 10 in the neighboring exons 9 and 11, in order to evaluate exactly the inclusion/exclusion of exon 10 (Figure 8B).

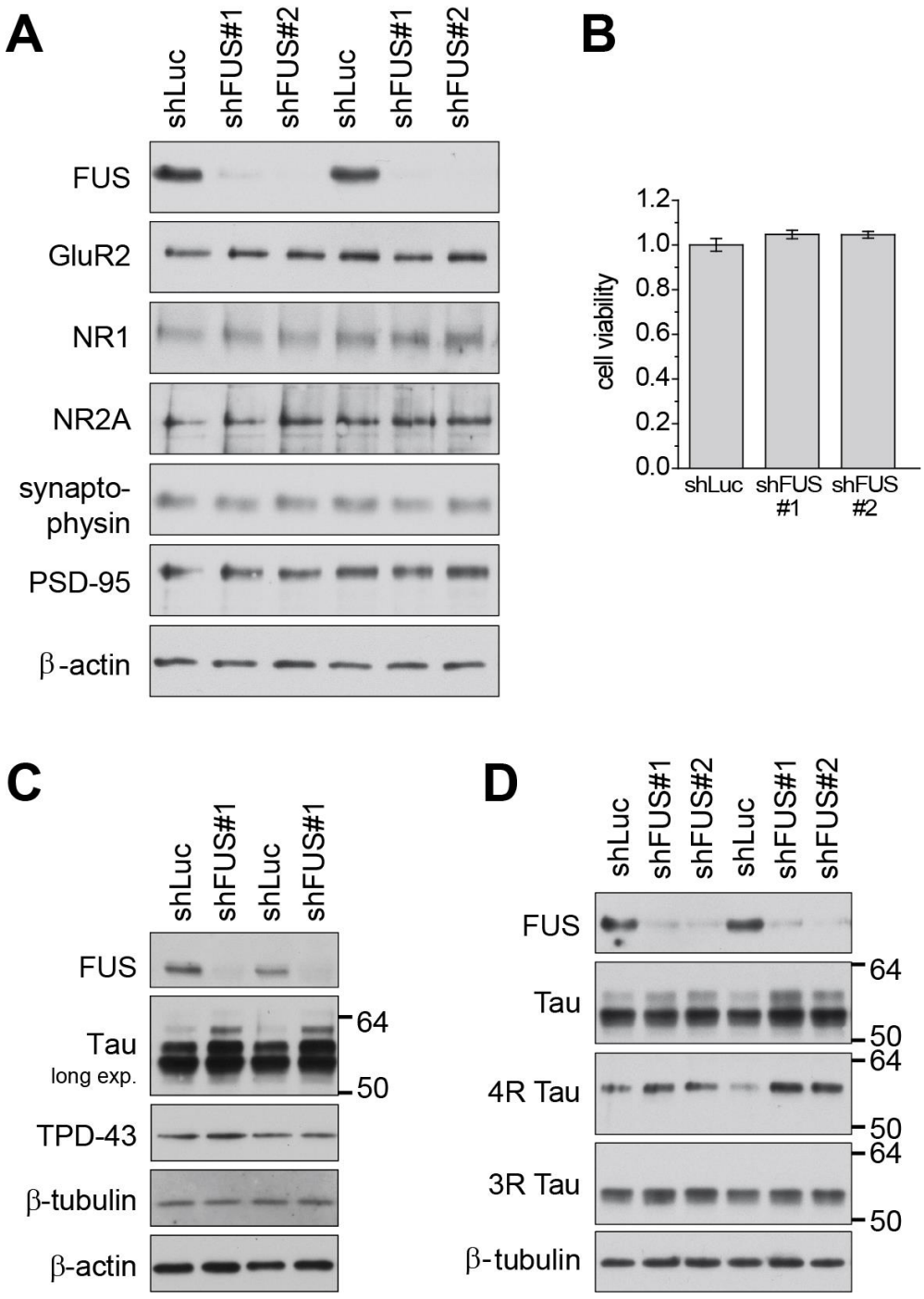

Figure 7 FUS knockdown in neurons is not toxic but enhances expression of 4R TAU isoform

Hippocampal neurons were transduced with lentivirus (DIV 2+7) to express the indicated shRNA directed against FUS (shFUS#1 or shFUS#2) or non-targeting control shRNA against firefly luciferase (shLuc). **(A)** Immunoblots with the indicated antibodies show expression of neuronal proteins, duplicates are shown. **(B)** Cell viability measured with XTT assay shows no significant alteration in FUS knockdown condition, mean +/- SEM are shown, one-way ANOVA, n = 12. **(C)** Immunoblots with the indicated antibodies. Note that the disease related DNA/RNA-binding protein TDP-43 remains unaltered in FUS knockdown conditions. The TAU blot shows a longer exposure (long exp.) and additional isoforms are visible. **(D)** Immunoblots with the indicated antibodies show total TAU protein and isoforms 4R and 3R, duplicates are shown. Note the increase in 4R Tau expression in the FUS knockdown samples.

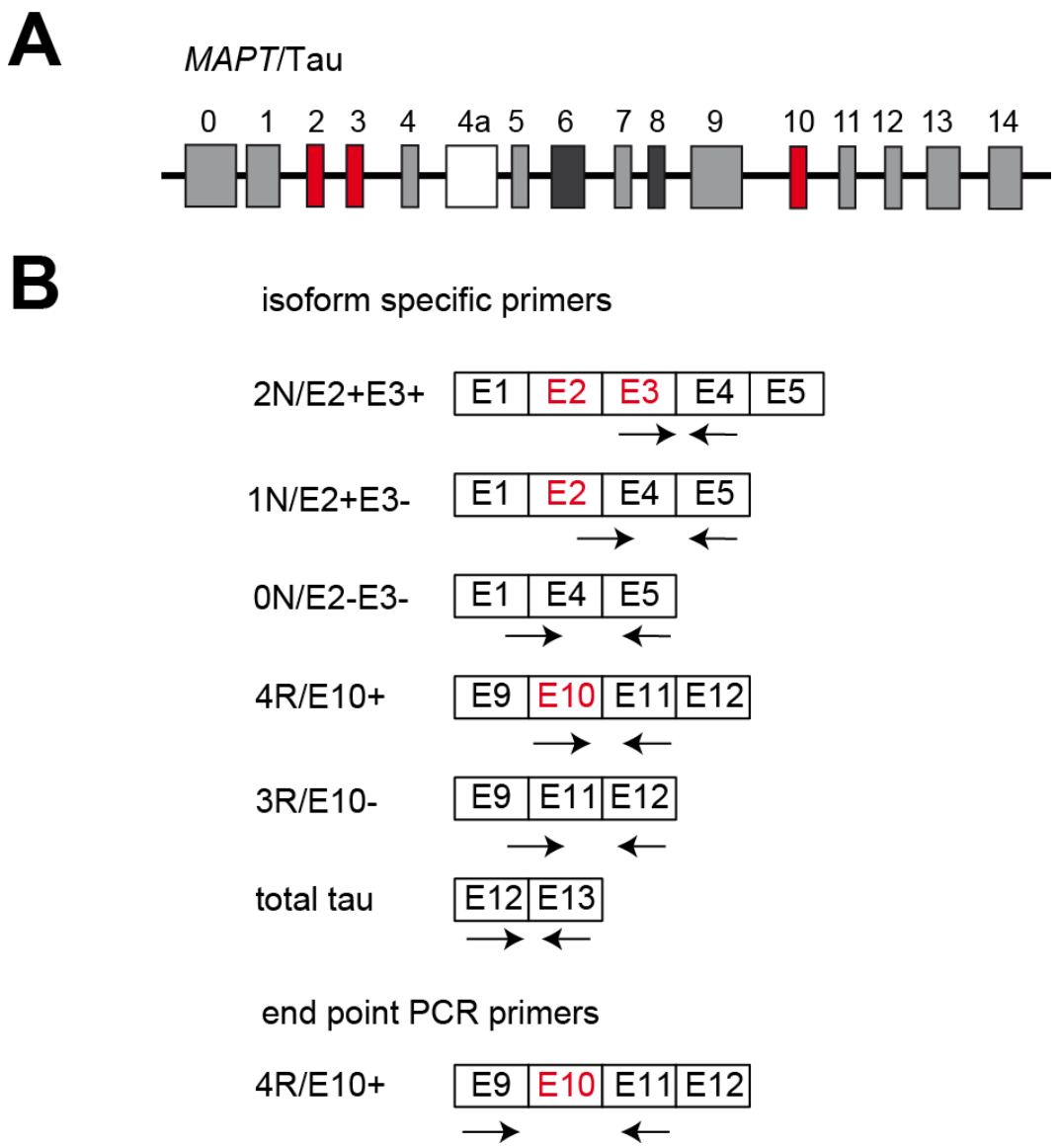

Figure 8 *MAPT*/TAU genomic structure and primer design for quantitative PCR and endpoint PCR

(A) Exon structure of the human *MAPT* gene. Alternatively spliced exons in the CNS are shown in red. Exon 4a (white) is included only in the peripheral nervous system and exon 6 and exon 8 (dark grey) are not expressed in the human CNS. **(B)** Isoform specific primers for quantitative PCR. In the case of 0N, 1N and 3R, forward primers bind to the splice sites between exons E1-E4, E2-E4 and E9-E11, respectively. Primers for the 2N and 4R isoforms bind in exon 3 or exon 10, which are unique for the respective isoform. Specificity was confirmed by sequencing the PCR products. Endpoint PCR primers bind around exon 10 in the neighboring exons 9 and 11.

The results from the endpoint PCR showed a significant increase (70%) of exon 10 inclusion in neurons after FUS knockdown (Figure 9A). The qPCR results confirmed the knockdown efficiency and also revealed a specific increase in expression of TAU exon 3 and exon 10 (resulting in isoforms 2N and 4R TAU). Total levels of TAU and splicing events involving 0N, 1N or 3R TAU, remained unaffected (Figure 9B).

In summary, end point PCR and qPCR confirm and clarify the exact splicing events altered upon FUS knockdown. Specifically 2N and 4R TAU levels are increased in hippocampal neurons after FUS knockdown.

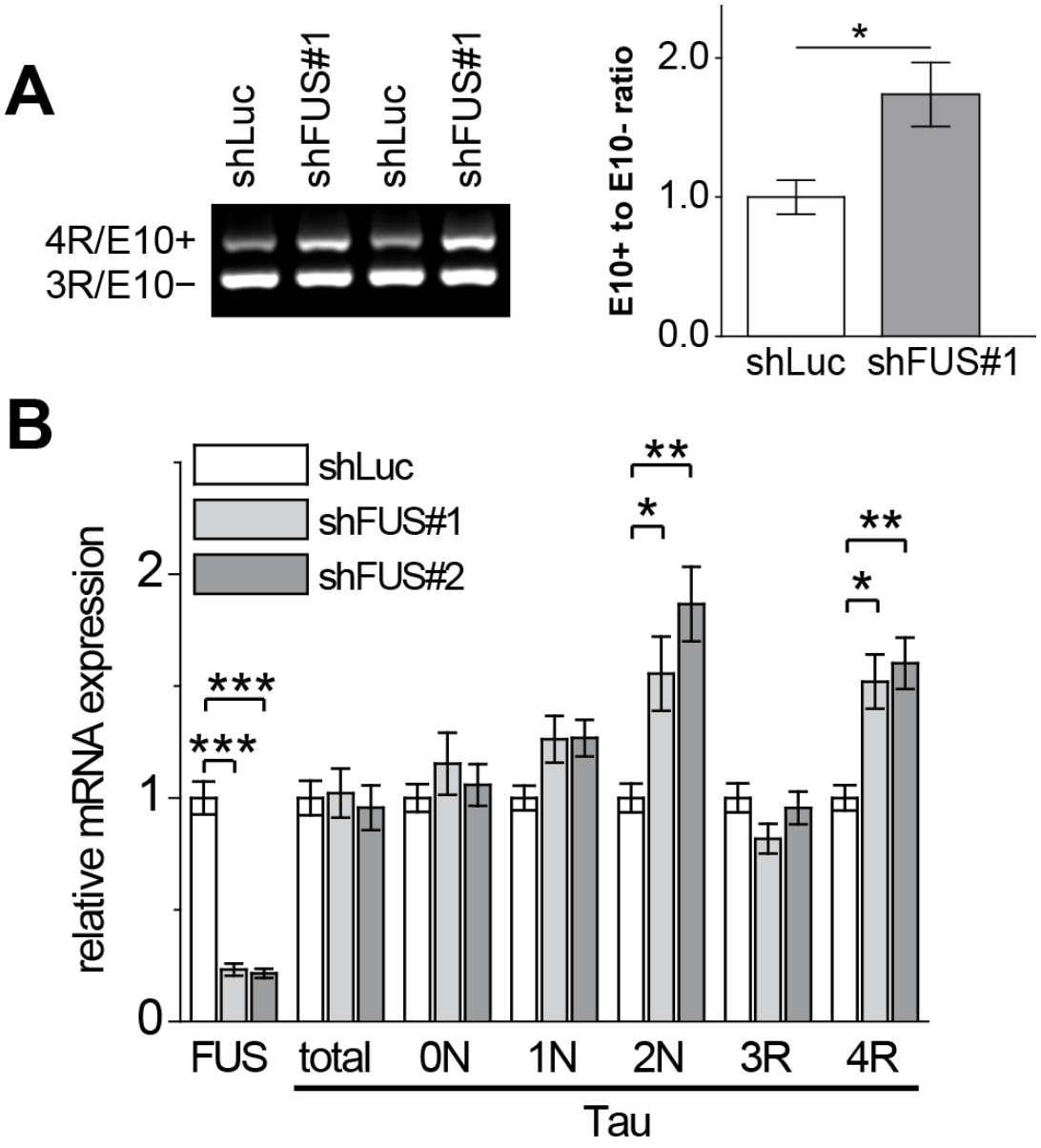

Figure 9 FUS knockdown enhaces inclusion of TAU exon 3 and exon 10 at mRNA level

Hippocampal neurons were transduced with lentivirus (DIV 2+7) to express the indicated shRNA against FUS (shFUS#1 or shFUS#2) or non-targeting control shRNA (shLuc). Total RNA was analyzed by end-point PCR or quantitative PCR (qPCR) and shows enhanced expression of TAU exon 3 and exon 10 upon FUS knockdown. **(A)** Endpoint PCR after 30 cycles. PCR products were visualized in an agarose gel, duplicates are shown. The ratio of E10 inclusion to E10 exclusion is quantified in the right panel. n=3, mean +/-SEM are shown, student's t-test: *p<0.05. Note the significant increase in E10 inclusion upon FUS knockdown. **(B)** Total RNA was analyzed by qPCR for FUS, total TAU and TAU isoforms. FUS and total TAU expression was normalized to the housekeeping gene YWHAZ and TAU isoform expression was normalized to total TAU levels. n=4, mean +/-SEM are shown, one-way ANOVA with Dunnett's post-test: *p<0.05, **p<0.01, ***p<0.001.

4.1.4. Neurons in culture reflect the *in vivo* developmental changes in TAU alternative splicing

In order to evaluate the applicability of our primary neuron model, I tested whether TAU alternative splicing in cultured neurons reflects the changes seen during postnatal development. For this, RNA was collected from cultured neurons at four different time points: DIV 1, DIV 7, DIV 14 and DIV 21. I then evaluated the expression of TAU isoforms by qPCR.

With time, I detected increased expression of 4R TAU in comparison to 3R TAU. Also 2N TAU became more preferentially expressed than the initial 0N TAU (Figure 10). The shift in TAU isoform expression showed the pattern expected based on the reported TAU expression in the murine brain (Kosik et al, 1989). *In vivo*, the shortest isoform 0N3R is highly expressed early in development. With time there is a shift in expression towards the longer TAU isoforms, reaching a peak in expression of the longest isoform 2N4R at adult stages. Regarding FUS expression over time, I detected a slight decrease of FUS expression, this was however not statistically significant (Figure 10). Interestingly, a similar decrease in FUS expression has been reported after differentiation of SY5Y cells with retinoic acid (Andersson et al, 2008).

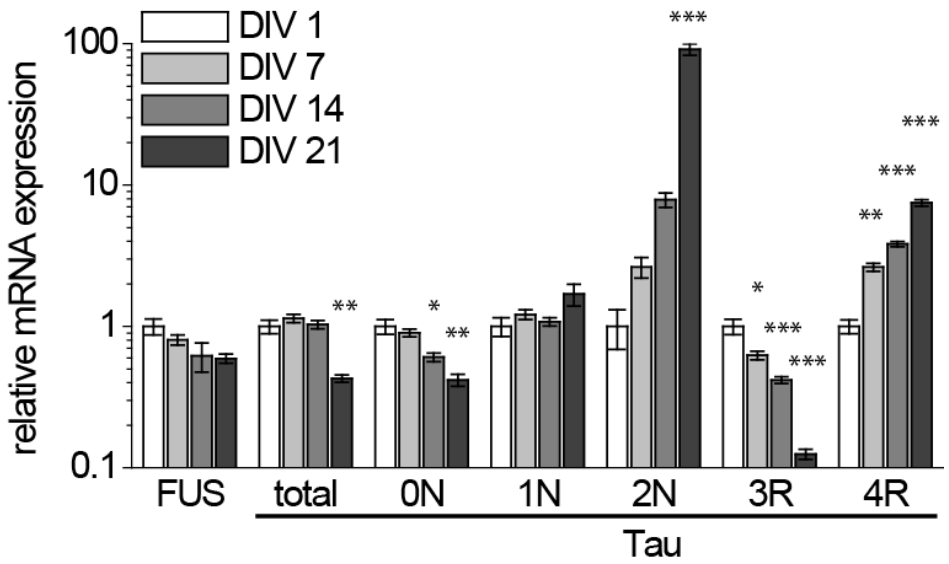

Figure 10 TAU isoform expression in cultured hippocampal neurons recapitulates *in vivo* TAU isoform expression during development

Total RNA, collected form untreated hippocampal neurons at DIV1, DIV7, DIV14 and DIV21, was analyzed by quantitative PCR for FUS, total TAU and TAU isoforms. FUS and total TAU expression was normalized to the housekeeping gene YWHAZ and TAU isoform expression was normalized to total TAU levels. n=3, mean +/-SEM are shown, ANOVA with Dunnett's post-test: *p<0.05, **p<0.01, ***p<0.001. Note the significant increase 2N and 4R TAU expression and decreased 0N and 3R TAU expression with time.

Altogether this result confirms that cultured rat hippocampal neurons reflect the normal development *in vivo*. Therefore, the increased expression of 2N and 4R TAU isoforms observed upon FUS knockdown in 9 day old neurons reflects the shift in isoform expression seen in older neurons (DIV 21).

4.1.5. 2N TAU specific antibody detects overexpressed TAU isoforms

The lack of commercial antibodies specific for the 0N, 1N or 2N TAU isoforms has hampered research on TAU splicing and its implications in disease. The results presented above highlighted the importance of having an antibody to detect 2N-TAU isoforms. Therefore, we set out to generate a 2N TAU specific antibody. For this, rabbits were immunized with rat TAU exon 3 fused to an N-terminal GST (Figure 11A).

I transfected constructs expressing different TAU isoforms in HEK 293-FT cells (Figure 11A) to validate antibody specificity. The final bleed serum specifically detected the 2N TAU isoform (Figure 11B). Although affinity-purification with the GST-exon 3 TAU antigen did reduce the background in immunoblotting, the purified antibody only detected overexpressed 2N TAU and was not sensitive enough to detect endogenous 2N TAU in cultured neurons (data not shown). Similar results were obtained in immunofluorescence staining. The antibody against 2N TAU labeled only those neurons that had been transfected to overexpress the 2N4R TAU isoform but not the surrounding untransfected neurons (Figure 11D).

Taken together, the production and purification of an antibody against 2N TAU was successful. However, this antibody detects only overexpressed 2N TAU isoforms in cultured neurons. Furthermore, the detection limit might be overcome by using samples with higher abundance of 2N TAU isoforms, for instance in brain lysate of adult mouse tissue.

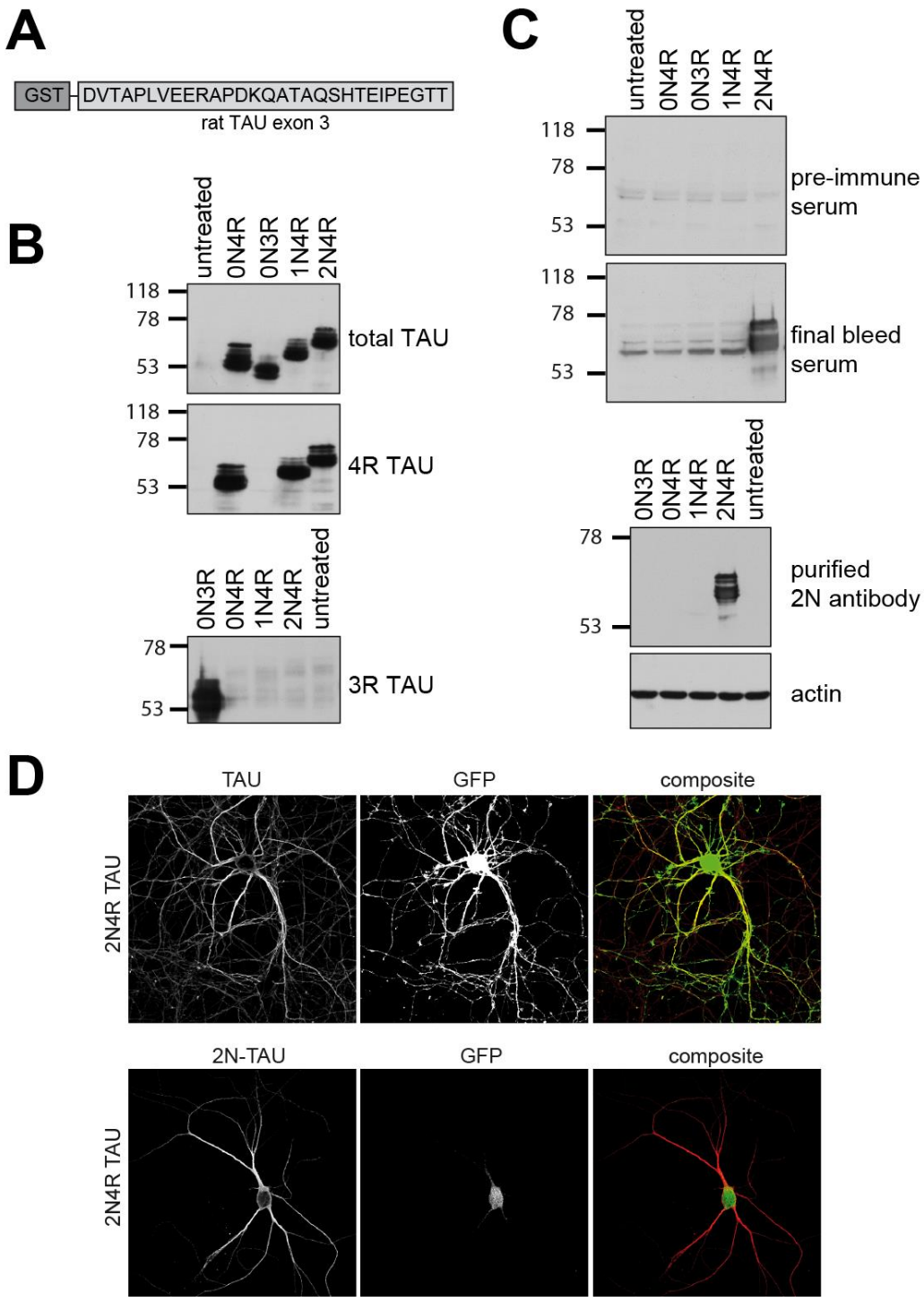

Figure 11 2N TAU specific antibody detects overexpressed TAU isoform

(A) Anti-2N TAU polyclonal antibody produced by immunizing rabbits with the depicted antigen was purified and tested in immunoblots **(C)** and immunofluorescence **(D)**. **(B)** Characterization of rat TAU isoform constructs used to test 2N TAU polyclonal antibody. Immunoblots with the indicated antibodies. **(C)** Immunoblots using the indicated sera and antibody. The purified antibody detects only the 2N4R TAU isoform without additional unspecific bands, compared to the final bleed serum. **(D)** Hippocampal neurons transfected to overexpress rat 2N4R TAU isoform and GFP to control the transfection. Immunofluorescence using the indicated antibodies. Note the specific signal of the 2N TAU antibody solely at the transfected cell but not surrounding processes as observed for the TAU antibody staining.

4.1.6. Knockdown of ALS/FTLD related proteins TDP-43, C9orf72, EWS or TAF15 does not alter TAU isoform expression

In order to evaluate the specificity of the FUS effect on TAU splicing, I evaluated how the knockdown of other ALS/FTLD related proteins influences TAU splicing. Hippocampal neurons were transduced with lentivirus to express shRNAs (shLuc control or shRNA for knockdown). RNA samples were collected 7 days after transduction and analyzed by qPCR.

TDP-43 and FUS are functionally related proteins that define different subgroups of ALS and FTLD pathology. Hippocampal neurons treated with lentivirus to knockdown TDP-43 showed significant reduction of TDP-43 (>80% reduction). TAU isoform abundance and total TAU levels remained, however, largely unchanged compared to shLuc control samples (Figure 12A).

Recently a higher frequency of AD pathology (including NFTs), has been reported in FTLD cases with *C9orf72* mutation compared to FTLD cases with *GRN* mutation (Bieniek et al, 2013). I evaluated therefore if C9orf72 knockdown could alter TAU splicing. As seen in Figure 12B, the C9orf72 knockdown in neurons was highly efficient (>90% knockdown). Similar to the TDP-43 knockdown, there were no significant differences in the abundance of TAU isoforms between shLuc control and C9orf72 knockdown. A slight decrease in 4R TAU was detected; however it did not reach statistical significance. Total TAU expression also remained unchanged (Figure 12B).

FUS belongs to the FET family of proteins (including EWS and TAF15) that shares similar protein domain structure and potentially cellular functions. Hippocampal neurons treated with lentivirus showed good individual knockdowns of EWS (75% knockdown) or TAF15 (70% knockdown) respectively. TAU isoform abundance was not significantly altered in the knockdown samples compared to the control. There was, however, a trend towards a reduction in the abundance of 2N and 4R TAU in shTAF15 samples. Total TAU levels remained largely unchanged (Figure 12C).

Taken together, this data confirms that TAU splicing is specifically altered in FUS knockdown and none of the ALD/FTLD related proteins tested (TDP-43, C9orf72, EWS, or TAF15) showed similar effects. This implicates FUS mediated TAU aberrant splicing directly with ALS/FTLD-FUS pathophysiology and not to ALS/FTLD-TDP.

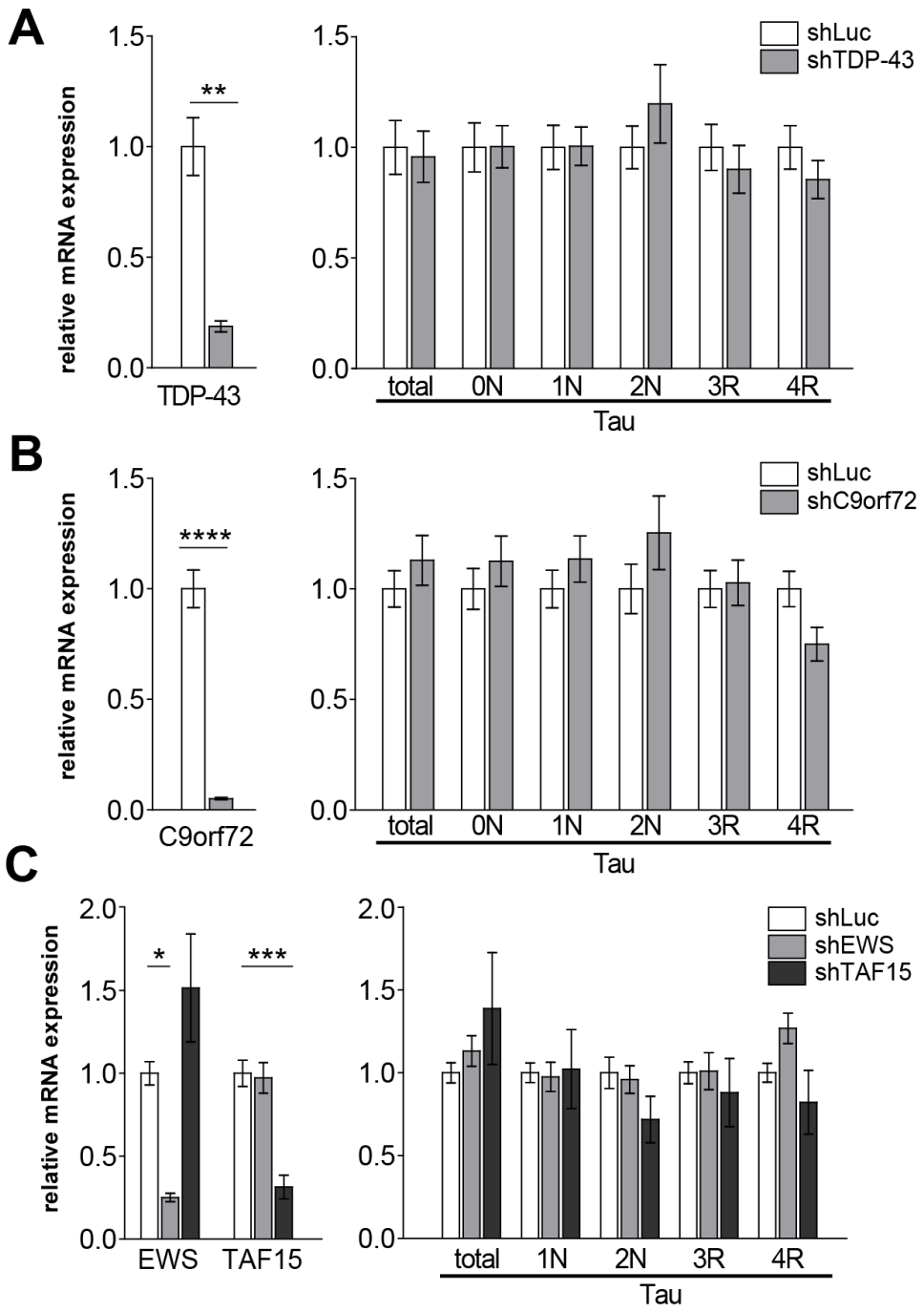

Figure 12 Knockdown of ALS/FTLD related genes TDP-43, C9orf72, EWS or TAF-15 does not alter TAU isoform expression

Hippocampal neurons were transduced with lentivirus (DIV 2+7) to express the indicated shRNA against **(A)** TDP-43, **(B)** C9orf72, **(C)** EWS, TAF-15 or non-targeting control shRNA (shLuc). Total RNA was analyzed by quantitative PCR. **(A)** TDP-43 and total TAU expression was normalized to the housekeeping gene YWHAZ and TAU isoform expression was normalized to total TAU levels. n=6, mean +/-SEM are shown, student's t-test: **p<0.01. **(B)** C9orf72 and total TAU expression was normalized to the housekeeping gene YWHAZ and TAU isoform expression was normalized to total TAU levels. n=6, mean +/-SEM are shown, student's t-test: ****p<0.0001. **(C)** EWS, TAF-15 and total TAU expression was normalized to the housekeeping gene YWHAZ and TAU isoform expression was normalized to total TAU levels. n=4, mean +/-SEM are shown, one-way ANOVA with Dunnett's post-test: **p<0.01.

4.1.7. Reintroduction of human FUS rescues aberrant TAU splicing

In order to confirm that aberrant TAU splicing is a direct consequence of FUS knockdown and to exclude an off-target effect, I performed rescue experiments by reintroducing human FUS into rat neurons treated to knockdown FUS. The human FUS construct was HA-tagged and was resistant to the shRNA due to a silent mutation of the shRNA seed region. Hippocampal neurons were doubly transduced with lentivirus to express shRNA (shLuc or FUS shRNA) and human wildtype FUS on day 2 and samples for immunoblotting and RNA were recovered 7 days after transduction.

Reintroduction of HA-human FUS strongly increased the level of FUS in both control and FUS shRNA treated neurons compared to the shLuc control, that shows endogenous levels (Figure 13A). In the immunoblot, the HA-human FUS is observed slightly higher than endogenous FUS due to the HA-tag. Importantly, the expression of human FUS did not affect cell viability, compared to the control neurons expressing GFP (Figure 13B). Both immunoblots and qPCR showed that reintroduction of HA-human FUS completely rescued the altered splicing of TAU exon 3 and exon 10 (Figure 13A,C). The immunoblot using 4R TAU antibody shows that HA-human FUS not only rescues the increase in 4R TAU but it even suppresses 4R TAU expression below endogenous level (Figure 13A). In contrast, 3R TAU levels remained largely unchanged on protein level and showed a slight increase on mRNA level upon reintroduction of human FUS (Figure 13A,C).

This data corroborates the specific effect of FUS in TAU splicing and confirms that the splicing events involving exon 3 and exon 10 are highly responsive to the levels of FUS in the neurons.

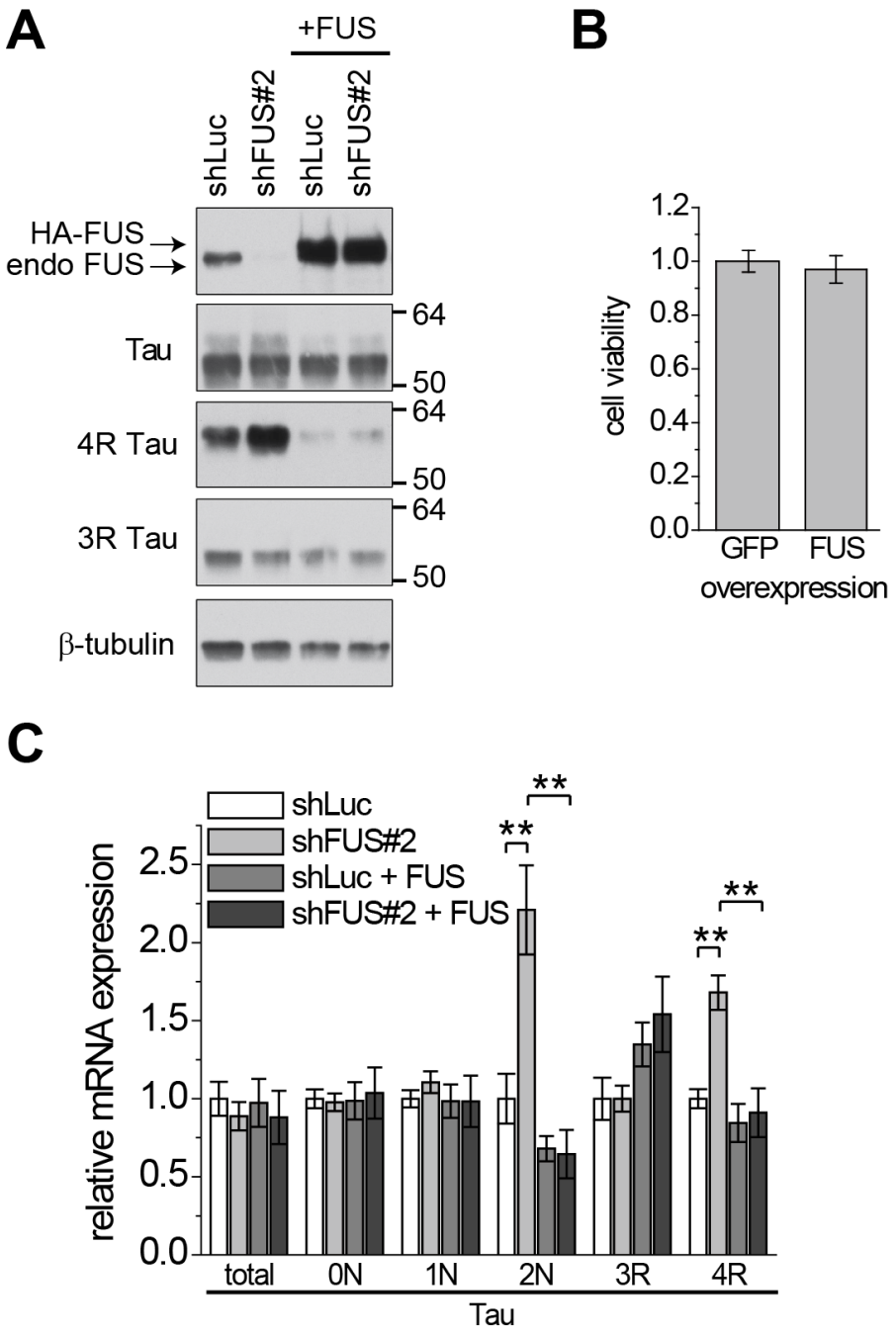

Figure 13 Reintroduction of human FUS fully rescues aberrant TAU splicing

Hippocampal neurons were transduced (DIV2+7) with lentivirus to express the indicated shRNA against FUS (shFUS#2) or non-targeting control shRNA (shLuc) and co-transduced with lentivirus to express HA-tagged shRNA resistant human FUS. **(A)** Immunoblots using indicated antibodies. Note that overexpression of human FUS leads to a marked decrease in 4R TAU levels in both shLuc and shFUS conditions. **(B)** Cell viability measured with XTT assay shows no significant alteration upon FUS overexpression, compared to control cells expressing GFP. mean +/- SEM are shown, student's t-test, n = 12. **(C)** Total RNA was analyzed by quantitative PCR for total TAU and TAU isoforms. Total TAU expression was normalized to the housekeeping gene YWHAZ and TAU isoform expression was normalized to total TAU levels. Note that samples from shLuc and shFUS treated neurons were statistically indistinguishable when co-transduced to express HA-tagged shRNA resistant human FUS. n=3, mean +/-SEM are shown, ANOVA with Bonferroni correction: **p<0.01.

4.1.8. Overexpression of FUS in hippocampal neurons alters TAU splicing

After confirming the effect of reintroducing FUS to a control or knockdown condition, the question arose if the overexpression of FUS alone would also alter TAU alternative splicing. Animal models overexpressing wildtype or mutant FUS often show detrimental effects (Lanson Jr & Pandey, 2012; Shelkovnikova, 2013). It is, however, not known if these models also show altered TAU splicing. *FUS* mutations that cause ALS cluster around the NLS domain at the C-terminus of the protein (Dormann & Haass, 2013). This observation led to the notion that the NLS has an important role in the pathomechanism behind the disease. Therefore, for the overexpression experiments I also used FUS ΔC mutant, which lacks the NLS domain (deletion of amino acids 514-526).

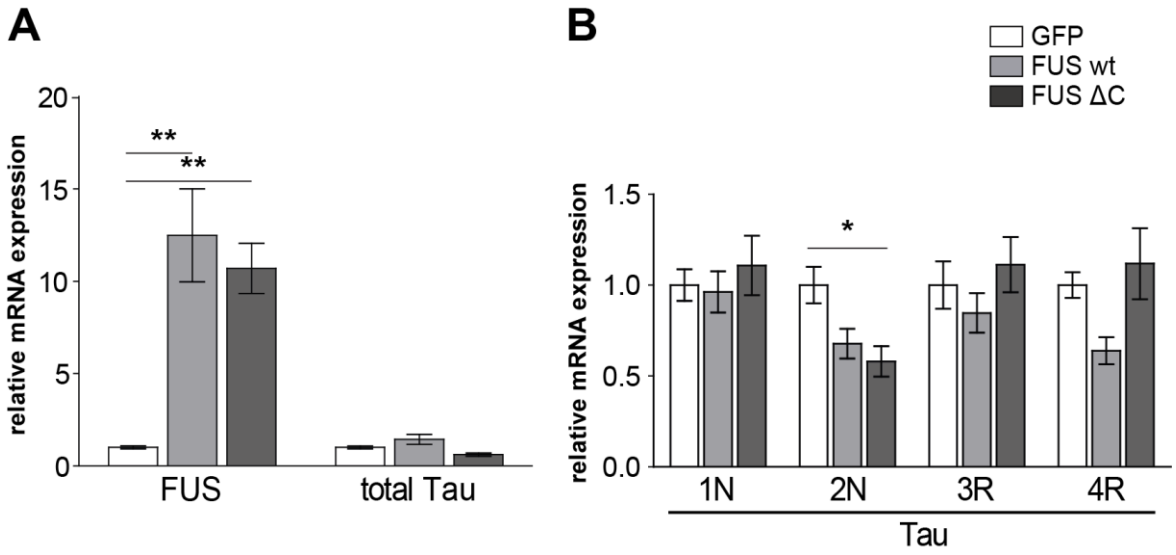

Figure 14 Overexpression of FUS in hippocampal neurons alters TAU splicing

Hippocampal neurons were transduced (DIV3+6) with lentivirus to express either HA-tagged human wildtype FUS (FUS wt), human mutant FUS (FUS ΔC) or GFP as a control. **(A)** Total RNA was analyzed by quantitative PCR for FUS and total TAU expression, normalized to housekeeping gene YWHAZ **(B)** TAU isoform expression was normalized to total TAU levels. n=4, mean +/-SEM are shown, one-way ANOVA with Dunnett's post-test.

Hippocampal neurons were treated with lentivirus on day 3 after plating to express GFP, wildtype or mutant FUS individually. RNA samples were collected after 6 days of transduction. The overexpression was assessed with qPCR, and both wildtype and mutant FUS showed a 10-12 fold higher expression than the GFP control (Figure 14A). Total TAU levels were decreased in mutant FUS samples, however, the difference was not statistically significant. As expected from the previous results, overexpression of wildtype FUS resulted in decreased expression of 2N and 4R TAU. Interestingly, mutant FUS overexpression reduced only 2N TAU levels and not 4R TAU levels (Figure 14B).

Overall, these results confirm the influence of FUS on TAU alternative splicing because increased wildtype FUS levels result in altered splicing of TAU exon 3 and exon 10. In contrast, overexpressed mutant FUS did not alter 4R TAU expression, which could indicate a loss of FUS function in regulating alternative splicing of TAU exon 10.

4.2. FUS interacts with TAU pre-mRNA

4.2.1. FUS associates with TAU pre-mRNA in mouse brain

FUS binds RNA and is known to be part of the spliceosome (Hartmuth et al, 2002; Rappsilber et al, 2002; Zhou et al, 2002). To test whether FUS associates with TAU mRNA, I performed immunoprecipitations (IP) of endogenous FUS from mouse brain (P15) extracts using a FUS antibody. A GST antibody was used as a negative control. The bound RNA was isolated from the immunoprecipitated samples and the abundance of RNA transcripts was estimated by comparing the percentage of recovery between control and FUS IP after reverse transcription and qPCR. Pre-mRNA levels were analyzed using intronic primers (Figure 15A) and mRNA levels using exonic primers.

Immunoblotting confirmed specific immunoprecipitation of endogenous FUS compared to control IP with GST antibody (Figure 15B). The relative recovery of TAU pre-mRNA bound to FUS was significantly higher than the control IP, with about 1% recovery of the input material in the FUS IP sample (Figure 15C). Also total TAU mRNA was significantly enriched in the FUS IP, but to a lesser extent than TAU pre-mRNA. Two recently identified FUS binding targets SON and FUS mRNA (Hoell et al, 2011), served as positive controls and also showed significant association with FUS at comparable levels to the TAU mRNA. In contrast, neither glyceraldehyde-3-phosphate dehydrogenase (GAPDH) pre-mRNA nor mRNA showed a significant association to FUS, compared to the control IP (Figure 15C). The qPCR end product was visualized in an agarose gel and also confirms the qPCR results (Figure 15B,C). Additionally, PCR products were confirmed by sequencing.

Taken together, these results show that FUS is associated with TAU pre-mRNA and mRNA in the mouse brain.

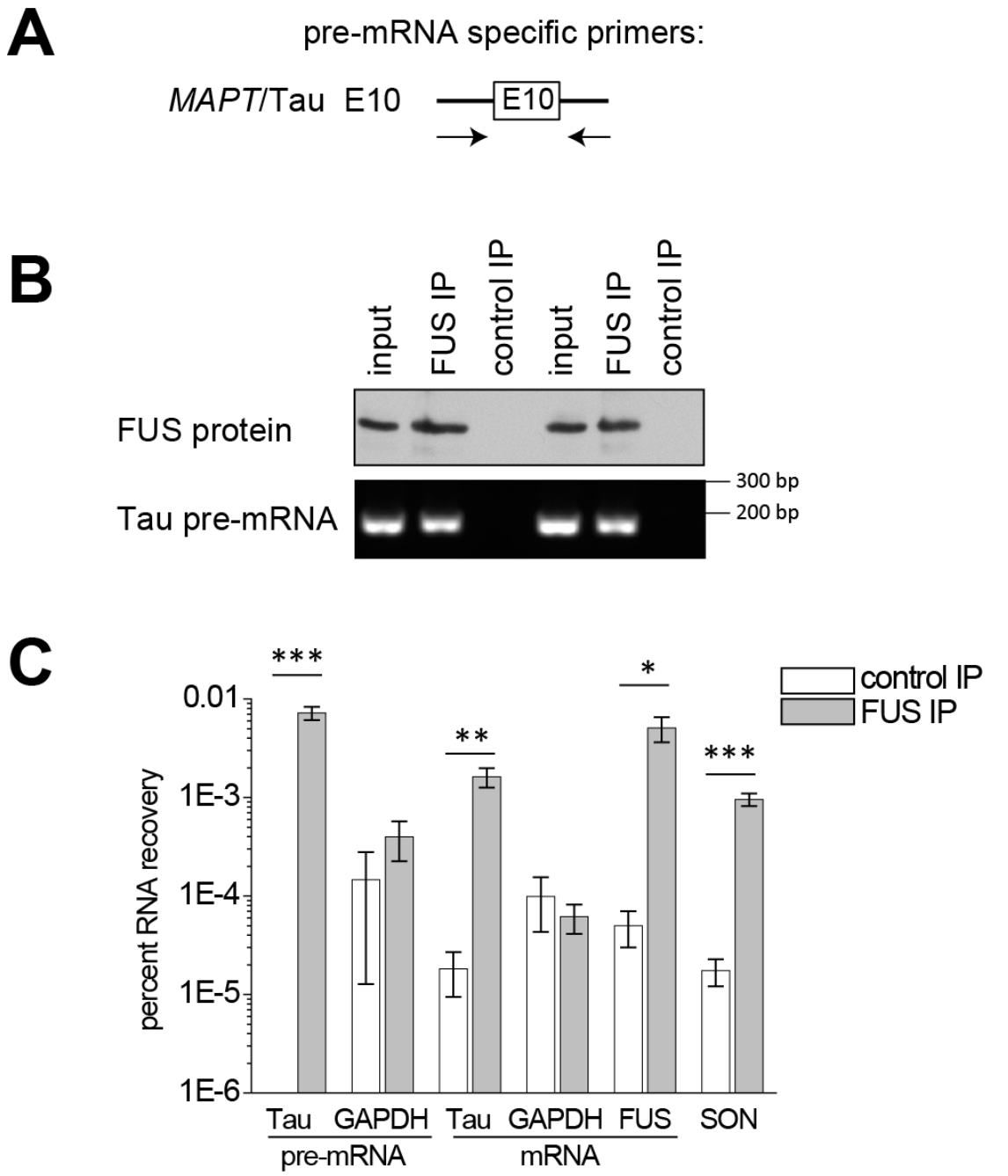

Figure 15 Endogenous FUS associates with TAU pre-mRNA in the mouse brain

Mouse brain (age 15 days) lysates were used to perform immunoprecipiations with anti-FUS antibody and control anti-GST antibody followed by RNA extraction and quantitative analysis of the bound RNA. RNA associated with FUS was reverse transcribed and analyzed by quantitative PCR. **(A)** Primers used for TAU E10 pre-mRNA quantitative PCR bind in introns adjacent to TAU exon 10. **(B)** Immunoblot using anti-FUS antibody shows input material, FUS- and control-immunoprecipitates (upper panel). PCR product after quantitative PCR analysis shown in (C) (lower panel). PCR products were confirmed by sequencing. **(C)** RNA recovery from FUS- and control-immunoprecipitates. For each group, individual immunoprecipitations from six mouse brains were analyzed by quantitative PCR. n=6, mean +/- SEM are shown, student's t-test: *p<0.05, **p<0.01, ***p<0.001. Note that SON primers span a verified FUS-binding motif within a large exon and therefore amplify both pre-mRNA and mRNA. SON and FUS mRNA binding serve as positive controls.

4.2.2. Endogenous FUS directly binds TAU pre-mRNA

To test whether the association of FUS to TAU pre-mRNA is direct and not mediated by an unknown co-immunoprecipitated protein, I performed RNA binding assays with biotin labeled RNA probes and a UV-crosslinking step. I used mouse TAU RNA probes surrounding the regulated exons 3 and exon 10 to roughly map the FUS binding regions (Figure 16A). Genomic TAU fragments covering the regions of interest were PCR amplified from mouse genomic DNA and cloned in a vector under a T7 promoter (pGEM3). Labeled RNA was generated by *in vitro* transcription using biotin-UTP as the labelling nucleotide.

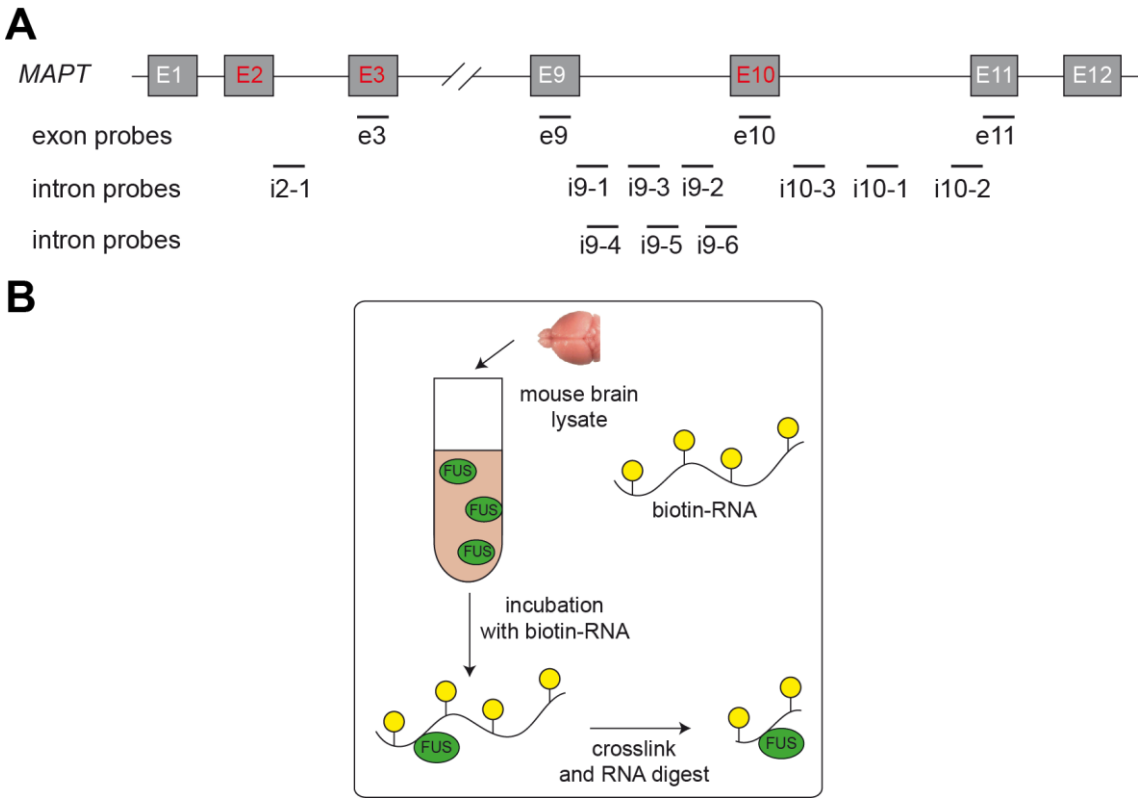

Figure 16 RNA binding assay setup to evaluate FUS interaction with TAU pre-mRNA in mouse brain lysates

(A) Scheme of regions covered by the TAU RNA probes used for RNA-binding assay. The alternatively spliced exons are marked in red. **(B)** Experimental setup of RNA-binding assay. Biotin-labelled RNA probes (yellow) were incubated with mouse brain lysates. After crosslinking with ultraviolet (UV)-light, the samples were digested with RNAase A, followed by immunoprecipitation using anti-FUS antibody or control anti-GST antibody. Immunoprecipiated protein-RNA complexes were analyzed by immunoblotting with streptavidin-HRP and anti-FUS antibody.

For the cross-linking experiments, biotinylated RNA probes were first incubated with a mouse brain extract. After incubation, the samples were subjected to UV crosslinking to capture interacting partners. In order to remove excess RNA, the samples were treated

with RNase A to digest unbound RNA. In this process, the protein-RNA interaction protects a short RNA fragment from being digested and the remaining peptide is sufficient to label the protein with biotin. FUS endogenous protein is then immunoprecipitated from the lysate to evaluate the potential binding to the labeled RNA probes. At the end, biotinylation of FUS, detected by immunoblot using streptavidin-HRP, indicates a direct interaction with the labeled RNA (Figure 17).

The mouse brain lysate used as an input for the RNA binding assay had to first be pre-cleared from endogenous biotinylated proteins to allow a better signal detection. The pre-clearing was successful as shown by the streptavidin-HRP immunoblot, with approximately less than 50% biotin signal left after pre-clearing (Figure 17A). Note that the prominent biotin bands in the brain lysate do not run in the SDS-PAGE gel at the same height as FUS (arrow, Figure 17A). Interestingly, the pre-clearing step does not influence the endogenous FUS levels suggesting that FUS is not endogenously biotinylated in the brain. As expected from the previous results, exonic GAPDH probes (GAPDH e3 and e5) showed no biotin signal in the FUS immunoprecipitates (compare Figure 15 to Figure 17C). Also the no-RNA control showed no positive signal. In general, FUS binding to TAU probes was more prominent at intronic regions. Exonic RNA probes e3 and e9 showed no binding, whereas probes e10 and e11 showed some binding. Significant binding was observed using intronic probes: i2-1, i10-1, i10-2, i9-4, i9-6, i9-1, i9-2 and i9-3 (Figure 17C,D). TAU intronic probes that were not bound at all (i10-3 and i9-5) further show the specificity of the binding in this assay because not all intronic probes show a biotin signal (Figure 17B,C). Interestingly, the probes with the most significant binding (i9-1, i9-2, i10-2) are all located around the regulated exon 10.

These results indicate a direct binding of endogenous FUS to TAU pre-mRNA specifically at sites around the FUS-regulated exons 3 and 10.

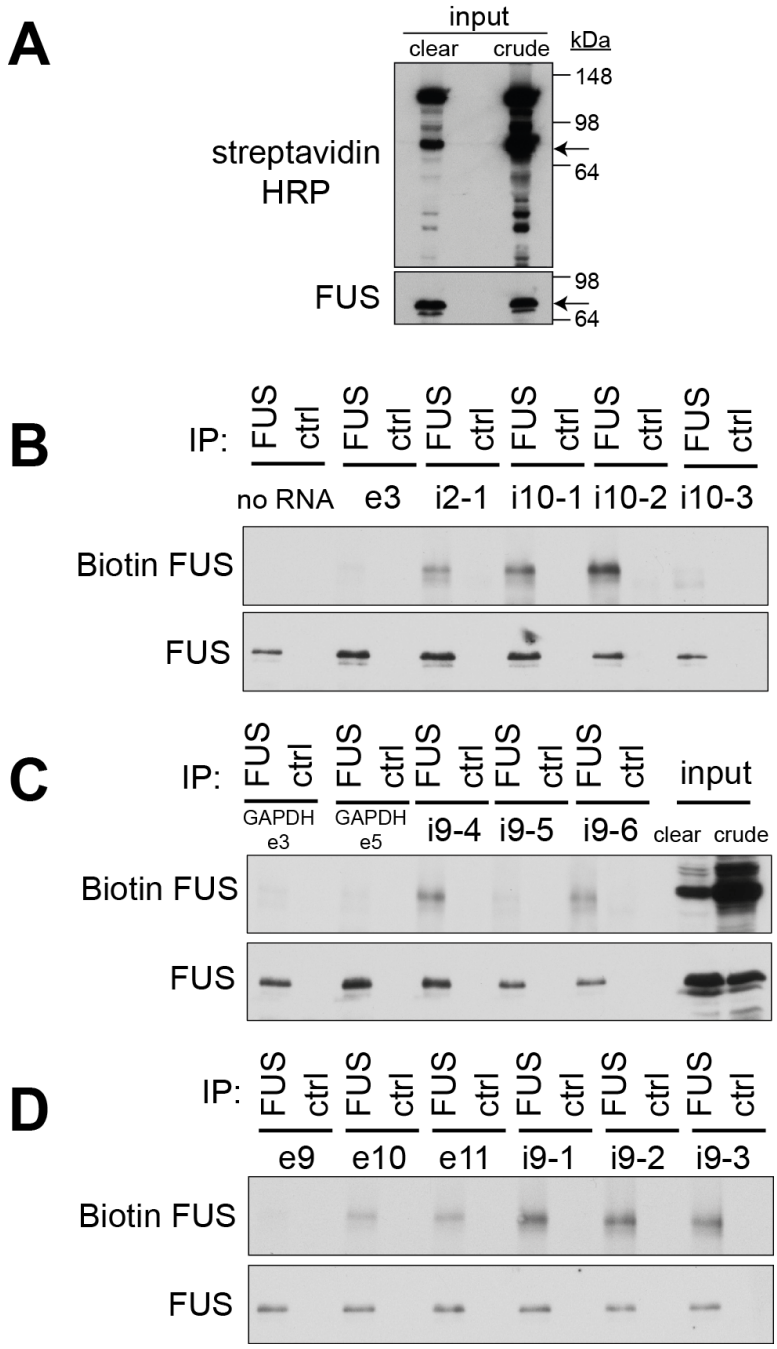

Figure 17 Endogenous FUS directly binds TAU pre-mRNA in the mouse brain

Mouse brain lysates (age 15 days) were incubated with biotin-labeled TAU RNA probes and crosslinked with ultraviolet (UV)-light. Protein-RNA complexes were immunoprecipitated with anti-FUS or anti-GST antibody as control and analyzed by immunoblotting with streptavidin-HRP and anti-FUS antibody. **(A)** Immunoblot with streptavidin-HRP of the mouse brain lysate after (clear) and before (crude) clearing. Note that the input was successfully cleared from biotin-proteins without altering the FUS levels in the samples. The arrow points the location of the FUS band in the blot. Note that none of the prominent biotin bands runs exactly at the same position as FUS. (**B, C, D**) Immunoblots from FUS- and control-immunoprecipitates. Positive signal with streptavidin-HRP (Biotin-FUS signal) indicates direct binding between FUS protein and labeled TAU RNA probe. Lysates that were not incubated with RNA (no RNA) but otherwise treated as the other samples served as a negative control **(B)**. **(C)** GAPDH RNA probes were also used as negative controls.

4.2.3. Endogenous FUS preferentially binds TAU pre-mRNA at conserved regions in introns

In order to identify a sequence that could determine FUS binding to RNA, I first evaluated the conservation of sequences between mouse/rat/human in probes that showed strong binding. I then evaluated emerging sequence patterns among those probes.

First, sequences from bound probes showed a good conservation between human and rodent, despite being intronic sequences (Figure 18). Such conserved regions in introns can point to regulatory elements in the sequence. Second, I evaluated the frequency of AUU-rich regions, which are reported to be a RNA motif preferentially bound by FUS in a recent crosslinking and immunoprecipitation (CLIP) study in HEK 293-FT cells (Hoell et al, 2011). I found many such AUU motifs in the binding probes. Interestingly, mouse TAU pre-mRNA contains three AUU-rich regions in intron 9 (9-17 AUUs in 300 nucleotides). Probe i9-2, which is located closest to exon 10, encompasses 17x AUU motifs and shows a good conservation between rodents and humans (Figure 18B). AUUs were however not absolutely required, as a probe with low AUU content (e.g. i2-1) also showed strong binding (compare Figure 18A to Figure 17B).

These results lead to the conclusion, that endogenous FUS in mouse brain binds TAU mRNA at conserved regions preferentially in introns. These regions were often, but not always, AUU-rich sequences.

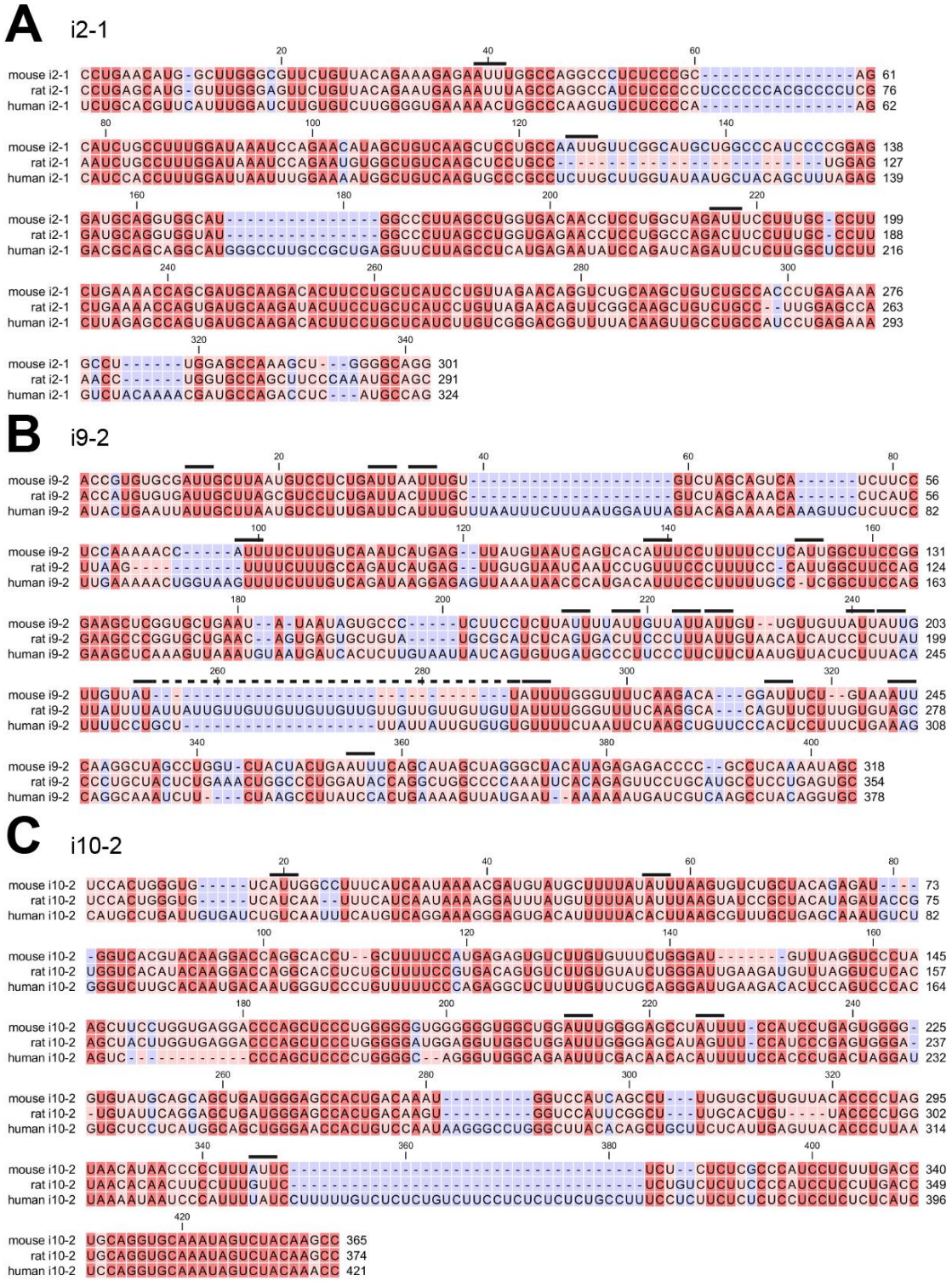

Figure 18 Alignment of mouse, rat and human TAU pre-mRNA for FUS interacting probes i2-1, i9-2 and i10-2

Alignment of sequences retrieved from Ensembl for the mouse TAU pre-mRNA probes i2-1 **(A)**, i9-2 **(B)**, i10-2 **(C)** and the homologue sequences in rat and human *MAPT*. Conserved residues are marked in red, semi-conserved in pink and gaps or residues not-conserved are marked in blue. AUU motifs in the mouse sequence are marked with a black bar above the mouse sequence. Note the high degree of conservation for probes that show strong binding to FUS protein (compare to Figure 17).

4.3. FUS regulates TAU alternative splicing in human cell culture systems

4.3.1. TAU minigene constructs to study alternative splicing in cell lines

After confirming that FUS regulates alternative splicing of TAU through direct binding using rat hippocampal neurons and mouse brain extracts, the question arose if it would be possible to detect the influence of FUS on TAU splicing using a heterologous system. For this, two TAU minigenes constructs were cloned covering mouse exons 9 through 11 and exons 1 through 4, to evaluate the splicing events around exon 10 and exon 2/3 separately (Figure 19). The minigene constructs include the full intron sequences between the exons evaluated. Two tags, myc and HA, at the N-terminal and C-terminal part of the sequences respectively, allow detection of the spliced fragments at protein level by immunoblotting.

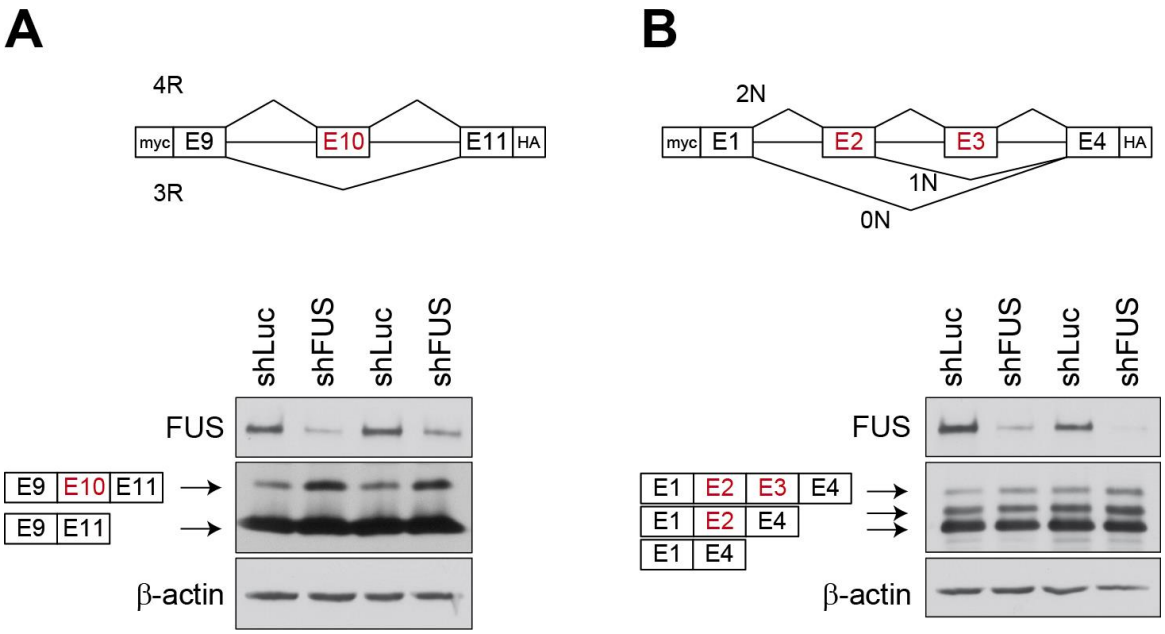

Figure 19 FUS knockdown alters splicing of a TAU minigene in HEK 293-FT cells

HEK 293-FT cells were co-transfected with TAU minigenes and the indicated shRNAs. The shRNA against FUS targets specifically the human FUS gene. The TAU minigenes reflect splicing events around exon 10 **(A)** or around exon 2 and exon 3 **(B)**. The processed reporter protein is HA-tagged and is detected in immunoblotting with HA antibody. FUS and beta-actin blots confirm the knockdown efficiency. Note that FUS knockdown in HEK 293-FT cells results in a strong shift in alternative splicing only in the E9-E11 TAU minigene and not the E1-E4 TAU minigene.

HEK 293-FT cells were first transfected on day 1 with constructs expressing shRNAs (shLuc control or FUS shRNA) to allow for sufficient knockdown. After re-plating on day 2, control and FUS knockdown HEK 293-FT cells were additionally transfected on day 3 with the TAU minigene constructs. The protein samples were analyzed with immunoblotting. HEK 293-FT cells transfected with the E9-E11 minigene construct and

control shRNA (shLuc) predominantly expressed the smaller TAU fragment corresponding to the 3R isoform and some 4R fragment. Upon FUS knockdown, however, there was a strong increase in expression of the 4R corresponding TAU fragment, indicating preferential exon 10 inclusion upon loss of FUS (Figure 19A). In contrast, the E1-E4 TAU minigene was processed similarly in both shLuc control and FUS knockdown HEK 293-FT cells. The samples showed similar abundance of the three protein products corresponding to the 0N isoform, lacking exon 2 and 3; 1N isoform containing only exon 2; and 2N isoform containing both exon 2 and exon 3 (Figure 19B).

Together, these results confirm, in a heterologous system, that FUS knockdown results in preferential inclusion of exon 10. The splicing event involving exons 2 and 3 could not be confirmed in HEK 293-FT cells, which may be due to the lack of additional neuron-specific splicing factors in these cells.

4.3.2. LUHMES cells: human neuronal-like cell culture system to study TAU

The alternative splicing of TAU is markedly different between mouse/rat and humans. Although the shift during development towards longer TAU isoforms is common to mouse, rat and humans, there is a marked difference in the ratio between 3R and 4R TAU reached in adulthood. Adult mice and rats express predominantly the largest 4R TAU isoform (Kosik et al, 1989). Adult humans, in contrast, express both 3R and 4R TAU isoforms at a delicately controlled 1:1 ratio (Gao et al, 2000). This ratio, when disturbed for example by *MAPT* mutations, can cause FTD (Brunden et al, 2008). In order to link the role of FUS on TAU splicing to human neurodegenerative diseases, it was very important to confirm the results also in human cells expressing TAU.

For this, I used the human mesenchymal cell line LUHMES (Lund human mesencephalic), which is immortalized by myc-expression (Lotharius et al, 2002; Lotharius et al, 2005; Scholz et al, 2011). LUHMES cells, in the dividing culture, are small irregularly shaped cells that tend to form colonies (Figure 20B). By changing growth factors and adding tetracycline to repress the transgenic v-myc oncogene, LUHMES cells stop dividing and differentiate into postmitotic neuronal-like cells (Figure 20A). The differentiation process is fast and cells begin to elongate and take a neuronal-like shape already after 3 days of differentiation. By day 6, the cells reach the typical morphology of a mature neuron, including long neuronal processes and small rounded

cell bodies (Figure 20B). Cells at this stage show expression of neuronal and synaptic markers and lose expression of embryonic cell markers (Scholz et al, 2011).

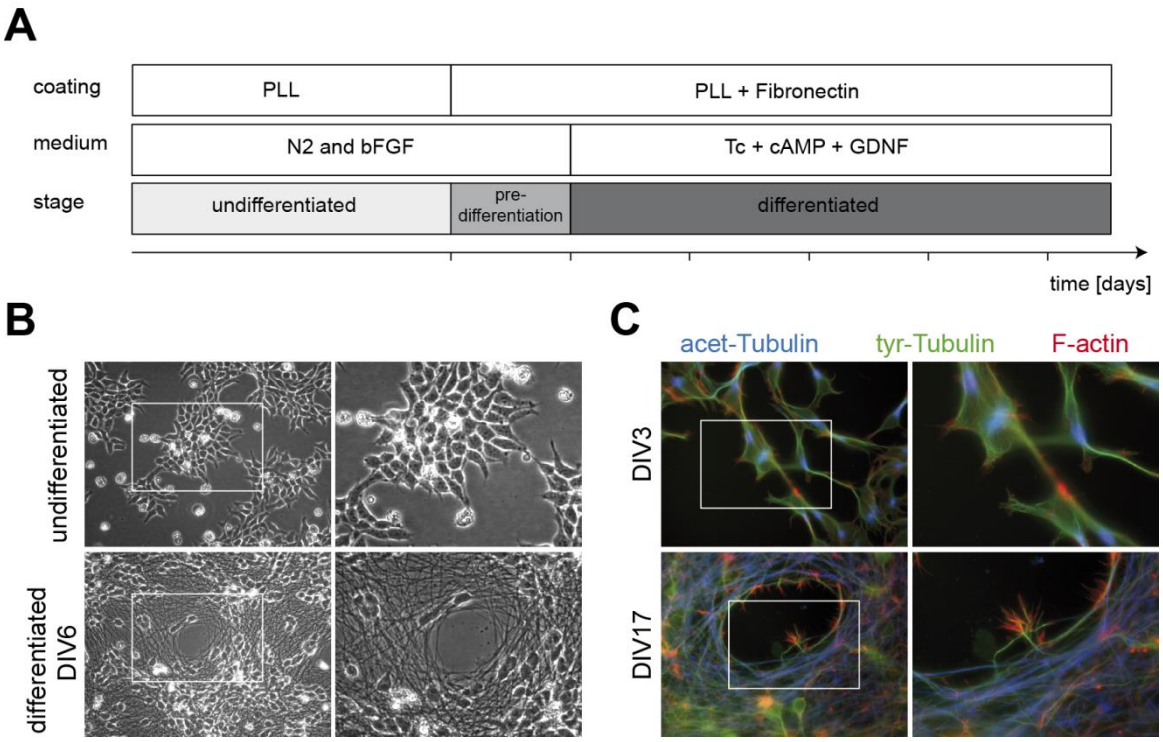

Figure 20 LUHMES cells as a human cell culture model to study TAU

Lund human mesencephalic (LUHMES) cells are human mesencephalic cells transformed by overexpressing the v-myc oncogene controlled by tetracycline. The cell line is a subclone of the MESC2.10 cell line originating in Lund University, Sweden (Lotharius et al, 2002). **(A)** Scheme followed to differentiate the LUHMES cells line into neuronal-like cells. The coating condition (PLL or PLL + Fibronectin) and the medium supplemented with (N2 + bFGF) or (Tetracycline + cAMP + GDNF) provide the signals for the cells to stop dividing and to differentiate. After 6 days, LUHMES cells have completed the differentiation process. Adapted from: (Lotharius et al, 2005; Scholz et al, 2011). **(B)** Bright field images of living cells at the undifferentiated stage (upper panel) and after six days of differentiation (lower panel). Right panels show a higher magnification view of the area marked with white boxes in the left panel. Note the marked morphological changes that LUHMES cells undergo during differentiation. **(C)** Immunostaining of LUHMES cells after 3 days (upper panel) or 17 days (lower panel) of differentiation using phalloidin (red) to stain F-actin and using antibodies against acetylated tubulin (blue) or tyrosinated tubulin (green), to evaluate the stable and dynamic tubulin populations. The acetylated tubulin population generally represents stabilized microtubules and the tyrosinated tubulin population represents dynamic microtubules. Note that the acetylated population becomes prominent at later stages of differentiation. Right panels show a high magnification view of the area marked with white boxes in the left panel.

The differentiation process and maturation of the cytoskeleton was monitored by immunofluorescence with cells fixed at different time points. The growth cone structure was visible from DIV 3 and showed typical neuronal growth cone shape with F-actin staining at DIV 17. Both acetylated and tyrosinated tubulins, used here as markers for

stabilized and dynamic microtubules respectively, showed the expected normal distribution, as in primary cultured neurons (Figure 20C) (Witte et al, 2008).

In summary, LUHMES cells were successfully differentiated into neuronal-like cells with typical neuronal morphology of the cytoskeleton.

4.3.3. FUS knockdown in LUHMES cells results in increased 4R TAU expression

Transduction of differentiated LUHMES cells with lentivirus to knockdown or overexpress human FUS was successful, although compared to rat neurons, higher lentivirus concentration was needed to achieve >90% transduction efficiency. FUS knockdown was >95% efficient, as confirmed by immunoblotting and qPCR (Figure 21A,B). Overexpression of HA-human FUS was also efficient and reached a 13x increase compared to control cells expressing GFP. Total TAU mRNA level was not significantly altered neither by FUS knockdown nor by FUS overexpression (Figure 21B). Interestingly, immunoblots with TAU antibody showed altered running behavior of the TAU isoforms in FUS knockdown samples (Figure 21A). The band pattern was, however, not identical to that of rat neurons (compare Figure 7 to Figure 21) and corresponded mainly to the 3R TAU isoforms. 4R TAU was undetectable in immunoblots. qPCR analysis revealed 0N3R as the most abundant TAU isoform expressed in LUHMES cells at DIV7+9 and confirmed the low expression of 4R TAU with markedly higher Ct values (data not shown). Further, qPCR analysis revealed a significant increase in 4R TAU expression upon FUS knockdown similar to the effect seen in rat primary neurons. Also as expected, FUS overexpression resulted in a slight decrease in 4R TAU expression. In contrast, TAU exon 3 splicing remained largely unchanged in LUHMES cells upon FUS knockdown.

In summary, these results demonstrate that altering FUS levels in human neuronal-like cells also influences alternative splicing specifically of TAU exon 10. Different reasons could account for the discrepancies between rat primary neurons and human neuronal-like cells regarding splicing of exon 2 and exon 3, including missing co-regulatory factors in the differentiated human cell line compared to the rat primary neurons.

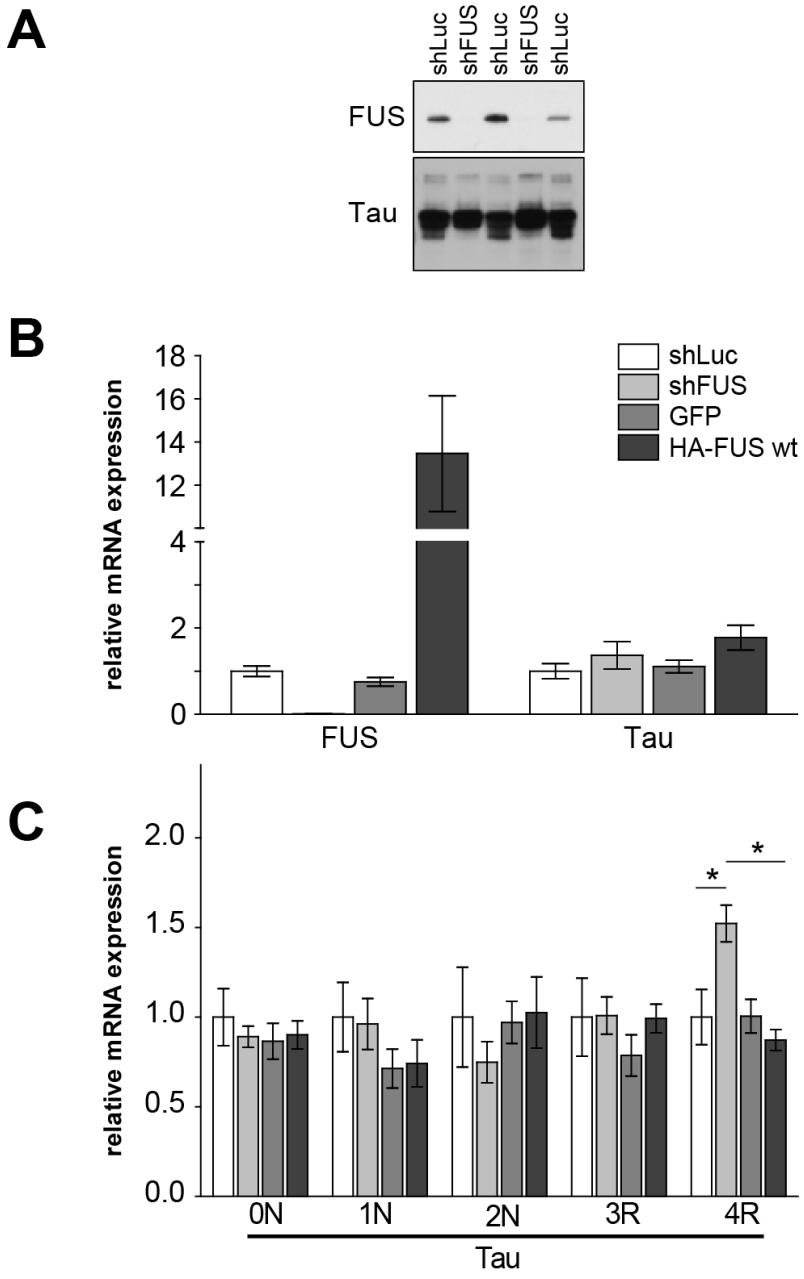

Figure 21 FUS knockdown in differentiated LUHMES cells results in increased 4R TAU expression

LUHMES cells were transduced with lentivirus to express shRNAs (shLuc control or shFUS) after 7 days of differentiation. The shFUS construct used here targets specifically human FUS. Lentivirus was also used to overexpress GFP or HA-FUS wildtype in LUHMES cells. Protein and RNA samples were collected 9 days after transduction and analyzed with immunobloting or quantitative PCR respectively. **(A)** Immunoblot of LUHMES cell samples using anti-FUS and anti-TAU antibodies. The FUS blot confirms the efficiency of the knockdown and the TAU blot shows marked differences in the running behavior of TAU. **(B)** Quantitative PCR analysis of FUS knockdown or overexpression LUHMES cell samples. FUS and total TAU expression was normalized to the housekeeping gene YWHAZ. n=3, mean +/-SEM are shown. Note the efficiency of the FUS knockdown and HA-FUS overexpression. Total TAU levels were not significantly altered. **(C)** Quantitative PCR analysis of FUS knockdown or overexpression in LUHMES cell. TAU isoforms expression was normalized to total TAU levels. n=3, mean +/-SEM are shown, one-way ANOVA with Dunnett's post-test: *p<0.05.

4.4. Functional consequences of FUS knockdown in neurons

4.4.1. Early FUS knockdown in neurons results in shorter axons and aberrant growth cone morphology

Based on the results presented here showing that FUS regulates the alternative splicing of TAU, I focused my evaluation of functional consequences of FUS knockdown on the development and morphology of neuronal axons. Additionally, neurons cultured from FUS knockout mice show altered spine morphology (Fujii et al, 2005), which also prompted an evaluation of the axonal morphology in FUS deficient neurons.

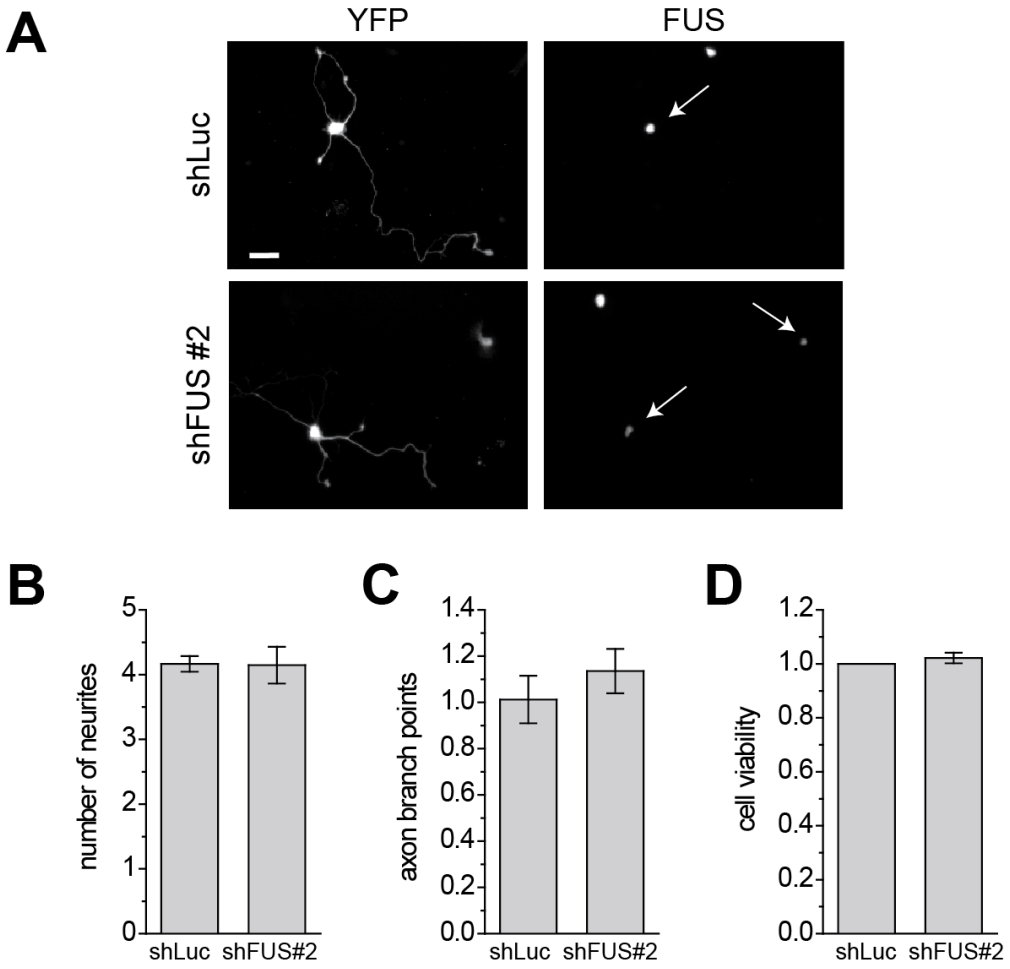

Figure 22 Early FUS knockdown in hippocampal neurons does not affect neurite growth, axonal branching or cell viability

Rat hippocampal neurons were co-transfected before plating with the indicated shRNAs (shLuc or shFUS) and pEYFP-C1 to control the transfection. **(A)** Immunostaining after 4 days in culture with the indicated antibodies. The arrows mark transfected cells. **(B)** Quantification of number of neurites, **(C)** number of axonal branch points, and **(D)** cell viability (DIV14) of neurons with early knockdown of FUS. Note that prolonged FUS knockdown did not significantly alter cell viability. Note also that control and FUS knockdown cells are statistically indistinguishable regarding number of neurites, number of axonal branch points or cell viability. Values presented as mean +/-SEM, n=3, student's t-test, all not significant.

To address this question, freshly isolated rat hippocampal neurons were transfected before plating with shRNA control (shLuc) or against FUS (shFUS) using nucleofection (Lonza). After 4 days *in vitro* (DIV 4), FUS knockdown was confirmed by immunostaining. The transfected cells (arrows) expressed significantly less FUS compared to the non-transfected neighboring cells (Figure 22A). Cell viability was not affected and around 90% of the cells had formed an axon by day 4 in both control and knockdown conditions (Figure 22D). Also the number of neurites and the number of axonal branch points did not significantly change with FUS knockdown (Figure 22B,C).

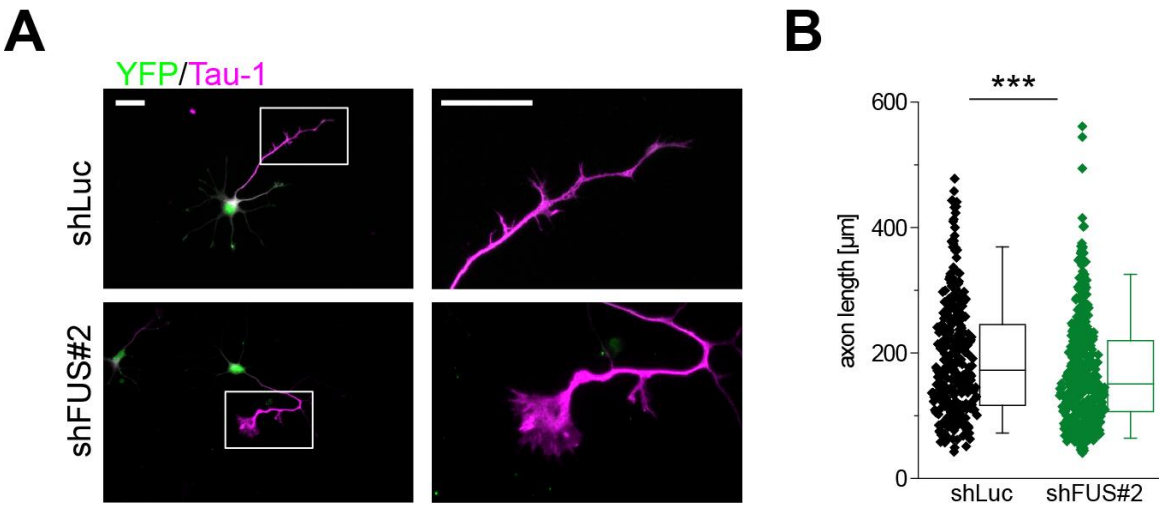

Figure 23 Early FUS knockdown in hippocampal neurons reduces axon length

Rat hippocampal neurons were co-transfected before plating with the indicated shRNAs (shLuc or shFUS) and pEYFP-C1 to control the transfection. **(A)** Immunostaining after 4 days in culture with the indicated antibodies. TAU1 is used as axonal marker. The field marked with a white box in the left panel is shown in higher magnification in the right panel. **(B)** Quantification of axonal length (n= 325 shLuc, n= 388 shFUS#2) measured blinded to the experimental condition. The box-plots represent the lower quartile, median, and upper quartile. The whiskers represent the 5th and 95th percentile. For the morphometric analysis, the axon was defined as the longest process with proximal-to-distal TAU1 gradient. Mann–Whitney test: ***P<0.001. Scale bars: 25 µm.

Despite the unchanged viability and normal axonal branching, the quantification of axonal length did show a small but significant decrease in axonal length in the FUS knockdown group (Figure 23).

While quantifying images, I constantly noticed a disturbed morphology of the axonal growth cone in the FUS knockdown condition (Figure 23, 24). FUS knockdown neurons developed severely enlarged growth cones that, in contrast to the control conditions, showed prominent TAU staining.

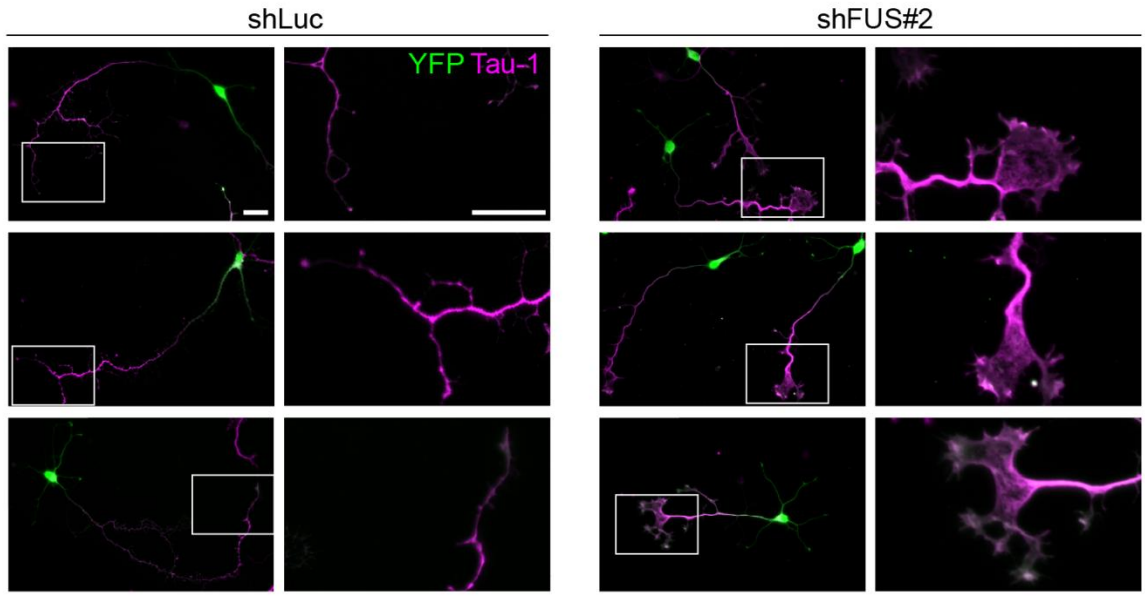

Figure 24 Extensive TAU staining observed in enlarged axonal growth cone of FUS depleted hippocampal neurons

Rat hippocampal neurons were co-transfected before plating with the indicated shRNAs (shLuc or shFUS) and pEYFP-C1 to control the transfection. Immunostaining after 4 days in culture with the indicated antibodies. TAU1 is used as axonal marker. The field marked with a white box in the left panel is shown in higher magnification in the right panel. For the morphologic analysis, the axon was defined as the longest process with proximal-to-distal TAU1 gradient. Scale bars: 25 µm.

F-actin and β3-tubulin stainings of control and FUS depleted neurons were used to better visualize the axonal growth cone (Figure 25). This staining corroborated the results previously obtained with TAU, since also the β3-tubulin staining showed prominent spreading of the microtubules further into the enlarged growth cone area, which had a less bundled appearance compared to the control transfected neurons (Figure 25). The quantification of the growth cone area showed a significant shift in the frequency of neurons showing enlarged growth cones. On average, the growth cones of FUS depleted neurons were twice as large as in the control cells (Figure 26).

Interestingly, the cytoskeletal phenotype (shorter axons with enlarged growth cones) of FUS depleted neurons strongly resembles the aberrant growth cone structure observed in TAU/MAP1B-double knockout neurons (Takei et al, 2000).

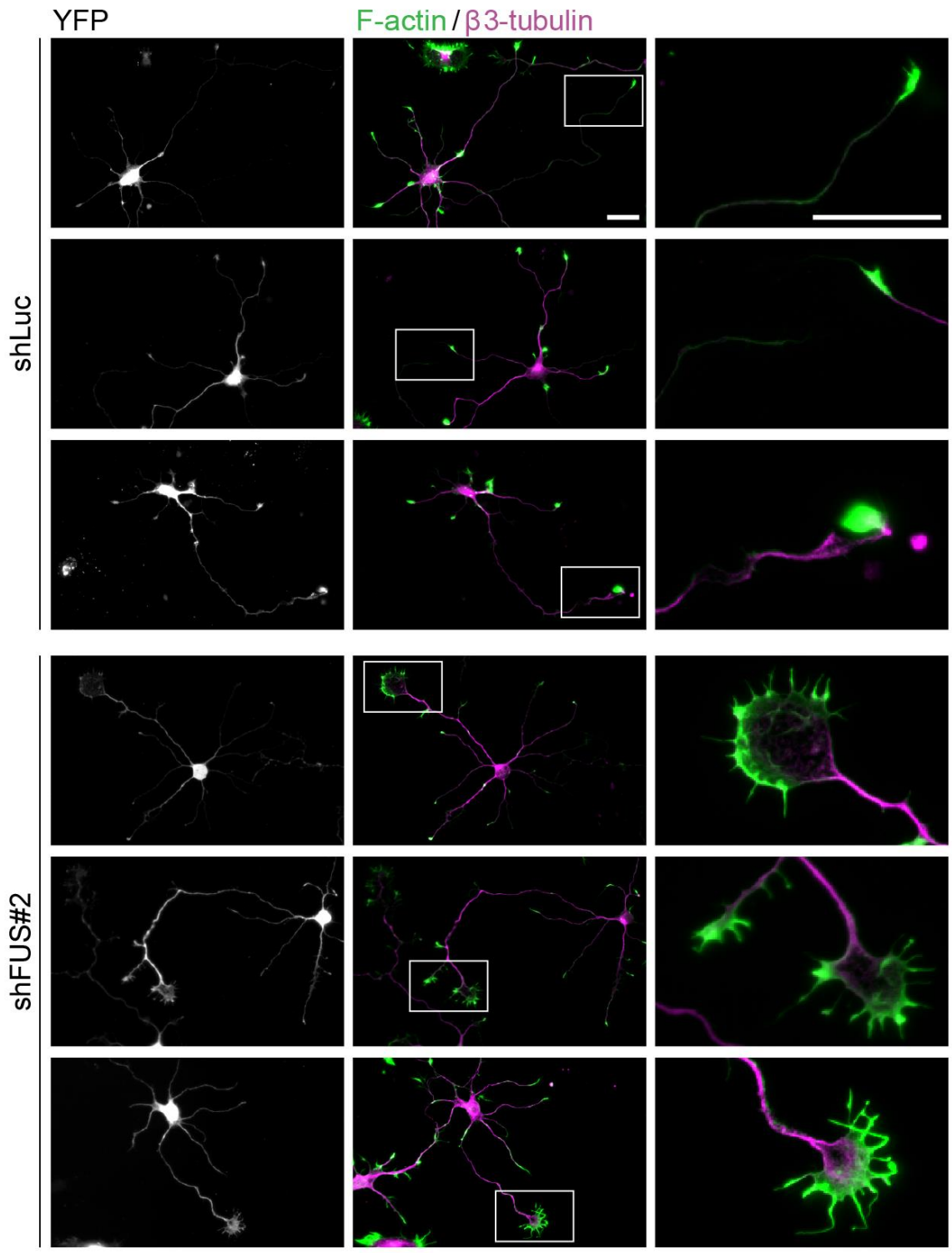

Figure 25 Early FUS knockdown in hippocampal neurons results in microtubules spreading further into the axonal growth cone area

Rat hippocampal neurons were co-transfected before plating with the indicated shRNAs (shLuc or shFUS) and pEYFP-C1. Immunostaining after 4 days in culture with the indicated antibodies and phalloidin to stain F-actin. Rightmost panels show a high magnification view of axonal growth cones, marked with white boxes in the middle panel. Scale bars: 25 µm.

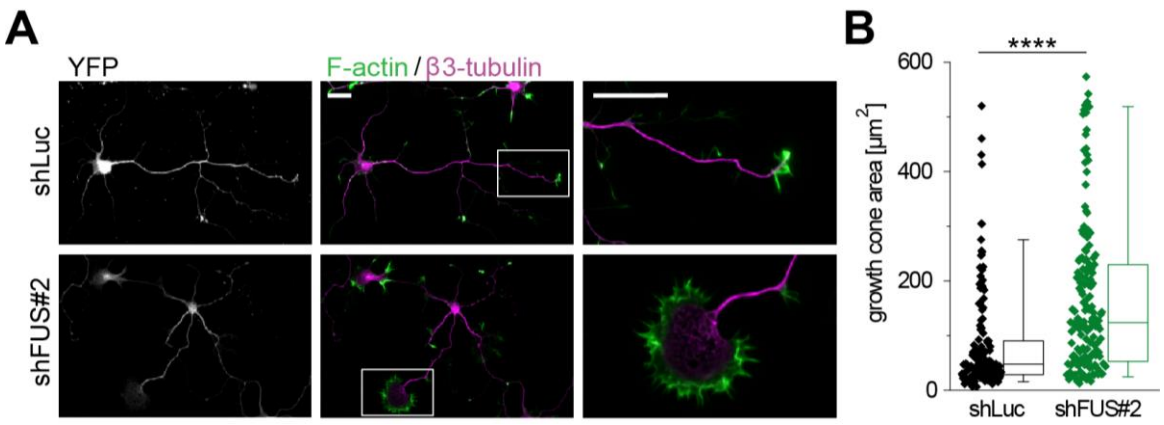

Figure 26 Early FUS knockdown in hippocampal neurons results in significantly enlarged growth cones

Rat hippocampal neurons were co-transfected before plating with the indicated shRNAs (shLuc or shFUS) and pEYFP-C1. **(A)** Immunostaining after 4 days in culture with the indicated antibodies and phalloidin to stain F-actin. Right panels show a high magnification view of axonal growth cones, marked with white boxes in the middle panel. **(B)** Quantification of growth cone area (n=147 shLuc, n= 164 shFUS#2) measured blinded to the experimental condition. The box-plots represent the lower quartile, median, and upper quartile. The whiskers represent the 5^{th} and 95^{th} percentile. For the morphometric analysis, the axon was defined as the longest process. Mann–Whitney test: ****P<0.0001. Scale bars: 25 µm.

All together, these results show that FUS has a crucial role in cytoskeletal organization especially at the axonal endings. In FUS knockdown cells, axons were significantly shorter and showed enlarged and disorganized growth cones.

5. Discussion

5.1. Identification of TAU as the first physiological FUS splicing target in neurons

FUS is genetically and pathologically linked to ALS and FTLD. On the one hand, pathogenic *FUS* mutations cause ALS, on the other hand, FUS positive neuronal cytoplasmic inclusions are found in a subset of ALS and FTLD cases (Kwiatkowski et al, 2009; Neumann et al, 2009a; Vance et al, 2009). The majority of pathogenic mutations disrupts the nuclear localization signal of FUS and cause cytoplasmic mislocalization of the protein (Bosco et al, 2010; Dormann et al, 2010). Thus, the loss of important nuclear functions of FUS could contribute to disease progression. FUS is also known to be a part of the spliceosome (Hartmuth et al, 2002; Rappsilber et al, 2002; Zhou et al, 2002), however, the physiological splice targets were unknown. In this study I identified and confirmed TAU as the first physiological splice target of FUS in neurons. FUS knockdown in rat neurons resulted in increased inclusion of TAU exon 3 and exon 10, leading to increased levels of 2N and 4R TAU. Reintroduction of human wild type FUS fully rescued aberrant splicing and demonstrated the specificity of the effect. Overexpression of wild type FUS had the opposite effect and caused a decrease in 2N and 4R TAU expression. In contrast, overexpression of mutant FUS lacking the nuclear localization signal (FUS ΔC) only influenced skipping of exon 3, but not of exon 10. These results confirmed that the N-terminal splice cassette (exons 2 and exon 3), and the C-terminal exon 10 can be regulated independently (Andreadis, 2005). They also suggest that FUS ΔC is somehow functionally impaired to influence specifically TAU exon 10 splicing, probably by a missing correct interaction with other proteins.

5.1.1. TAU splicing and functional consequences

The expression of TAU isoforms is tightly regulated during development, with predominant expression of the shortest isoform (0N3R) early in development and increased expression of the longest isoforms (2N4R and 2N3R) in adult stages (Andreadis, 2005; Liu & Gong, 2008). In adult human brain, the overall levels of 4R to 3R TAU are tightly regulated and kept at a 1 to 1 ratio. In contrast, adult mice and rats predominantly express 4R TAU.

Due to this difference, I also determined whether the FUS regulation of TAU splicing is conserved in humans using a twofold strategy. First, I analyzed splicing of a mouse *MAPT* minigene in FUS knockdown HEK 293-FT cells. Second, I evaluated alternative splicing of endogenous TAU in human neuronal-like cells (LUHMES) also with FUS

knockdown. Both approaches showed a significant increase in exon 10 inclusion upon FUS knockdown, which demonstrates that human FUS is also able to regulate splicing of TAU exon 10. In contrast, FUS knockdown had no effect on the splicing of exon 2 and exon 3 in the minigene and endogenous TAU. These results strongly suggest that FUS regulates primarily TAU exon 10 splicing in human neurons without affecting splicing of exon 3.

4R TAU isoforms have higher affinity to microtubules and contain additional phosphorylation sites, which can also regulate protein-protein interactions (Andreadis, 2005). The function of the TAU N-terminal part, including the conserved exon 2 and exon 3, is still poorly understood (Andreadis, 2005). It has been shown to associate with the plasma membrane (Brandt et al, 1995) and could regulate microtubules spacing (Chen et al, 1992). Changes in microtubule spacing in axons could have important consequences for axonal transport and microtubule dynamics. In addition, the N-terminus of TAU mediates the interaction with the membrane associated tyrosine kinase Fyn (Lee et al, 1998). Fyn functions in signaling pathways that regulate axon guidance, cell adhesion and cell differentiation by activating the small GTPase RAS. Interestingly, dendritic TAU has been shown *in vivo* to target Fyn to the postsynaptic compartment thereby transducing NMDA receptor mediated amyloid beta cytotoxicity (Ittner et al, 2010). Therefore, the cell signaling and structural functions of TAU could be directly affected by loss of FUS in neurons due to aberrant TAU alternative splicing.

5.2. *MAPT*/TAU is one of the top hits in genome-wide studies of FUS target genes

Concurrent unbiased studies have addressed the question of FUS splice targets and RNA binding partners on a genome wide level. They combined crosslinking immunoprecipiation (CLIP) and RNA sequencing to analyze changes in RNA metabolism upon loss of FUS in the mouse brain or in cultured neurons (Ishigaki et al, 2012; Lagier-Tourenne et al, 2012; Nakaya, 2013; Rogelj et al, 2012). These studies reinforce the notion that FUS is a key regulator of alternative splicing in the brain, because loss of FUS mainly alters splicing rather than transcription (Rogelj et al, 2012).

Importantly, the recent CLIP studies have robustly confirmed TAU as a FUS splice target (Ishigaki et al, 2012; Lagier-Tourenne et al, 2012; Rogelj et al, 2012). This finding is truly remarkable, because the overlap among studies is otherwise very limited. Most splice targets were identified in only one study and only six targets are reported in at least

three out of four studies. Additionally, the exact splice event reported was not always identical among studies, with the exception of TAU and NTNG1 (see below) (Annex 2). Such discrepancies may be attributed to differences in experimental conditions, because alternative splicing events are often specific to the type and age of tissue studied (Orozco & Edbauer, 2013).

In line with my results, the CLIP studies reported an increase of TAU exon 10 inclusion (Ishigaki et al, 2012; Lagier-Tourenne et al, 2012; Orozco et al, 2012; Rogelj et al, 2012) and an increase in exon 2 and exon 3 inclusion upon loss of FUS (Annex 2) (Lagier-Tourenne et al, 2012; Orozco et al, 2012). Very recently, the effect of FUS on splicing of TAU exon 10 was also reported in primary motor neurons, the primary site of ALS (Fujioka et al, 2013). Interestingly, the other robustly identified FUS splice target is Netrin-G1 (NTNG1), a membrane protein that functions in axon guidance. NTNG1 was previously linked to Parkinson's disease and schizophrenia (Aoki-Suzuki et al, 2005; Lin et al, 2009).

The biological relevance of hits identified in genome wide studies is validated with in depth analysis of the mechanism and functional consequences. In the case of FUS regulation of splicing, the candidate based approach presented here complements and expands the knowledge gained in the FUS CLIP studies.

Lastly, I also demonstrated the FUS specific regulation of TAU splicing with knockdowns of other ALS/FTD related proteins, such as TDP-43, TAF15, EWS or the uncharacterized C9orf72 which did not alter TAU splicing in neurons. This is in line with reports showing that there is only a small overlap of common target RNAs between FUS and TDP-43 and that TAU splicing is not affected by TDP-43 (Honda et al, 2014; Lagier-Tourenne et al, 2012; Rogelj et al, 2012). Also the binding pattern of RNA targets is markedly different between TDP-43 and FUS. TDP-43 binds the targets with surgical precision, whereas FUS binds targets more broadly along the nascent transcripts, which indicates a possible role in the stabilization of nascent RNA during transcriptional elongation and alternative splicing (Lagier-Tourenne et al, 2012; Rogelj et al, 2012).

5.2.1. Specificity of FUS RNA binding

When evaluating changes in alternative splicing, it is crucial to confirm a direct interaction between the protein and the target pre-mRNA, in order to exclude an indirect effect by other RNA-binding proteins or a general impairment of the spliceosome. In this

study, I first showed that endogenous TAU pre-mRNA is associated with FUS protein in mouse brain lysates using FUS-IP and qPCR analysis. Then, aiming for a more detailed understanding of the interaction, I corroborated the direct binding of FUS to TAU mRNA with RNA immunoprecipitation experiments using labeled-RNA probes. Interestingly, FUS was able to bind TAU pre-mRNA at the introns near the alternatively spliced exons.

Based on a previous report on a preference for AUU-rich regions (Hoell et al, 2011), I evaluated the presence of this motif and found that, indeed, FUS bound RNA probes often contained multiple AUU motifs. However, this motif was not an absolute prerequisite for binding. Other studies could not identify a consensus sequence for FUS binding (Ishigaki et al, 2012; Lagier-Tourenne et al, 2012; Nakaya, 2013; Rogelj et al, 2012). In a subset of targets researchers found a significant preference for G/C (Ishigaki et al, 2012), C/U (Nakaya, 2013), GGU (Rogelj et al, 2012) or GUGGU (Lagier-Tourenne et al, 2012) motifs. The preferred sequences overlap with the motif GGUG originally identified with *in vitro* studies (Lerga et al, 2001). Alternatively, the RNA secondary structure might mediate FUS binding specificity. One study proposed a short stem loop motif (Hoell et al, 2011), which was confirmed by some but not all studies (Ishigaki et al, 2012; Rogelj et al, 2012). In conclusion, until further biochemical studies clarify RNA binding specificity (Nakaya, 2013), GGU and AUU rich sequences remain the best consensus sequence mediating FUS RNA binding.

5.3. Functional consequences of FUS knockdown

Based on the observation that the axonal protein TAU is mis-spliced upon FUS knockdown, I focused on the axonal architecture of FUS depleted neurons as a read out for the functional consequences on axonal development. After 4 days in culture FUS depleted neurons developed axons that were significantly shorter than those from the control cells. Neurite outgrowth and axonal branching events were, however, not affected. This is in line with previous studies that show decreased axon length but no effect on the length of minor processes in siRNA treated neurons to knockdown TAU (Qiang et al, 2006). Also neurons cultured from MAP1b/TAU double knockout mice show significantly reduced axon length compared to the controls (Takei et al, 2000). In addition to the reduced axon length, I also observed a significant shift in the frequency of neurons with enlarged axonal growth cones in FUS depleted neurons. This phenotype was strikingly similar to the disturbed growth cone structure seen in neurons cultured from MAP1b/TAU double knockout mice (Takei et al, 2000). Remarkably, the two most robust

FUS phenotypes reported here (shorter axons and enlarged growth cones) have been previously reported in TAU/MAP1b deficient neurons. Although FUS target genes other than TAU may still contribute to the axonal phenotype, these results clearly indicate that loss of FUS regulates cytoskeletal dynamics. Neuronal growth cones have an important role not only in the development but also the repair of the adult nervous system. At adult stages, healthy growth cones are essential structures to repair damaged axons, as determined with *in vivo* studies (Bradke et al, 2012).

Interestingly, gene ontology analysis of splice targets reported in CLIP studies consistently showed enrichment for proteins with axonal function, including axonogenesis, axon guidance, cell adhesion, neuron projection, vesicle transport, and cytoskeletal organization (Ishigaki et al, 2012; Lagier-Tourenne et al, 2012; Nakaya, 2013; Rogelj et al, 2012). Therefore, FUS seems to regulate the alternative splicing of a network of genes responsible for maintaining and growing axons. Consequently, loss of FUS function in ALS/FTLD-FUS cases could have direct adverse effect on physiological axon regeneration and thus promote disease progression by reducing the repair capacity.

5.4. Pathomechanism model centered on FUS regulation of alternative splicing

A new model for the pathomechanism behind ALS/FTLD-FUS emerges from the recent finding that FUS splice targets maintain and repair axons (Figure 27) (Orozco & Edbauer, 2013). The model presented here is based on the multiple-hit hypothesis (Dormann & Haass, 2011) and on the role of FUS as central regulator of alternative splicing with RNA targets clustering in similar pathways (Ishigaki et al, 2012; Lagier-Tourenne et al, 2012; Nakaya, 2013; Orozco & Edbauer, 2013; Rogelj et al, 2012). Such a central regulation of specific pathways is a common feature of RNA-binding proteins (Hogan et al, 2008; Keene, 2007; Ule et al, 2005).

The model includes the following events. **(1)** The first step in the pathological cascade is the mislocalization of FUS to the cytoplasm caused, for example, by mutations in the NLS (Dormann & Haass, 2011). **(2)** The loss of nuclear FUS function leads to aberrant alternative splicing of several targets involved in axon maintenance and repair. As a consequence, neuronal connections with neighboring and distant cells are weakened. Cytoplasmic aggregates can also reinforce the mechanism by sequestering FUS and other RNA-binding proteins into the aggregates or by evoking aberrant protein-protein interactions. **(3)** In addition to the initial weakening, aging and other stressors (Dormann

& Haass, 2011; Dormann & Haass, 2013) can disturb neuronal integrity which results in denervation and may trigger early clinical symptoms. **(4)** Finally, progressive neurodegeneration is the consequence of disrupted repair mechanisms and limited tissue renewal in the brain.

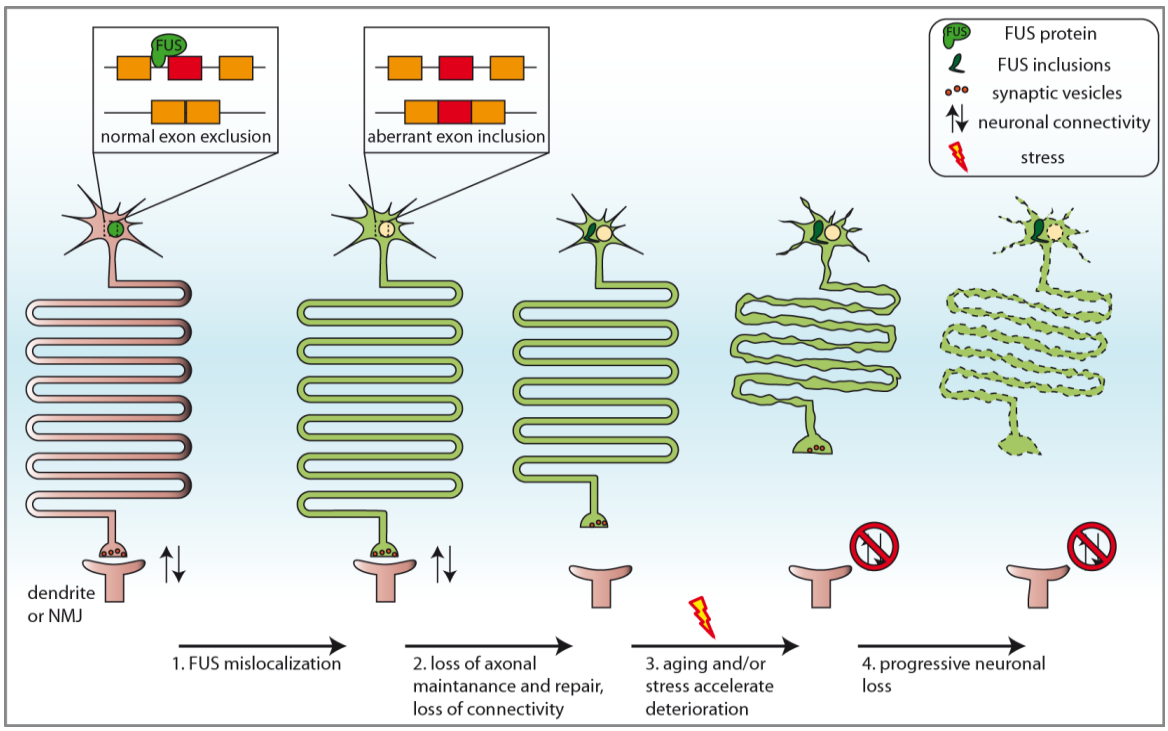

Figure 27 Hypothesis for pathomechanism in ALS/FTLD-FUS focused on FUS mediated alternative splicing

(1) Impaired nuclear import of FUS, due to mutations in the NLS or transport defects, causes mislocalization of FUS to the cytoplasm. This leads to loss of nuclear function and thus changes in alternative splicing of axonal and cytoskeleton related genes. **(2)** Altered splicing disturbs axonal maintenance and repair resulting in axonal atrophy and loss of connectivity. **(3)** Aging and stress accelerate the process of neuronal denervation and lead to the first clinical symptoms, since synapses or neuromuscular junctions (NMJ) start to fade out. **(4)** Due to disturbed repair mechanisms, the affected neurons are not able to cope with the stress and to repair damaged connections. The result is progressive degeneration observed in disease. From (Orozco & Edbauer, 2013).

5.4.1. Open questions

Although the model offers an initial hypothesis to understand the role of FUS in the pathogenesis of ALS and FTLD, many new questions arise and need further investigation. FUS binds many RNAs that are apparently not affected in splicing or expression upon loss of FUS. Are all of these RNAs only transport targets or are they affected in other ways, for example in their stability? Also, FUS binds many long non-coding RNAs (lncRNA), which can regulate, among others, transcription, chromosomal dynamics and subcellular organization (Mercer et al, 2009). What is the function of FUS binding to

lncRNAs? Two interesting lncRNA targets are the maternally expressed 3 (Meg 3) and nuclear enriched abundant transcript 1 (NEAT 1) (Lagier-Tourenne et al, 2012), because of their reported dysregulated expression in HD (Johnson, 2012). Interestingly, in FTLD-TDP cases TDP-43 showed increased binding of NEAT1, an essential regulator of paraspeckles in the nucleus, when compared to controls (Clemson et al, 2009; Tollervey et al, 2011). Furthermore, the nature of FUS aggregates in the cytoplasm remains unclear; how are they formed? Can that process be reversed? And finally, beside FUS function in alternative splicing, how are other functions affected by the mislocalization? One recurring theme among animal models has been the role of FUS in genomic stability (Hicks et al, 2000; Kuroda et al, 2000; Wang et al, 2013). This role could also be essential for normal cell function, as recent studies show that healthy post-mitotic neurons require constant genome repair, as double strand breaks result from normal synaptic activity (Suberbielle et al, 2013). In summary, loss of FUS could be detrimental to normal neuronal function by disturbing multiple pathways that together lead to ALS/FTLD.

5.5. The link between TAU and FUS in disease

In order to finally link FUS regulation of TAU alternative splicing to ALS/FTLD, it will be crucial to evaluate TAU alternative splicing and cytoskeletal aberrations in ALS/FTLD-FUS tissue, ideally using laser microdissection of neurons with FUS inclusions. Also, it will be important to investigate if other TAU related diseases (tauopathies) show FUS pathology or even *FUS* mutations.

Tauopathies are defined neuropathologically by the presence of hyperphosphorylated TAU aggregates (Brunden et al, 2008; Lee et al, 2001). However, several animal models have shown that neuronal toxicity precedes TAU aggregation, demonstrating that non-fibrillary TAU can cause neurodegeneration and cognitive symptoms (Brunden et al, 2008; de Calignon et al, 2010). *MAPT* mutations around exon 10 in some inherited tauopathies suggest that misbalanced expression of TAU isoforms may cause disease (Goedert & Jakes, 2005; Lee et al, 2001). Importantly, enhanced expression of either 4R TAU or 3R TAU both result in disease in humans and animal models. This emphasizes the importance of TAU isoform balance for physiologic function (Brunden et al, 2008; Ishihara et al, 1999; Sergeant et al, 1997). In PD, for example, 4R TAU expression levels correlate with co-occuring dementia, although PD cases do not show overt TAU pathology (Caffrey et al, 2006; Tobin et al, 2008; Williams-Gray et al, 2009). Also the H1

haplotype at the *MAPT* locus, which enhances 4R TAU expression, was identified as a strong genetic risk factor for PD (Caffrey et al, 2006; Tobin et al, 2008).

Interestingly, downregulation of FUS has been reported in PD (Stamper et al, 2008), again showing a link between FUS and TAU in disease. Furthermore, the role of FUS in essential tremor (ET), an adult-onset movement disorder, is still debated after a report that genetically associated FUS to ET through exome sequencing (Agúndez et al, 2013; Merner et al, 2012; Ortega-Cubero et al, 2013). Of note, TAU has also been genetically (Sundar et al, 2007) and pathologically (Buée-Scherrer et al, 1995) linked to the Guam variant of ALS, which demonstrates that alterations in TAU can also cause ALS. In summary, genetic and pathology aspects of neurodegenerative diseases may have previously linked FUS and TAU indirectly. The results presented in this thesis now provide a direct molecular link between FUS and TAU, by showing that loss of FUS enhances expression of 4R TAU, which is a well-established cause of disease even in the absence of TAU pathology (Brunden et al, 2008; Hutton et al, 1998; Tobin et al, 2008).

5.5.1. Future challenges

Future challenges include the generation of better animal models for ALS/FTLD-FUS and human TAU splicing. Emerging genome editing technologies could for the first time enable the study of *FUS* pathogenic mutations with endogenous expression. Also, in order to circumvent lethality in FUS KO mice, an inducible mouse line with neuron specific FUS depletion could be generated. Although the current FUS animal models already indicate that balanced FUS levels are essential for normal development and function, future models should also address the role of FUS in non-neuronal cells, since FUS patients also often show inclusions in glia cells (Ling et al, 2013; Neumann et al, 2009a). In a TDP-43 rat model, for instance, expression of human mutant TDP-43 specifically in astrocytes was sufficient to induce progressive paralysis due to denervation of skeletal muscles and motor neuron loss (Tong et al, 2013).

Furthermore, new models are needed that recapitulate the unique regulation of human TAU alternative splicing, which is remarkably different than the regulation in the murine nervous system (Gao et al, 2000; Kosik et al, 1989). For this, one could apply human induced pluripotent stem cells (iPS) that are then differentiated into motor neurons suitable for longer cultures. Such powerful tools could help investigate the influence of misbalanced isoform expression on emerging roles of TAU protein, such as signal

transduction, stress response and neuronal signaling (Morris et al, 2011; Timm et al, 2006).

In conclusion, classification of different disease subtypes based on molecular pathology is a useful tool; however we should be aware of exceptions and embrace the opportunities behind shared pathomechanisms. Especially infrequent conditions such as ALS/FTLD-FUS could benefit from ongoing clinical and pre-clinical studies focusing on other tauopathies. One example is the microtubule stabilizing agent NAP/davunetide which is currently tested in phase II clinical trials for FTLD-TAU patients and individuals with mild cognitive impairment (Morimoto et al, 2013; Morris et al, 2011; Trojanowski et al, 2008).

A greater understanding in the molecular mechanism behind the disease is the first step in the effective translation of our findings into treatment of patients suffering from devastating progressive neurodegeneration.

6. References

Aggarwal A, Shashiraj (2006) Juvenile amyotrophic lateral sclerosis. *Indian J Pediatr* **73:** 225-226

Agúndez JA, Jiménez-Jiménez FJ, Alonso-Navarro H, García-Martín E (2013) FUS: a putative biomarker for essential tremor raised by whole-exome sequencing analyses. *Pharmacogenomics* **14:** 1680-1681

Al-Bassam J, Ozer RS, Safer D, Halpain S, Milligan RA (2002) MAP2 and tau bind longitudinally along the outer ridges of microtubule protofilaments. *The Journal of Cell Biology* **157:** 1187-1196

Al-Chalabi A, Andersen PM, Nilsson P, Chioza B, Andersson JL, Russ C, Shaw CE, Powell JF, Nigel Leigh P (1999) Deletions of the Heavy Neurofilament Subunit Tail in Amyotrophic Lateral Sclerosis. *Human Molecular Genetics* **8:** 157-164

Al-Chalabi A, Jones A, Troakes C, King A, Al-Sarraj S, den Berg L (2012) The genetics and neuropathology of amyotrophic lateral sclerosis. *Acta Neuropathol* **124:** 339-352

Amador-Ortiz C, Lin W-L, Ahmed Z, Personett D, Davies P, Duara R, Graff-Radford NR, Hutton ML, Dickson DW (2007) TDP-43 immunoreactivity in hippocampal sclerosis and Alzheimer's disease. *Annals of Neurology* **61:** 435-445

Andersson M, Stahlberg A, Arvidsson Y, Olofsson A, Semb H, Stenman G, Nilsson O, Aman P (2008) The multifunctional FUS, EWS and TAF15 proto-oncoproteins show cell type-specific expression patterns and involvement in cell spreading and stress response. *BMC Cell Biology* **9:** 37

Andreadis A (2005) Tau gene alternative splicing: expression patterns, regulation and modulation of function in normal brain and neurodegenerative diseases. *Biochimica et Biophysica Acta (BBA) - Molecular Basis of Disease* **1739:** 91-103

Andreadis A (2012) Tau splicing and the intricacies of dementia. *Journal of Cellular Physiology* **227:** 1220-1225

Aoki-Suzuki M, Yamada K, Meerabux J, Iwayama-Shigeno Y, Ohba H, Iwamoto K, Takao H, Toyota T, Suto Y, Nakatani N, Dean B, Nishimura S, Seki K, Kato T, Itohara S, Nishikawa T, Yoshikawa T (2005) A family-based association study and gene expression analyses of netrin-G1 and -G2 genes in schizophrenia. *Biological psychiatry* **57:** 382-393

Arai T, Hasegawa M, Akiyama H, Ikeda K, Nonaka T, Mori H, Mann D, Tsuchiya K, Yoshida M, Hashizume Y, Oda T (2006) TDP-43 is a component of ubiquitin-positive tau-negative inclusions in frontotemporal lobar degeneration and amyotrophic lateral sclerosis. *Biochemical and Biophysical Research Communications* **351:** 602-611

Bahia VS, Takada LT, Deramecourt V (2013) Neuropathology of frontotemporal lobar degeneration. **7:** 19-26

Bai B, Hales CM, Chen P-C, Gozal Y, Dammer EB, Fritz JJ, Wang X, Xia Q, Duong DM, Street C, Cantero G, Cheng D, Jones DR, Wu Z, Li Y, Diner I, Heilman CJ, Rees HD, Wu H, Lin L, Szulwach KE, Gearing M, Mufson EJ, Bennett DA, Montine TJ, Seyfried NT, Wingo TS, Sun YE, Jin P, Hanfelt J, Willcock DM, Levey A, Lah JJ, Peng J (2013) U1 small nuclear

ribonucleoprotein complex and RNA splicing alterations in Alzheimer's disease. *Proceedings of the National Academy of Sciences* **110:** 16562-16567
Baker M, Litvan I, Houlden H, Adamson J, Dickson D, Perez-Tur J, Hardy J, Lynch T, Bigio E, Hutton M (1999) Association of an Extended Haplotype in the Tau Gene with Progressive Supranuclear Palsy. *Human Molecular Genetics* **8:** 711-715

Ballatore C, Lee VMY, Trojanowski JQ (2007) Tau-mediated neurodegeneration in Alzheimer's disease and related disorders. *Nat Rev Neurosci* **8:** 663-672

Belly A, Moreau-Gachelin F, Sadoul R, Goldberg Y (2005) Delocalization of the multifunctional RNA splicing factor TLS/FUS in hippocampal neurones: exclusion from the nucleus and accumulation in dendritic granules and spine heads. *Neuroscience Letters* **379:** 152-157

Belzil V, Bauer P, Prudencio M, Gendron T, Stetler C, Yan I, Pregent L, Daughrity L, Baker M, Rademakers R, Boylan K, Patel T, Dickson D, Petrucelli L (2013) Reduced C9orf72 gene expression in c9FTD/ALS is caused by histone trimethylation, an epigenetic event detectable in blood. *Acta Neuropathol* **126:** 895-905

Bentmann E, Haass C, Dormann D (2013) Stress granules in neurodegeneration – lessons learnt from TAR DNA binding protein of 43 kDa and fused in sarcoma. *FEBS Journal* **280:** 4348-4370

Bertram L, Tanzi RE (2005) The genetic epidemiology of neurodegenerative disease. *The Journal of Clinical Investigation* **115:** 1449-1457

Bieniek K, Murray M, Rutherford N, Castanedes-Casey M, DeJesus-Hernandez M, Liesinger A, Baker M, Boylan K, Rademakers R, Dickson D (2013) Tau pathology in frontotemporal lobar degeneration with C9ORF72 hexanucleotide repeat expansion. *Acta Neuropathol* **125:** 289-302

Bird T, Knopman D, VanSwieten J, Rosso S, Feldman H, Tanabe H, Graff-Raford N, Geschwind D, Verpillat P, Hutton M (2003) Epidemiology and genetics of frontotemporal dementia/Pick's disease. *Annals of Neurology* **54:** S29-S31

Blauw HM, Barnes C, van Vught PW, van Rheenen W, Verheul M, Cuppen E, Veldink JH, Van Den Berg L (2012) SMN1 gene duplications are associated with sporadic ALS. *Neurology* **78:** 776-780

Bosco DA, Lemay N, Ko HK, Zhou H, Burke C, Kwiatkowski TJ, Sapp P, McKenna-Yasek D, Brown RH, Hayward LJ (2010) Mutant FUS proteins that cause amyotrophic lateral sclerosis incorporate into stress granules. *Human Molecular Genetics* **19:** 4160-4175

Bradke F, Fawcett JW, Spira ME (2012) Assembly of a new growth cone after axotomy: the precursor to axon regeneration. *Nat Rev Neurosci* **13:** 183-193

Brady OA, Zheng Y, Murphy K, Huang M, Hu F (2013) The frontotemporal lobar degeneration risk factor, TMEM106B, regulates lysosomal morphology and function. *Human Molecular Genetics* **22:** 685-695

Brandt R, Léger J, Lee G (1995) Interaction of tau with the neural plasma membrane mediated by tau's amino-terminal projection domain. *The Journal of Cell Biology* **131:** 1327-1340

Brunden KR, Trojanowski JQ, Lee VMY (2008) Evidence that Non-Fibrillar Tau Causes Pathology Linked to Neurodegeneration and Behavioral Impairments. *Journal of Alzheimer's Disease* **14:** 393-399

Buée-Scherrer V, Buee L, Hof PR, Leveugle B, Gilles C, Loerzel AJ, Perl DP, Delacourte A (1995) Neurofibrillary degeneration in amyotrophic lateral sclerosis/parkinsonism-dementia complex of Guam. Immunochemical characterization of tau proteins. *The American journal of pathology* **68:** 924-932

Buratti E, Baralle FE (2008) Multiple roles of TDP-43 in gene expression, splicing regulation, and human disease. *Front Biosci* **13:** 867-878

Buratti E, Baralle FE (2010) The multiple roles of TDP-43 in pre-mRNA processing and gene expression regulation. *RNA Biology* **7:** 420-429

Burghes AHM, Beattie CE (2009) Spinal muscular atrophy: why do low levels of survival motor neuron protein make motor neurons sick? *Nat Rev Neurosci* **10:** 597-609

Caffrey TM, Joachim C, Paracchini S, Esiri MM, Wade-Martins R (2006) Haplotype-specific expression of exon 10 at the human MAPT locus. *Human Molecular Genetics* **15:** 3529-3537

CDC CfDCP (2003) Trends in aging-United States and worldwide. *MMWR Morbidity and mortality weekly report* **52:** 101-106

Chen-Plotkin AS, Unger TL, Gallagher MD, Bill E, Kwong LK, Volpicelli-Daley L, Busch JI, Akle S, Grossman M, Van Deerlin V, Trojanowski JQ, Lee VM-Y (2012) TMEM106B, the Risk Gene for Frontotemporal Dementia, Is Regulated by the microRNA-132/212 Cluster and Affects Progranulin Pathways. *The Journal of Neuroscience* **32:** 11213-11227

Chen J, Kanai Y, Cowan N, Hirokawa N (1992) Projection domains of MAP2 and tau determine spacings between microtubules in dendrites and axons. *Nature* **360:** 674-677

Chen Y, Yang M, Deng J, Chen X, Ye Y, Zhu L, Liu J, Ye H, Shen Y, Li Y, Rao E, Fushimi K, Zhou X, Bigio E, Mesulam M, Xu Q, Wu J (2011) Expression of human FUS protein in Drosophila leads to progressive neurodegeneration. *Protein Cell* **2:** 477-486

Chiò A, Logroscino G, Traynor BJ, Collins J, Simeone JC, Goldstein LA, White LA (2013) Global Epidemiology of Amyotrophic Lateral Sclerosis: A Systematic Review of the Published Literature. *Neuroepidemiology* **41:** 118-130

Ciura S, Lattante S, Le Ber I, Latouche M, Tostivint H, Brice A, Kabashi E (2013) Loss of function of C9orf72 causes motor deficits in a zebrafish model of amyotrophic lateral sclerosis. *Annals of Neurology* **74:** 180-187

Clemson CM, Hutchinson JN, Sara SA, Ensminger AW, Fox AH, Chess A, Lawrence JB (2009) An Architectural Role for a Nuclear Noncoding RNA: NEAT1 RNA Is Essential for the Structure of Paraspeckles. *Molecular Cell* **33:** 717-726

Cleveland DW, Rothstein JD (2001) From charcot to lou gehrig: deciphering selective motor neuron death in als. *Nat Rev Neurosci* **2:** 806-819

Cooper TA, Wan L, Dreyfuss G (2009) RNA and Disease. *Cell* **136:** 777-793

Cox LE, Ferraiuolo L, Goodall EF, Heath PR, Higginbottom A, Mortiboys H, Hollinger HC, Hartley JA, Brockington A, Burness CE, Morrison KE, Wharton SB, Grierson AJ, Ince PG, Kirby J, Shaw PJ (2010) Mutations in <italic>CHMP2B</italic> in Lower Motor Neuron Predominant Amyotrophic Lateral Sclerosis (ALS). *PLoS ONE* **5:** 1-16

Crozat A, Aman P, Mandahl N, Ron D (1993) Fusion of CHOP to a novel RNA-binding protein in human myxoid liposarcoma. *Nature* **363:** 640-644

Cruts M, Theuns J, Van Broeckhoven C (2012) Locus-specific mutation databases for neurodegenerative brain diseases. *Human Mutation* **33:** 1340-1344

Das R, Yu J, Zhang Z, Gygi MP, Krainer AR, Gygi SP, Reed R (2007) SR Proteins Function in Coupling RNAP II Transcription to Pre-mRNA Splicing. *Molecular Cell* **26:** 867-881

de Calignon A, Fox LM, Pitstick R, Carlson GA, Bacskai BJ, Spires-Jones TL, Hyman BT (2010) Caspase activation precedes and leads to tangles. *Nature* **464:** 1201-1204

DeJesus-Hernandez M, Mackenzie Ian R, Boeve Bradley F, Boxer Adam L, Baker M, Rutherford Nicola J, Nicholson Alexandra M, Finch NiCole A, Flynn H, Adamson J, Kouri N, Wojtas A, Sengdy P, Hsiung G-Yuek R, Karydas A, Seeley William W, Josephs Keith A, Coppola G, Geschwind Daniel H, Wszolek Zbigniew K, Feldman H, Knopman David S, Petersen Ronald C, Miller Bruce L, Dickson Dennis W, Boylan Kevin B, Graff-Radford Neill R, Rademakers R (2011) Expanded GGGGCC Hexanucleotide Repeat in Noncoding Region of C9ORF72 Causes Chromosome 9p-Linked FTD and ALS. *Neuron* **72:** 245-256

Deng H-X, Chen W, Hong S-T, Boycott KM, Gorrie GH, Siddique N, Yang Y, Fecto F, Shi Y, Zhai H, Jiang H, Hirano M, Rampersaud E, Jansen GH, Donkervoort S, Bigio EH, Brooks BR, Ajroud K, Sufit RL, Haines JL, Mugnaini E, Pericak-Vance MA, Siddique T (2011) Mutations in UBQLN2 cause dominant X-linked juvenile and adult-onset ALS and ALS/dementia. *Nature* **477:** 211-215

Dixit R, Ross JL, Goldman YE, Holzbaur ELF (2008) Differential Regulation of Dynein and Kinesin Motor Proteins by Tau. *Science* **319:** 1086-1089

Doi H, Koyano S, Suzuki Y, Nukina N, Kuroiwa Y (2010) The RNA-binding protein FUS/TLS is a common aggregate-interacting protein in polyglutamine diseases. *Neuroscience Research* **66:** 131-133

Doi H, Okamura K, Bauer PO, Furukawa Y, Shimizu H, Kurosawa M, Machida Y, Miyazaki H, Mitsui K, Kuroiwa Y, Nukina N (2008) RNA-binding Protein TLS Is a Major Nuclear Aggregate-interacting Protein in Huntingtin Exon 1 with Expanded Polyglutamine-expressing Cells. *Journal of Biological Chemistry* **283:** 6489-6500

Dormann D, Haass C (2011) TDP-43 and FUS: a nuclear affair. *Trends in neurosciences* **34:** 339-348

Dormann D, Haass C (2013) Fused in sarcoma (FUS): An oncogene goes awry in neurodegeneration. *Molecular and Cellular Neuroscience* **56:** 475-486

Dormann D, Madl T, Valori CF, Bentmann E, Tahirovic S, Abou-Ajram C, Kremmer E, Ansorge O, Mackenzie IRA, Neumann M, Haass C (2012) Arginine methylation next to the PY-NLS modulates Transportin binding and nuclear import of FUS. *EMBO J* **31:** 4258-4275

Dormann D, Rodde R, Edbauer D, Bentmann E, Fischer I, Hruscha A, Than ME, Mackenzie IRA, Capell A, Schmid B, Neumann M, Haass C (2010) ALS-associated fused in sarcoma (FUS) mutations disrupt Transportin-mediated nuclear import. *EMBO J* **29:** 2841-2857

Dredge BK, Polydorides AD, Darnell RB (2001) The splice of life: Alternative splicing and neurological disease. *Nat Rev Neurosci* **2:** 43-50

Du AT, Jahng GH, Hayasaka S, Kramer JH, Rosen HJ, Gorno-Tempini ML, Rankin KP, Miller BL, Weiner MW, Schuff N (2006) Hypoperfusion in frontotemporal dementia and Alzheimer disease by arterial spin labeling MRI. *Neurology* **67:** 1215-1220
Eriksen JL, Mackenzie IRA (2008) Progranulin: normal function and role in neurodegeneration. *Journal of Neurochemistry* **104:** 287-297

Feany MB, Dickson DW (1995) Widespread cytoskeletal pathology characterizes corticobasal degeneration. *The American journal of pathology* **146:** 1388

Ferrer I, Santpere G, van Leeuwen FW (2008) Argyrophilic grain disease. *Brain* **131:** 1416-1432

Ferri CP, Prince M, Brayne C, Brodaty H, Fratiglioni L, Ganguli M, Hall K, Hasegawa K, Hendrie H, Huang Y, Jorm A, Mathers C, Menezes PR, Rimmer E, Scazufca M (2005) Global prevalence of dementia: a Delphi consensus study. *The Lancet* **366:** 2112-2117

Frappier TF, Georgieff IS, Brown K, Shelanski ML (1994) τ Regulation of Microtubule-Microtubule Spacing and Bundling. *Journal of Neurochemistry* **63:** 2288-2294

Fujii R, Okabe S, Urushido T, Inoue K, Yoshimura A, Tachibana T, Nishikawa T, Hicks GG, Takumi T (2005) The RNA Binding Protein TLS Is Translocated to Dendritic Spines by mGluR5 Activation and Regulates Spine Morphology. *Current Biology* **15:** 587-593

Fujii R, Takumi T (2005) TLS facilitates transport of mRNA encoding an actin-stabilizing protein to dendritic spines. *Journal of Cell Science* **118:** 5755-5765

Fujioka Y, Ishigaki S, Masuda A, Iguchi Y, Udagawa T, Watanabe H, Katsuno M, Ohno K, Sobue G (2013) FUS-regulated region- and cell-type-specific transcriptome is associated with cell selectivity in ALS/FTLD. *Sci Rep* **3:** 1-12

Gao Q-S, Memmott J, Lafyatis R, Stamm S, Screaton G, Andreadis A (2000) Complex Regulation of Tau Exon 10, Whose Missplicing Causes Frontotemporal Dementia. *Journal of Neurochemistry* **74:** 490-500

Gerbino V, Carrì MT, Cozzolino M, Achsel T (2013) Mislocalised FUS mutants stall spliceosomal snRNPs in the cytoplasm. *Neurobiology of Disease* **55:** 120-128

Geschwind D, Karrim J, Nelson SF, Miller B (1998) The apolipoprotein E ε4 allele is not a significant risk factor for frontotemporal dementia. *Annals of Neurology* **44:** 134-138

Gijselinck I, Van Langenhove T, van der Zee J, Sleegers K, Philtjens S, Kleinberger G, Janssens J, Bettens K, Van Cauwenberghe C, Pereson S, Engelborghs S, Sieben A, De Jonghe P, Vandenberghe R, Santens P, De Bleecker J, Maes G, Bäumer V, Dillen L, Joris G, Cuijt I, Corsmit E, Elinck E, Van Dongen J, Vermeulen S, Van den Broeck M, Vaerenberg C, Mattheijssens M, Peeters K, Robberecht W, Cras P, Martin J-J, De Deyn PP, Cruts M, Van Broeckhoven C (2012) A C9orf72 promoter repeat expansion in a Flanders-Belgian cohort with disorders of the frontotemporal lobar degeneration-amyotrophic lateral sclerosis spectrum: a gene identification study. *The Lancet Neurology* **11:** 54-65

Gitler AD, Shorter J (2011) RNA-binding proteins with prion-like domains in ALS and FTLD-U. *Prion* **5:** 179-187

Goedert M, Jakes R (2005) Mutations causing neurodegenerative tauopathies. *Biochimica et Biophysica Acta (BBA) - Molecular Basis of Disease* **1739:** 240-250

Goedert M, Spillantini MG (2006) A Century of Alzheimer's Disease. *Science* **314:** 777-781

Gorno-Tempini ML, Hillis AE, Weintraub S, Kertesz A, Mendez M, Cappa SF, Ogar JM, Rohrer JD, Black S, Boeve BF, Manes F, Dronkers NF, Vandenberghe R, Rascovsky K, Patterson K, Miller BL, Knopman DS, Hodges JR, Mesulam MM, Grossman M (2011) Classification of primary progressive aphasia and its variants. *Neurology* **76:** 1006-1014

Gustke N, Trinczek B, Biernat J, Mandelkow E-M, Mandelkow E (1994) Domains of tau protein and interactions with microtubules. *Biochemistry* **33:** 9511-9522

Haass C, Mandelkow E (2010) Fyn-Tau-Amyloid: A Toxic Triad. *Cell* **142:** 356-358

Han J-H, Ryu H-H, Jun M-H, Jang D-J, Lee J-A (2012) The functional analysis of the CHMP2B missense mutation associated with neurodegenerative diseases in the endo-lysosomal pathway. *Biochemical and Biophysical Research Communications* **421:** 544-549

Hartmann AM, Rujescu D, Giannakouros T, Nikolakaki E, Goedert M, Mandelkow E-M, Gao QS, Andreadis A, Stamm S (2001) Regulation of Alternative Splicing of Human Tau Exon 10 by Phosphorylation of Splicing Factors. *Molecular and Cellular Neuroscience* **18:** 80-90

Hartmuth K, Urlaub H, Vornlocher H-P, Will CL, Gentzel M, Wilm M, Lührmann R (2002) Protein composition of human prespliceosomes isolated by a tobramycin affinity-selection method. *Proceedings of the National Academy of Sciences* **99:** 16719-16724

Hattori D, Millard SS, Wojtowicz WM, Zipursky SL (2008) Dscam-Mediated Cell Recognition Regulates Neural Circuit Formation. *Annual Review of Cell and Developmental Biology* **24:** 597-620

Hicks GG, Singh N, Nashabi A, Mai S, Bozek G, Klewes L, Arapovic D, White EK, Koury MJ, Oltz EM, Van Kaer L, Ruley HE (2000) Fus deficiency in mice results in defective B-lymphocyte development and activation, high levels of chromosomal instability and perinatal death. *Nat Genet* **24:** 175-179

Hoell JI, Larsson E, Runge S, Nusbaum JD, Duggimpudi S, Farazi TA, Hafner M, Borkhardt A, Sander C, Tuschl T (2011) RNA targets of wild-type and mutant FET family proteins. *Nat Struct Mol Biol* **18:** 1428-1431

Hogan DJ, Riordan DP, Gerber AP, Herschlag D, Brown PO (2008) Diverse RNA-Binding Proteins Interact with Functionally Related Sets of RNAs, Suggesting an Extensive Regulatory System. *PLoS Biol* **6:** 2297-2313

Honda D, Ishigaki S, Iguchi Y, Fujioka Y, Udagawa T, Masuda A, Ohno K, Katsuno M, Sobue G (2014) The ALS/FTLD-related RNA-binding proteins TDP-43 and FUS have common downstream RNA targets in cortical neurons. *FEBS Open Bio* **4:** 1-10

Hong M, Zhukareva V, Vogelsberg-Ragaglia V, Wszolek Z, Reed L, Miller BI, Geschwind DH, Bird TD, McKeel D, Goate A, Morris JC, Wilhelmsen KC, Schellenberg GD, Trojanowski JQ, Lee VM-Y (1998) Mutation-Specific Functional Impairments in Distinct Tau Isoforms of Hereditary FTDP-17. *Science* **282:** 1914-1917

Houlden H, Baker M, Morris HR, MacDonald N, Pickering–Brown S, Adamson J, Lees AJ, Rossor MN, Quinn NP, Kertesz A, Khan MN, Hardy J, Lantos PL, St. George–Hyslop P, Munoz DG, Mann D, Lang AE, Bergeron C, Bigio EH, Litvan I, Bhatia KP, Dickson D, Wood NW, Hutton M (2001) Corticobasal degeneration and progressive supranuclear palsy share a common tau haplotype. *Neurology* **56:** 1702-1706

Hsiung G-YR, Feldman HH (2013) GRN-Related Frontotemporal Dementia. *GeneReviews™(Internet) Seattle (WA): University of Washington, Seattle*

Huang C, Zhou H, Tong J, Chen H, Liu Y-J, Wang D, Wei X, Xia X-G (2011) FUS Transgenic Rats Develop the Phenotypes of Amyotrophic Lateral Sclerosis and Frontotemporal Lobar Degeneration. *PLoS Genet* **7:** 1-10

Husi H, Ward MA, Choudhary JS, Blackstock WP, Grant SGN (2000) Proteomic analysis of NMDA receptor-adhesion protein signaling complexes. *Nat Neurosci* **3:** 661-669

Hutton M, Lendon CL, Rizzu P, Baker M, Froelich S, Houlden H, Pickering-Brown S, Chakraverty S, Isaacs A, Grover A, Hackett J, Adamson J, Lincoln S, Dickson D, Davies P, Petersen RC, Stevens M, de Graaff E, Wauters E, van Baren J, Hillebrand M, Joosse M, Kwon JM, Nowotny P, Che LK, Norton J, Morris JC, Reed LA, Trojanowski J, Basun H, Lannfelt L, Neystat M, Fahn S, Dark F, Tannenberg T, Dodd PR, Hayward N, Kwok JBJ, Schofield PR, Andreadis A, Snowden J, Craufurd D, Neary D, Owen F, Oostra BA, Hardy J, Goate A, van Swieten J, Mann D, Lynch T, Heutink P (1998) Association of missense and 5[prime]-splice-site mutations in tau with the inherited dementia FTDP-17. *Nature* **393:** 702-705

Iko Y, Kodama TS, Kasai N, Oyama T, Morita EH, Muto T, Okumura M, Fujii R, Takumi T, Tate S-i, Morikawa K (2004) Domain Architectures and Characterization of an RNA-binding Protein, TLS. *Journal of Biological Chemistry* **279:** 44834-44840

Ishigaki S, Masuda A, Fujioka Y, Iguchi Y, Katsuno M, Shibata A, Urano F, Sobue G, Ohno K (2012) Position-dependent FUS-RNA interactions regulate alternative splicing events and transcriptions. *Sci Rep* **2:** 1-8

Ishihara T, Hong M, Zhang B, Nakagawa Y, Lee MK, Trojanowski JQ, Lee VMY (1999) Age-Dependent Emergence and Progression of a Tauopathy in Transgenic Mice Overexpressing the Shortest Human Tau Isoform. *Neuron* **24:** 751-762

Ittner LM, Ke YD, Delerue F, Bi M, Gladbach A, van Eersel J, Wölfing H, Chieng BC, Christie MJ, Napier IA, Eckert A, Staufenbiel M, Hardeman E, Götz J (2010) Dendritic Function of Tau Mediates Amyloid-β Toxicity in Alzheimer's Disease Mouse Models. *Cell* **142:** 387-397

Jakovcevski M, Akbarian S (2012) Epigenetic mechanisms in neurological disease. *Nat Med* **18:** 1194-1204

Johnson JO, Mandrioli J, Benatar M, Abramzon Y, Van Deerlin VM, Trojanowski JQ, Gibbs JR, Brunetti M, Gronka S, Wuu J, Ding J, McCluskey L, Martinez-Lage M, Falcone D, Hernandez DG, Arepalli S, Chong S, Schymick JC, Rothstein J, Landi F, Wang Y-D, Calvo A, Mora G, Sabatelli M, Monsurrò MR, Battistini S, Salvi F, Spataro R, Sola P, Borghero G, Galassi G, Scholz SW, Taylor JP, Restagno G, Chiò A, Traynor BJ (2010) Exome Sequencing Reveals VCP Mutations as a Cause of Familial ALS. *Neuron* **68:** 857-864

Johnson R (2012) Long non-coding RNAs in Huntington's disease neurodegeneration. *Neurobiology of Disease* **46:** 245-254

Josephs KAM, MD; Ahmed, Zeshan BS; Katsuse, Omi MD; Parisi, Joseph F. MD; Boeve, Bradley F. MD; Knopman, David S. MD; Petersen, Ronald C. MD, PhD; Davies, Peter PhD; Duara, Ranjan MD; Graff-Radford, Neill R. MD; Uitti, Ryan J. MD; Rademakers, Rosa PhD; Adamson, Jennifer BS; Baker, Matthew BS; Hutton, Michael L. PhD; Dickson, Dennis W. MD (2007) Neuropathologic Features of Frontotemporal Lobar Degeneration With Ubiquitin-Positive Inclusions With Progranulin Gene (PGRN) Mutations. *Journal of Neuropathology & Experimental Neurology* **66:** 142-151

Kar S, Fan J, Smith MJ, Goedert M, Amos LA (2003) Repeat motifs of tau bind to the insides of microtubules in the absence of taxol. *The EMBO Journal* **22:** 70-77

Kato M, Han Tina W, Xie S, Shi K, Du X, Wu Leeju C, Mirzaei H, Goldsmith Elizabeth J, Longgood J, Pei J, Grishin Nick V, Frantz Douglas E, Schneider Jay W, Chen S, Li L, Sawaya Michael R, Eisenberg D, Tycko R, McKnight Steven L (2012) Cell-free Formation of RNA Granules: Low Complexity Sequence Domains Form Dynamic Fibers within Hydrogels. *Cell* **149:** 753-767

Kawahara Y, Kwak S (2005) Excitotoxicity and ALS: What is unique about the AMPA receptors expressed on spinal motor neurons? *Amyotrophic Lateral Sclerosis* **6:** 131-144

Kawahara Y, Mieda-Sato A (2012) TDP-43 promotes microRNA biogenesis as a component of the Drosha and Dicer complexes. *Proceedings of the National Academy of Sciences* **109:** 3347-3352

Keene JD (2007) RNA regulons: coordination of post-transcriptional events. *Nat Rev Genet* **8:** 533-543

Kiernan MC, Vucic S, Cheah BC, Turner MR, Eisen A, Hardiman O, Burrell JR, Zoing MC (2011) Amyotrophic lateral sclerosis. *The Lancet* **377:** 942-955

King OD, Gitler AD, Shorter J (2012) The tip of the iceberg: RNA-binding proteins with prion-like domains in neurodegenerative disease. *Brain Research* **1462:** 61-80

Kinsley L, Siddique T, Pagon R, Bird T, Dolan C, Stephens K, Adam M (2001) Amyotrophic lateral sclerosis overview. *GeneReviews™(Internet) Seattle (WA): University of Washington, Seattle*

Klint P, Hellman U, Wernstedt C, Åman P, Ron D, Claesson-Welsh L (2004) Translocated in liposarcoma (TLS) is a substrate for fibroblast growth factor receptor-1. *Cellular Signalling* **16:** 515-520

Kosik KS, Orecchio LD, Bakalis S, Neve RL (1989) Developmentally regulated expression of specific tau sequences. *Neuron* **2:** 1389-1397

Kuroda M, Sok J, Webb L, Baechtold H, Urano F, Yin Y, Chung P, de Rooij DG, Akhmedov A, Ashley T, Ron D (2000) Male sterility and enhanced radiation sensitivity in TLS-/- mice. *EMBO J* **19:** 453-462

Kwiatkowski TJ, Bosco DA, LeClerc AL, Tamrazian E, Vanderburg CR, Russ C, Davis A, Gilchrist J, Kasarskis EJ, Munsat T, Valdmanis P, Rouleau GA, Hosler BA, Cortelli P, de Jong PJ, Yoshinaga Y, Haines JL, Pericak-Vance MA, Yan J, Ticozzi N, Siddique T, McKenna-Yasek D, Sapp PC, Horvitz HR, Landers JE, Brown RH (2009) Mutations in the FUS/TLS Gene on Chromosome 16 Cause Familial Amyotrophic Lateral Sclerosis. *Science* **323:** 1205-1208

Lagier-Tourenne C, Polymenidou M, Cleveland DW (2010) TDP-43 and FUS/TLS: emerging roles in RNA processing and neurodegeneration. *Human Molecular Genetics* **19:** R46-R64

Lagier-Tourenne C, Polymenidou M, Hutt KR, Vu AQ, Baughn M, Huelga SC, Clutario KM, Ling S-C, Liang TY, Mazur C, Wancewicz E, Kim AS, Watt A, Freier S, Hicks GG, Donohue JP, Shiue L, Bennett CF, Ravits J, Cleveland DW, Yeo GW (2012) Divergent roles of ALS-linked proteins FUS/TLS and TDP-43 intersect in processing long pre-mRNAs. *Nat Neurosci* **15:** 1488-1497

Lang CM, Fellerer K, Schwenk BM, Kuhn P-H, Kremmer E, Edbauer D, Capell A, Haass C (2012) Membrane Orientation and Subcellular Localization of Transmembrane Protein 106B (TMEM106B), a Major Risk Factor for Frontotemporal Lobar Degeneration. *Journal of Biological Chemistry* **287:** 19355-19365

Lanson Jr NA, Pandey UB (2012) FUS-related proteinopathies: Lessons from animal models. *Brain Research* **1462:** 44-60

Lanson NA, Maltare A, King H, Smith R, Kim JH, Taylor JP, Lloyd TE, Pandey UB (2011) A Drosophila model of FUS-related neurodegeneration reveals genetic interaction between FUS and TDP-43. *Human Molecular Genetics* **20:** 2510-2523

Lashley T, Rohrer JD, Bandopadhyay R, Fry C, Ahmed Z, Isaacs AM, Brelstaff JH, Borroni B, Warren JD, Troakes C, King A, Al-Saraj S, Newcombe J, Quinn N, Ostergaard K, Schrøder HD, Bojsen-Møller M, Braendgaard H, Fox NC, Rossor MN, Lees AJ, Holton JL, Revesz T (2011) A comparative clinical, pathological, biochemical and genetic study of fused in sarcoma proteinopathies. *Brain* **134:** 2548-2564

Lattante S, Rouleau GA, Kabashi E (2013) TARDBP and FUS Mutations Associated with Amyotrophic Lateral Sclerosis: Summary and Update. *Human Mutation* **34:** 812-826

Law WJ, Cann KL, Hicks GG (2006) TLS, EWS and TAF15: a model for transcriptional integration of gene expression. *Briefings in Functional Genomics & Proteomics* **5:** 8-14

Lee BJ, Cansizoglu AE, Süel KE, Louis TH, Zhang Z, Chook YM (2006) Rules for Nuclear Localization Sequence Recognition by Karyopherinβ2. *Cell* **126:** 543-558

Lee EB, Lee VMY, Trojanowski JQ (2012) Gains or losses: molecular mechanisms of TDP43-mediated neurodegeneration. *Nat Rev Neurosci* **13:** 38-50

Lee G, Newman ST, Gard DL, Band H, Panchamoorthy G (1998) Tau interacts with src-family non-receptor tyrosine kinases. *Journal of Cell Science* **111:** 3167-3177

Lee VM-Y, Goedert M, Trojanowski JQ (2001) Neurodegenerative Tauopathies. *Annual Review of Neuroscience* **24:** 1121-1159

Lerga A, Hallier M, Delva L, Orvain C, Gallais I, Marie J, Moreau-Gachelin F (2001) Identification of an RNA Binding Specificity for the Potential Splicing Factor TLS. *Journal of Biological Chemistry* **276:** 6807-6816

Leung CL, He CZ, Kaufmann P, Chin SS, Naini A, Liem RKH, Mitsumoto H, Hays AP (2004) A Pathogenic Peripherin Gene Mutation in a Patient with Amyotrophic Lateral Sclerosis. *Brain Pathology* **14:** 290-296

Li Q, Lee J-A, Black DL (2007) Neuronal regulation of alternative pre-mRNA splicing. *Nat Rev Neurosci* **8:** 819-831

Licatalosi DD, Darnell RB (2010) RNA processing and its regulation: global insights into biological networks. *Nat Rev Genet* **11:** 75-87

Lin L, Lesnick TG, Maraganore DM, Isacson O (2009) Axon guidance and synaptic maintenance: preclinical markers for neurodegenerative disease and therapeutics. *Trends in neurosciences* **32:** 142-149

Ling S-C, Polymenidou M, Cleveland Don W (2013) Converging Mechanisms in ALS and FTD: Disrupted RNA and Protein Homeostasis. *Neuron* **79:** 416-438

Liu F, Gong C-X (2008) Tau exon 10 alternative splicing and tauopathies. *Mol Neurodegener* **3:** 1326-1338

Lois C, Hong EJ, Pease S, Brown EJ, Baltimore D (2002) Germline Transmission and Tissue-Specific Expression of Transgenes Delivered by Lentiviral Vectors. *Science* **295:** 868-872

Lomen-Hoerth C, Anderson T, Miller B (2002) The overlap of amyotrophic lateral sclerosis and frontotemporal dementia. *Neurology* **59:** 1077-1079

Lorson CL, Androphy EJ (1998) The Domain Encoded by Exon 2 of the Survival Motor Neuron Protein Mediates Nucleic Acid Binding. *Human Molecular Genetics* **7:** 1269-1275

Lotharius J, Barg S, Wiekop P, Lundberg C, Raymon HK, Brundin P (2002) Effect of Mutant α-Synuclein on Dopamine Homeostasis in a New Human Mesencephalic Cell Line. *Journal of Biological Chemistry* **277:** 38884-38894

Lotharius J, Falsig J, van Beek J, Payne S, Dringen R, Brundin P, Leist M (2005) Progressive Degeneration of Human Mesencephalic Neuron-Derived Cells Triggered by Dopamine-Dependent Oxidative Stress Is Dependent on the Mixed-Lineage Kinase Pathway. *The Journal of Neuroscience* **25:** 6329-6342

Mackenzie IA, Munoz D, Kusaka H, Yokota O, Ishihara K, Roeber S, Kretzschmar H, Cairns N, Neumann M (2011a) Distinct pathological subtypes of FTLD-FUS. *Acta Neuropathol* **121:** 207-218

Mackenzie IA, Neumann M, Baborie A, Sampathu D, Plessis D, Jaros E, Perry R, Trojanowski J, Mann DA, Lee VY (2011b) A harmonized classification system for FTLD-TDP pathology. *Acta Neuropathol* **122:** 111-113

Mandelkow EM, Schweers O, Drewes G, Biernat J, Gustke N, Trinczek B, Mandelkow E (1996) Structure, Microtubule Interactions, and Phosphorylation of Tau Protein. *Annals of the New York Academy of Sciences* **777:** 96-106

Marko M, Vlassis A, Guialis A, Leichter M (2012) Domains involved in TAF15 subcellular localisation: Dependence on cell type and ongoing transcription. *Gene* **506:** 331-338

Meissner M, Lopato S, Gotzmann J, Sauermann G, Barta A (2003) Proto-oncoprotein tls/fus is associated to the nuclear matrix and complexed with splicing factors ptb, srm160, and sr proteins. *Experimental Cell Research* **283:** 184-195

Mercer TR, Dinger ME, Mattick JS (2009) Long non-coding RNAs: insights into functions. *Nat Rev Genet* **10:** 155-159

Merner Nancy D, Girard Simon L, Catoire H, Bourassa Cynthia V, Belzil Véronique V, Rivière J-B, Hince P, Levert A, Dionne-Laporte A, Spiegelman D, Noreau A, Diab S, Szuto A, Fournier H, Raelson J, Belouchi M, Panisset M, Cossette P, Dupré N, Bernard G, Chouinard S, Dion Patrick A, Rouleau Guy A (2012) Exome Sequencing Identifies FUS Mutations as a Cause of Essential Tremor. *The American Journal of Human Genetics* **91:** 313-319

Miguel L, Avequin T, Delarue M, Feuillette S, Frébourg T, Campion D, Lecourtois M (2012) Accumulation of insoluble forms of FUS protein correlates with toxicity in Drosophila. *Neurobiology of Aging* **33:** e1-15

Mitchell J, McGoldrick P, Vance C, Hortobagyi T, Sreedharan J, Rogelj B, Tudor E, Smith B, Klasen C, Miller CJ, Cooper J, Greensmith L, Shaw C (2012) Overexpression of human wild-type FUS causes progressive motor neuron degeneration in an age- and dose-dependent fashion. *Acta Neuropathol***:** 1-16

Momeni P, Rogaeva E, van Deerlin V, Yuan W, Grafman J, Tierney M, Huey E, Bell J, Morris CM, Kalaria RN, van Rensburg SJ, Niehaus D, Potocnik F, Kawarai T, Salehi-Rad S, Sato C, St. George-Hyslop P, Hardy J (2006) Genetic Variability in CHMP2B and Frontotemporal Dementia. *Neurodegenerative Diseases* **3:** 129-133

Morahan JM, Yu B, Trent RJ, Pamphlett R (2009) A genome-wide analysis of brain DNA methylation identifies new candidate genes for sporadic amyotrophic lateral sclerosis. *Amyotrophic Lateral Sclerosis* **10:** 418-429

Mori K, Lammich S, Mackenzie IA, Forné I, Zilow S, Kretzschmar H, Edbauer D, Janssens J, Kleinberger G, Cruts M, Herms J, Neumann M, Broeckhoven C, Arzberger T, Haass C (2013a) hnRNP A3 binds to GGGGCC repeats and is a constituent of p62-positive/TDP43-negative inclusions in the hippocampus of patients with C9orf72 mutations. *Acta Neuropathol* **125:** 413-423

Mori K, Weng S-M, Arzberger T, May S, Rentzsch K, Kremmer E, Schmid B, Kretzschmar HA, Cruts M, Van Broeckhoven C, Haass C, Edbauer D (2013b) The C9orf72 GGGGCC Repeat Is Translated into Aggregating Dipeptide-Repeat Proteins in FTLD/ALS. *Science* **339:** 1335-1338

Morimoto BH, Fox AW, Stewart AJ, Gold M (2013) Davunetide: a review of safety and efficacy data with a focus on neurodegenerative diseases. *Expert Rev Clin Pharmacol* **6:** 483-502

Morris M, Maeda S, Vossel K, Mucke L (2011) The Many Faces of Tau. *Neuron* **70:** 410-426

Morrison JH, Hof PR (1997) Life and Death of Neurons in the Aging Brain. *Science* **278:** 412-419

Munoz D, Neumann M, Kusaka H, Yokota O, Ishihara K, Terada S, Kuroda S, Mackenzie I (2009) FUS pathology in basophilic inclusion body disease. *Acta Neuropathol* **118:** 617-627

Nakashima-Yasuda H, Uryu K, Robinson J, Xie S, Hurtig H, Duda J, Arnold S, Siderowf A, Grossman M, Leverenz J, Woltjer R, Lopez O, Hamilton R, Tsuang D, Galasko D, Masliah E, Kaye J, Clark C, Montine T, Lee VY, Trojanowski J (2007) Co-morbidity of TDP-43 proteinopathy in Lewy body related diseases. *Acta Neuropathol* **114:** 221-229

Nakaya TA, Panagiotis; Maragkakis, Manolis; Chang, Alexandra; Mourelatos, Zissimos (2013) FUS regulates genes coding for RNA-binding proteins in neurons by binding to their highly conserved introns. *RNA* **19:** 498-509

Neumann M, Mackenzie IR, Cairns NJ, Boyer PJ, Markesbery WR, Smith CD, Taylor JP, Kretzschmar HA, Kimonis VE, Forman MS (2007) TDP-43 in the Ubiquitin Pathology of Frontotemporal Dementia With VCP Gene Mutations. *Journal of Neuropathology & Experimental Neurology* **66:** 152-157

Neumann M, Rademakers R, Roeber S, Baker M, Kretzschmar HA, Mackenzie IR (2009a) A new subtype of frontotemporal lobar degeneration with FUS pathology. *Brain* **132:** 2922-2931

Neumann M, Roeber S, Kretzschmar H, Rademakers R, Baker M, Mackenzie IA (2009b) Abundant FUS-immunoreactive pathology in neuronal intermediate filament inclusion disease. *Acta Neuropathol* **118:** 605-616

Neumann M, Sampathu DM, Kwong LK, Truax AC, Micsenyi MC, Chou TT, Bruce J, Schuck T, Grossman M, Clark CM, McCluskey LF, Miller BL, Masliah E, Mackenzie IR, Feldman H, Feiden W, Kretzschmar HA, Trojanowski JQ, Lee VM-Y (2006) Ubiquitinated TDP-43 in Frontotemporal Lobar Degeneration and Amyotrophic Lateral Sclerosis. *Science* **314:** 130-133

NINDS. (2013) Amyotrophic Lateral Sclerosis (ALS) Fact Sheet. In (NINDS) NIoNDaS (ed.), *NIH Publication No. 13-916*. NIH.

Nishimaru H, Restrepo CE, Ryge J, Yanagawa Y, Kiehn O (2005) Mammalian motor neurons corelease glutamate and acetylcholine at central synapses. *Proceedings of the National Academy of Sciences of the United States of America* **102:** 5245-5249

Orozco D, Edbauer D (2013) FUS-mediated alternative splicing in the nervous system: consequences for ALS and FTLD. *J Mol Med* **91:** 1343-1354

Orozco D, Tahirovic S, Rentzsch K, Schwenk BM, Haass C, Edbauer D (2012) Loss of fused in sarcoma (FUS) promotes pathological Tau splicing. *EMBO Rep* **13:** 759-764

Ortega-Cubero S, Lorenzo-Betancor O, Lorenzo E, Alonso E, Coria F, Pastor MA, Fernández-Santiago R, Martí MJ, Ezquerra M, Valldeoriola F, Compta Y, Tolosa E, Agundez JA, Jiménez-Jiménez FJ, Gironell A, Clarimon J, de Castro P, García-Martín E, Alonso-Navarro H, Pastor P (2013) Fused in Sarcoma (FUS) gene mutations are not a frequent cause of essential tremor in Europeans. *Neurobiology of Aging* **34:** e9-e11

Parkinson N, Ince PG, Smith MO, Highley R, Skibinski G, Andersen PM, Morrison KE, Pall HS, Hardiman O, Collinge J, Shaw PJ, Fisher EC, Study obotMPiA, Consortium tF (2006) ALS phenotypes with mutations in CHMP2B (charged multivesicular body protein 2B). *Neurology* **67:** 1074-1077

Pick A (1892) Über die Beziehungen der senilen Hirnatrophie zur Aphasie. *Prag Med Wochenschr* **17:** 165-167

Polymenidou M, Lagier-Tourenne C, Hutt KR, Huelga SC, Moran J, Liang TY, Ling S-C, Sun E, Wancewicz E, Mazur C, Kordasiewicz H, Sedaghat Y, Donohue JP, Shiue L, Bennett CF, Yeo GW, Cleveland DW (2011) Long pre-mRNA depletion and RNA missplicing contribute to neuronal vulnerability from loss of TDP-43. *Nat Neurosci* **14:** 459-468

Powers CA, Mathur M, Raaka BM, Ron D, Samuels HH (1998) TLS (translocated-in-liposarcoma) is a high-affinity interactor for steroid, thyroid hormone, and retinoid receptors. *Molecular Endocrinology* **12:** 4-18

Prasad D, Ouchida M, Lee L, Rao VN, Reddy E (1994) TLS/FUS fusion domain of TLS/FUS-erg chimeric protein resulting from the t (16; 21) chromosomal translocation in human myeloid leukemia functions as a transcriptional activation domain. *Oncogene* **9:** 3717-3729

Puls I, Jonnakuty C, LaMonte BH, Holzbaur ELF, Tokito M, Mann E, Floeter MK, Bidus K, Drayna D, Oh SJ, Brown RH, Ludlow CL, Fischbeck KH (2003) Mutant dynactin in motor neuron disease. *Nat Genet* **33:** 455-456

Qiang L, Yu W, Andreadis A, Luo M, Baas PW (2006) Tau Protects Microtubules in the Axon from Severing by Katanin. *The Journal of Neuroscience* **26:** 3120-3129

Qiu H, Lee S, Shang Y, Wang W-Y, Au KF, Kamiya S, Barmada SJ, Finkbeiner S, Lui H, Carlton CE (2014) ALS-associated mutation FUS-R521C causes DNA damage and RNA splicing defects. *The Journal of clinical investigation* **124:** 981–999

Rabbitts TH, Forster A, Larson R, Nathan P (1993) Fusion of the dominant negative transcription regulator CHOP with a novel gene FUS by translocation t(12;16) in malignant liposarcoma. *Nat Genet* **4:** 175-180

Rademakers R, Cruts M, van Broeckhoven C (2004) The role of tau (MAPT) in frontotemporal dementia and related tauopathies. *Human Mutation* **24:** 277-295

Rademakers R, Neumann M, Mackenzie IR (2012) Advances in understanding the molecular basis of frontotemporal dementia. *Nat Rev Neurol* **8:** 423-434

Rappsilber J, Friesen WJ, Paushkin S, Dreyfuss G, Mann M (2003) Detection of Arginine Dimethylated Peptides by Parallel Precursor Ion Scanning Mass Spectrometry in Positive Ion Mode. *Analytical Chemistry* **75:** 3107-3114

Rappsilber J, Ryder U, Lamond AI, Mann M (2002) Large-Scale Proteomic Analysis of the Human Spliceosome. *Genome Research* **12:** 1231-1245

Rascovsky K, Hodges JR, Knopman D, Mendez MF, Kramer JH, Neuhaus J, van Swieten JC, Seelaar H, Dopper EGP, Onyike CU, Hillis AE, Josephs KA, Boeve BF, Kertesz A, Seeley WW, Rankin KP, Johnson JK, Gorno-Tempini M-L, Rosen H, Prioleau-Latham CE, Lee A, Kipps CM, Lillo P, Piguet O, Rohrer JD, Rossor MN, Warren JD, Fox NC, Galasko D, Salmon DP, Black SE, Mesulam M, Weintraub S, Dickerson BC, Diehl-Schmid J, Pasquier F, Deramecourt V, Lebert F, Pijnenburg Y, Chow TW, Manes F, Grafman J, Cappa SF, Freedman M, Grossman M, Miller BL (2011) Sensitivity of revised diagnostic criteria for the behavioural variant of frontotemporal dementia. *Brain* **134:** 2456-2477

Reed R (2003) Coupling transcription, splicing and mRNA export. *Current Opinion in Cell Biology* **15:** 326-331

Renton AE, Chio A, Traynor BJ (2014) State of play in amyotrophic lateral sclerosis genetics. *Nat Neurosci* **17:** 17-23

Renton Alan E, Majounie E, Waite A, Simón-Sánchez J, Rollinson S, Gibbs JR, Schymick Jennifer C, Laaksovirta H, van Swieten John C, Myllykangas L, Kalimo H, Paetau A, Abramzon Y, Remes Anne M, Kaganovich A, Scholz Sonja W, Duckworth J, Ding J, Harmer Daniel W, Hernandez Dena G, Johnson Janel O, Mok K, Ryten M, Trabzuni D, Guerreiro Rita J, Orrell Richard W, Neal J, Murray A, Pearson J, Jansen Iris E, Sondervan D, Seelaar H, Blake D, Young K, Halliwell N, Callister Janis B, Toulson G, Richardson A, Gerhard A, Snowden J, Mann D, Neary D, Nalls Michael A, Peuralinna T, Jansson L, Isoviita V-M, Kaivorinne A-L, Hölttä-Vuori M, Ikonen E, Sulkava R, Benatar M, Wuu J, Chiò A, Restagno G, Borghero G, Sabatelli M, Heckerman D, Rogaeva E, Zinman L, Rothstein Jeffrey D, Sendtner M, Drepper C, Eichler Evan E, Alkan C, Abdullaev Z, Pack Svetlana D, Dutra A, Pak E, Hardy J, Singleton A, Williams Nigel M, Heutink P, Pickering-Brown S, Morris Huw R, Tienari Pentti J, Traynor Bryan J (2011) A Hexanucleotide Repeat Expansion in C9ORF72 Is the Cause of Chromosome 9p21-Linked ALS-FTD. *Neuron* **72:** 257-268

Ringholz GM, Appel SH, Bradshaw M, Cooke NA, Mosnik DM, Schulz PE (2005) Prevalence and patterns of cognitive impairment in sporadic ALS. *Neurology* **65:** 586-590

Rogelj B, Easton LE, Bogu GK, Stanton LW, Rot G, Curk T, Zupan B, Sugimoto Y, Modic M, Haberman N, Tollervey J, Fujii R, Takumi T, Shaw CE, Ule J (2012) Widespread binding of FUS along nascent RNA regulates alternative splicing in the brain. *Sci Rep* **2:** 1-10

Rohrer JD, Guerreiro R, Vandrovcova J, Uphill J, Reiman D, Beck J, Isaacs AM, Authier A, Ferrari R, Fox NC, Mackenzie IRA, Warren JD, de Silva R, Holton J, Revesz T, Hardy J, Mead S,

Rossor MN (2009) The heritability and genetics of frontotemporal lobar degeneration. *Neurology* **73:** 1451-1456

Rosen DR, Siddique T, Patterson D, Figlewicz DA, Sapp P, Hentati A, Donaldson D, Goto J, O'Regan JP, Deng H-X, Rahmani Z, Krizus A, McKenna-Yasek D, Cayabyab A, Gaston SM, Berger R, Tanzi RE, Halperin JJ, Herzfeldt B, Van den Bergh R, Hung W-Y, Bird T, Deng G, Mulder DW, Smyth C, Laing NG, Soriano E, Pericak-Vance MA, Haines J, Rouleau GA, Gusella JS, Horvitz HR, Brown RH (1993) Mutations in Cu/Zn superoxide dismutase gene are associated with familial amyotrophic lateral sclerosis. *Nature* **362:** 59-62

Ross CA, Poirier MA (2004) Protein aggregation and neurodegenerative disease. **10:** S10-S17

Rothstein JD, Martin LJ, Kuncl RW (1992) Decreased glutamate transport by the brain and spinal cord in amyotrophic lateral sclerosis. *New England Journal of Medicine* **326:** 1464-1468

Santarella RA, Skiniotis G, Goldie KN, Tittmann P, Gross H, Mandelkow E-M, Mandelkow E, Hoenger A (2004) Surface-decoration of Microtubules by Human Tau. *Journal of Molecular Biology* **339:** 539-553

Santillo AF, Nilsson C, Englund E (2013) von Economo neurones are selectively targeted in frontotemporal dementia. *Neuropathology and Applied Neurobiology* **39:** 572-579

Schägger H, Von Jagow G (1987) Tricine-sodium dodecyl sulfate-polyacrylamide gel electrophoresis for the separation of proteins in the range from 1 to 100 kDa. *Analytical biochemistry* **166:** 368-379

Scholz D, Pöltl D, Genewsky A, Weng M, Waldmann T, Schildknecht S, Leist M (2011) Rapid, complete and large-scale generation of post-mitotic neurons from the human LUHMES cell line. *Journal of Neurochemistry* **119:** 957-971

Schwab C, Arai T, Hasegawa M, Yu S, McGeer PL (2008) Colocalization of transactivation-responsive DNA-binding protein 43 and huntingtin in inclusions of Huntington disease. *Journal of Neuropathology & Experimental Neurology* **67:** 1159-1165

Schwartz JC, Ebmeier CC, Podell ER, Heimiller J, Taatjes DJ, Cech TR (2012) FUS binds the CTD of RNA polymerase II and regulates its phosphorylation at Ser2. *Genes & Development* **26:** 2690-2695

Schwenk BM, Lang CM, Hogl S, Tahirovic S, Orozco D, Rentzsch K, Lichtenthaler SF, Hoogenraad CC, Capell A, Haass C, Edbauer D (2013) The FTLD risk factor TMEM106B and MAP6 control dendritic trafficking of lysosomes. *The EMBO Journal* **33:** 450-467

Seeley WW (2008) Selective functional, regional, and neuronal vulnerability in frontotemporal dementia. *Current Opinion in Neurology* **21:** 701-707

Seeley WW, Bauer AM, Miller BL, Gorno-Tempini ML, Kramer JH, Weiner M, Rosen HJ (2005) The natural history of temporal variant frontotemporal dementia. *Neurology* **64:** 1384-1390

Sergeant N, David JP, Lefranc D, Vermersch P, Wattez A, Delacourte A (1997) Different distribution of phosphorylated tau protein isoforms in Alzheimer's and Pick's diseases. *FEBS Letters* **412:** 578-582

Shaw PJ, Ince PG (1997) Glutamate, excitotoxicity and amyotrophic lateral sclerosis. *J Neurol* **244:** S3-S14

Shelkovnikova T (2013) Modelling FUSopathies: focus on protein aggregation. *Biochemical Society transactions* **41:** 1613-1617

Sieben A, Van Langenhove T, Engelborghs S, Martin J-J, Boon P, Cras P, De Deyn P-P, Santens P, Van Broeckhoven C, Cruts M (2012) The genetics and neuropathology of frontotemporal lobar degeneration. *Acta Neuropathol* **124:** 353-372

Skovronsky DM, Lee VM-Y, Trojanowski JQ (2006) NEURODEGENERATIVE DISEASES: New Concepts of Pathogenesis and Their Therapeutic Implications. *Annual Review of Pathology: Mechanisms of Disease* **1:** 151-170

Smith CL (1994) Cytoskeletal movements and substrate interactions during initiation of neurite outgrowth by sympathetic neurons in vitro. *The Journal of Neuroscience* **14:** 384-398

Snowden J, Hu Q, Rollinson S, Halliwell N, Robinson A, Davidson Y, Momeni P, Baborie A, Griffiths T, Jaros E, Perry R, Richardson A, Pickering-Brown S, Neary D, Mann DA (2011) The most common type of FTLD-FUS (aFTLD-U) is associated with a distinct clinical form of frontotemporal dementia but is not related to mutations in the FUS gene. *Acta Neuropathol* **122:** 99-110

Sobrido M-J, Abu–Khalil A, Weintraub S, Johnson N, Quinn B, Cummings JL, Mesulam M-M, Geschwind DH (2003) Possible association of the tau H1/H1 genotype with primary progressive aphasia. *Neurology* **60:** 862-864

Stamper C, Siegel A, Liang WS, Pearson JV, Stephan DA, Shill H, Connor D, Caviness JN, Sabbagh M, Beach TG, Adler CH, Dunckley T (2008) Neuronal gene expression correlates of Parkinson's disease with dementia. *Movement Disorders* **23:** 1588-1595

Steele JC, McGeer PL (2008) The ALS/PDC syndrome of Guam and the cycad hypothesis. *Neurology* **70:** 1984-1990

Suberbielle E, Sanchez PE, Kravitz AV, Wang X, Ho K, Eilertson K, Devidze N, Kreitzer AC, Mucke L (2013) Physiologic brain activity causes DNA double-strand breaks in neurons, with exacerbation by amyloid-[beta]. *Nat Neurosci* **16:** 613-621

Sun Z, Diaz Z, Fang X, Hart MP, Chesi A, Shorter J, Gitler AD (2011) Molecular Determinants and Genetic Modifiers of Aggregation and Toxicity for the ALS Disease Protein FUS/TLS. *PLoS Biol* **9:** 1-25

Sundar PD, Yu C-E, Sieh W, Steinbart E, Garruto RM, Oyanagi K, Craig U-K, Bird TD, Wijsman EM, Galasko DR, Schellenberg GD (2007) Two sites in the MAPT region confer genetic risk for Guam ALS/PDC and dementia. *Human Molecular Genetics* **16:** 295-306

Takei Y, Teng J, Harada A, Hirokawa N (2000) Defects in Axonal Elongation and Neuronal Migration in Mice with Disrupted tau and map1b Genes. *The Journal of Cell Biology* **150:** 989-1000

Tan AY, Manley JL (2009) The TET Family of Proteins: Functions and Roles in Disease. *Journal of Molecular Cell Biology* **1:** 82-92

Tan AY, Riley TR, Coady T, Bussemaker HJ, Manley JL (2012) TLS/FUS (translocated in liposarcoma/fused in sarcoma) regulates target gene transcription via single-stranded DNA response elements. *Proceedings of the National Academy of Sciences* **109:** 6030-6035

Tateishi T, Hokonohara T, Yamasaki R, Miura S, Kikuchi H, Iwaki A, Tashiro H, Furuya H, Nagara Y, Ohyagi Y, Nukina N, Iwaki T, Fukumaki Y, Kira J-i (2010) Multiple system degeneration with basophilic inclusions in Japanese ALS patients with FUS mutation. *Acta Neuropathol* **119:** 355-364

Taylor JP, Hardy J, Fischbeck KH (2002) Toxic Proteins in Neurodegenerative Disease. *Science* **296:** 1991-1995

Thomas M, Alegre-Abarrategui J, Wade-Martins R (2013) RNA dysfunction and aggrephagy at the centre of an amyotrophic lateral sclerosis/frontotemporal dementia disease continuum. *Brain* **136:** 1345-1360

Timm T, Matenia D, Li XY, Griesshaber B, Mandelkow EM (2006) Signaling from MARK to Tau: Regulation, Cytoskeletal Crosstalk, and Pathological Phosphorylation. *Neurodegenerative Diseases* **3:** 207-217

Tobin JE, Latourelle JC, Lew MF, Klein C, Suchowersky O, Shill HA, Golbe LI, Mark MH, Growdon JH, Wooten GF, Racette BA, Perlmutter JS, Watts R, Guttman M, Baker KB, Goldwurm S, Pezzoli G, Singer C, Saint-Hilaire MH, Hendricks AE, Williamson S, Nagle MW, Wilk JB, Massood T, Laramie JM, DeStefano AL, Litvan I, Nicholson G, Corbett A, Isaacson S, Burn DJ, Chinnery PF, Pramstaller PP, Sherman S, Al-hinti J, Drasby E, Nance M, Moller AT, Ostergaard K, Roxburgh R, Snow B, Slevin JT, Cambi F, Gusella JF, Myers RH (2008) Haplotypes and gene expression implicate the MAPT region for Parkinson disease: The GenePD Study. *Neurology* **71:** 28-34

Tollervey JR, Curk T, Rogelj B, Briese M, Cereda M, Kayikci M, Konig J, Hortobagyi T, Nishimura AL, Zupunski V, Patani R, Chandran S, Rot G, Zupan B, Shaw CE, Ule J (2011) Characterizing the RNA targets and position-dependent splicing regulation by TDP-43. *Nat Neurosci* **14:** 452-458

Tong J, Huang C, Bi F, Wu Q, Huang B, Liu X, Li F, Zhou H, Xia XG (2013) Expression of ALS-linked TDP-43 mutant in astrocytes causes non-cell-autonomous motor neuron death in rats. *The EMBO Journal* **32:** 1917-1926

Tradewell ML, Yu Z, Tibshirani M, Boulanger M-C, Durham HD, Richard S (2012) Arginine methylation by PRMT1 regulates nuclear-cytoplasmic localization and toxicity of FUS/TLS harbouring ALS-linked mutations. *Human Molecular Genetics* **21:** 136-149

Trojanowski JQ (2008) PENN Neurodegenerative Disease Research – In the Spirit of Benjamin Franklin. *Neurosignals* **16:** 5-10

Trojanowski JQ, Duff K, Fillit H, Koroshetz W, Kuret J, Murphy D, Refolo L (2008) New directions for frontotemporal dementia drug discovery. *Alzheimer's & Dementia* **4:** 89-93

Ule J, Ule A, Spencer J, Williams A, Hu J-S, Cline M, Wang H, Clark T, Fraser C, Ruggiu M, Zeeberg BR, Kane D, Weinstein JN, Blume J, Darnell RB (2005) Nova regulates brain-specific splicing to shape the synapse. *Nat Genet* **37:** 844-852

Urwin H, Authier A, Nielsen JE, Metcalf D, Powell C, Froud K, Malcolm DS, Holm I, Johannsen P, Brown J, Fisher EMC, van der Zee J, Bruyland M, Consortium tF, Van Broeckhoven C, Collinge J, Brandner S, Futter C, Isaacs AM (2010a) Disruption of endocytic trafficking in frontotemporal dementia with CHMP2B mutations. *Human Molecular Genetics* **19:** 2228-2238

Urwin H, Josephs K, Rohrer J, Mackenzie I, Neumann M, Authier A, Seelaar H, Swieten J, Brown J, Johannsen P, Nielsen J, Holm I, Dickson D, Rademakers R, Graff-Radford N, Parisi J,

Petersen R, Hatanpaa K, White Iii C, Weiner M, Geser F, Deerlin V, Trojanowski J, Miller B, Seeley W, Zee J, Kumar-Singh S, Engelborghs S, Deyn P, Broeckhoven C, Bigio E, Deng H-X, Halliday G, Kril J, Munoz D, Mann D, Pickering-Brown S, Doodeman V, Adamson G, Ghazi-Noori S, Fisher EC, Holton J, Revesz T, Rossor M, Collinge J, Mead S, Isaacs A (2010b) FUS pathology defines the majority of tau- and TDP-43-negative frontotemporal lobar degeneration. *Acta Neuropathol* **120:** 33-41

Vaccaro A, Tauffenberger A, Aggad D, Rouleau G, Drapeau P, Parker JA (2012) Mutant TDP-43 and FUS Cause Age-Dependent Paralysis and Neurodegeneration in <italic>C. elegans</italic>. *PLoS ONE* **7:** 1-10

Van Deerlin VM, Sleiman PMA, Martinez-Lage M, Chen-Plotkin A, Wang L-S, Graff-Radford NR, Dickson DW, Rademakers R, Boeve BF, Grossman M, Arnold SE, Mann DMA, Pickering-Brown SM, Seelaar H, Heutink P, van Swieten JC, Murrell JR, Ghetti B, Spina S, Grafman J, Hodges J, Spillantini MG, Gilman S, Lieberman AP, Kaye JA, Woltjer RL, Bigio EH, Mesulam M, al-Sarraj S, Troakes C, Rosenberg RN, White CL, Ferrer I, Llado A, Neumann M, Kretzschmar HA, Hulette CM, Welsh-Bohmer KA, Miller BL, Alzualde A, de Munain AL, McKee AC, Gearing M, Levey AI, Lah JJ, Hardy J, Rohrer JD, Lashley T, Mackenzie IRA, Feldman HH, Hamilton RL, Dekosky ST, van der Zee J, Kumar-Singh S, Van Broeckhoven C, Mayeux R, Vonsattel JPG, Troncoso JC, Kril JJ, Kwok JBJ, Halliday GM, Bird TD, Ince PG, Shaw PJ, Cairns NJ, Morris JC, McLean CA, DeCarli C, Ellis WG, Freeman SH, Frosch MP, Growdon JH, Perl DP, Sano M, Bennett DA, Schneider JA, Beach TG, Reiman EM, Woodruff BK, Cummings J, Vinters HV, Miller CA, Chui HC, Alafuzoff I, Hartikainen P, Seilhean D, Galasko D, Masliah E, Cotman CW, Tunon MT, Martinez MCC, Munoz DG, Carroll SL, Marson D, Riederer PF, Bogdanovic N, Schellenberg GD, Hakonarson H, Trojanowski JQ, Lee VMY (2010) Common variants at 7p21 are associated with frontotemporal lobar degeneration with TDP-43 inclusions. *Nat Genet* **42:** 234-239

van der Zee J, Urwin H, Engelborghs S, Bruyland M, Vandenberghe R, Dermaut B, De Pooter T, Peeters K, Santens P, De Deyn PP, Fisher EM, Collinge J, Isaacs AM, Van Broeckhoven C (2008) CHMP2B C-truncating mutations in frontotemporal lobar degeneration are associated with an aberrant endosomal phenotype in vitro. *Human Molecular Genetics* **17:** 313-322

van der Zee J, Van Langenhove T, Kleinberger G, Sleegers K, Engelborghs S, Vandenberghe R, Santens P, Van den Broeck M, Joris G, Brys J, Mattheijssens M, Peeters K, Cras P, De Deyn PP, Cruts M, Van Broeckhoven C (2011) TMEM106B is associated with frontotemporal lobar degeneration in a clinically diagnosed patient cohort. *Brain* **134:** 808-815

Van Langenhove T, van der Zee J, Gijselinck I, Engelborghs S, Vandenberghe R, Vandenbulcke M, De Bleecker J, Sieben A, Versijpt J, Ivanoiu A (2013) Distinct Clinical Characteristics of C9orf72 Expansion Carriers Compared With GRN, MAPT, and Nonmutation Carriers in a Flanders-Belgian FTLD CohortC9orf72 Characteristics in a FTLD Cohort. *JAMA neurology* **70:** 365-373

Van Langenhove T, van der Zee J, Sleegers K, Engelborghs S, Vandenberghe R, Gijselinck I, Van den Broeck M, Mattheijssens M, Peeters K, De Deyn PP, Cruts M, Van Broeckhoven C (2010) Genetic contribution of FUS to frontotemporal lobar degeneration. *Neurology* **74:** 366-371

van Langenhove T, van der Zee J, van Broeckhoven C (2012) The molecular basis of the frontotemporal lobar degeneration–amyotrophic lateral sclerosis spectrum. *Annals of Medicine* **44:** 817-828

Vance C, Rogelj B, Hortobágyi T, De Vos KJ, Nishimura AL, Sreedharan J, Hu X, Smith B, Ruddy D, Wright P, Ganesalingam J, Williams KL, Tripathi V, Al-Saraj S, Al-Chalabi A, Leigh PN, Blair IP, Nicholson G, de Belleroche J, Gallo J-M, Miller CC, Shaw CE (2009) Mutations in

FUS, an RNA Processing Protein, Cause Familial Amyotrophic Lateral Sclerosis Type 6. *Science* **323:** 1208-1211

Verpillat P, Camuzat A, Hannequin D, Thomas-Anterion C, Puel M, Belliard S, Dubois B, Didic M, Lacomblez L, Moreaud O (2002) Apolipoprotein E gene in frontotemporal dementia: an association study and meta-analysis. *European journal of human genetics: EJHG* **10:** 399-405

Wang W-Y, Pan L, Su SC, Quinn EJ, Sasaki M, Jimenez JC, Mackenzie IRA, Huang EJ, Tsai L-H (2013) Interaction of FUS and HDAC1 regulates DNA damage response and repair in neurons. *Nat Neurosci* **16:** 1383-1391

Wang Y, Wang J, Gao L, Stamm S, Andreadis A (2011) An SRp75/hnRNPG complex interacting with hnRNPE2 regulates the 5′ splice site of tau exon 10, whose misregulation causes frontotemporal dementia. *Gene* **485:** 130-138

Watts GDJ, Wymer J, Kovach MJ, Mehta SG, Mumm S, Darvish D, Pestronk A, Whyte MP, Kimonis VE (2004) Inclusion body myopathy associated with Paget disease of bone and frontotemporal dementia is caused by mutant valosin-containing protein. *Nat Genet* **36:** 377-381

Wei M-L, Andreadis A (1998) Splicing of a Regulated Exon Reveals Additional Complexity in the Axonal Microtubule-Associated Protein Tau. *Journal of Neurochemistry* **70:** 1346-1356

Weingarten MD, Lockwood AH, Hwo S-Y, Kirschner MW (1975) A protein factor essential for microtubule assembly. *Proceedings of the National Academy of Sciences* **72:** 1858-1862

WHO WHO. (2012) Dementia Fact sheet Number 362.

Williams-Gray CH, Evans JR, Goris A, Foltynie T, Ban M, Robbins TW, Brayne C, Kolachana BS, Weinberger DR, Sawcer SJ, Barker RA (2009) The distinct cognitive syndromes of Parkinson's disease: 5 year follow-up of the CamPaIGN cohort. *Brain* **132:** 2958-2969

Williams KL, Warraich ST, Yang S, Solski JA, Fernando R, Rouleau GA, Nicholson GA, Blair IP (2012) UBQLN2/ubiquilin 2 mutation and pathology in familial amyotrophic lateral sclerosis. *Neurobiology of Aging* **33:** e3-e10

Witte H, Neukirchen D, Bradke F (2008) Microtubule stabilization specifies initial neuronal polarization. *The Journal of Cell Biology* **180:** 619-632

Xia R, Liu Y, Yang L, Gal J, Zhu H, Jia J (2012) Motor neuron apoptosis and neuromuscular junction perturbation are prominent features in a Drosophila model of Fus-mediated ALS. *Molecular Neurodegeneration* **7:** 10-27

Yang L, Embree LJ, Hickstein DD (2000) TLS-ERG Leukemia Fusion Protein Inhibits RNA Splicing Mediated by Serine-Arginine Proteins. *Molecular and Cellular Biology* **20:** 3345-3354

Yang L, Embree LJ, Tsai S, Hickstein DD (1998) Oncoprotein TLS Interacts with Serine-Arginine Proteins Involved in RNA Splicing. *Journal of Biological Chemistry* **273:** 27761-27764

Yeo G, Holste D, Kreiman G, Burge C (2004) Variation in alternative splicing across human tissues. *Genome Biology* **5:** R74.71-15

Zakaryan RP, Gehring H (2006) Identification and Characterization of the Nuclear Localization/Retention Signal in the EWS Proto-oncoprotein. *Journal of Molecular Biology* **363:** 27-38

Zhou Z, Licklider LJ, Gygi SP, Reed R (2002) Comprehensive proteomic analysis of the human spliceosome. *Nature* **419:** 182-185

Zinszner H, Albalat R, Ron D (1994) A novel effector domain from the RNA-binding protein TLS or EWS is required for oncogenic transformation by CHOP. *Genes & Development* **8:** 2513-2526

Zinszner H, Sok J, Immanuel D, Yin Y, Ron D (1997) TLS (FUS) binds RNA in vivo and engages in nucleo-cytoplasmic shuttling. *Journal of Cell Science* **110:** 1741-1750

7. Annex

Annex I

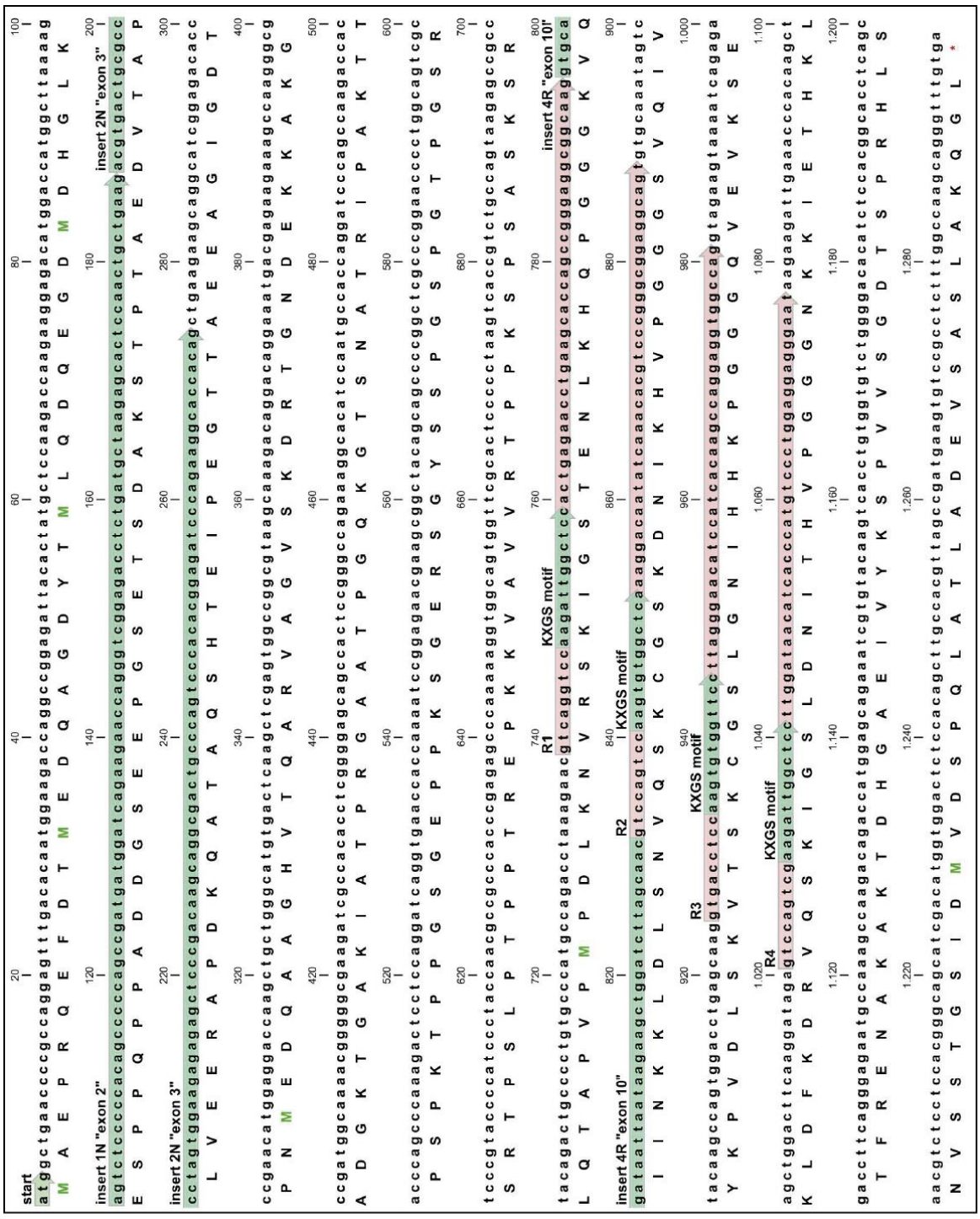

Figure 28 Rat *MAPT*/TAU 2N4R isoform

The *MAPT* nucleotide and protein sequence presented here is supported by cloning data and is based on the *MAPT* rat isoform sequences annotated in NCBI and Ensembl databases. Note that the exon names are given with quotation marks to avoid confusion, because the exon number can vary depending on the isoform. Characteristic protein domains, as the N-terminal inserts and microtubule binding domains (R1-4), are also labeled. Note that the microtubule domains contain the typical KXGS motif.

Annex II

Table 1 Alternative splicing upon loss of FUS: hits identified in at least 3 studies

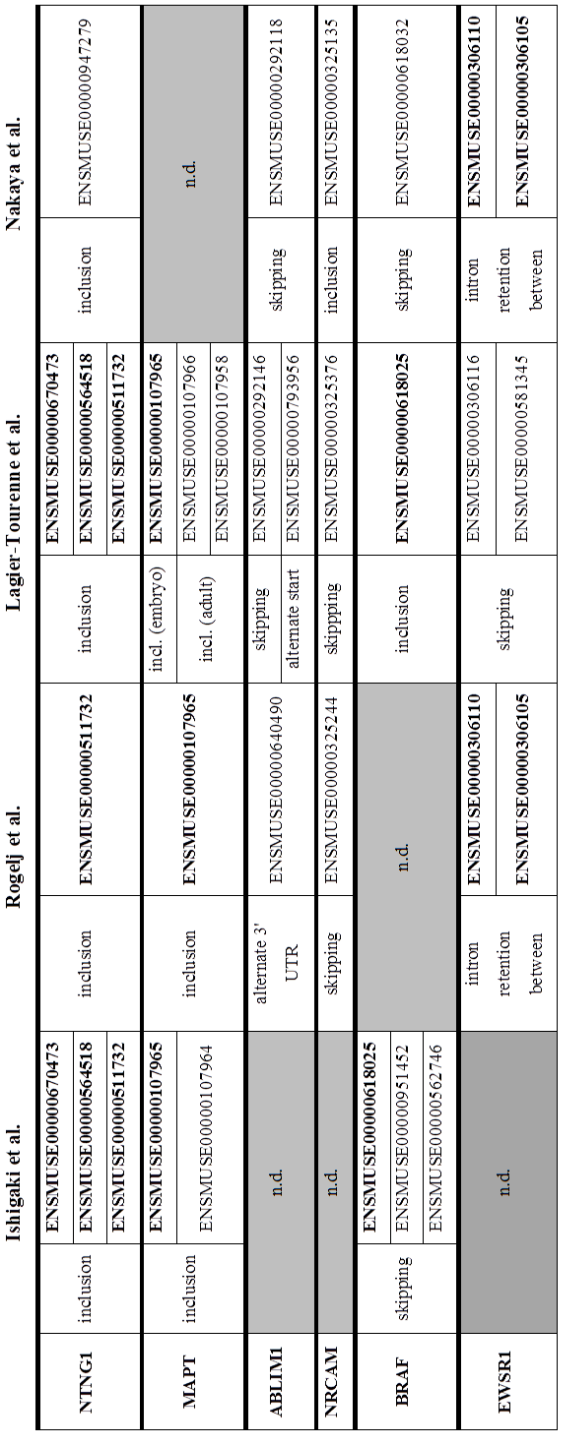

	Ishigaki et al.		Rogelj et al.		Lagier-Tourenne et al.		Nakaya et al.	
NTNG1	inclusion	**ENSMUSE00000670473**	inclusion	**ENSMUSE00000511732**	inclusion	**ENSMUSE00000670473**	inclusion	ENSMUSE00000947279
		ENSMUSE00000564518				**ENSMUSE00000564518**		
		ENSMUSE00000511732				**ENSMUSE00000511732**		
MAPT	inclusion	**ENSMUSE00000107965**	inclusion	**ENSMUSE00000107965**	incl. (embryo)	**ENSMUSE00000107965**	n.d.	
		ENSMUSE00000107964			incl. (adult)	ENSMUSE00000107966		
						ENSMUSE00000107958		
ABLIM1	n.d.		alternate 3' UTR	ENSMUSE00000640490	skipping	ENSMUSE00000292146	skipping	ENSMUSE00000292118
					alternate start	ENSMUSE00000793956		
NRCAM	n.d.		skipping	ENSMUSE00000325244	skippping	ENSMUSE00000325376	inclusion	ENSMUSE00000325135
BRAF	skipping	**ENSMUSE00000618025**	n.d.		inclusion	**ENSMUSE00000618025**	skipping	ENSMUSE00000618032
		ENSMUSE00000951452						
		ENSMUSE00000562746						
EWSR1	n.d.		intron retention between	**ENSMUSE00000306110**	skipping	ENSMUSE00000306116	intron retention between	**ENSMUSE00000306110**
				ENSMUSE00000306105		ENSMUSE00000581345		**ENSMUSE00000306105**

The columns list the splicing event reported in each publication for the genes marked in the row headers. Each splicing event includes the type of event (eg. inclusion) and the identifier of the exon involved. All coordinates were analyzed with the Ensembl mouse genome NCBIM37. In case of ambiguity, all exons in the chromosomal region are listed. Exons identified more than once are marked in bold. ENSMUSE00000xxxxxx Ensembl unique and stable mouse exon identifier n.d. not detected. Adapted from (Orozco & Edbauer, 2013) and based on the publications (Ishigaki et al, 2012; Lagier-Tourenne et al, 2012; Nakaya, 2013; Rogelj et al, 2012).

8. Acknowledgements

Gratitude is not only the greatest of virtues, but the parent of all others.
-Cicero

I am very grateful to all the people that contributed directly or indirectly to this work, including the FTD/ALS patients and their families that contribute to and motivate our research. I am especially grateful to...

Prof. Dr. Dieter Edbauer for excellent supervision and hours of scientific discussion. Thank you for letting me be part of your growing lab and for your constant support and encouraging words.

Prof. Dr. Christian Haass for giving me the opportunity to work in his institute, for being part of my Thesis Advisory Committee and for his constant support.

Prof. Dr. Magdalena Götz and **Prof. Dr. Dieter Chichung Lie** for their interest in my work and for scientific discussions as part of my Thesis Advisory Committee.

The **International Max Planck Research School** for Molecular and Cellular Life Sciences: From Biology to Medicine, (IMPRS-LS) for financial support to expand our scientific knowledge, and the excellent IMPRS coordinators **Dr. Hans-Joerg Schäffer, Dr. Ingrid Wolf,** and **Maximiliane Reif** for their warm welcome in Munich, for their interest in our research and taking care of us.

Der **Deutsche Akademische Austauschdienst** (DAAD) for their interest in my work and financial support during my university studies in Hamburg. Without their help, this thesis wouldn't have been possible.

All colleagues from the **Adolf Butenandt Institute** for Metabolic Biochemistry at the LMU and the **Deutsches Zentrum für Neurodegenerative Erkrankungen** (DZNE) for their scientific and administrative help and for the friendly atmosphere.

My colleagues from the Edbauer Lab, **Dr. Julia Banzhaf**, **Benjamin Schwenk**, **Kristin Rentzsch**, **Stephanie May**, **Martin Schludi**, **Franzi Boneberg** and **Lorenz Dreßen** and former members **Dr. ShihMing Weng (Jonas)** and **Claudia Lermer**, for the friendly atmosphere in the lab, technical advice and most of all for being truly inspiring colleagues.

Thanks to **Dr. Eva Bentmann** and **Benjamin Schwenk** for carefully reading my thesis and for excellent advice.

Dr. Dorothee Dormann and **Dr. Eva Bentmann** for sharing their expertise in RNA-binding proteins and for showing interest in new projects.

Sabina Tahirovic, for sharing her expertise in axonal biology and her team especially **Andrea Wenninger-Weinzierl** and **Stephanie Kunath**, for their excellent technical support with the neuronal cultures.

Dr. Peer-Hendrik Kuhn, **Prof. Günter Höglinger**, **Anderson de Andrade**, **Dr. Sven Lammich**, **Dr. Bettina Schmid**, **Alexander Hruscha**, **Dr. Daniela Dirndorfer** and **Dr. Jacki Heraud**, for scientific discussion and technical advice regarding TAU splicing, and RNA-binding proteins.

Sabine Odoy for excellent management of the lab, for her patience, understanding and help with urgent situations.

My IMPRS-sive friends, especially **Maria Patra**, **Katrin Strecker**, **Laura Hasenkamp**, **Barbara Solchenberger**, **Nicole Teichmann**, **Amit Gupta**, **Shoh Asano**, **Vladimiros Thoma**, **Dhawal Jain**, **Mathias Rosam**, for sharing this adventure with me.

Teresa Bachhuber and **Joanna McCarter** for, without even knowing, convincing me to come to Munich and for sharing the ups and downs of this journey.

Thanks to my friends around the world for their encouraging words and constant support.

Gracias a mis abuelos, tíos, primos y sobrinos de la Familia Orozco y Familia Moisa por su energía y apoyo incondicional.

Especialmente a mis Tíos, **Jaime Ernesto Octavio Orozco Mayén**, Doctor en Medicina, y **Claudia Denise Elena Orozco Mayén**, Arquitecta y Socióloga, cuyas especiales vidas, y aún sin compartir mucho tiempo, me han inspirado y motivado siempre.

A mis amados y ejemplares padres **Alvaro Juan Antonio Orozco Mayén**, Ingeniero Industial y Master en Dirección de Empresas y en Gestión Ambiental, y **Marta Eugenia Moisa de Orozco**, Licenciada en Ciencias Económicas, Licenciada en Contaduría Públicas y Master en Administración de Empresas. Gracias infinitas, no tengo palabras para describir la dicha de tener padres como ustedes.

A mis hermanos **Adrián José Orozco Moisa** y **Juan Carlos Orozco Moisa**, de quienes soy la más fiel admiradora. Gracias por enseñarme cómo se sigue apasionadamente un ideal.

Y especialmente a **Victor**, gracias. Danke für deine Geduld, Unterstützung und Verständnis. Thanks for picking me up when it got late and thanks for packing my lunch for my weekends in the lab.

9. Curriculum Vitae

Personal Details

Denise Marie Orozco Moisa

San Salvador, El Salvador

Scientific Publications

- Orozco D and Edbauer D. "*FUS mediated alternative splicing in the nervous system - consequences for ALS and FTLD"*. J Mol Med. 2013, **Impact Factor: 4.7**
- Orozco D, Tahirovic S, Rentzsch K, Schwenk BM, Haass C, Edbauer D. "*Loss of fused in sarcoma (FUS) promotes pathological Tau splicing*". EMBO Rep. 2012, **Impact Factor: 7.2**
- Schwenk BM, Lang CM, Hogl S, Tahirovic S, Orozco D, Rentzsch K, Lichtenthaler SF, Hoogenraad CC, Capell A, Haass C, Edbauer D. "*The FTLD risk factor TMEM106B and MAP6 control dendritic trafficking of lysosomes*." EMBO Journal. 2013, **Impact Factor: 9.8**
- Heraud-Farlow J, Sharangdhar T, Li X, Pfeifer P, Tauber S, Orozco D, Hörmann A, Thomas S, Bakosova A, Farlow A, Edbauer D, Lipshitz H, Morris Q, Bilban M, Doyle M, Kiebler M. "*Staufen2 regulates neuronal target RNAs*". Cell Reports. 2013, **Impact Factor: 7.2**
- Gelderblom M, Leypoldt F, Lewerenz J, Birkenmayer G, Orozco D, Ludewig P, Thundyil J, Arumugam TV, Gerloff C, Tolosa E, Maher P, Magnus T. "*The flavonoid fisetin attenuates postischemic immune cell infiltration, activation and infarct size after transient cerebral middle artery occlusion in mice*". J Cereb Blood Flow Metab. 2012, **Impact Factor: 5.4**

International Conferences

International Conference on Alzheimer's & Parkinson's Diseases – Florence, Italy 2013

- Poster presentation

Interact 2013 – Munich, Germany 2013

- Poster presentation

Federation of European Neuroscience Societies (FENS) Forum – Barcelona, Spain 2012

- Project presented in an invited talk (Prof. Dr. Edbauer)

10. Publications

EMBO reports

scientific report

Loss of fused in sarcoma (FUS) promotes pathological Tau splicing

Denise Orozco[1,2], Sabina Tahirovic[1], Kristin Rentzsch[1], Benjamin M. Schwenk[1], Christian Haass[1,3] & Dieter Edbauer[1,3+]

[1]German Center for Neurodegenerative Diseases (DZNE), Munich, Germany, [2]The International Max Planck Research School for Molecular and Cellular Life Sciences, Martinsried, Germany, and [3]Adolf Butenandt Institute, Biochemistry, Ludwig-Maximilians University Munich, Munich, Germany

A subset of amyotrophic lateral sclerosis (ALS) and frontotemporal lobar degeneration (FTLD) patients present pathological redistribution and aggregation of the nuclear protein fused in sarcoma (FUS) in the cytoplasm. Although FUS associates with the spliceosomal complex, no endogenous neuronal splicing targets have been identified. Here we identify Tau mRNA as a physiological splicing target of FUS. In mouse brain, FUS directly binds to Tau pre-mRNA, and knockdown of FUS in hippocampal neurons leads to preferential inclusion of Tau exons 3 and 10. FUS knockdown causes significant growth cone enlargement and disorganization reminiscent of Tau loss of function. These findings suggest that disturbed cytoskeletal function and enhanced expression of the neurodegeneration-associated Tau exon 10 might contribute to FTLD/ALS with FUS inclusions.

Keywords: neurodegeneration; FUS; RNA-binding protein; splicing; Tau (MAPT)

EMBO *reports* advance online publication 19 June 2012; doi:10.1038/embor.2012.90

INTRODUCTION

Frontotemporal lobar degeneration (FTLD) and amyotrophic lateral sclerosis (ALS) have recently been recognized as opposite ends of a disease spectrum with overlapping clinical symptoms, genetics and pathology [1,2]. These devastating neurodegenerative diseases are now subdivided by specific marker proteins identified in abnormal aggregates, including Fused in sarcoma (FUS) [2–4]. The RNA/DNA-binding protein FUS normally resides predominantly in the nucleus, but is found in cytosolic inclusions of both FTLD and ALS patients. FUS binds to numerous mRNAs in HEK293 cells, however with little correlation to transcript abundance [5]. Although FUS associates with the spliceosomal complex [6], no endogenous neuronal splicing target is known so far and the role of FUS-mediated splicing in FTLD/ALS remains unclear. Two observations suggest that the loss of nuclear FUS activity contributes to FTLD/ALS pathophysiology: First, mutations disrupting the C-terminal nuclear targeting sequence of FUS cause early-onset ALS [3,4,7]. Second, even in the absence of *FUS* mutations, a partial nuclear clearing of FUS is apparent in neurons with FUS aggregates [1].

Here we identify the microtubule-associated protein Tau (MAPT) as a physiological splicing target of FUS in neurons and found morphological alterations in axons and growth cones that are reminiscent of Tau-knockout mice [8]. The *MAPT* gene consists of 16 exons and gives rise to six main transcripts in the central nervous system (supplementary Fig S1A online) [9,10]. The shortest Tau isoform, termed 0N3R, lacks exons 2, 3 and 10. Inclusion of exon 2 or exons 2 and 3 leads to insertion of one or two 29-amino acid regions (1N, 2N). Inclusion of exon 10 gives rise to a fourth microtubule-binding region (4R). The composition of the N-terminal projection domain determines microtubule spacing and might affect cellular signalling [9,11]. Somatodendritic Tau aggregates with characteristic isoform composition are found in Alzheimer's disease and a subset of FTLD collectively termed FTLD–Tau, including Pick's disease and corticobasal degeneration [2,12]. Mutations that lead to the preferential inclusion of exon 10 cause frontotemporal dementia and parkinsonism [13], showing the importance of exon 10 inclusion for FTLD–Tau disease pathology. Our data show that FUS knockdown enhances expression of Tau exon 10. Tau aggregation has so far not been described in patients with FUS pathology. However, there is evidence that non-fibrillar Tau can cause neurodegeneration and cognitive symptoms [14,15]. For example, the H1 haplotype at the MAPT locus moderately enhances exon 10 inclusion and is a strong genetic risk factor for Parkinson's disease, which also lacks overt Tau pathology [16,17].

RESULTS AND DISCUSSION

FUS knockdown affects levels of 4R Tau

Tau has been linked to many neurodegenerative disorders including FTLD–Tau. Therefore, we analysed Tau expression

[1]German Center for Neurodegenerative Diseases (DZNE), Schillerstr. 44, Munich 80336, Germany
[2]The International Max Planck Research School for Molecular and Cellular Life Sciences, Am Klopferspitz 18, Martinsried 82152, Germany
[3]Adolf Butenandt Institute, Biochemistry, Ludwig-Maximilians University Munich, Schillerstr. 44, Munich 80336, Germany
[+]Corresponding author. Tel: +49 8921 8075462; Fax: +49 8921 8075432; E-mail: dieter.edbauer@dzne.de

Received 17 January 2012; revised 22 May 2012; accepted 1 June 2012; published online 19 June 2012

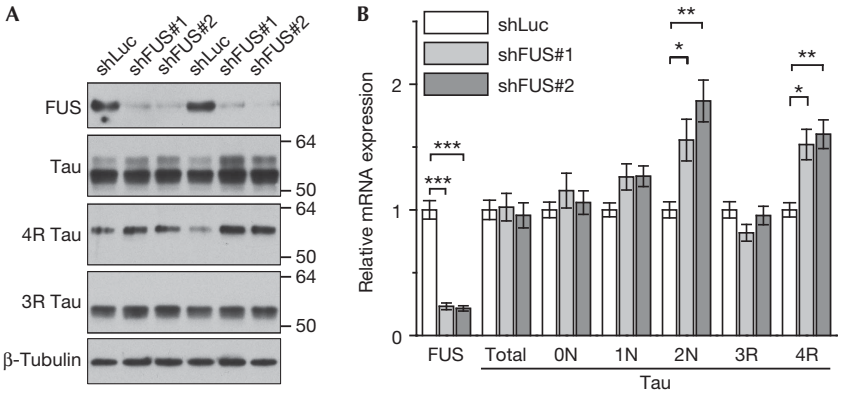

Fig 1 | FUS knockdown enhances expression of Tau exons 3 and 10. Hippocampal neurons (DIV2 + 7) were infected with lentivirus to knockdown FUS (shFUS#1 and #2) or non-targeting control (shLuc). (**A**) Immunoblots with the indicated antibodies. Note that the two main Tau isoforms comigrate with 4 R and 3 R Tau. Two replicates are shown. (**B**) Total RNA was analysed by quantitative PCR for FUS, total Tau and Tau isoforms. FUS and total Tau expression was normalized to the housekeeping gene YWHAZ. Tau isoform expression was normalized to total Tau levels. $n = 4$, mean ± s.e.m., one-way analysis of variance with Dunnett's post-test: $^{*}P < 0.05$, $^{**}P < 0.01$, $^{***}P < 0.001$. FUS, Fused in sarcoma; shFUS, short hairpin FUS; shLuc, short hairpin RNA targeting the luciferase transcript; YWHAZ, tyrosine 3-monooxygenase/tryptophan 5-monooxygenase activation protein zeta/14-3-3-zeta.

upon FUS knockdown in rat primary hippocampal neurons using lentiviral expression of short hairpin RNAs (shRNAs). We transduced neurons at day 2 *in vitro* and collected proteins 7 days later (DIV2 + 7). Two FUS-specific shRNAs (shFUS#1 and shFUS#2) specifically suppressed FUS protein expression compared with a control shRNA targeting the luciferase transcript (shLuc; Fig 1A). An XTT-based cell viability assay confirmed that FUS knockdown showed no overt toxicity in this context (supplementary Fig S2A online). Although the main Tau isoform (lower band) was unchanged, a larger isoform (upper band) appeared upregulated in FUS-knockdown neurons (Fig 1A). A Tau exon 10-specific antibody showed robustly increased levels of 4R Tau (comigrating with the upper Tau band), suggesting an effect of FUS on Tau splicing. In contrast, 3R Tau expression was not significantly affected by FUS knockdown. The amount and running behaviour of several other key synaptic proteins were unaffected by FUS knockdown, including synaptic scaffold proteins (PSD95), glutamate-receptor subunits (NR1, NR2A and GluR2), synaptic vesicle proteins (synaptophysin) and cytoskeletal proteins (β-actin and β-tubulin, Fig 1A; supplementary Fig S2B online). Together, these data strongly indicate that FUS knockdown affects splicing of Tau exon 10.

FUS knockdown affects Tau mRNA splicing

To further explore how FUS knockdown modifies Tau splicing in neurons, we designed isoform-specific primers for the alternatively spliced exons 2, 3 and 10 (supplementary Fig S1B online). Reverse transcription and quantitative real-time PCR (qPCR) allowed for quantitative comparison of exon insertion between FUS knockdown and control shRNA-infected neurons. About 80% reduction of FUS levels did not significantly affect total Tau mRNA expression (Fig 1B), but caused significant upregulation of the 2N and 4R Tau isoforms.

As FUS and TDP-43 aggregation cause similar clinical symptoms in FTLD and ALS patients, it is tempting to hypothesize that FUS and TDP-43 regulate overlapping mRNA targets [1]. We therefore used lentiviral shRNA to downregulate TDP-43 in hippocampal neurons and analysed the expression of Tau isoforms by qPCR. Consistent with previous results [18], splicing of exons 2, 3 and 10 was not significantly affected by TDP-43 knockdown (supplementary Fig S3 online). Thus, aberrant Tau splicing might contribute to FTLD/ALS pathophysiology with FUS inclusions, but not with TDP-43 inclusions.

FUS reintroduction rescues altered Tau splicing

To confirm that altered Tau splicing upon shFUS treatment is mediated by loss of FUS and not by off-target effects, we performed rescue experiments by reintroduction of FUS in shRNA-treated cells. We doubly infected neurons with lentiviral vectors expressing shRNA (shLuc or shFUS#2) and haemagglutinin (HA)-tagged wild-type human FUS resistant to shFUS#2. Transduction with HA–FUS strongly increased FUS-expression compared with the endogenous levels of shLuc control infected cells (Fig 2A). Importantly, HA–FUS co-transduction not only prevented the shFUS#2-mediated upregulation of 4R Tau, but even suppressed its expression below shLuc control levels (Fig 2A). Similarly, HA–FUS coexpression completely abolished the induction of 2N and 4R isoforms by shFUS on mRNA level (Fig 2B). The full rescue of the shFUS#2-mediated splicing effects by overexpression of FUS strongly argues for a FUS-specific effect.

FUS is associated with Tau transcripts in the brain

To test whether FUS is associated with Tau RNA, we performed immunoprecipitations from mouse brain (P15) extracts using a FUS antibody and a GST antibody as a negative control, followed by isolation of the bound RNA. By reverse transcription and qPCR we amplified Tau pre-mRNA using intronic primers and compared the recovery of Tau pre-mRNA from the immunoprecipitates. While the control immunoprecipitates contained no detectable Tau pre-mRNA (Fig 3A,B), FUS-immunoprecipitates recovered about 1% of the input material, which strongly suggests a specific interaction. Using intron-spanning primers, we also detected spliced Tau mRNA specifically enriched (but to a lesser extent than pre-mRNA) in FUS-immunoprecipitates. The enrichment of

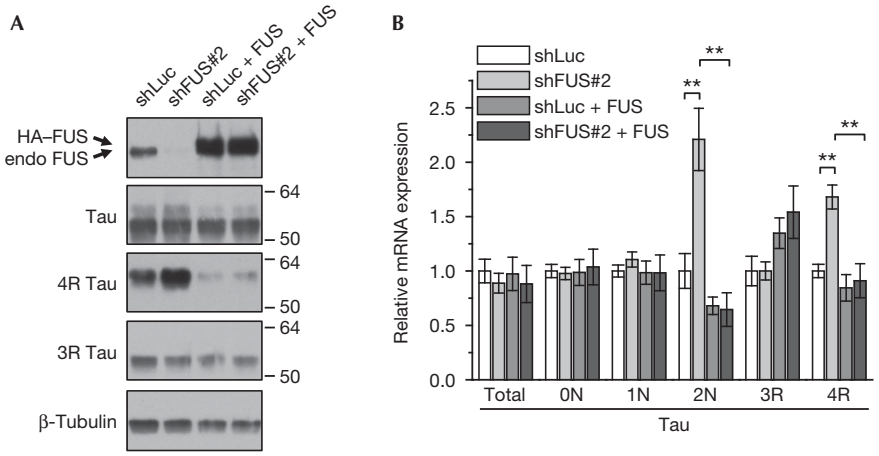

Fig 2 | FUS overexpression fully rescues the Tau splicing phenotype. Hippocampal neurons (DIV2 + 7) were coinfected with lentivirus expressing the shLuc or shFUS#2 and HA-tagged shRNA-resistant FUS. (**A**) Immunoblots with the indicated antibodies. (**B**) Total RNA was analysed by quantitative PCR for total Tau and isoforms. Total Tau expression was normalized to YWHAZ. Tau isoform expression was normalized to total Tau levels. $n = 3$, mean ± s.e.m, analysis of variance with Bonferroni correction: $^{**}P < 0.01$. Note that samples from shLuc- and shFUS-transduced neurons were statistically indistinguishable on coexpression of shFUS-resistant FUS. FUS, Fused in sarcoma; HA, haemagglutinin; shFUS, short hairpin FUS; shLuc, short hairpin RNA targeting the luciferase transcript.

Tau mRNA was comparable to two positive controls recently identified by crosslinking and immunoprecipitation (CLIP) analysis of FUS-bound RNAs in HEK293 cell, its own mRNA and SON (Fig 3B; [5]). In contrast, glyceraldehyde-3-phosphate dehydrogenase pre-mRNA and mRNA were not enriched in FUS-immunoprecipitates. Taken together, these data show that FUS is associated with Tau pre-mRNA and mRNA in mouse brain.

FUS directly binds to Tau transcripts at multiple sites

To analyse whether the interaction of FUS with Tau RNA is direct, we incubated mouse brain extracts with biotinylated RNA probes followed by ultraviolet crosslinking, RNase A digest and FUS immunoprecipitation [19]. RNA probes covering the FUS-regulated exon 10 and the neighbouring exon 11 resulted in significant biotinylation of FUS compared with an exon 9 spanning probe, indicating a direct and specific interaction of FUS with these RNA fragments (Fig 3C; supplementary Fig S5B online). CLIP analysis in HEK293 cells had revealed preferential interaction of FUS with AU-rich intronic RNA that was corroborated by *in vitro* binding assays with artificial AUU-repeats [5]. Interestingly, mouse Tau pre-mRNA contains three clusters with multiple AUU motifs in intron 9 (9–17 AUU within ~300 nucleotides) and RNA probes spanning these regions showed strong interaction with FUS in the crosslinking assay (compare i9-1, -2 and -3 in Fig 3C). Probe i9-2 is located closest to exon 10 and shows the strongest conservation between rodents and humans (supplementary Fig S5A,C online). Although FUS-knockdown led to preferential inclusion of Tau exon 3, we could not detect significant interaction of an exon 3 spanning RNA probe with FUS. However, the region within intron 2 with the highest conservation between mouse and human Tau (supplementary Fig S5A,D online) was strongly crosslinked to FUS, although it contained only four AUU motifs. Thus, FUS directly binds to Tau RNA at several sites near the FUS-regulated exons 3 and 10.

FUS knockdown promotes exon 10 inclusion in minigene

To further analyse the effects of FUS on pathologically relevant Tau splicing in a heterologous system, we used a minigene construct covering mouse exons 9 to 11 that contains the full intron sequences and expresses short HA-tagged Tau protein fragments, corresponding to the 3R/4R Tau domains. HEK293 cells co-transfected with the 3R/4R minigene and a control shRNA (shLuc) predominantly express fragments corresponding to 3R Tau and some 4R Tau. However, FUS knockdown (using shFUS-hu) led to a shift towards the longer fragment corresponding to 4R Tau, suggesting that endogenous FUS promotes skipping of exon 10 in the heterologous system (Fig 3D). These data corroborate the effects of FUS knockdown on Tau 4R expression in hippocampal neurons (Fig 1).

FUS knockdown disturbs cytoskeletal organization

To address whether FUS knockdown has functional consequences on neuronal development, we transfected hippocampal neurons before plating with shFUS#2 or an unspecific control (shLuc). FUS knockdown was apparent by immunostaining at DIV4 (supplementary Fig S4A online). Toxicity assays performed showed no difference between groups even after prolonged knockdown (supplementary Fig S4C online). After 4 days in culture, both neurons transfected with shLuc or shFUS sent out a similar number of neurites (Fig 4A; supplementary Fig S4B online) and had developed an axon (89% and 88%, respectively) that was identified by immunostaining with the axonal marker Tau1 [20]. Furthermore, neurons lacking FUS showed normal axonal branching (supplementary Fig S4B online). However, axons in FUS-knockdown neurons were slightly, but significantly shorter than in control cells (Fig 4B, left panel) and interestingly, the shFUS-transfected neurons typically developed severely enlarged growth cones. We found that the growth cone area of the shFUS-transfected neurons was in average twice as large as in the control cells (Fig 4B, right panel). When analysing tubulin and actin

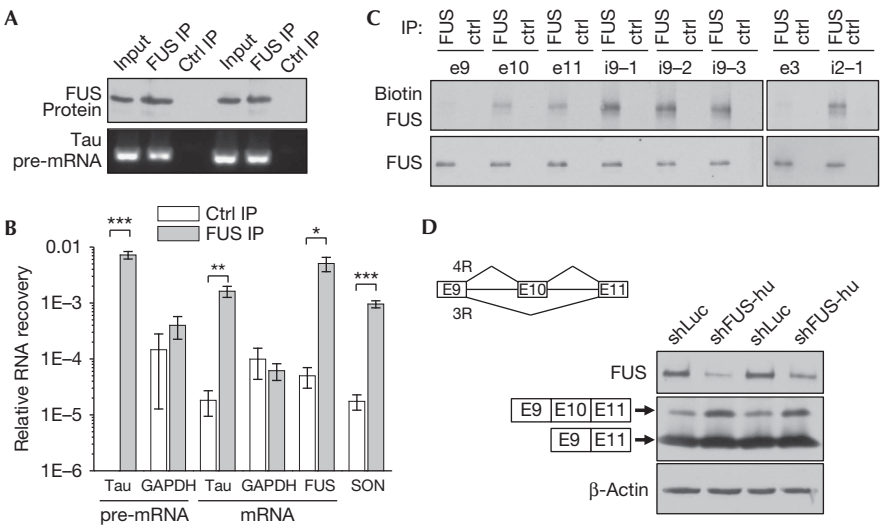

Fig 3 | FUS is associated with Tau pre-mRNA in brain and affects splicing of a minigene reporter construct. (**A**) Anti-FUS immunoblot of mouse brain (age 15 days) extracts, FUS- and control-immunoprecipitates. FUS-associated RNA was reverse transcribed and analysed by quantitative PCR. pre-mRNA-specific primers bind in introns 9 and 11 adjacent to Tau exon 10 (compare supplementary Fig S1C online). The end product after quantitative PCR analysis is shown. (**B**) RNA recovery from FUS-immunoprecipitates compared with control-immunoprecipitates. For both groups, individual immunoprecipitations from six mouse brains were analysed by quantitative PCR. SON primers spanning a verified FUS-binding motif within a large exon amplify both pre-mRNA and mRNA and served as positive control together with FUS mRNA [5]. $n = 6$, mean ± s.e.m, Student's *t*-test: $^{*}P < 0.05$, $^{**}P < 0.01$, $^{***}P < 0.001$. (**C**) Ultraviolet crosslinking of biotinylated RNA probes with FUS in mouse brain extracts (age 15 days). Detection of biotinylated FUS using strepatavidin and anti-FUS immunoblot of FUS- and control-immunoprecipitates. (**D**) HEK293 cells co-transfected with Tau exons 9 to 11 minigene construct (depicted in inset) and the indicated shRNAs. HA-tagged alternatively spliced protein product, FUS and β-actin were detected by immunoblotting. Ctrl, control; FUS, Fused in sarcoma; GAPDH, glyceraldehyde-3-phosphate dehydrogenase; IP, immunoprecipitation; shFUS, short hairpin FUS; shLuc, short hairpin RNA targeting the luciferase transcript.

localization in axonal growth cones (Fig 4C), we observed that in shFUS-transfected neurons microtubules spread further into the enlarged growth cone area and appeared less bundled, which resembles findings in Tau- and MAP1B-knockout neurons [8]. Together, these data indicate that FUS has an important role in cytoskeletal organization, particularly in the organization of microtubule network at axonal tips.

CONCLUSION

In this study, we established Tau as the first physiological splice target of FUS in neurons. This was corroborated on both mRNA and protein level. FUS knockdown promotes inclusion of exons 3 and 10 and thus expression of 2N- and 4R-containing Tau isoforms. Moreover, regulation of exon 10 was confirmed in a minigene reporter assay. We found that Tau pre-mRNA is associated with FUS in the brain and demonstrated direct binding to several intronic and exonic regions of Tau RNA, suggesting a direct role in Tau splicing. Consistent with recent CLIP analysis [5], we found the most robust binding of FUS to intronic regions containing multiple AUU motifs, although this was no absolute prerequisite for binding.

Enhanced expression of 4R Tau is a well-established cause of neurodegeneration both in the presence and absence of overt Tau aggregation [13–16]. Our data indicate that FTLD–Tau and FTLD–FUS share disease mechanisms through increased Tau 4R expression. Increased expression of 4R Tau has been linked to Parkinson's disease and is a strong predictor of progression to dementia [16,17,21]. Interestingly, FUS is downregulated in brains from Parkinson patients [22]. Furthermore, Tau variants are a risk factor for the Guam variant of ALS [23]. The consequences of enhanced 2N expression are poorly understood. Because the interaction of the Tau N-terminal region with Fyn has been linked to excitotoxicity, altered Tau splicing might contribute to the loss of mature dendritic spines observed in FUS-knockout mice potentially causing synaptic dysfunction in FTLD/ALS [9,24,25].

We observed shortened axonal length and growth cone enlargement on FUS-knockdown that are reminiscent of Tau-knockout mice [8]. Although we cannot exclude that other FUS-regulated genes contribute to this phenotype, altered Tau isoform expression might disturb cytoskeletal function in the axon and thus affect growth cone organization. It will be crucial to investigate Tau splicing and cytoskeletal aberrations in FTLD/ALS cases with FUS pathology and vice versa look for altered FUS expression in other tauopathies.

METHODS

Antibodies. FUS (Bethyl, A300-292A), Tau (Dako, A 0024), 3R Tau (Millipore, 8E6/C11), 4R Tau (Millipore, 1E1/A6), Tau1 (Millipore, PC1C6), β-actin (Sigma, AC-15), β3-Tubulin (Sigma, SDL.3D10 and Covance, Tuj1), synaptophysin (Millipore, SY38), PSD95 (Neuromab, K28/43), NR1 (BD, 54.1), NR2A (Covance, PRB-513P), GluR2 (Neuromab, L21/32), and GFP (rabbit, Fitzgerald Industries International) were used.

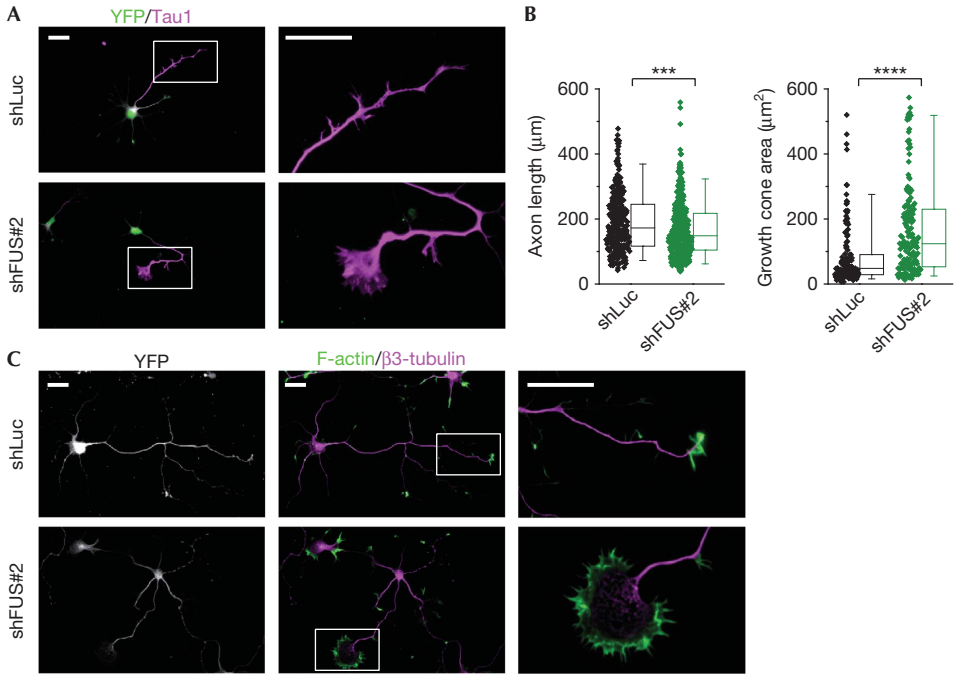

Fig 4 | FUS knockdown affects axon and growth cone morphology. Hippocampal neurons co-transfected with the shLuc or shFUS#2 and pEYFP-C1 before plating. (**A**) Immunostaining at day 4 with anti-YFP as transfection control and anti-Tau1 as axonal marker. Right panels show a high-magnification view of growth cones. For morphometric analysis processes with proximal-to-distal Tau1 gradient were defined as axons. (**B**) Quantification of axonal length (left, $n = 325$ for shLuc, $n = 388$ for shFUS#2) and growth cone area (right, $n = 147$ for shLuc, $n = 164$ for shFUS#2) measured blinded to the experimental condition. Box-plots represent lower quartile, median and upper quartile. Whiskers represent the 5th and 95th percentile. Mann–Whitney test: $^{***}P < 0.001$, $^{****}P < 0.0001$. (**C**) Staining for F-actin (using phalloidin) and β3-tubulin. Right panels show a high-magnification view of axonal growth cones. Scale bars, 25 μm. FUS, Fused in sarcoma; shFUS, short hairpin FUS; shLuc, short hairpin RNA targeting the luciferase transcript; YFP, yellow fluorescent protein.

DNA constructs and transfection. shRNA targeting FUS (rat #1 5′-ggcctaggcgagaatgtta-3′, rat #2 5′-gtgcaaggcctaggcgaga-3′, human 5′-ggacagcagcaaagctatg-3′), TDP-43 (5′-gtagatgtcttcattccc aaa-3′) and firefly luciferase (5′-cgtacgcggaatacttcga-3′) at the indicated sites were cloned into pSUPER (Oligoengine). For lentiviral knockdown, the shRNA-expression cassette was subcloned into a lentiviral vector coexpressing mCherry from human ubiquitin C promoter [26]. HA-tagged human FUS complementary DNA containing silent mutations in the shRNA-binding sites were expressed under the human synapsin promoter in a lentiviral vector [26].

A Tau minigene construct containing exons 9 to 11 was cloned by homologous recombination using the Red/ET system (Genebridges) from a mouse genomic BAC (Imagenes) into an expression vector (derived from pBUD-CE4, Invitrogen) containing an N-terminal myc-tag and a C-terminal HA-tag. For the splicing assay, the minigene construct was co-transfected in HEK293 cells that had been transfected with shRNAs two days earlier using Lipofectamine 2000 (Invitrogen) to allow sufficient FUS knockdown.

To generate RNA probes for the crosslinking experiments, 250–400 bp fragments of Tau pre-mRNA were cloned from mouse genomic DNA into pGEM3 (Promega) or pCR-blunt2 TOPO (Invitrogen) and transcribed into RNA using the MAXIscript T7 kit (Invitrogen) in the presence of biotin-16-UTP (Biotin RNA labelling mix, Roche) according to the manufacturer's instruction.

All constructs were verified by DNA sequencing. All oligos are listed in supplementary Table S1 online.

Neuronal culture, transfection and immunostaining. Hippocampal neurons for lentiviral infections were cultured from embryonic day 18 or 19 rats, as described previously, in a feeder-free system using B27 (Invitrogen) [26]. Neurons were lysed in Laemmli buffer and run on 10% denaturing SDS–PAGE gels. Cell viability was measured using the XTT cell proliferation kit (Roche). For the analysis of neuronal morphology (neurite number, axonal length and branching), we cultured rat hippocampal neurons on astrocyte feeder cells using N2 media [27]. The neurons were transfected before plating using an Amaxa 4D-Nucleofector (Lonza) with primary culture kit P3 (program EM110).

Hippocampal neurons were fixed with 4% paraformaldehyde, quenched in 50 mM ammonium chloride and permeabilized with 0.1% Triton X-100. After blocking with 2% fetal bovine serum (Invitrogen), 2% bovine serum albumin (Sigma-Aldrich), and 0.2% fish gelatin (Sigma-Aldrich) dissolved in phosphate-buffered saline neurons were incubated with primary antibodies diluted in 10% blocking solution.

For the quantification of growth cone area, neurite number and axonal branching, a minimum of 45 cells per condition were analysed in three independent experiments. For axonal length quantifications, a minimum of 99 cells per condition in three independent experiments were measured using AxioVision software (Zeiss).

Reverse transcription and quantitative PCR analysis. Total RNA was extracted using RNeasy Mini Kit (Qiagen) and reverse transcribed with random hexanucleotide primers using TaqMan Reverse Transcription Kit (Applied Biosystems, Invitrogen). The complementary DNA was amplified using qPCR SsoFast Evagreen Supermix (Biorad) and analysed in the CFX384 Real-Time System (Biorad).

FUS immunoprecipitation and RNA isolation. Mouse brains (day 15) were homogenized in 2-ml lysis buffer (20 mM Tris–HCl, pH 7.4, 450 mM NaCl, 0.1 mM EDTA, 1.5 mM $MgCl_2$, 1 mM $CaCl_2$, 0.6% Triton X-100) containing SUPERase RNase inhibitor (Ambion, 1 U/μl) and protease and phosphatase inhibitor cocktails (Sigma). After 70 000 *g* centrifugation (20 min), supernatants were immunoprecipitated for 1 h with Dynabeads Protein G (Invitrogen) precoupled with FUS or GST antibody (10 μg antibody/75 μl beads). After four washes with lysis buffer, the bound RNA was extracted using RNeasy Mini Kit including treatment with DNase (Qiagen).

Crosslinking of FUS with Tau pre-mRNA. Direct interaction of FUS with RNA was analysed analogous to protocols established for TDP-43 [19]. Mouse brains (day 15) were homogenized as described above (but in the absence of RNase inhibitor). After centrifugation, the supernatant was diluted with 2 volumes of lysis buffer lacking salt (20 mM Tris–HCl, pH 7.4, 0.1 mM EDTA, 1.5 mM $MgCl_2$, 1 mM $CaCl_2$, 0.6% Triton X-100). Endogenously biotinylated proteins in the lysates were depleted using streptavidin agarose (Sigma). Protein extracts (500 μg) were incubated with biotinylated RNA probes for 30 min at room temperature and crosslinked on ice by ultraviolet irradiation (254 nm, 400 mJ/cm^2) using a StrataLinker 1800 (Stratagene). After RNase A digestion (15 min, 10 μg/ml, Sigma), the lysates were subjected to immunoprecipitation using anti-FUS or anti-GST antibodies as described above. Crosslinking of biotinylated RNA was detected using Streptavidin-Peroxidase (Sigma).

Supplementary information is available at EMBO *reports* online (http://www.emboreports.org).

ACKNOWLEDGEMENTS

We thank S. Kunath and A. Seibel for technical assistance. We are grateful to B. Schmid, M. Müller, S. Lammich, E. Bentmann, D. Dormann, A. Capell and J. Strathmann for helpful discussion and reagents. DE was supported by the Helmholtz Young Investigator program HZ-NG-607.

Author contributions: D.O. performed and analysed most experiments. S.T. analysed the morphological phenotype. K.R. cloned most constructs. B.M.S. performed cytotoxicity assays and cloned constructs. C.H. supervised research. D.E. cloned the minigene construct, designed and supervised the project and wrote the manuscript with input from all authors.

CONFLICT OF INTEREST

The authors declare that they have no conflict of interest.

REFERENCES

1. Mackenzie IR, Rademakers R, Neumann M (2010) TDP-43 and FUS in amyotrophic lateral sclerosis and frontotemporal dementia. *Lancet Neurol* **9:** 995–1007
2. Josephs KA, Hodges JR, Snowden JS, Mackenzie IR, Neumann M, Mann DM, Dickson DW (2011) Neuropathological background of phenotypical variability in frontotemporal dementia. *Acta Neuropathol* **122:** 137–153
3. Vance C *et al* (2009) Mutations in FUS, an RNA processing protein, cause familial amyotrophic lateral sclerosis type 6. *Science* **323:** 1208–1211
4. Kwiatkowski TJ Jr. *et al* (2009) Mutations in the FUS/TLS gene on chromosome 16 cause familial amyotrophic lateral sclerosis. *Science* **323:** 1205–1208
5. Hoell JI *et al* (2011) RNA targets of wild-type and mutant FET family proteins. *Nat Struct Mol Biol* **18:** 1428–1431
6. Meissner M, Lopato S, Gotzmann J, Sauermann G, Barta A (2003) Proto-oncoprotein TLS/FUS is associated to the nuclear matrix and complexed with splicing factors PTB, SRm160, and SR proteins. *Exp Cell Res* **283:** 184–195
7. Dormann D *et al* (2010) ALS-associated fused in sarcoma (FUS) mutations disrupt Transportin-mediated nuclear import. *EMBO J* **29:** 2841–2857
8. Takei Y, Teng J, Harada A, Hirokawa N (2000) Defects in axonal elongation and neuronal migration in mice with disrupted tau and map1b genes. *J Cell Biol* **150:** 989–1000
9. Morris M, Maeda S, Vossel K, Mucke L (2011) The many faces of tau. *Neuron* **70:** 410–426
10. Andreadis A (2005) Tau gene alternative splicing: expression patterns, regulation and modulation of function in normal brain and neurodegenerative diseases. *Biochim Biophys Acta* **1739:** 91–103
11. Chen J, Kanai Y, Cowan NJ, Hirokawa N (1992) Projection domains of MAP2 and tau determine spacings between microtubules in dendrites and axons. *Nature* **360:** 674–677
12. Goedert M, Spillantini MG (2011) Pathogenesis of the tauopathies. *J Mol Neurosci* **45:** 425–431
13. Hutton M *et al* (1998) Association of missense and 5′-splice-site mutations in tau with the inherited dementia FTDP-17. *Nature* **393:** 702–705
14. Brunden KR, Trojanowski JQ, Lee VM (2008) Evidence that non-fibrillar tau causes pathology linked to neurodegeneration and behavioral impairments. *J Alzheimers Dis* **14:** 393–399
15. de Calignon A, Fox LM, Pitstick R, Carlson GA, Bacskai BJ, Spires-Jones TL, Hyman BT (2010) Caspase activation precedes and leads to tangles. *Nature* **464:** 1201–1204
16. Tobin JE *et al* (2008) Haplotypes and gene expression implicate the MAPT region for Parkinson disease: the GenePD Study. *Neurology* **71:** 28–34
17. Caffrey TM, Joachim C, Paracchini S, Esiri MM, Wade-Martins R (2006) Haplotype-specific expression of exon 10 at the human MAPT locus. *Hum Mol Genet* **15:** 3529–3537
18. Polymenidou M *et al* (2011) Long pre-mRNA depletion and RNA missplicing contribute to neuronal vulnerability from loss of TDP-43. *Nat Neurosci* **14:** 459–468
19. Fiesel FC *et al* (2010) Knockdown of transactive response DNA-binding protein (TDP-43) downregulates histone deacetylase 6. *EMBO J* **29:** 209–221
20. Mandell JW, Banker GA (1996) A spatial gradient of tau protein phosphorylation in nascent axons. *J Neurosci* **16:** 5727–5740
21. Williams-Gray CH *et al* (2009) The distinct cognitive syndromes of Parkinson's disease: 5 year follow-up of the CamPaIGN cohort. *Brain* **132:** 2958–2969
22. Stamper C *et al* (2008) Neuronal gene expression correlates of Parkinson's disease with dementia. *Mov Disord* **23:** 1588–1595
23. Sundar PD *et al* (2007) Two sites in the MAPT region confer genetic risk for Guam ALS/PDC and dementia. *Hum Mol Genet* **16:** 295–306
24. Fujii R, Okabe S, Urushido T, Inoue K, Yoshimura A, Tachibana T, Nishikawa T, Hicks GG, Takumi T (2005) The RNA binding protein TLS is translocated to dendritic spines by mGluR5 activation and regulates spine morphology. *Curr Biol* **15:** 587–593
25. Ittner LM *et al* (2010) Dendritic function of tau mediates amyloid-beta toxicity in Alzheimer's disease mouse models. *Cell* **142:** 387–397
26. Edbauer D *et al* (2010) Regulation of synaptic structure and function by FMRP-associated microRNAs miR-125b and miR-132. *Neuron* **65:** 373–384
27. Kaech S, Banker G (2006) Culturing hippocampal neurons. *Nat Protoc* **1:** 2406–2415

J Mol Med
DOI 10.1007/s00109-013-1077-2

JMolMed

REVIEW

FUS-mediated alternative splicing in the nervous system: consequences for ALS and FTLD

Denise Orozco · Dieter Edbauer

Received: 26 May 2013 / Revised: 1 August 2013 / Accepted: 6 August 2013

Abstract Mutations in fused in sarcoma (FUS) in a subset of patients with amyotrophic lateral sclerosis (ALS) linked this DNA/RNA-binding protein to neurodegeneration. Most of the mutations disrupt the nuclear localization signal which strongly suggests a loss-of-function pathomechanism, supported by cytoplasmic inclusions. FUS-positive neuronal cytoplasmic inclusions are also found in a subset of patients with frontotemporal lobar degeneration (FTLD). Here, we discuss recent data on the role of alternative splicing in FUS-mediated pathology in the central nervous system. Several groups have shown that FUS binds broadly to many transcripts in the brain and have also identified a plethora of putative splice targets; however, only ABLIM1, BRAF, Ewing sarcoma protein R1 (EWSR1), microtubule-associated protein tau (MAPT), NgCAM cell adhesion molecule (NRCAM), and netrin G1 (NTNG1) have been identified in at least three of four studies. Gene ontology analysis of all putative targets unanimously suggests a role in axon growth and cytoskeletal organization, consistent with the altered morphology of dendritic spines and axonal growth cones reported upon loss of FUS. Among the axonal targets, MAPT/tau and NTNG1 have been further validated in biochemical studies. The next challenge will be to confirm changes of FUS-mediated alternative splicing in patients and define their precise role in the pathophysiology of ALS and FTLD.

D. Orozco · D. Edbauer
German Center for Neurodegenerative Diseases (DZNE), Munich, Germany

D. Orozco
The International Max Planck Research School for Molecular and Cellular Life Sciences (IMPRS-LS), Martinsried, Germany

D. Orozco · D. Edbauer
Adolf-Butenandt-Institute, Biochemistry, Ludwig-Maximilians-University, Munich, Germany

D. Edbauer (✉)
Munich Center of Systems Neurology (SyNergy), Munich, Germany
e-mail: dieter.edbauer@med.uni-muenchen.de

Keywords FUS · Alternative splicing · ALS · FTLD · Tau · MAPT · NTNG1 · Neurodegeneration

Amyotrophic lateral sclerosis/frontotemporal lobar degeneration pathology and genetics

Cytoplasmic aggregates of the DNA/RNA-binding protein fused in sarcoma (FUS), also known as translocated in sarcoma (TLS), define a subgroup of both amyotrophic lateral sclerosis (ALS; also known as Lou Gehrig's disease) and frontotemporal lobar degeneration (FTLD) [1–3]. In ALS, motor neurons degenerate, and patients rapidly succumb to progressive muscular weakening and paralysis. ALS is the most common form of motor neuron disease in adults, with a lifetime risk of 1/600 to 1/1,000 [4]. Disease onset occurs on average at the age of 55 years, and the 3-year survival rate is close to 50 % [5]. In FTLD, patients suffer from region-specific neurodegeneration in the frontotemporal cortex that affects higher cognitive functions such as speech, language, and personality. FTLD is the second most common cause of dementia under 65 years [6]. Many patients show signs of both motor neuron loss and dementia, and thus, ALS and FTLD are now considered extreme ends of a disease spectrum [7, 8].

Both ALS and FTLD have a strong genetic component because 20–50 % of patients have a family history of neurodegeneration (familial cases) [5, 6, 9]. The discovery of dominant disease-causing mutations in several genes further linked these diseases and led to a pathological subdivision defined by the main aggregating protein (FUS, TAR DNA-binding protein 43 (TDP-43), tau, or SOD1) [8–11].

Aggregation of the microtubule-associated protein tau (MAPT) in the form of neurofibrillary tangles is often caused by pathogenic tau mutations that alter its affinity for microtubules [12]. Cytoplasmic redistribution and aggregation of the nuclear DNA/RNA-binding protein TDP-43 (or TARDBP) is the key pathological feature in most FTLD and ALS patients, hence called FTLD/ALS-TDP [13]. The nuclear DNA/RNA-binding protein FUS forms cytoplasmic inclusions in neurons

Published online: 24 August 2013

and glia in a distinct group of patients, termed FTLD/ALS-FUS [1–3, 14]. Mutations in TDP-43 cause predominantly ALS and rarely FTLD, and mutations in FUS cause exclusively ALS [8]. While loss-of-function mutations in the growth factor progranulin (GRN) cause FTLD-TDP [15], no other mutations have been linked to FTLD-FUS so far. The most common genetic cause for ALS and FTLD is the recently discovered massive expansion of a GGGGCC repeat in the first intron of the uncharacterized gene *C9orf72*, which causes TDP-43 pathology by an unclear mechanism possibly involving RNA toxicity [16–18]. Aggregation of TDP-43 and FUS strongly suggests that dysregulated RNA processing is an important factor in the pathogenesis of ALS and FTLD. In this review, we focus on the role of aberrant splicing in this process.

FUS pathophysiology in ALS and FTLD

FUS is ubiquitously expressed and is predominantly localized in the nucleus. FUS mediates mRNA transport by shuttling in and out of the nucleus [19, 20]. Mislocalization of FUS to the cytoplasm is presumably the first step in the pathophysiological cascade that leads to neurodegeneration. ALS-FUS mutations cluster around the C-terminal nuclear localization signal (NLS) and disrupt the nuclear import of FUS [1, 2, 21]. The other members of the FET family of proteins, Ewing sarcoma protein (EWS) and TATA-binding protein-associated factor 15 (TAF15), are imported normally into the nucleus. FUS inclusions therefore lack EWS and TAF15 [14]. In contrast, FTLD-FUS cases show inclusions where the entire FET family coaggregates [14]. Thus, in FTLD-FUS, which typically lacks FUS mutations, nuclear import of the FET family may be more broadly impaired, although other unrelated transportin 1 cargos are not affected. This topic was discussed in the recent review by Dormann and Haass [11].

Regardless of the mechanism, mislocalization of FUS results in a reduction of nuclear function and an increase of cytoplasmic FUS prone to aggregation [22]. Cytoplasmic FUS may result in toxic gain of function by disrupting extranuclear RNA metabolism [23].

FUS animal and cell culture models have been generated to dissect loss- and gain-of-function pathomechanisms. Two FUS knockout mouse lines show surprisingly different phenotypes. Inbred knockout mice fail to suckle and die within a few hours after birth [24]. In contrast, outbred knockout mice reach adulthood, but the males are sterile [25]. Despite the different phenotypes, both knockout mice show genomic instability. Furthermore, loss of FUS alters neuron morphology. Cultured neurons from knockout mice have fewer mature spines, but more filopodia-like dendritic protrusion than wild-type neurons [26]. Early FUS knockdown in hippocampal neurons results in enlarged axonal growth cones with disorganized cytoskeleton [27]. Gain-of-function mouse models that overexpress wild-type FUS succumb to progressive paralysis and die after 12 weeks. These mice show FUS-positive inclusions in spinal cord motor neurons and, therefore, replicate some aspects of human pathology [2, 28]. Together, these results suggest an important role of FUS in neurons during development. They also point to a combined loss-of-function and toxic gain-of-function pathomechanism in ALS/FTLD-FUS [29]. Thus, it is critical to understand the physiological function of FUS in the brain.

Alternative splicing in the brain

Alternative splicing drives and vastly extends the diversity of the transcriptome and proteome. One single gene may give rise to many different protein isoforms, often with distinct functions [30–32]. Tailored protein function is possible due to tissue- and development-dependent regulation of alternative splicing. Compared to other tissues, the human brain shows exceptionally high levels of alternative splicing, with more than 40 % of genes being alternatively spliced [33]. A complex interplay of *cis*- and *trans*-acting elements regulates alternative splicing. The *cis*-acting elements are splicing enhancer and inhibitory sequences within the pre-mRNA that recruit *trans*-acting RNA-binding proteins (RBP), which may themselves be further regulated by posttranscriptional modifications. The spliceosome, a RNA–protein complex consisting of small nuclear RNAs (U1, U2, U4, U5, and U6) and several RBPs, catalyzes splicing [34].

FUS is also part of the spliceosome and directly binds pre-mRNA [27, 35–38] and the splicing factors: splicing component 35 (SC35), polypyrimidine tract-binding protein (PTB), and the serine arginine (SR)-related proteins SRm160 and SRp75 [39–41]. Splicing of pre-mRNA transcripts starts during transcription, and both processes are tightly integrated [42]. FUS also regulates RNA polymerase II-mediated transcription by binding its C-terminal domain and regulating its phosphorylation [43]. Thus, FUS may integrate transcriptional and splicing regulation through RNA–protein and protein–protein interactions.

Until recently, the analysis of FUS-mediated splicing was limited to artificial exogenous splicing targets [39, 44]. The recent identification of endogenous neuronal splicing targets such as MAPT/tau [27] will allow detailed analysis of regulatory elements and will help to pinpoint the role of FUS in alternative splicing.

Pathogenic mutations highlight the importance of alternative splicing in neurodegeneration. In FTLD-tau patients, for example, MAPT mutations around exon 10 alter its splicing, thereby causing tau aggregation and impairing the axonal function of tau [45]. Moreover, mutations in *trans*-acting factors such as the RBP survival motor neuron protein 1 (SMN1) cause spinal muscular atrophy [46, 47]. Thus, identifying the splicing

targets of FUS will help us to understand the pathogenesis of ALS/FTLD-FUS.

FUS-mediated alternative splicing in the brain

RNA-binding and alternative splicing targets of FUS have been studied previously in cell culture models (human embryonic kidney 293 cells [23, 43], motor neuron-like cells NSC-34 [48]) or in *Xenopus laevis* embryos [49]. Recently, four independent studies analyzed RNA bound to FUS in neuronal tissue [35–38] using different cross-linking and immunoprecipitation (CLIP) technologies and next-generation sequencing [50, 51]. The four groups then correlated CLIP results to the splicing changes detected in FUS knockout brains or cultured neurons with FUS knockdown, in order to identify FUS splicing targets in the nervous system. The experimental approach and results are compared in Table 1.

The four studies are largely consistent in their conclusions: firstly, in the brain, FUS regulates primarily alternative splicing events rather than transcription or constitutive splicing. Secondly, FUS binds several thousand transcripts and favors very long introns. FUS-binding sites often flank the regulated alternatively spliced exon. However, only 42 % [38] to 55 % [37] of transcripts differentially spliced after FUS knockdown were direct binding targets of FUS. Additionally, two studies that applied CLIP technology to human and mouse brain tissue [37, 38] found highly comparable RNA-binding profiles and a high correlation of binding targets between humans and mice.

Thirdly, no simple RNA sequence can explain the RNA-binding pattern of FUS. In a fraction of targets ranging from 10 % [35] to 60 % [37], different groups detected a significant preference for G/C [35], C/U [38], GGU [36], or GUGGU [37] motifs, although the enrichment was rather low. The GGU and GUGGU motifs are similar to the GGUG motif identified previously through in vitro affinity selection [44]. Two groups also evaluated the enrichment of RNA structure motifs, such as the short-stem loop motif proposed by Hoell et al. [23]. Ishigaki et al. [35] found a modest enrichment of short-stem loop in FUS RNA targets, but Rogelj et al. [36] did not. Further biochemical studies are necessary to fully understand the RNA-binding specificity of FUS in the brain [38].

Fourthly, gene ontology analysis revealed that FUS splice targets are predominantly involved in the following pathways: axonogenesis, axon guidance, cell adhesion, neuron projection, vesicle transport, and cytoskeletal organization [35–38]. Among other splicing events, loss of FUS leads to inclusion/exclusion of exon cassettes (e.g., MAPT/tau) [35–37], selection of alternative 3′ untranslated regions (UTRs) (e.g., ABLIM1) [36] and intron retention (e.g., small nuclear ribonucleoprotein 70 (snRNP70)) [38]. Intron retention typically leads to insertion of a premature stop codon and may be a mechanism to regulate protein abundance through nonsense-mediated mRNA decay. Interestingly, a previous study using FUS knockdown in *X. laevis* observed extensive intron retention with functional effects on the fibroblast growth factor pathway [49].

Finally, the studies comparing binding targets of TDP-43 and FUS detected only few RNAs bound by both proteins. Despite their structural homology, these two proteins seem to regulate a vastly different set of genes [36, 37]. Also, TDP-43 binds its targets with surgical precision, whereas FUS typically binds broadly along nascent transcripts with long introns, leading to a characteristic saw-tooth pattern of binding [36, 37]. This could indicate a role of FUS in stabilizing nascent RNA during transcriptional elongation.

Despite the consensus regarding pathways regulated by alternative splicing, only six genes were identified in at least three studies (Table 2), and 71 genes were identified in at least two studies (Table 3). Only netrin G1 (NTNG1), previously linked to Parkinson's disease (PD) and schizophrenia, was identified in all four studies [35–38]. MAPT/tau was identified in three studies and, additionally, also in our candidate-based approach [27, 35–37]. FUS also binds MAPT/tau mRNA in the human brain [38]. The overlapping targets NTNG1, MAPT, ABLIM1, NRCAM and BRAF are discussed below.

The differences in experimental approach and statistical analysis are probably responsible for the limited overlap of splicing targets (Table 1). Differences in transcript abundance between whole brain tissue [36, 37], cultured neurons [35], or neurons differentiated from mouse embryonic stem cells [38] also limit the comparison. The use of FUS knockout brains [36, 37] in contrast to FUS knockdown in vitro [35, 38] or in vivo [37] could also account for the differences. Finally, Nakaya et al. [38] report several RBPs among the FUS targets, for example, EWS [36, 38] and snRNP70 [38], and suggest that FUS cross-regulates the RBP network. The lists of FUS-regulated genes inevitably include indirect splicing events.

Interestingly, independent studies of TDP-43 that applied CLIP technology [52–54] also showed limited overlap among targets [51]. A recent comparison of these studies also points to methodological differences as the underlying cause [51].

We considered only the top splicing targets for the discussion on potential implications for ALS/FTLD.

FUS regulates alternative splicing of proteins related to axonal biology

MAPT/tau

Three FUS CLIP/exon array studies and our candidate-based study identified increased MAPT/tau exon 10 inclusion upon loss of FUS [27, 35–37]. Additionally, both our study [27] and that of Lagier-Tourenne et al. [37] reported an enhanced

Table 1 Comparison of experimental conditions of FUS CLIP/exon array studies

Ref.	Experimental conditions				Results
	CLIP technology	Knockdown or knockout	Exon array or RNA-seq	Validation	
Ishigaki et al. [35]	HITS-CLIP 12 week C57BL6 mice Compared: FUS vs control	Primary cortical mouse neurons (E15) transduced with *Lentivirus* shRNA against FUS DIV5+6 for exon array	Mouse exon 1.0 ST Array (Affymetrix)	PCR of primary cortical mouse neurons (E15) transduced with *Lentivirus* shRNA against FUS DIV5+6	44 exons with increased (≥1.3-fold) and 55 exons with decreased (≥1.5-fold) expression upon FUS KD Validated: 37/37
Rogelj et al. [36]	iCLIP E18 C57BL6 mice Compared: FUS vs TDP vs U2AF65	FUS KO mouse [24] (E18) whole brain RNA for splice junction microarrays	mjay mouse GeneSplice Array (Affymetrix)	PCR of whole brain FUS KO mouse [24]	68 alternative spliced cassettes 48 other type of splicing event Validated: 14/17
Lagier-Tourenne et al. [37]	CLIP-seq 8 week C57BL6 mice and human brain Compared: 3 FUS antibodies with different epitopes	FUS KO mouse, [24] E18.5 for exon array In vivo KD: intrastriatal and intraventricular injections of single-stranded ASOs against FUS, TDP-43, or both in 8–10-week-old female C57BL6 mice	mjay mouse GeneSplice Array (Affymetrix) RNA-seq	PCR of ASO-mediated KD in vivo and FUS KO mouse	300 splicing events in embryonic brains from KO mouse 67 also in ASO-mediated FUS KD in the adult brain 65 in the same direction
Nakaya et al. [38]	HITS-CLIP Normal human brains, temporal lobe Compared: FUS vs control neurons differentiated from mouse ES cells	Mouse ES cell derived neurons treated with siRNA against FUS	Solid support directional RNA-seq (SSD-RNA-seq) [91]	PCR of mouse ES cell-derived neurons treated with siRNA for FUS KD or lentiviral transduction for overexpression of human FUS	631 exons with increased and 437 exons with decreased expression upon FUS KD

E18 embryonic day 18, *KO* knockout, *KD* knockdown, *ES cells* embryonic stem cells, *ASO* antisense oligonucleotides

Table 2 Alternative splicing upon loss of FUS. Hits were identified in at least three studies

	Ishigaki et al. [35]		Rogelj et al. [36]		Lagier-Tourenne et al. [37]		Nakaya et al. [38]	
NTNG1	Inclusion	**ENSMUSE00000670473** **ENSMUSE00000564518** **ENSMUSE00000511732**	Inclusion	**ENSMUSE00000511732**	Inclusion	**ENSMUSE00000670473** **ENSMUSE00000564518** **ENSMUSE00000511732**	Inclusion	ENSMUSE00000947279
MAPT	Inclusion	**ENSMUSE00000107965** ENSMUSE00000107964	Inclusion	**ENSMUSE00000107965**	Inclusion (embryo) Inclusion (adult)	**ENSMUSE00000107965** ENSMUSE00000107966 ENSMUSE00000107958	n.d.	
ABLIM1	n.d.		Alternate 3′ UTR	ENSMUSE00000640490	Skipping Alternate start	ENSMUSE00000292146 ENSMUSE00000793956	Skipping	ENSMUSE00000292118
NRCAM	n.d.		Skipping	ENSMUSE00000325244	Skipping	ENSMUSE00000325376	Inclusion	ENSMUSE00000325135
BRAF	Skipping	**ENSMUSE00000618025** ENSMUSE00000951452 ENSMUSE00000562746	n.d.		Inclusion	**ENSMUSE00000618025**	Skipping	ENSMUSE00000618032
EWSR1	n.d.		Intron retention between	**ENSMUSE00000306110** **ENSMUSE00000306105**	Skipping	ENSMUSE00000306116 ENSMUSE00000581345 **ENSMUSE00000306110**	Intron retention between	**ENSMUSE00000306110** **ENSMUSE00000306105**

All coordinates were analyzed with the Ensemble mouse genome NCBIM37. In case of ambiguity, all exons in the chromosomal region are listed. Exons identified more than once are marked in bold. ENSMUSE00000xxxxxx, Ensembl unique and stable mouse exon identifier

n.d. not detected

Table 3 Putative splicing targets of FUS. Hits were identified in at least two studies

	Gene	Ishigaki et al. [35]	Rogelj et al. [36]	Lagier-Tourenne et al. [37]	Nakaya et al. [38]
1	NTNG1	✓	✓	✓	✓
2	MAPT[a]	✓	✓	✓	
3	ABLIM1		✓	✓	✓
4	NRCAM		✓	✓	✓
5	BRAF	✓		✓	✓
6	EWSR1		✓	✓	✓
7	2700081O15RIK			✓	✓
8	5330434G04RIK			✓	✓
9	5730419I09RIK			✓	✓
10	ALCAM			✓	✓
11	ANKRD32			✓	✓
12	ANKS1	✓			✓
13	ANKS1B	✓			✓
14	BIRC6			✓	✓
15	CAPN10			✓	✓
16	CLEC16A			✓	✓
17	CNKSR2			✓	✓
18	COPE			✓	✓
19	DLGAP1	✓		✓	
20	DNAJA1			✓	✓
21	DTNA		✓	✓	
22	EIF4G2			✓	✓
23	ENAH		✓	✓	
24	ENO2			✓	✓
25	EPB4.1L2			✓	✓
26	EPB4.9			✓	✓
27	ERC2	✓		✓	
28	ETL4			✓	✓
29	GRIA2			✓	✓
30	GTF2IRD1			✓	✓
31	H13		✓	✓	
32	HNRNPK			✓	✓
33	HUWE1			✓	✓
34	INPP5F			✓	✓
35	LPHN3			✓	✓
36	LSM14B			✓	✓
37	MAGI1			✓	✓
38	MARCH8			✓	✓
39	MBOAT7			✓	✓
40	MEAF6			✓	✓
41	MMP11			✓	✓
42	MVD			✓	✓
43	NEO1	✓			✓
44	NRXN1			✓	✓
45	PHKB			✓	✓
46	PITPNC1			✓	✓
47	POT1A			✓	✓
48	PRRT2			✓	✓
49	PTDSS2			✓	✓
50	RABL2			✓	✓
51	RAP1GDS1			✓	✓
52	RAPGEF4	✓			✓
53	RASGRF1		✓		✓
54	RASGRP2			✓	✓
55	RRAGD			✓	✓
56	SEC63			✓	✓
57	SLC25A14			✓	✓
58	SLITRK4		✓	✓	
59	SMG7		✓	✓	
60	SORBS1		✓	✓	
61	SORT1		✓	✓	
62	SPP1		✓	✓	
63	ST3GAL3			✓	✓
64	TECR			✓	✓
65	TIA1	✓		✓	
66	TMEM150C			✓	✓
67	TSC22D2	✓		✓	
68	TTLL12			✓	✓
69	UBA3			✓	✓
70	ZFML			✓	✓
71	ZFP273			✓	✓
72	ZFP553			✓	✓

[a] MAPT is also an alternative splicing target of FUS in the study of Orozco et al. [27]

inclusion of exon 2 (ENSMUSE00000107966) and exon 3 (ENSMUSE00000107958) upon FUS knockdown (Table 2). Although formal proof that FUS regulates splicing of MAPT/tau in the human brain is still missing, there is strong evidence for functional conservation [37, 38].

The *MAPT* gene, encoding the protein tau, consists of 16 exons and is mainly expressed in the nervous system. Tau shows a complex alternative splicing regulation of an N-terminal cassette (exons 2 and 3) and exon 10 that leads to six different isoforms (0N3R, 1N3R, 2N3R, 0N4R, 1N4R, 2N4R) [55] (Fig. 1a). Inclusion of exon 2 or exons 2 and 3 adds one or two short acidic regions (termed 1N and 2N) in the so-called projection domain. Inclusion of exon 10 inserts a fourth microtubule binding region (4R), which increases affinity to microtubules compared to the shorter 3R isoforms [56]. During development, expression shifts toward longer isoforms.

Tauopathies are characterized by neurofibrillary tangles, which consist of aggregated hyperphosphorylated tau. Such aggregates are found in corticobasal degeneration, progressive supranuclear palsy, frontotemporal dementia and parkinsonism linked to chromosome 17 (FTDP-17), as well as Alzheimer's

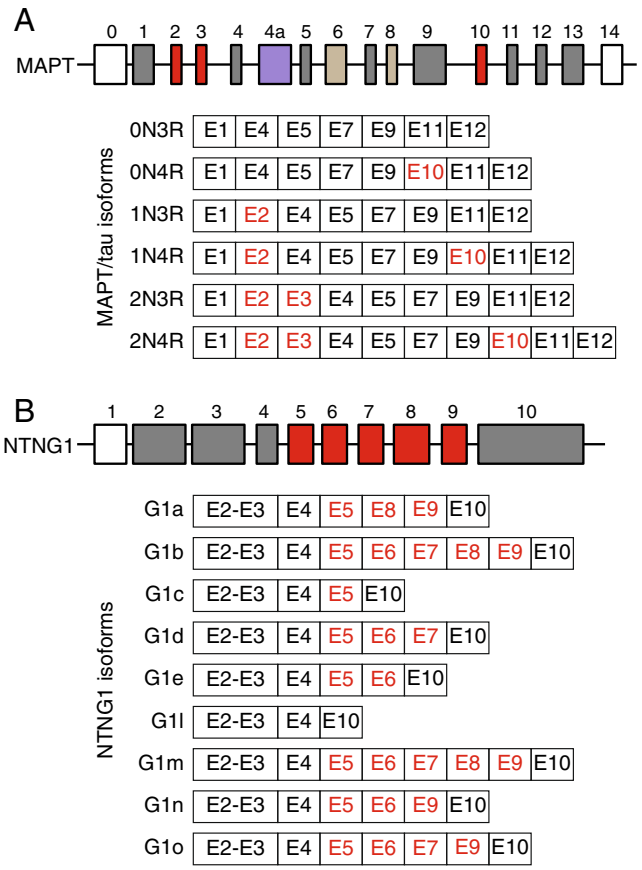

Fig. 1 Genomic structures and isoforms of MAPT/tau and NTNG1. **a** The human MAPT gene encodes for the tau protein and contains 16 exons. E0 and E14 (*white*) are noncoding, E6 and E8 (*brown*) are not expressed in the human brain, and E4a is only expressed in the peripheral nervous system. The N-terminal part of the protein shows a complex alternative splicing of the cassettes E2 and E3. Inclusion of E3 is coupled to the inclusion of E2. Inclusion of E2 or E2/E3 adds one or two acidic regions (1N, 2N) in the projection domain (N-terminal part). Alternative splicing of E10 is regulated independently. Exons 9–12 code for microtubule binding domains. Inclusion of E10 adds extra fourth microtubule binding region (4R). **b** The human NTNG1 gene contains 10 exons. E1 (*white*) is noncoding. Complex alternative splicing of E5, E6, E7, E8, and E9 results in at least nine different isoforms termed G1a, G1b, G1c, G1d, G1-e, G1-l, G1-m, G1-n, and G1-o. *E* exon

disease [57]. Tau mutations in FTDP-17 patients promote tau aggregation either by disturbing the tightly controlled 4R/3R ratio [58] or by affecting the interaction of tau with microtubules [56]. The changes in microtubule stability directly affect the transport along microtubules. Interestingly, increased 4R expression may cause neurodegeneration even in the absence of visible tau aggregation [59]. In mouse models of tauopathies, toxicity precedes tau aggregation [60]. In PD, 4R expression is correlated with progression to dementia without detectable tangles [61–63]. The H1 MAPT haplotype, which enhances 4R expression [64], has been genetically linked to PD. Finally, tau is also genetically [65] and pathologically [66] linked to the Guam variant of ALS. Thus, a shift toward 4R tau may contribute to neurodegeneration in ALS/FTLD-FUS, despite the lack of overt tau aggregation [67, 68].

Netrin G1

NTNG1, also known as laminet-1, belongs to the netrin family, with the distinction of being membrane bound via a glycosylphosphatidylinositol (GPI) anchor [69–71]. Netrins provide important guidance cues during brain development [72]. For example, NTNG1 and its ligand NGL-1 regulate axon guidance as well as synapse formation and maintenance [70]. Nine different isoforms resulting from alternative splicing of the exons 5–9 have been reported so far [71]. The protein contains several laminin- and non-laminin-type epidermal growth factor (EGF) domains.

NTNG1 is the only target identified in all four FUS CLIP/exon array studies. Rogelj et al. [36] report an increased inclusion of exon 9 (ENSMUSE00000511732) upon FUS knockdown, while Ishigaki et al. and Lagier-Tourenne et al. [35, 37] report exon inclusion in a PCR amplicon spanning exon 7 (ENSMUSE00000670473) to exon 9 (ENSMUSE00000511732). Exons 8 and 9 insert laminin-type EGF domains. In contrast, Nakaya et al. [38] report an increased inclusion of exon 10 (ENSMUSE00000947279) that codes for an extracellular EGF domain. Little is known about the differential function of NTNG1 isoforms. Based on the number of EGF-like domains, the isoforms might have different affinities for the ligand NGL-1 [69]. Selective reduction of the G1c isoform has been observed in familiar cases of schizophrenia [73] and bipolar disorders [69]. Interestingly, NTNG1 is also linked to PD in a genome-wide association study [74].

ABLIM1, NRCAM, and BRAF

Altered splicing of ABLIM1, NRCAM, and BRAF upon loss of FUS was reported in at least three studies (Table 2). The actin-binding *LIM* protein ABLIM1 is expressed throughout the body and exists in three different isoforms ABLIM1-s, ABLIM1-m, and ABLIM1-l, which differ in the number of LIM domains [75]. In contrast to NTNG1 and MAPT/tau, the reported effects in splicing vary among the studies. Lagier-Tourenne et al. and Nakaya et al. detected preferential skipping of exons ENSMUSE00000292146 and ENSMUSE00000292118, respectively [37, 38]. The specific function of these exons is unknown. Rogelj et al. [36] detected an alternative 3′ splice site event at ENSMUSE00000640490, which is almost identical to exon ENSMUSE00000292146 except that it is annotated to be 5 bp longer. The protein product of this transcript lacks the C-terminal vinillin headpiece that mediates the binding of F-actin. Lastly, Lagier-Tourenne et al. [37] detected an alternative start site at ENSMUSE00000793956. The mouse genome database (NCBIM37) lists only one short transcript with this alternative

start site, which also lacks the C-terminal vinillin headpiece. ABLIM1 binds F-actin, bridges the actin cytoskeleton, and is known to mediate axon guidance and outgrowth [76]. Interestingly, netrin signaling has been shown to activate ABLIM1 [77].

NRCAM is a transmembrane protein that belongs to the L1 family of cell adhesion molecules [78]. Alternative splicing of NRCAM results in more than a dozen isoforms that are differentially regulated during development [79]. The function of the different isoforms is unknown. Similar to ABLIM1, there is limited overlap in the reported affected exons upon loss of FUS. Rogelj et al. [36] reported skipping of exon ENSMUSE00000325244, which codes for an Ig-like beta sandwich domain. In contrast, Lagier-Tourenne et al. and Nakaya et al. [37, 38] report skipping of exon ENSMUSE00000325376 and inclusion of exon ENSMUSE00000325135, respectively (Table 2). Interestingly, these are neighboring exons, and the latter also encodes an Ig-like domain. NRCAM is crucial for axon growth and guidance, synapse formation, and neurite outgrowth [78] and has been linked to different forms of cancer and autism [78].

The *BRAF* gene codes for the B-raf protein member of the Raf family of kinases (including A-raf and C-raf). Raf kinases are part of the mitogen-activated protein kinase (MAPK) cascade, which activates gene expression upon growth factor stimulation. B-raf is highly expressed in the CNS [80] and is the major activator of the extracellular signal-regulated kinase (ERK)1/2 pathway in neurons [81, 82]. Both in vitro and in vivo studies have demonstrated the essential role of B-raf in neuronal survival and differentiation [82, 83]. Interestingly, conditional double knockout of B-raf and C-raf resulted in reduced axon growth [83]. Alternative splicing of *BRAF* results in 10 isoforms expressed in different tissues. The longest isoforms are abundant in the CNS [80]. Ishigaki et al. [35] report exon skipping in the region encompassing exons ENSMUSE00000618025, ENSMUSE00000951452, and ENSMUSE00000562746 after FUS knockdown. Lagier-Tourenne et al. [37], however, report preferential inclusion of exon ENSMUSE00000618025. This discrepancy could reflect differences in FUS regulation of alternative splicing in different cell populations in the brain, since Ishigaki et al. [35] analyzed cultured neurons, and Lagier-Tourenne et al. [37] analyzed whole mouse brain. Nakaya et al. [38] report skipping of exon ENSMUSE00000618032 upon loss of FUS. All known isoforms can activate ERK1/2

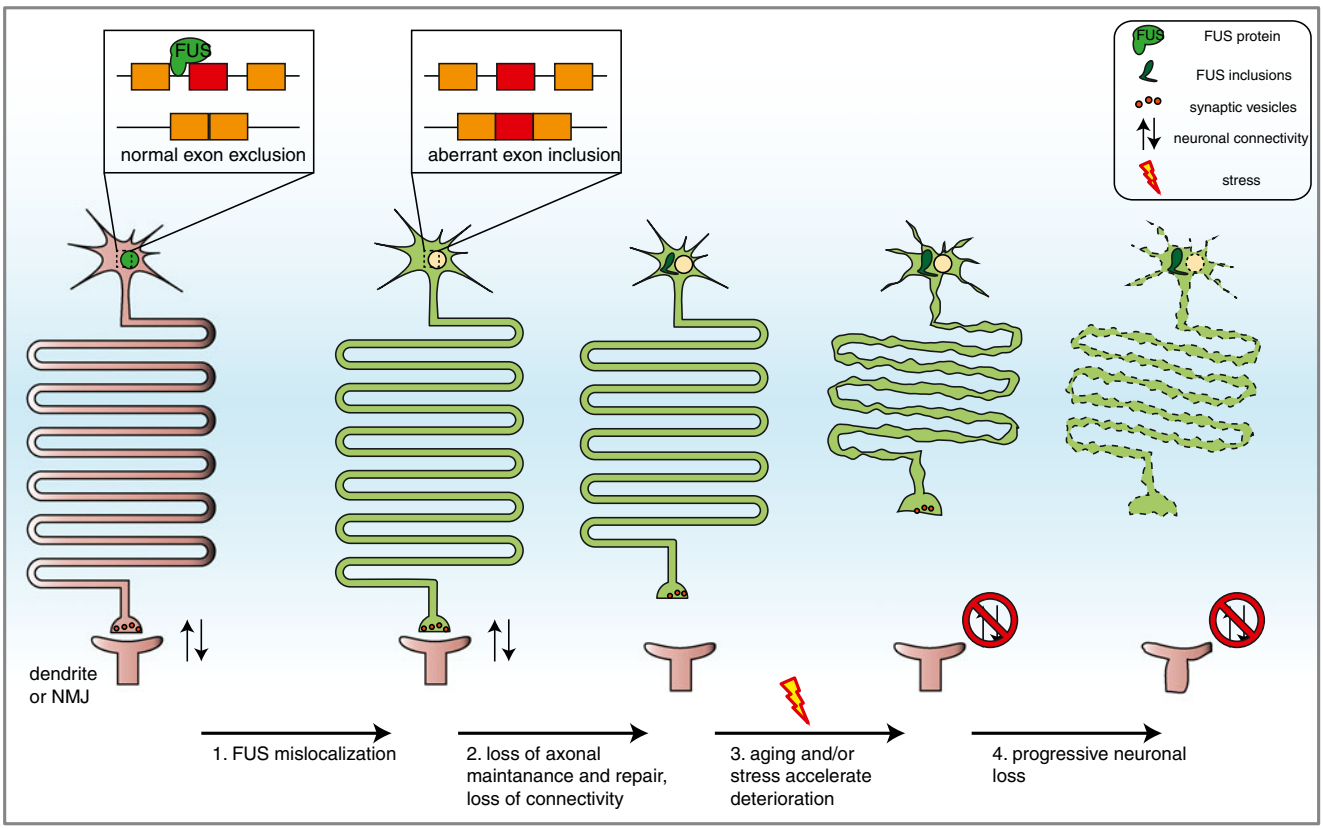

Fig. 2 Hypothesis of splicing centered pathomechanism in ALS/FTLD-FUS. *1* Impaired nuclear import of FUS, due to mutations in the NLS or transport defects, causes mislocalization of FUS to the cytoplasm. This leads to loss of nuclear function and thus changes in alternative splicing of axonal and cytoskeleton related genes. *2* Altered splicing disturbs axonal growth and maintenance and results in axonal atrophy and loss of connectivity. *3* Aging and stress accelerate the process of neuronal denervation and lead to the first clinical symptoms. Connections to dendrites or neuromuscular junction (*NMJ*) are affected. *4* Due to disturbed repair mechanisms, the affected neurons are not able to cope with the stress and to repair damaged connections. The result is progressive degeneration observed in disease

signaling [80], but alternative splicing might modulate kinase activity and substrate specificity, thus altering growth factor signaling [80].

Consequences for ALS and FTLD

Tau, NTNG1, ABLIM1, NRCAM, and B-raf exemplify a common theme among FUS splice targets, because they all affect cytoskeletal organization and, in particular, axon growth and maintenance. The recent identification of ALS-causing mutations in profilin 1 [84], a protein that regulates actin polymerization, as well as mutations in the neurofilament subunit H [85], further highlights the importance of the cytoskeleton in the pathogenesis of neurodegenerative diseases. Altogether, FUS mislocalization to the cytoplasm may impair maintenance and repair of long axons. Interestingly, the earliest signs of ALS are axon retraction and denervation, which clearly occur before the loss of neuronal cell bodies [86, 87].

How could impaired FUS-mediated alternative splicing render neurons more vulnerable in ALS/FTLD-FUS? We propose the following model (Fig. 2): (1) in ALS or FTLD, pathogenic mutations or impaired nuclear import causes cytoplasmic mislocalization of FUS [88]. Reduction of nuclear FUS results in aberrant alternative splicing of axonal and cytoskeleton-related transcripts, such as MAPT/tau. (2) The network responsible for axonal growth, maintenance, and repair deteriorates, and neuronal connections are weakened. Secondary effects, such as misregulation of other RBPs [38] or their sequestration into aggregates, may enhance neurodegeneration. (3) Aging and other stressors [11, 88] can trigger denervation and early clinical symptoms. Lastly, (4) due to disrupted repair mechanisms, the damaged tissue cannot be repaired resulting in progressive neurodegeneration.

Conclusions and key open questions

We have reviewed here the alternative splicing targets of FUS reported by four independent groups. The most robustly identified targets are linked to cytoskeleton, axon growth, and maintenance [35–38]. However, FUS binds many more RNAs apparently without changing splicing or expression. How are these RNAs affected by FUS? Furthermore, it is unclear how FUS affects the bound long noncoding RNAs, for example, maternally expressed 3 (*Meg3*) and nuclear enriched abundant transcript 1 (*NEAT1*) [37]. *Meg3* and *NEAT1* have been linked to neurodegeneration, because their expression is significantly dysregulated in Huntington's disease [89]. Moreover, it will be important to understand how FUS aggregates might impair cytoplasmic RNA metabolism [23]. Finally, to fully understand the pathomechanism of ALS and FTLD with FUS pathology, we should also consider other potential roles of FUS in the nervous system, particularly genomic stability. Even postmitotic neurons seem to require constant genome repair, because cellular stress and normal synaptic activity can cause double-strand breaks [90].

In conclusion, we now know that loss of FUS alters splicing of key components of the cytoskeleton and related proteins that promote axonal maintenance and repair. The next challenge will be to confirm these findings in ALS and FTLD patients and relate them with the pathology and symptoms. Only then, we can begin to translate these findings into therapeutic approaches for these devastating diseases.

Acknowledgments We thank D. Dormann, B. Schmid, S. Tahirovic, J. McCarter, E. Bentmann, K. Strecker, B. Schwenk, and J. Banzhaf for critically reading the manuscript.

Conflict of interest The authors declare no conflict of interests.

References

1. Kwiatkowski TJ, Bosco DA, LeClerc AL, Tamrazian E, Vanderburg CR, Russ C, Davis A, Gilchrist J, Kasarskis EJ, Munsat T et al (2009) Mutations in the FUS/TLS gene on chromosome 16 cause familial amyotrophic lateral sclerosis. Science 323:1205–1208
2. Vance C, Rogelj B, Hortobágyi T, De Vos KJ, Nishimura AL, Sreedharan J, Hu X, Smith B, Ruddy D, Wright P et al (2009) Mutations in FUS, an RNA processing protein, cause familial amyotrophic lateral sclerosis type 6. Science 323:1208–1211
3. Neumann M, Rademakers R, Roeber S, Baker M, Kretzschmar HA, Mackenzie IR (2009) A new subtype of frontotemporal lobar degeneration with FUS pathology. Brain 132:2922–2931
4. Pasinelli P, Brown RH (2006) Molecular biology of amyotrophic lateral sclerosis: insights from genetics. Nat Rev Neurosci 7:710–723
5. Kiernan MC, Vucic S, Cheah BC, Turner MR, Eisen A, Hardiman O, Burrell JR, Zoing MC (2011) Amyotrophic lateral sclerosis. Lancet 377:942–955
6. Bird T, Knopman D, VanSwieten J, Rosso S, Feldman H, Tanabe H, Graff-Raford N, Geschwind D, Verpillat P, Hutton M (2003) Epidemiology and genetics of frontotemporal dementia/Pick's disease. Ann Neurol 54:S29–S31
7. Thomas M, Alegre-Abarrategui J, Wade-Martins R (2013) RNA dysfunction and aggrephagy at the centre of an amyotrophic lateral sclerosis/frontotemporal dementia disease continuum. Brain 136(Pt 5):1345–1360
8. Mackenzie IRA, Rademakers R, Neumann M (2010) TDP-43 and FUS in amyotrophic lateral sclerosis and frontotemporal dementia. Lancet Neurol 9:995–1007
9. Rademakers R, Neumann M, Mackenzie IR (2012) Advances in understanding the molecular basis of frontotemporal dementia. Nat Rev Neurol 8:423–434
10. Josephs KA, Hodges JR, Snowden JS, Mackenzie IR, Neumann M, Mann DM, Dickson DW (2011) Neuropathological background of phenotypical variability in frontotemporal dementia. Acta Neuropathol 122:137–153
11. Dormann D, Haass C (2013) Fused in sarcoma (FUS): an oncogene goes awry in neurodegeneration. Mol Cell Neurosci. doi:10.1016/j.mcn.2013.03.006
12. Hutton M, Lendon CL, Rizzu P, Baker M, Froelich S, Houlden H, Pickering-Brown S, Chakraverty S, Isaacs A, Grover A et al (1998)

Association of missense and 5′-splice-site mutations in tau with the inherited dementia FTDP-17. Nature 393:702–705
13. Neumann M, Sampathu DM, Kwong LK, Truax AC, Micsenyi MC, Chou TT, Bruce J, Schuck T, Grossman M, Clark CM et al (2006) Ubiquitinated TDP-43 in frontotemporal lobar degeneration and amyotrophic lateral sclerosis. Science 314:130–133
14. Neumann M, Bentmann E, Dormann D, Jawaid A, DeJesus-Hernandez M, Ansorge O, Roeber S, Kretzschmar HA, Munoz DG, Kusaka H et al (2011) FET proteins TAF15 and EWS are selective markers that distinguish FTLD with FUS pathology from amyotrophic lateral sclerosis with FUS mutations. Brain 134:2595–2609
15. Cruts M, Gijselinck I, van der Zee J, Engelborghs S, Wils H, Pirici D, Rademakers R, Vandenberghe R, Dermaut B, Martin JJ et al (2006) Null mutations in progranulin cause ubiquitin-positive frontotemporal dementia linked to chromosome 17q21. Nature 442:920–924
16. Renton AE, Majounie E, Waite A, Simón-Sánchez J, Rollinson S, Gibbs JR, Schymick JC, Laaksovirta H, van Swieten JC, Myllykangas L et al (2011) A hexanucleotide repeat expansion in C9ORF72 is the cause of chromosome 9p21-linked ALS-FTD. Neuron 72:257–268
17. DeJesus-Hernandez M, Mackenzie IR, Boeve BF, Boxer AL, Baker M, Rutherford NJ, Nicholson AM, Finch NiCole A, Flynn H et al (2011) Expanded GGGGCC hexanucleotide repeat in noncoding region of C9ORF72 causes chromosome 9p-linked FTD and ALS. Neuron 72:245–256
18. Gijselinck I, Van Langenhove T, van der Zee J, Sleegers K, Philtjens S, Kleinberger G, Janssens J, Bettens K, Van Cauwenberghe C, Pereson S et al (2012) A C9orf72 promoter repeat expansion in a Flanders-Belgian cohort with disorders of the frontotemporal lobar degeneration-amyotrophic lateral sclerosis spectrum: a gene identification study. Lancet Neurol 11:54–65
19. Åman P, Panagopoulos I, Lassen C, Fioretos T, Mencinger M, Toresson H, Höglund M, Forster A, Rabbitts TH, Ron D et al (1996) Expression patterns of the human sarcoma-associated genes FUS and EWS and the genomic structure of FUS. Genomics 37:1–8
20. Zinszner H, Sok J, Immanuel D, Yin Y, Ron D (1997) TLS (FUS) binds RNA in vivo and engages in nucleo-cytoplasmic shuttling. J Cell Sci 110:1741–1750
21. Dormann D, Rodde R, Edbauer D, Bentmann E, Fischer I, Hruscha A, Than ME, Mackenzie IRA, Capell A, Schmid B et al (2010) ALS-associated fused in sarcoma (FUS) mutations disrupt transportin-mediated nuclear import. EMBO J 29:2841–2857
22. Kato M, Han Tina W, Xie S, Shi K, Du X, Wu Leeju C, Mirzaei H, Goldsmith EJ, Longgood J, Pei J et al (2012) Cell-free formation of RNA granules: low complexity sequence domains form dynamic fibers within hydrogels. Cell 149:753–767
23. Hoell JI, Larsson E, Runge S, Nusbaum JD, Duggimpudi S, Farazi TA, Hafner M, Borkhardt A, Sander C, Tuschl T (2011) RNA targets of wild-type and mutant FET family proteins. Nat Struct Mol Biol 18:1428–1431
24. Hicks GG, Singh N, Nashabi A, Mai S, Bozek G, Klewes L, Arapovic D, White EK, Koury MJ, Oltz EM et al (2000) Fus deficiency in mice results in defective B-lymphocyte development and activation, high levels of chromosomal instability and perinatal death. Nat Genet 24:175–179
25. Kuroda M, Sok J, Webb L, Baechtold H, Urano F, Yin Y, Chung P, de Rooij DG, Akhmedov A, Ashley T et al (2000) Male sterility and enhanced radiation sensitivity in TLS(−/−) mice. EMBO J 19:453–462
26. Fujii R, Okabe S, Urushido T, Inoue K, Yoshimura A, Tachibana T, Nishikawa T, Hicks GG, Takumi T (2005) The RNA binding protein TLS is translocated to dendritic spines by mGluR5 activation and regulates spine morphology. Curr Biol CB 15:587–593
27. Orozco D, Tahirovic S, Rentzsch K, Schwenk BM, Haass C, Edbauer D (2012) Loss of fused in sarcoma (FUS) promotes pathological tau splicing. EMBO Rep 13:759–764
28. Mitchell J, McGoldrick P, Vance C, Hortobagyi T, Sreedharan J, Rogelj B, Tudor E, Smith B, Klasen C, Miller CJ et al (2013) Overexpression of human wild-type FUS causes progressive motor neuron degeneration in an age- and dose-dependent fashion. Acta Neuropathol 125(2):273–288
29. Lanson NA Jr, Pandey UB (2012) FUS-related proteinopathies: lessons from animal models. Brain Res 1462:44–60
30. Licatalosi DD, Darnell RB (2010) RNA processing and its regulation: global insights into biological networks. Nat Rev Genet 11:75–87
31. Li Q, Lee J-A, Black DL (2007) Neuronal regulation of alternative pre-mRNA splicing. Nat Rev Neurosci 8:819–831
32. Dredge BK, Polydorides AD, Darnell RB (2001) The splice of life: alternative splicing and neurological disease. Nat Rev Neurosci 2:43–50
33. Yeo G, Holste D, Kreiman G, Burge C (2004) Variation in alternative splicing across human tissues. Genome Biol 5:R74
34. Wahl MC, Will CL, Lührmann R (2009) The spliceosome: design principles of a dynamic RNP machine. Cell 136:701–718
35. Ishigaki S, Masuda A, Fujioka Y, Iguchi Y, Katsuno M, Shibata A, Urano F, Sobue G, Ohno K (2012) Position-dependent FUS-RNA interactions regulate alternative splicing events and transcriptions. Sci Rep 2. http://www.nature.com/srep/2012/120724/srep00529/abs/srep00529.html#supplementary-information
36. Rogelj B, Easton LE, Bogu GK, Stanton LW, Rot G, Curk T, Zupan B, Sugimoto Y, Modic M, Haberman N, Tollervey J, Fujii R, Takumi T, Shaw CE, Ule J (2012) Widespread binding of FUS along nascent RNA regulates alternative splicing in the brain. Sci Rep 2. http://www.nature.com/srep/2012/120828/srep00603/abs/srep00603.html#supplementary-information
37. Lagier-Tourenne C, Polymenidou M, Hutt KR, Vu AQ, Baughn M, Huelga SC, Clutario KM, Ling S-C, Liang TY, Mazur C et al (2012) Divergent roles of ALS-linked proteins FUS/TLS and TDP-43 intersect in processing long pre-mRNAs. Nat Neurosci 15:1488–1497
38. Nakaya TA, Panagiotis M, Manolis C, Alexandra M, Zissimos (2013) FUS regulates genes coding for RNA-binding proteins in neurons by binding to their highly conserved introns. RNA 19(4):498–509
39. Meissner M, Lopato S, Gotzmann J, Sauermann G, Barta A (2003) Proto-oncoprotein TLS/FUS is associated to the nuclear matrix and complexed with splicing factors PTB, SRm160, and SR proteins. Exp Cell Res 283:184–195
40. Yang L, Embree LJ, Tsai S, Hickstein DD (1998) Oncoprotein TLS interacts with serine-arginine proteins involved in RNA splicing. J Biol Chem 273:27761–27764
41. Gerbino V, Carrì MT, Cozzolino M, Achsel T (2013) Mislocalised FUS mutants stall spliceosomal snRNPs in the cytoplasm. Neurobiol Dis 55:120–128
42. Braunschweig U, Gueroussov S, Plocik AM, Graveley Brenton R, Blencowe Benjamin J (2013) Dynamic integration of splicing within gene regulatory pathways. Cell 152:1252–1269
43. Schwartz JC, Ebmeier CC, Podell ER, Heimiller J, Taatjes DJ, Cech TR (2012) FUS binds the CTD of RNA polymerase II and regulates its phosphorylation at Ser2. Genes Dev 26:2690–2695
44. Lerga A, Hallier M, Delva L, Orvain C, Gallais I, Marie J, Moreau-Gachelin F (2001) Identification of an RNA binding specificity for the potential splicing factor TLS. J Biol Chem 276:6807–6816
45. Hong M, Zhukareva V, Vogelsberg-Ragaglia V, Wszolek Z, Reed L, Miller BI, Geschwind DH, Bird TD, McKeel D, Goate A et al (1998) Mutation-specific functional impairments in distinct tau isoforms of hereditary FTDP-17. Science 282:1914–1917
46. Cooper TA, Wan L, Dreyfuss G (2009) RNA and disease. Cell 136:777–793
47. Lorson CL, Androphy EJ (1998) The domain encoded by exon 2 of the survival motor neuron protein mediates nucleic acid binding. Hum Mol Genet 7:1269–1275

48. Colombrita C, Onesto E, Megiorni F, Pizzuti A, Baralle FE, Buratti E, Silani V, Ratti A (2012) TDP-43 and FUS RNA-binding proteins bind distinct sets of cytoplasmic messenger RNAs and differently regulate their post-transcriptional fate in motoneuron-like cells. J Biol Chem 287:15635–15647
49. Dichmann DS, Harland RM (2012) fus/TLS orchestrates splicing of developmental regulators during gastrulation. Genes Dev 26:1351–1363
50. König J, Zarnack K, Luscombe NM, Ule J (2012) Protein–RNA interactions: new genomic technologies and perspectives. Nat Rev Genet 13:77–83
51. Buratti E, Romano M, Baralle FE (2013) TDP-43 high throughput screening analyses in neurodegeneration: advantages and pitfalls. Mol Cell Neurosci. doi:10.1016/j.mcn.2013.03.001
52. Sephton CF, Cenik C, Kucukural A, Dammer EB, Cenik B, Han Y, Dewey CM, Roth FP, Herz J, Peng J et al (2011) Identification of neuronal RNA targets of TDP-43-containing ribonucleoprotein complexes. J Biol Chem 286:1204–1215
53. Tollervey JR, Curk T, Rogelj B, Briese M, Cereda M, Kayikci M, Konig J, Hortobagyi T, Nishimura AL, Zupunski V et al (2011) Characterizing the RNA targets and position-dependent splicing regulation by TDP-43. Nat Neurosci 14:452–458
54. Polymenidou M, Lagier-Tourenne C, Hutt KR, Huelga SC, Moran J, Liang TY, Ling S-C, Sun E, Wancewicz E, Mazur C et al (2011) Long pre-mRNA depletion and RNA missplicing contribute to neuronal vulnerability from loss of TDP-43. Nat Neurosci 14:459–468
55. Goedert M, Spillantini M (2011) Pathogenesis of the tauopathies. J Mol Neurosci 45:425–431
56. Buée L, Bussière T, Buée-Scherrer V, Delacourte A, Hof PR (2000) Tau protein isoforms, phosphorylation and role in neurodegenerative disorders. Brain Res Rev 33:95–130
57. Lee VM-Y, Goedert M, Trojanowski JQ (2001) Neurodegenerative tauopathies. Annu Rev Neurosci 24:1121–1159
58. Panda D, Samuel JC, Massie M, Feinstein SC, Wilson L (2003) Differential regulation of microtubule dynamics by three- and four-repeat tau: implications for the onset of neurodegenerative disease. Proc Natl Acad Sci 100:9548–9553
59. Brunden KR, Trojanowski JQ, Lee VMY (2008) Evidence that Non-fibrillar tau causes pathology linked to neurodegeneration and behavioral impairments. J Alzheimers Dis 14:393–399
60. de Calignon A, Fox LM, Pitstick R, Carlson GA, Bacskai BJ, Spires-Jones TL, Hyman BT (2010) Caspase activation precedes and leads to tangles. Nature 464:1201–1204
61. Tobin JE, Latourelle JC, Lew MF, Klein C, Suchowersky O, Shill HA, Golbe LI, Mark MH, Growdon JH, Wooten GF et al (2008) Haplotypes and gene expression implicate the MAPT region for Parkinson disease: the GenePD study. Neurology 71:28–34
62. Caffrey TM, Joachim C, Paracchini S, Esiri MM, Wade-Martins R (2006) Haplotype-specific expression of exon 10 at the human MAPT locus. Hum Mol Genet 15:3529–3537
63. Williams-Gray CH, Evans JR, Goris A, Foltynie T, Ban M, Robbins TW, Brayne C, Kolachana BS, Weinberger DR, Sawcer SJ et al (2009) The distinct cognitive syndromes of Parkinson's disease: 5 year follow-up of the CamPaIGN cohort. Brain 132:2958–2969
64. Skipper L, Wilkes K, Toft M, Baker M, Lincoln S, Hulihan M, Ross OA, Hutton M, Aasly J, Farrer M (2004) Linkage disequilibrium and association of MAPT H1 in Parkinson disease. Am J Hum Genet 75:669–677
65. Sundar PD, Yu C-E, Sieh W, Steinbart E, Garruto RM, Oyanagi K, Craig U-K, Bird TD, Wijsman EM, Galasko DR et al (2007) Two sites in the MAPT region confer genetic risk for Guam ALS/PDC and dementia. Hum Mol Genet 16:295–306
66. Mawal-Dewan M, Schmidt LM, Balin B, Perl DP, Lee VM-Y, Trojanowski JQ (1996) Identification of phosphorylation sites in PHF-TAU from patients with Guam amyotrophic lateral sclerosis/parkinsonism-dementia complex. J Neuropathol Exp Neurol 55:1051–1059
67. Urwin H, Josephs K, Rohrer J, Mackenzie I, Neumann M, Authier A, Seelaar H, Swieten J, Brown J, Johannsen P et al (2010) FUS pathology defines the majority of tau- and TDP-43-negative frontotemporal lobar degeneration. Acta Neuropathol 120:33–41
68. Arai T, Hasegawa M, Akiyama H, Ikeda K, Nonaka T, Mori H, Mann D, Tsuchiya K, Yoshida M, Hashizume Y et al (2006) TDP-43 is a component of ubiquitin-positive tau-negative inclusions in frontotemporal lobar degeneration and amyotrophic lateral sclerosis. Biochem Biophys Res Commun 351:602–611
69. Eastwood SL, Harrison PJ (2007) Decreased mRNA expression of netrin-G1 and netrin-G2 in the temporal lobe in schizophrenia and bipolar disorder. Neuropsychopharmacology 33:933–945
70. Yin Y, Miner JH, Sanes JR (2002) Laminets: laminin- and netrin-related genes expressed in distinct neuronal subsets. Mol Cell Neurosci 19:344–358
71. Meerabux JMA, Ohba H, Fukasawa M, Suto Y, Aoki-Suzuki M, Nakashiba T, Nishimura S, Itohara S, Yoshikawa T (2005) Human netrin-G1 isoforms show evidence of differential expression. Genomics 86:112–116
72. Cirulli V, Yebra M (2007) Netrins: beyond the brain. Nat Rev Mol Cell Biol 8:296–306
73. Aoki-Suzuki M, Yamada K, Meerabux J, Iwayama-Shigeno Y, Ohba H, Iwamoto K, Takao H, Toyota T, Suto Y, Nakatani N et al (2005) A family-based association study and gene expression analyses of netrin-G1 and -G2 genes in schizophrenia. Biol Psychiatry 57:382–393
74. Lin L, Lesnick TG, Maraganore DM, Isacson O (2009) Axon guidance and synaptic maintenance: preclinical markers for neurodegenerative disease and therapeutics. Trends Neurosci 32:142–149
75. Roof DJ, Hayes A, Adamian M, Chishti AH, Li T (1997) Molecular characterization of abLIM, a novel actin-binding and double zinc finger protein. J Cell Biol 138:575–588
76. Lundquist EA, Herman RK, Shaw JE, Bargmann CI (1998) UNC-115, a conserved protein with predicted LIM and actin-binding domains, mediates axon guidance in C. Elegans. Neuron 21:385–392
77. Erkman L, Yates PA, McLaughlin T, McEvilly RJ, Whisenhunt T, O'Connell SM, Krones AI, Kirby MA, Rapaport DH, Bermingham JR et al (2000) A POU domain transcription factor dependent program regulates axon pathfinding in the vertebrate visual system. Neuron 28:779–792
78. Sakurai T (2012) The role of NrCAM in neural development and disorders—beyond a simple glue in the brain. Mol Cell Neurosci 49:351–363
79. Wang B, Williams H, Du J-S, Terrett J, Kenwrick S (1998) Alternative splicing of human NrCAM in neural and nonneural tissues. Mol Cell Neurosci 10:287–295
80. Barnier JV, Papin C, Eychène A, Lecoq O, Calothy G (1995) The mouse B-raf gene encodes multiple protein isoforms with tissue-specific expression. J Biol Chem 270:23381–23389
81. Frebel K, Wiese S (2006) Signalling molecules essential for neuronal survival and differentiation. Biochem Soc Trans 34(Pt 6):1287–1290
82. Wiese S, Pei G, Karch C, Troppmair J, Holtmann B, Rapp UR, Sendtner M (2001) Specific function of B-Raf in mediating survival of embryonic motoneurons and sensory neurons. Nat Neurosci 4:137–142
83. Zhong J, Li X, McNamee C, Chen AP, Baccarini M, Snider WD (2007) Raf kinase signaling functions in sensory neuron differentiation and axon growth in vivo. Nat Neurosci 10:598–607
84. Wu C-H, Fallini C, Ticozzi N, Keagle PJ, Sapp PC, Piotrowska K, Lowe P, Koppers M, McKenna-Yasek D, Baron DM et al (2012)

Mutations in the profilin 1 gene cause familial amyotrophic lateral sclerosis. Nature 488:499–503
85. Al-Chalabi A, Andersen PM, Nilsson P, Chioza B, Andersson JL, Russ C, Shaw CE, Powell JF, Nigel Leigh P (1999) Deletions of the heavy neurofilament subunit tail in amyotrophic lateral sclerosis. Hum Mol Genet 8:157–164
86. Fischer LR, Culver DG, Tennant P, Davis AA, Wang M, Castellano-Sanchez A, Khan J, Polak MA, Glass JD (2004) Amyotrophic lateral sclerosis is a distal axonopathy: evidence in mice and man. Exp Neurol 185:232–240
87. Saxena S, Caroni P (2011) Selective neuronal vulnerability in neurodegenerative diseases: from stressor thresholds to degeneration. Neuron 71:35–48
88. Dormann D, Haass C (2011) TDP-43 and FUS: a nuclear affair. Trends Neurosci 34:339–348
89. Johnson R (2012) Long non-coding RNAs in Huntington's disease neurodegeneration. Neurobiol Dis 46:245–254
90. Suberbielle E, Sanchez PE, Kravitz AV, Wang X, Ho K, Eilertson K, Devidze N, Kreitzer AC, Mucke L (2013) Physiologic brain activity causes DNA double-strand breaks in neurons, with exacerbation by amyloid-β. Nat Neurosci 16:613–621
91. Vourekas A, Zheng Q, Alexiou P, Maragkakis M, Kirino Y, Gregory BD, Mourelatos Z (2012) Mili and Miwi target RNA repertoire reveals piRNA biogenesis and function of Miwi in spermiogenesis. Nat Struct Mol Biol 19:773–781